Developments in non-relativistic field theory and complexity

Stefano Baiguera

Advisor: Silvia Penati

Co-advisor: Roberto Auzzi

Department of Physics
University of Milan-Bicocca

This dissertation is submitted for the degree of
Doctor of Philosophy

PhD coordinator: Marta Calvi
Curriculum in Theoretical Physics
Cycle XXXII
Matricola: 814546
Academic year: 2018/2019

October 2019

Declaration

This dissertation is a result of my own efforts. The work to which it refers is based on my PhD research projects:

1. "Trace anomaly for non-relativistic fermions," with R. Auzzi and G. Nardelli, JHEP **1708** (2017) 042 [arXiv:1705.02229 [hep-th]].

2. "Nonrelativistic trace and diffeomorphism anomalies in particle number background," with R. Auzzi and G. Nardelli, Phys. Rev. D **97** (2018) no.8, 085010 [arXiv:1711.00910 [hep-th]].

3. "Volume and complexity for warped AdS black holes," with R. Auzzi and G. Nardelli, JHEP **1806** (2018) 063 [arXiv:1804.07521 [hep-th]].

4. "Complexity and action for warped AdS black holes," with R. Auzzi, G. Nardelli and N. Zenoni, JHEP **1809** (2018) 013 [arXiv:1806.06216 [hep-th]].

5. "Renormalization properties of a Galilean Wess-Zumino model," with R. Auzzi, G. Nardelli and S. Penati, JHEP **1906** (2019) 048 [arXiv:1904.08404 [hep-th]].

6. "Subsystem complexity in warped AdS," with R. Auzzi, A. Mitra, G. Nardelli and N. Zenoni, JHEP **1909** (2019) 114 [arXiv:1906.09345 [hep-th]].

7. "On subregion action complexity in AdS_3 and in the BTZ black hole," with R. Auzzi, A. Legramandi, G. Nardelli, P. Roy and N. Zenoni, [arXiv:1910.00526 [hep-th]].

I hereby declare that except where specific reference is made to the work of others, the contents of this dissertation are original and have not been submitted in whole or in part for consideration for any other degree or qualification in this, or any other university.

Stefano Baiguera
October 2019

Acknowledgements

There are a lot of people I need to thank a lot for the continuous support during the PhD and whose help was determinant to finish this work. First of all, the biggest acknowledgments go to my supervisors[1] Roberto Auzzi, Giuseppe Nardelli and Silvia Penati, who explained me a lot of things and supported me during all these years. The experience I lived in these years surely helped me to grow up professionally and, more importantly, as a person, also due to the various schools, workshops, trips where I met a lot of new people and I learnt new things.

In this sense, I thank for the professional and daily experiences all the professors and postdocs in Milan-Bicocca, *i.e.* Alessandro Tomasiello, Alberto Zaffaroni, Sara Pasquetti, Noppadol Mekareeya, Carlo Oleari, Simone Alioli, Antonio Amariti, Valentin Reys, Francesco Aprile, Paul Richmond, Yegor Zenkevich, Kate Eckerle, Vladimir Bashmakov ... Moreover, I thank a lot all the people working in Università Cattolica del Sacro Cuore di Brescia, where I studied during the bachelor and master degrees and who allowed me to work in the institute in a joint program with the Bicocca university: in particular I thank the professors Fausto Borgonovi, Alfredo Marzocchi, Marco Marzocchi, Silvia Pianta, Mauro Spera, Dario Mazzoleni, Stefania Pagliara, Marco Degiovanni, Claudio Giannetti ...

I also greatly thank Niels Obers and Shira Chapman, who accepted to evaluate the thesis and gave me a lot of valuable comments and insights

To continue the acknowledgments, I find more convenient to switch now to italian.

I più grandi ringraziamenti vanno alle persone con cui ho passato più tempo, allietando incredibilmente le mie giornate e anche moltissime serate. Parto dagli amici in Bicocca: grazie intanto ai miei coetanei con cui siamo entrati massivamente nello stesso anno del PhD: Andrea Legramandi, Giuseppe Bruno de Luca, Gabriele Lo Monaco, Carolina Gomez. Grazie a chi si è aggiunto l'anno dopo, Ivan Garozzo e Marco Rocco, e poi due anni dopo, Matteo Sacchi, Lorenzo Coccia, Nicola Gorini e Simone (notevoli i memes prodotti per la temperatura nel nostro ufficio quest'estate). Già presenti dagli anni prima, ci sono Morteza Seyed Hosseini, Luca Cassia, Silvia Ferrario Ravasio, Erika Colombo, Michele Turelli e Anton Nedelin (che era già postdoc, ma ha passato moltissimo tempo con noi). Grazie a tutti voi[2]! Rimarranno sempre tra i miei ricordi migliori i pranzi insieme, e soprattutto le serate cinema o giochi (Mario Kart o altri giochi retrò, anche se purtroppo abbiamo

[1] Someone was official, someone not, but this is irrelevant.

[2] Ho sorvolato sui soprannomi, ma alcuni meritevoli sono EP, Cicci, cumpà, picciò ... L'intepretazione della prima sigla è tuttora oggetto di ampi dibattiti.

fatto solo una sessione . . .), le discussioni su Pokémon e su altri giochi[3], la costruzione della cucina e del *trio* nel nostro ufficio, il pane tostato con la Nutella[4] e il burro d'arachidi, la piantina di menta seguita da quella di zenzero, la visione a pranzo delle puntate di Death Note (per me era tipo la sesta volta!). A questi si aggiungono i viaggi insieme alle varie scuole di dottorato, dove abbiamo alloggiato insieme e vissuto grandi e divertenti esperienze, tra cui potrei citare episodi come "*Ma quell'orologio ha due lancette!*", lo streatching durante la pausa di una certa lezione, il test di dialetto bresciano che ho dovuto affrontare, la Nintendo Wii in appartamento a Trieste con il controller senza batterie, il viaggio su Flixbus giocando a Pokémon Showdown in competitivo per 5-6 ore, le partitelle a basket[5] e tanto altro. Tra gli studenti di PhD con cui ho condiviso momenti divertenti tra le varie scuole al GGI o all'ICTP ci sono Carlo Heissenberg, Sara Bonansea, Stefano Speziali, Luca Buoninfante, Alberto Merlano, Riccardo Conti, Luca Ciambelli, Lorenzo Menculini, Paolo Soresina, Paolo Milan . . .

Proseguendo cronologicamente a ritroso con i miei amici, troviamo i colleghi del DMF a Brescia: Tommaso Tosi, Giulia Zani, Silvia Bianchetti, Michele Zubani, Sara Zanini, Ilario Medaglia, Debora Coltrini, Eugenio Guarneri e Francesco Filippini[6]. Con loro posso ricordare tante serate di giochi da tavolo, da Maschera (uno dei miei preferiti, adoro troppo il bluff e gli azzardi sensati nei giochi da tavolo) a Seven Wonders, da Bang! a Citadels . . . A questo si aggiungono i tanti compleanni festeggiati insieme, il weekend a Firenze durante il ponte del primo maggio qualche anno fa, i dibattiti sulle mie battute e il loro valore, gli episodi divertenti in Università (per chi può intendere, credo che negli ultimi mesi abbiamo dormito tutti sonni molto tranquilli), le varie camminate in montagna che ho saltato, le partitelle fisici contro matematici che avevamo fatto con clamorosi risultati, la tintura imperiale . . . Tra le tante serate insieme, meritano sicuramente una menzione particolare Nick Fiini, Chiara Co', Gabriele Calzavara, Melania Fava, Pippo, e in dipartimento o altrove anche Mauro, Fede Armanti, Steve e poi Sara Rizzini, Mattia Angeli, Paolo Stornati, Paolo Franceschini, Andrea Tognazzi . . . Un grazie per le giornate insieme ai miei compagni di ufficio a Brescia, Silvia Pagani, Sara Mastaglio, Antonio Miti, e anche a Chahan e Sonia Freddi. In particolare, un grande ringraziamento va a Nicolò Zenoni, co-autore di vari paper e praticamente compagno di ufficio, con cui ci sono state varie discussioni scientifiche e riguardanti anime come Dragon Ball, Naruto, partite di tennis e altro.

Continuando indietro nel tempo ci sono gli amici del liceo, tra cui merita una menzione particolare Lavneet Banger detto Bunch, con i suoi straordinari e divertenti racconti di episodi realmente accaduti nella sua permanenza in Canada, che mi hanno notevolmente rallegrato. E qui la lista arriva ai membri della Fellowship, che seppure abbia iniziato a diffondersi per il mondo, resta saldamente un punto di riferimento: Fede, Mix, Ken, Rocco (e le loro sorelle ahah), Paolo, Riccardo (da Ric, aggiungerei per chi può intendere), Marci, Sam. Anche qui gli episodi esaltanti sono davvero molti (a malapena numerabili): citerei sicuramente Hulk, partite a Tekken, le grondaie, i *tutti tutti*, i nobili tornei degli

[3] Menzione d'onore per i giochi del genere soulsborne e per le discussioni sullo splendido lavoro e sulle gaffe di Sabaku no Maiku.

[4] Quanto mi manca! Ahah.

[5] A quando la partita a calcetto?

[6] Scientificamente, menzione d'onore per gli ultimi due: abbiamo collaborato intensamente durante la tesi triennale e magistrale, rispettivamente.

scacchi, le partite a Risiko, Monopoli, cooperative al Signore degli Anelli[7], alla Serenissima, a Diplomacy (molto tempo fa ormai), le coperte durante il soggiorno a Monaco di Baviera, frasi come "*è tratto da un fumetto!*", le chiamate della Farnesina in Crimea, il Pedro all'eredità, le discussioni sulle partite del Milan (ahimé, sono brutti tempi), le discussioni su anime di grande qualità e i consigli su giochi come Undertale (assolutamente straordinario, Toby Fox è un genio) . . . Mi viene anche nostalgia ripensando alle discussioni sulle classifiche degli anime o sulle mono tech da giocare nei mazzi di Yu-gi-oh!, cose che ormai risalgono a una decina di anni fa. Un grande ringraziamento anche a Giulia Ferrari, che ha letto e commentato il poster che ho preparato sulla partecipazione delle donne nel mondo scientifico! A ciò si aggiungono diversi consigli in tema di anime.

Infine, un ringraziamento particolare a mia mamma, che mi ha sempre supportato, sopportato e sostenuto con affetto in tutte le mie scelte (oltre a far da mangiare e tutte le altre cose tipiche delle mamme! Mi piace molto vivere da solo perché posso organizzarmi come voglio, ma trovo noioso far sempre da mangiare ahah), e a mio papà, tra le innumerevoli partite a carte e i consigli di vita. Grazie anche a tutti gli zii, cugini e nonni!

Concludo questi lunghi ringraziamenti (sono stato prolisso anche in questa parte della tesi, yeah!) ancora una volta con un "*Grazie, ragazzi!*" come direbbe Seb Vettel[8], senza tutti voi, questa tesi non sarebbe stata possibile.

[7] Qui vanno necessariamente citati un "*Giammai mi sacrificherò per tutti*" e il ruolo di causalità e casualità nel gioco in questione.

[8] A proposito di sport, come per il Milan, anche in F1 sono tempi magri . . .

Abstract

This thesis focuses on the investigation of two research areas: non-relativistic field theories and holographic complexity.

In the first part we review the general classification of the trace anomaly for 2+1 dimensional field theories coupled to a Newton-Cartan background and we also review the heat kernel method, which is used to study one-loop effective actions and then allows to compute anomalies for a given theory. We apply this technique to extract the exact coefficients of the curvature terms of the trace anomaly for both a non-relativistic free scalar and a fermion, finding a relation with the conformal anomaly of the 3+1 dimensional relativistic counterpart which suggests the existence of a non-relativistic version of the a-theorem on which we comment. We continue the analysis of non-relativistic free scalar and fermion with the heat kernel method by turning on a source for the particle mass: on this background, we find that there is no gravitational anomaly, but the trace anomaly is not gauge invariant.

We then consider a specific model realizing a $\mathscr{N} = 2$ supersymmetric extension of the Bargmann group in 2+1 dimensions with non-vanishing superpotential, obtained by null reduction of a relativistic Wess-Zumino model. We check that the superpotential is protected against quantum corrections as in the relativistic parent theory, thus finding a non-relativistic version of the non-renormalization theorem. Moreover, we find strong evidence that the theory is one-loop exact, due to the causal structure of the non-relativistic propagator together with mass conservation.

In the second part of the thesis we review the holographic conjectures proposed by Susskind to describe the time-evolution of the Einstein-Rosen bridge in gravitational theories: the complexity=volume and complexity=action. These quantities may be used as a tool to investigate dualities, and we investigate both the volume and the action for black holes living in warped AdS_3 spacetime, which is a non-trivial modification of usual AdS_3 with non-relativistic boundary isometries. In particular, we analytically compute the time dependence of complexity finding an asymptotic growth rate proportional to the product of Hawking temperature and Bekenstein-Hawking entropy. In this context, there exist extensions of the holographic proposals when the dual state from the field theory side is mixed, *i.e.* we consider only a subregion on the boundary. We study the structure of UV divergences, the sub/super-additivity behaviour of complexity and its temperature dependence for warped black holes in 2+1 dimensions when the subregion is taken to be one of the two disconnected boundaries. Finally, we analytically compute the subregion action complexity for a general segment on the boundary in the BTZ black hole background, finding that it is equal to the sum of a linearly divergent term proportional to the size of the subregion and of a term proportional to the entanglement

entropy. While this result suggests a strong relation of complexity with entanglement entropy, we find after investigating the case of two disjoint segments in the BTZ background that there are additional finite contributions: as a consequence, mutual holographic complexity carries a different content compared to mutual information. This means that entropy is not enough!

Table of contents

Chapter 1

Introduction

Symmetries play a crucial role in modern physics: when a law of physics does not change upon some transformation, this is said to exhibit an invariance. The use of symmetries allows to obtain conserved quantities which simplify the description of the system, or imposes restrictions on the way a model needs to be formulated. An important example of a symmetry and of the consequences of its existence is Poincaré invariance, which was understood to be a fundamental symmetry of Nature after the formulation of the theory of relativity. Translation and rotation invariances imply the existence of a symmetric and conserved energy-momentum tensor, and requiring that the symmetry holds gives restrictions on the theoretical model describing a physical system, *e.g.* it constrains the action and the form of correlation functions.

A broader way in which the concept of symmetry can be applied is in the context of the Renormalization Group: it refers to an invariance of the observables under changes of the scales at which physical quantities are defined. In this case, the independence of the theory from such an arbitrary scale implies the existence of a differential equation of the kind

$$\frac{d}{d\mu}\mathscr{O} = 0\,, \tag{1.1}$$

where $\mathscr{O}$ is a physical observable and μ is a mass scale. The solutions of such a relation consist in trajectories in the space of Quantum Field Theories. The application of these ideas allows to understand the asymptotic behaviour of gauge theories and to find relevant physical quantities like the critical exponents of second order phase transitions.

In this context, the search for emergent symmetries has recently acquired great relevance: a new symmetry may arise in the infrared, even if absent from the microscopic Hamiltonian, due to the presence of an interacting infrared fixed point in the renormalization group flow.

The material contained in the Introduction to this thesis is organized as follows. In section 1.1 we will discuss the relevance of the conformal symmetry and of the corresponding quantum anomaly in relation to universal properties of the Renormalization Group flow, *i.e.* the irreversibility of a trajectory in the space of Quantum Field Theories. Moreover, we will justify why non-relativistic symmetry

can play a meaningful role in the discussion, and which insights can provide in the context of a better understanding of the laws of physics. In section 1.2 the special role played by Supersymmetry will be discussed, in particular in relation to the powerful exact results that this invariance provides, such as non-renormalization theorems. We will be interested in studying the implementation of Supersymmetry as a graded extension of the Galilean algebra in order to analyze if similar results apply to non-relativistic models. In section 1.3 we will tackle a different problem related to quantum information and geometry, a nice realization of the AdS/CFT correspondence. In particular, we will discuss the relation between the evolution in time of the Einstein-Rosen bridge in connection with computational complexity, and we will study this quantity for black holes in spacetimes which do not contain the Lorentz group as an isometry at the boundary, thus providing insights on the investigation of non-relativistic realizations of holography.

1.1 Non-relativistic trace anomalies

Weyl invariance gives important restrictions on relativistic field theories, implying that the classical energy-momentum tensor is traceless. However Weyl symmetry is in general lost after quantization, and the trace of the energy-momentum tensor is non-vanishing when the system is coupled to curved backgrounds (*trace anomaly*)

$$\langle T^{\mu}_{\mu} \rangle \equiv \mathscr{A} \neq 0 \,. \tag{1.2}$$

It is possible to write the most general expression of the trace anomaly in d spacetime dimensions consistent with diffeomorphism invariance and satisfying the Wess-Zumino consistency conditions

$$\Delta^{\mathrm{WZ}}_{\sigma_1\sigma_2} W = (\delta_{\sigma_1}\delta_{\sigma_2} - \delta_{\sigma_2}\delta_{\sigma_1})W = 0 \,, \tag{1.3}$$

where W is the generating functional of connected diagrams. In particular, it is well known that in 2 dimensions

$$\mathscr{A}_{\mathrm{d}=2} = cR \,, \tag{1.4}$$

where c is the *central charge* of the corresponding Conformal Field theory and it is related to the Lorentz structure of the matter fields. In 4 dimensions, the anomaly is

$$\mathscr{A}_{\mathrm{d}=4} = aE_4 - cW^2_{\mu\nu\rho\sigma} + \mathscr{A}_{\mathrm{ct}} \,, \tag{1.5}$$

where E_4 and $W^2_{\mu\nu\rho\sigma}$ are the Euler density and the square of the Weyl tensor, respectively. The term $\mathscr{A}_{\mathrm{ct}}$ refers the scheme-dependent part[1].

Trace anomalies allow to characterize in the relativistic case the irreversibility properties of the Renormalization Group. In the case of relativistic (1+1)-dimensional theories, this is established by Zamolodchikov's c-theorem [1]: there exists a function defined in the space of Quantum Field

[1] More precisely, the classification of the terms entering the trace anomaly is a cohomological problem and the scheme-dependent part refers to expressions which are not only closed, but also exact under Weyl variations.

Theories which is monotonically decreasing along a Renormalization Group trajectory and coincides at fixed points with the central charge c of the corresponding Conformal Field Theory.

Some of these results can be extended to four dimensional theories. In particular it was conjectured in [2] that such monotonically decreasing function exists and coincides with the conformal anomaly coefficient a at the fixed point (a-theorem). A perturbative proof of this conjecture based on local Renormalization Group flow equations was given by Osborn [3], while a non-perturbative proof based on 't Hooft anomaly matching was given by Komargodski and Schwimmer in 2011 [4].

The terms composing the anomaly can be divided into type A and type B terms depending from their Weyl variation[2] [5]. It turns out that the coefficients of type A anomalies[3] are candidates for an a-theorem. This can be understood in the framework of local Renormalization Group followed in [3]: since type B anomalies are Weyl invariant scalars, they are trivial solutions of the Wess-Zumino consistency conditions (1.3), and then they do not give any non-trivial contraint on their coefficients. On the other hand, type A anomalies have non-vanishing Weyl variation and then the local Renormalization Group equations following from application of (1.3) give meaningful constraints.

One can asks if the previous results are related to the relativistic content of the theory, and if an analogue of the Weyl group exists for Galilean-invariant field theories. At first sight, the two cases look very different. First of all, the Klein-Gordon equation

$$(-\hbar^2 c^2 \Box + m^2 c^4)\Phi = 0 \tag{1.6}$$

is evidently invariant under a dilatation parametrized by a constant factor σ as

$$x^\mu \to e^{2\sigma} x^\mu \,. \tag{1.7}$$

This behaviour is a consequence of the fact that the coordinates of Minkowski spacetime can be described in terms of a common four-vector containing both time and space.

On the other hand, the Schrödinger equation for a free particle is

$$i\hbar \frac{\partial}{\partial t}\psi(\vec{x},t) = -\frac{\triangle}{2m}\psi(\vec{x},t)\,, \tag{1.8}$$

which is not invariant under scale transformations (1.7). Indeed, in non-relativistic theories the scaling of time and spatial coordinates must be different in order to keep the kinetic term invariant.

We can interpret the discrepancy between the two cases due to the appearance in the Klein-Gordon equation of both the speed of light and the mass of the particle, which allows to interpret the latter as an inverse length. On the other hand, this is not true for the Schrödinger equation and ultimately allows the mass to not be interpreted as an inverse length. In this way we can rescale space and time

[2] Type B anomalies are invariant under Weyl transformations, while type A are not.

[3] In the relativistic case there exists a general procedure to show that type A anomalies must give scale-free contributions to the effective action in dimensional regularization, which in turn implies that they are related to topological invariants [5].

while retaining quantities (such as the mass) which have inequivalent dimensions and no scaling properties.

This allows to consider transformations of kind

$$x^i \to e^{\sigma} x^i\,, \quad t \to e^{z\sigma} t\,, \tag{1.9}$$

where the dynamical exponent z parametrizes the anisotropy between space and time. The Lifshitz case is characterized by invariance under the previous transformations for a general value of z. The relativistic conformal case can be recovered for $z=1$, whereas by requiring symmetry under Galilean boosts we need to choose $z=2$, which leads to the invariance of the Schrödinger equation.

In the case of Lifshitz theories, a detailed study of trace anomalies for various dimensions and values of z was carried on in [6–9]. The result does not give any reasonable candidate for a decreasing a-function; several anomalies are indeed possible at the scale-invariant fixed points, but their Weyl variation vanishes identically (type B anomalies). An analysis like the one developed in [3, 10, 11] for relativistic theories would suggest that no monotonically-decreasing anomaly coefficient is present in the Lifshitz case.

A more promising arena for searching decreasing $a-$functions along a Renormalization Group flow is the Schrödinger case. The algebra contains the generators H for time translations and P_i for spatial translations, L_{ij} for spatial rotations, K_i for Galilean boosts, D for dilatations and C for special conformal transformations, satisying the commutation relations

$$\begin{gathered}
[P_j,K_k] = i\delta_{jk}M\,, \qquad [H,K_j] = iP_j\,,\\
[L_{ij},P_k] = i\left(\delta_{ik}P_j - \delta_{jk}P_i\right)\,, \qquad [L_{ij},K_k] = i\left(\delta_{ik}K_j - \delta_{jk}K_i\right)\,,\\
[L_{ij},L_{kl}] = i\left(\delta_{ik}L_{jl} - \delta_{jk}L_{il} + \delta_{il}L_{kj} - \delta_{jl}L_{ki}\right)\,,\\
[P_i,D] = iP_i\,, \qquad [P_i,C] = iK_i\,, \qquad [K_i,D] = -iK_i\,,\\
[H,D] = 2iH\,, \qquad [H,C] = iD\,, \qquad [C,D] = -2iC\,.
\end{gathered} \tag{1.10}$$

Physical representations of this algebra require the mass to be conserved, which is implemented via the introduction of a $U(1)$ central extension (called Bargmann algebra) with the generator M.

Galilean invariance is usually thought as a low-energy approximation of theories with Poincaré invariance, and as such it can be found by performing the $c\to\infty$ limit in the corresponding relativistic setting[4]. On the other hand, it is possible to obtain the Galilean group by discrete light cone quantization, which consists in a dimensional reduction along a null direction of a relativistic theory living in one higher dimension [13]. A simple example where the procedure can be shown is the null reduction of the Klein-Gordon equation for a massless scalar field in $d+2$ dimensional Minkowski

[4]When performing this procedure, divergent expressions in the speed of light appear and we need to introduce some subtraction terms via a chemical potential and by appropriately rescaling the fields [12].

spacetime [14]

$$\Box\Phi = -\partial_0^2\Phi + \sum_{i=1}^{d+1}\partial_i^2\Phi = 0\,, \tag{1.11}$$

which is conformally-invariant.

We define the light-cone coordinates

$$x^{\pm} = \frac{x^{d+1} \pm x^0}{\sqrt{2}}\,, \tag{1.12}$$

so that the Klein-Gordon equation becomes

$$\left(2\frac{\partial}{\partial x^-}\frac{\partial}{\partial x^+} + \sum_{i=1}^{d}\partial_i^2\right)\Phi = 0\,. \tag{1.13}$$

Making the identification $\partial/\partial x^- = im$ we obtain

$$\left(2im\frac{\partial}{\partial x^+} + \sum_{i=1}^{d}\partial_i^2\right)\Phi = 0\,, \tag{1.14}$$

also written as

$$i\frac{\partial}{\partial x^+}\Phi = -\frac{1}{2m}\sum_{i=1}^{d}\partial_i^2\Phi\,. \tag{1.15}$$

This is the Schrödinger equation with the interpretation of the coordinate x^+ with time.

This relation is clearly invariant under transformations of the Schrödinger group in $d+1$ dimensions, and it was derived from the Klein-Gordon equation, invariant under the conformal group in the enlarged $d+2$ dimensional spacetime. This means that the Schrödinger group in d spatial dimensions is a subgroup of the conformal group in $d+2$ spacetime dimensions, *i.e.* $O(d+2,2)$.

In nonrelativistic theories the mass spectrum is usually discrete, because there is not a direct relation with energy and the gap corresponds to the mass of the lightest particle of the system. A way to obtain the discreteness of the mass spectrum consists in requiring periodicity along a light-cone coordinate, so that the field Φ can be decomposed as

$$\Phi(x^M) = e^{imx^-}\phi(x^\mu)\,, \tag{1.16}$$

where ϕ does not depend on the x^- coordinate, in fact $x^M = (x^-, x^\mu) = (x^-, x^+, x^i)$. This decomposition of the field allows to interpret $\partial/\partial x^- = im$, where m is the eigenvalue of the $U(1)$ mass generator M.

The previous case is an explicit realization of Discrete Light Cone Quantization which shows how the Galilean-invariant case is related to the Lorentz-invariant case in one higher dimension. In this way we understand that there is a relation between the relativistic trace anomaly in even dimensional

spacetimes and the non-relativistic anomaly in odd dimensional ones[5]. On the other hand, the fact that many tensorial quantities in the non-relativistic framework can be found by null reduction does not imply that the relativistic results can be immediately imported from the parent theory. In fact, the quantization of a theory does not commute in general with the non-relativistic limit, and this gives rise to meaningful results that we will investigate in this thesis.

In order to study the trace anomaly, the field theory must be coupled to a curved background whose metric acts as a source for the definition of the energy-momentum tensor. In the relativistic case the natural candidate is a pseudo-Riemannian manifold, while the analog concept in the non-relativistic setting is the Newton-Cartan geometry, a coordinate-independent way to describe Newtonian gravity. The main properties of this geometry will be described in chapter 2, where we will also address the problem of defining Weyl invariance in this context.

Due to the relation between Lorentz and Galilean-invariant quantities given by null reduction, the minimal non-trivial case where a Newton-Cartan trace anomaly can be investigated is $2+1$ dimensions[6]. The analysis of the Newton-Cartan conformal anomaly was initiated in [15], where an infinite number of possible terms entering the anomaly was found. In this situation, it is difficult to figure out the existence of an a-theorem, due to the infinitely many coefficients that are in principle present, and the infinite number of Wess-Zumino consistency conditions to solve. With these premises, the natural conclusion would be that non-relativistic theories cannot admit an a-theorem: either there are not type A anomalies (Lifshitz theories) or there are too many (Schrödinger theories).

It turns out that there is a selection rule which splits the possible scalars entering the trace anomaly into distinct sectors, each with a finite numbers of terms [16]. The structure of the anomaly critically depends whether causal backgrounds are or not allowed. If backgrounds satisying the causality condition are considered, the possible scalars collapse to only one sector and there is just a finite number of terms in the anomaly [17]. However only one term with vanishing Weyl variation (type B term) survives, spoiling the possibility of an a-theorem in this case.

On the other hand, the coupling to Newton-Cartan gravity may be seen as a formal trick to introduce sources for the energy-momentum tensor. We can then decide to study non-causal backgrounds and consider each sector composing the anomaly separately. It is also possible to study the local Renormalization Group flow equations using Wess-Zumino consistency conditions: the idea is to consider arbitrary local rescaling of the lengths via a Weyl transformation and to introduce a space-time dependence for the couplings, that act as sources for local operators [3]. The result is that there is a sector which is the analogue of the 3+1 dimensional relativistic case, and the coefficient of the corresponding type A anomaly is the natural candidate for a non relativistic a-theorem [18].

The analysis of the Newton-Cartan trace anomaly by means of the classification of terms satisying the dimensional requirements plus the Wess-Zumino consistency conditions gives a general expression,

[5] It is well known that the relativistic trace anomaly is non-vanishing only in even spacetime dimensions. This result can be found *e.g.* by dimensional analysis.

[6] It can be shown that in $0+1$ dimensions there is not enough structure to obtain non-vanishing curvature invariants, while in even spacetime dimensions arguments similar to the odd-dimensional relativistic case forbid the existence of curvature invariants with the correct scaling dimension.

but does not ensure that the coefficients multiplying the curvature terms are non-vanishing. When considering specific models, functional techniques such as the Fujikawa method can be used to determine the exact expression of the trace anomaly. In chapter 3 we will face the problem with the heat kernel procedure.

From a condensed-matter perspective, there are many motivations for studying field theories with non-relativistic symmetries, in particular using descriptions in terms of a Schrödinger conformal field theory [19–21]. Such an example is given by fermions at unitarity in 3+1 dimensions, which interact in a fine-tuned way such that their scattering length is infinite[7] [22, 23]. Another interesting class of non-relativistic conformal field theories involves anyons in 2+1 dimensions. They play an important role in the fractional quantum Hall effect, where a theoretical treatment requires a diffeomorphism invariance for the model, then naturally leading to a coupling with torsional Newton-Cartan geometry [24, 25]. The technique of effective actions to analyze non-relativistic systems has become very useful in many other context: in nuclear physics *e.g.* [26], for cold atoms [27], and even for quantum mechanical problems like the Efimov effect [28–30].

1.2 Non-relativistic supersymmetry

Supersymmetry is a special invariance which rotates bosonic into fermionic degrees of freedom and that has been studied for several decades, mostly from high energy physicist's perspective. Introduced in the context of extensions to the Standard Model as a symmetry able to explain the hierarchy problem of the Higgs mass, supersymmetry gives a strong analytic control on several quantum physical quantities, which in some cases can be exactly computed. Indeed, when the effective action or the superpotential have a holomorphic dependence on the quantum fields and coupling constants, it is possible to get restrictions on the flow of these quantities under renormalization, leading to the non-renormalization theorem [31, 32].

To get a feeling of the power of holomorphicity, we briefly review the original argument by Seiberg. We consider the high-energy physics of a system at scale μ_0 to be described by a SUSY-invariant theory with bare action S_{μ_0}. We assume that the bare action contains a superpotential $W_{\mu_0}(g_i, \Phi_a)$ that depends on a set of chiral superfields Φ_a and coupling constants g_i. The key observation is that each coupling in the Lagrangian can be interpreted as the vacuum expectation value of the scalar component of a heavy chiral superfield.

This makes manifest that the superpotential of the bare action is holomorphic not only in the chiral superfields, but also in the coupling constants. This can also be proven in terms of a supersymmetric Ward identity. Therefore, the low-energy Wilsonian effective action with superpotential $W_{\mu<\mu_0}$ must be holomorphic in the coupling constants.

[7] This kind of system can be realized experimentally, but it is very difficult to treat theoretically due to the absence of a perturbative parameter which allows to perform a series expansion. On the other hand, the power of effective field theory and the symmetry arguments coming from the Schrödinger invariance allow to investigate properties of the model which were not accesible before.

Moreover the coupling constants, viewed as the expectation value of heavy chiral superfields, spontaneously break global symmetries of the free action. Assuming that these symmetries do not acquire anomalies at quantum level, the Wilsonian effective action must be invariant under these symmetries. Holomorphicity and global symmetries can then be used to infer the exact expression of the effective superpotential.

We now apply this general statement to the specific case in which the UV physics is described by the WZ model for a single massive chiral superfield Φ. Thus

$$S_{\text{int}} = \int d^4x d^2\theta \, W_{\mu_0} + \text{c.c.} = \int d^4x d^2\theta \left(\frac{m}{2}\Phi^2 + \frac{\lambda}{3!}\Phi^3 \right) + \text{h.c.} \tag{1.17}$$

where m, λ are promoted to background chiral superfields.

This action is invariant under the global group $U(1)_G \times U(1)_R$ if we assign the following set of charges

Superfields	$U(1)_G$	$U(1)_R$
Φ	1	1
m	-2	0
λ	-3	-1

The $U(1)_R$ factor is the ordinary R-symmetry of $\mathcal{N} = 1$ SUSY theories in four dimensions, under which the $(\theta, \bar{\theta})$ coordinates conventionally carry charge $(-1, 1)$. Spinorial coordinates are instead neutral under $U(1)_G$.

Due to the previous discussion, and assuming global symmetries to be not anomalous at low energies, the form of the superpotential $W_{\mu<\mu_0}$ is constrained by holomorphicity and invariance under $U(1)_G \times U(1)_R$ group to be of the form

$$W_\mu = m\Phi^2 f\left(\frac{\lambda\Phi}{m}\right) \tag{1.18}$$

This is in fact the most general expression which has charge 0 under $U(1)_G$ and charge 2 under $U(1)_R$.

Now, taking the Laurent expansion of f we can write

$$W_\mu = m\Phi^2 \sum_n a_n \left(\frac{\lambda\Phi}{m}\right)^n = \sum_n a_n m^{1-n} \lambda^n \Phi^{n+2} \tag{1.19}$$

However, the holomorphic dependence of the superpotential on the couplings m, λ requires

$$n \geq 0, \qquad n \leq 1 \quad \Rightarrow \quad n = 0, 1 \tag{1.20}$$

This fixes the superpotential at any scale to be

$$W_\mu = \frac{m}{2}\Phi^2 + \frac{\lambda}{3!}\Phi^3 \tag{1.21}$$

The bare superpotential is quantum exact, and has not received any loop correction. This shows how the homolorphicity of the effective action in the superfields and in the coupling constants produced a non-perturbative result with simple arguments and without any loop computation.

There are several interesting settings where supersymmetry also appears as an emergent symmetry in condensed matter systems. For example, superconformal invariance in two dimensions arises in the tricritical Ising model [33]. Supersymmetry also appears in the description of quantum phase transitions at the boundary of topological superconductors [34], in optical lattices [35], and in many other settings [36–40]. It is then a natural question to investigate non-relativistic incarnations of supersymmetry, since this kind of invariance might be emergent in the infrared of some real world systems.

In addition, even if supersymmetry plays an indirect role in holography, most of the explicit examples where the AdS/CFT correspondence is verified by quantitative checks are supersymmetric. So, in order to find the precise holographic dual of a given gravity background which geometrically realizes the Schrödinger symmetry [14], it may be useful to focus on an explicitly supersymmetric theoretical setting.

Supersymmetric extensions of the Galilean algebra were first introduced in 3+1 dimensions [41], where two super-Galilean algebras were constructed, $\mathscr{S}_1\mathscr{G}$ which includes a single two-component spinorial supercharge and $\mathscr{S}_2\mathscr{G}$, which contains two supercharges. They can be obtained as the non-relativistic limit of $\mathscr{N}=1$ and $\mathscr{N}=2$ Super-Poincaré algebras, respectively. Alternatively, $\mathscr{S}_2\mathscr{G}$ can be obtained performing a null reduction of the super-Poincarè algebra in 4+1 dimensions. It turns out that $\mathscr{S}_1\mathscr{G} \subset \mathscr{S}_2\mathscr{G}$.

We give an explicit example of these supersymmetric extensions of the Galilean group in the $2+1$ dimensional case. The bosonic part of the algebra is simply given by eq. (1.11) with the identification $L_{12}=J$, since the angular momentum is a pseudo-scalar on the plane. The fermionic part is

$$\begin{gathered}
[Q,J] = \tfrac{1}{2}Q\,, \qquad \{Q,Q^\dagger\} = \sqrt{2}M\,, \\
[\tilde{Q},J] = -\tfrac{1}{2}\tilde{Q}\,, \quad [\tilde{Q},K_1 - iK_2] = -iQ\,, \quad \{\tilde{Q},\tilde{Q}^\dagger\} = \sqrt{2}H\,, \\
\{Q,\tilde{Q}^\dagger\} = -(P_1 - iP_2)\,, \quad \{\tilde{Q},Q^\dagger\} = -(P_1 + iP_2)\,,
\end{gathered} \tag{1.22}$$

where $Q,\tilde{Q}$ are two complex supercharges. This is the non-relativistic $\mathscr{N}=2$ SUSY algebra in 2+1 dimensions, which first appeared in the non-relativistic SUSY extension of Chern-Simons matter systems, where an enhanced superconformal symmetry arises [42]. Removing $\tilde{Q}$ from (4.2) we obtain the $\mathscr{S}_1\mathscr{G}$ algebra.

In 3+1 dimensions theories with $\mathscr{S}_1\mathscr{G}$ and $\mathscr{S}_2\mathscr{G}$ invariance have been considered in [41, 43–45], while in 2+1 dimensions Chern-Simons theories with $\mathscr{S}_2\mathscr{G}$ symmetry were studied in [42, 45, 46].

Moreover, supersymmetric generalizations of the Schrödinger algebra have been investigated [42, 47–49], as well as Lifshitz supersymmetry [50]. Recent developments about the power of holomorphicity applied to the renormalization of supersymmetric Lifshitz theories are treated in [51].

In chapter 4 we will build an example of a theory with $\mathscr{S}_2\mathscr{G}$ Supersymmetry in $2+1$ dimensions, which we obtain by null reduction from a $3+1$ dimensional $\mathscr{N}=1$ Wess-Zumino model, and we will investigate its renormalization properties.

1.3 Holographic complexity

The AdS/CFT correspondence gives a non-perturbative formulation of quantum gravity in asymptotically AdS spacetimes in terms of the Quantum Field theory living on the boundary. The geometry of the gravitational theory in the bulk hiddenly encodes quantum information properties: for example the Bekenstein-Hawking entropy is proportional to the area of the event horizon of a black hole

$$S_{\text{BH}} = \frac{A}{4G}\,, \tag{1.23}$$

and the area of a minimal surface in AdS is dual to the entanglement entropy of the boundary subregion [52].

The entropy is related to the counting of degrees of freedom in the dual quantum description of a black hole and the microscopic interpretation was given in the context of string theory [53], where the number of microstates is identified with

$$n_{\text{microstates}} = e^{S_{\text{BH}}}\,. \tag{1.24}$$

However, entropy does not seem the right quantity in order to describe the evolution of the Einstein-Rosen bridge in the interior of a black hole because it grows with time far after the black hole reaches thermal equilibrium [54]. We can indeed follow the time evolution of the Einstein-Rosen bridge in the context of general relativity by considering a foliation of spacetime with global spacelike slices satisfying some regularity properties, *i.e.*

- Geodesically complete causal curves must intersect these slices once.
- Slices must stay away from curvature singularities.
- The entire region outside the horizon must be foliated by these slices.

Given the set of spacelike slices anchored on a spatial sphere with infinite radius, it can be proven that there exists one with maximum volume. After choosing this one, we let the time t to vary and this gives a foliation of spacetime with maximal slices. An example of such a procedure is shown in fig. 1.1 for a kind of eternal black hole that will be considered in chapter 5.

We observe that as time increases, the maximal slices go even further in the interior of the black hole until when $t=\infty$ we find the top final slice, which is completely inside the horizon.

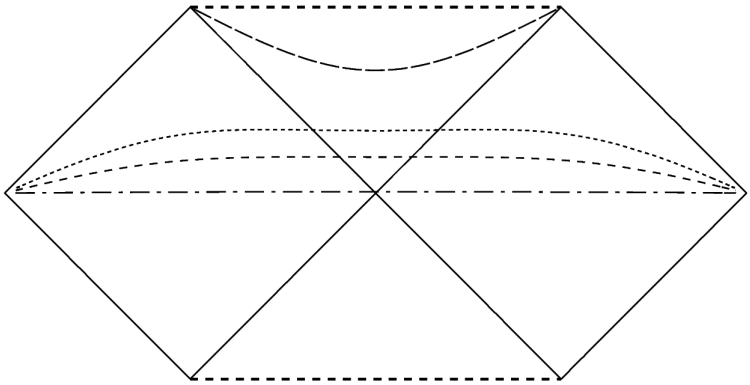

Figure 1.1: Set of extremal slices for an eternal black hole. The top slice is obtained when time goes to infinity in this effective decription.

In the AdS/CFT correspondence, a two-sided eternal black hole is dual to a thermofield double state, in which the two Conformal Field Theories living on the left and right boundaries are entangled [55]. Taking the two boundary times going in the same direction, this entangled state is time-dependent, and the geometry of the Einstein-Rosen bridge connecting the two sides grows linearly with time. This suggests that the investigation of the properties of the Einstein-Rosen bridge can give insights on the internal part of a black hole, which is expected to be related to quantum gravity aspects. Moreover, we notice that the Einstein-Rosen bridge grows for a much longer timescale compared to the thermalization time, and then entropy appears not a valid quantity to describe this process.

In order to find a boundary dual to such behaviour, a new quantum information tool has joined the discussion: computational complexity. For a quantum-mechanical system, it is defined as the minimal number of basic unitary operations which are needed to prepare a given state starting from a simple reference state.

There is a simple example which shows how the order of magnitude of entropy and complexity differ [54]. Consider a system composed by K classical bits, which are identified by associating the binary values 0 or 1 for each of them. We identify:

- A simple state[8] as $(0,0,\ldots,0)$.
- A generic state as a random collection of 0 and 1.
- A simple operation as the flip of a single bit $(0 \leftrightarrow 1)$.

In this case, the maximum entropy is the logarithm of the number of microstates (which are 2^K)

$$S_{\max}^{\mathrm{cl}} = K \log 2\,, \tag{1.25}$$

[8] We could as well identify the simple state as $(1,1,\ldots,1)$. Since there is not much difference between the two choices, we assume to identify states under a global $\mathbb{Z}_2$ transformation acting simultanesouly on all the classical bits.

while the maximal complexity corresponds to the least number of flips to perform in order to go from the reference state $(0,0,\ldots,0)$ to the most complex one, which is

$$(\underbrace{0,\ldots,0}_{K/2},\underbrace{1,\ldots,1}_{K/2}). \tag{1.26}$$

This shows that

$$\mathscr{C}^{\rm cl}_{\rm max} = K/2\,. \tag{1.27}$$

We observe that the classical entropy and complexity are both linear in the number K of classical bits.

Things drastically change at the quantum level. First of all, we need to take an Hilbert state instead of a generic set of states, and operations are required to be unitary. Furthermore, we identify

- A simple state[9] as $|00\ldots0\rangle$.
- A generic state as a generic superposition of qubits with complex coefficients $|\psi\rangle = \sum_{i=1}^{2^K} \alpha_i |i\rangle$.
- A simple operation as the action on 2 qubits, which is the simplest procedure which creates a non-vanishing entanglement in the system.

While the maximum entropy is the same (the number of microstates does not change between the classical and quantum cases)

$$S^{\rm qu}_{\rm max} = K\log 2\,, \tag{1.28}$$

now the most complex state is obtained by changing the coefficients of the generic superpositions, which are in number 2^K. This implies that the number of operations to perform is

$$\mathscr{C}^{\rm qu}_{\rm max} \sim e^K\,. \tag{1.29}$$

We observe that in this case we have an exponential behaviour for complexity instead of the power-law dependence for the entropy. Correspindingly, the time to get maximal entropy and maximal complexity are very different at quantum level, justifying heuristically the proposal that complexity can describe the time evolution of the Einstein-Rosen bridge.

In addition, from tensor network expectations the computational complexity is thought to behave as in fig. 1.2: there should be a short period of time when complexity grows linearly, and it reaches a constant value of saturation after an exponential time in the order of the size of the system, when quantum effects arise.

After a time of order e^{e^K} (not shown in the previous graph) Poincaré recurrencies are expected to arise, leading to a decreasing of complexity to the original value, and a periodic behaviour should manifest.

A proper definition of complexity in quantum field theory has several subtleties: the choice of the reference state, the allowed set of elementary quantum gates and the amount of tolerance which is

[9] In this case we identify states under a global $SU(2)$ transformation.

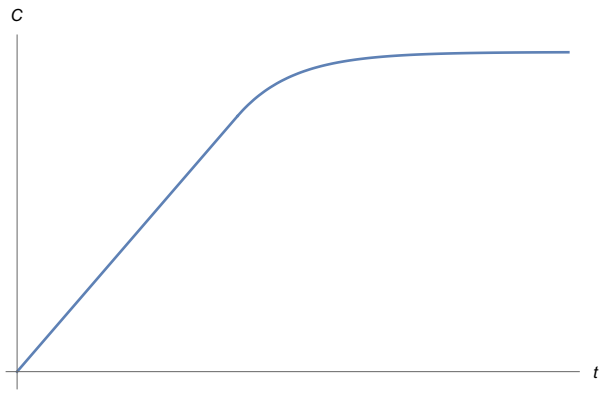

Figure 1.2: Expected time evolution of complexity in a typical chaotic system. The period of time where the effective description for the black holes is expected to be valid corresponds to the linear behaviour of complexity with respect to time in the graph.

introduced in order to specify the accuracy with which the state should be produced. Two different gravity duals of the quantum complexity of a state have been proposed so far: the complexity=volume [56] and the complexity=action [57] conjectures[10].

In the Volume conjecture, complexity is proportional to the volume of a maximal codimension-one sub-manifold hanging from the boundary

$$C_V \sim \frac{\text{Max}(V)}{Gl}\,. \tag{1.30}$$

While this proposal is a natural generalization of the entanglement entropy and has a physical interpretation as the volume of the Einstein-Rosen bridge, it requires the introduction of an *ad hoc* length scale l, which can be the AdS or the Schwarzschild radius or other relevant quantities dependent from the holographic dictionary.

In the Action conjecture, complexity is proportional to the gravitational action I evaluated in the Wheeler-De Witt patch, *i.e.* the bulk domain of dependence of a Cauchy surface anchored at the boundary state

$$C_A = \frac{I}{\pi\hbar}\,. \tag{1.31}$$

In this case the action has several contributions beyond the traditional bulk Einstein-Hilbert and boundary Gibbons-Hawking-York terms: they come from the null surfaces and from the joints at the intersection of boundary segments, which are necessary to compute the full time dependence of the Wheeler-De Witt action in AdS spacetime [58].

This conjecture appears more universal than the volume one because of the absence of the length scale in the definition of complexity, and the late time behaviour is the same of the volume case. On the other hand, the behaviour for intermediate times of the two proposals is different, which is a reason why it is interesting to investigate both of them.

[10] Various other similar versions exist, but they are all based on the Volume and Action proposals.

There are some minimal requirements that we ask complexity to satisfy. Based on dimensional grounds and on the observation that complexity is an extensive quantity, we require that the linear behaviour in time should have the rate

$$\frac{d\mathscr{C}}{dt} \sim TS, \tag{1.32}$$

being T the temperature of the black hole and S the entropy[11].

Moreover, extremal black holes are ground states and therefore static, which means that

$$\left(\frac{d\mathscr{C}}{dt}\right)_{\text{extr}} = 0. \tag{1.33}$$

This is also expected from the fact that extremal black holes usually have vanishing temperature.

Quantum complexity can access some informations that the entopy by itself cannot. First of all, from the gravity side, complexity should be able to access to regimes of the black hole evolution which are much longer than the thermalization time. We may also hope that an investigation of complexity for evaporating black holes can shed light on the information paradox: while the usual way to follow the process is by means of the Page curve for the entropy, the relation between the internal of the black hole and the Hawking radiation can be better understood in the context of complexity (in the spirit of ER=EPR interpretation [59]). In this sense, since complexity is an object that investigate the interior of the black hole, it goes in principle beyond the territory of entanglement entropy computations, whose holographic dual is given by the Ryu-Takayanagi curve which usually stays ouside the horizon. Another interesting topic that we can hope to better understand with complexity concerns the technique of bulk reconstruction. In particular, proposals like [60–62] aim to investigate the inside of a black hole and even part of the other asymptotic region by starting from one of the boundaries of the spacetime. We think that complexity can give some hints to tackle this kind of problems.

It is interesting to consider extensions of holography to spacetimes that are not asymptotically AdS. A non-trivial deformation of AdS_3 which only preserves the isometries $SL(2,\mathbb{R}) \times U(1)$ is given by Warped AdS_3. This spacetime is conjectured to be dual to a class of non-relativistic theories in 1+1 dimensions, called Warped Conformal Field Theories. They can be interpreted to be Lifshitz-invariant with dynamical exponent $z = \infty$ and in curved backgrounds they naturally couple to Newton-Cartan geometry. The entanglement entropy was studied in this context and an analog of the Cardy formula was found [63].

The conjectured duality is still far from being understood, in particular the field theory side is still in its infancy: it is then important to pursue the study of the subject in order to gain valuable insights when the duality involves non-AdS asymptotic. Furthermore explicit realizations of Warped Conformal Field Theories seem to be pathologic or at the brink of non-locality: they admit an infinite number of exactly marginal non-local deformations which must be tuned away [64]. In this

[11] This regime corresponds to late times in the semiclassical effective description where the black hole is studied; instead phenomena like the saturation of complexity are expected to arise after the Page time, when the effects of the Hawking radiation become important.

framework, it is useful to analyze quantities which do not require the introduction of an explicit action, like anomalies, entanglement entropy or complexity. We will test the holographic proposals for complexity in chapter 5 by computing the Volume and the Action for black holes in Warped AdS_3.

When the state on the boundary is mixed, *i.e.* we anchor the extremal slice to a subregion, holographic proposals for complexity similar to the case of entanglement entropy exist [65]. We will apply both these proposals for black holes in Warped AdS_3 in chapter 6 in a specific case where the subregion is taken to be one of the asymptotic boundaries. In chapter 7 we will further investigate the properties of subregion complexity=action for more general mixed states in the context of the BTZ black hole.

Conclusions and discussions on the results obtained in this thesis are collected in chapter 8. We put technical details of computations and conventions to the Appendices.

Part I

Non-relativistic quantum field theory

Chapter 2

Non-relativistic actions

In this chapter we will describe all the ingredients necessary for the investigation of the non-relativistic trace anomaly: a local version of the Galilean group (the Newton-Cartan geometry), how the Weyl transformations act on such a background, and the action for Galilean-invariant bosons and fermions. This material is intended as the set up necessary to undergo the investigation of the trace anomaly in explicit cases with the heat kernel technique that will be developed in chapter 3.

The discussion will be mostly referred to a general $d+1$ dimensional spacetime with non-relativistic symmetry, but in the derivation of the action for a fermion coupled to Newton-Cartan (NC) geometry we will focus on the case of interest, *i.e.* $2+1$ dimensions. While there are various methods to approach the problem of defining a local version of the Galilean group, we will focus on the Discrete Light-Cone Quantization (DLCQ) technique, which consists in the dimensional reduction of a $d+2$ dimensional spacetime along a null direction. The reason is that such procedure automatically implements all the non-relativistic symmetries[1], thus overcoming various problems that must be treated carefully with an intrinsic formulation without referring to a relativistic parent theory.

The NC geometry was first introduced as a tool to write newtonian gravity in a diffeomorphism-invariant fashion; for a review see [66]. Recently, works by Son and collaborators [25, 22, 67, 24] showed that it can be used as a powerful tool to study condensed matter systems with galilean invariance; the main idea is to use it as source for energy-momentum tensor for quantum field theory description of several condensed matter systems. Strongly-coupled system with Galilean invariance can be studied holographically [14, 68]; also in this approach the NC geometry is a natural formalism [69–71]. A theoretical approach to fermions invariant under the Galilean group was firstly faced in [72]; the coupling to a NC background by using the $c \to \infty$ limit was done in [25, 73], while other studies on fermions with the null reduction were performed in [74].

[1] This procedure is particularly convenient when dealing with the $U(1)$ gauge invariance and the local version of Galilean boosts (Milne boosts), which are very difficult to implement simultaneously.

2.1 Newton-Cartan geometry

We consider as a starting point a $d+2$ dimensional Lorentzian manifold whose coordinates are denoted with late capital latin indices x^M. In order to deal with spinors, we introduce early capital latin indices x^A to denote the tangent space, where the metric is locally flat. We introduce light-cone coordinates

$$x^{\pm} = \frac{x^{d+1} \pm x^0}{\sqrt{2}} \tag{2.1}$$

which allow to decompose the spacetime and tangent space structures as

$$\begin{aligned} x^M &= (x^-, x^\mu) = (x^-, x^+, x^i) \qquad (i = 1, \dots, d) \\ x^A &= (x^-, x^\alpha) = (x^-, x^+, x^a) \qquad (a = 1, \dots, d)\,. \end{aligned} \tag{2.2}$$

Latin lower-case letters refer to the spatial indices, while greek letters refer to the spacetime content of the $d+1$ dimensional non-relativistic theory. As for the relativistic parent, early and late letters refer to flat and curved indices, respectively.

Ambiguities can arise since the light-cone indices appear in the curved manifold and in the tangent space; in these cases we distinguish them by adding a subscript

$$\underset{(A)}{\pm}\,, \qquad \underset{(M)}{\pm}\,. \tag{2.3}$$

The null reduction is realized by compactifying x^- on a small circle of radius R. For convenience, we rescale $x^- \to x^-/R$ in such a way that the rescaled coordinate is adimensional. In order to keep the metric tensor adimensional, we also rescale $x^+ \to R x^+$. In the DLCQ dictionary, the light-cone direction x^+ after the compactification is interpreted as the time of the $d+1$ dimensional non-relativistic theory.

On a curved manifold, this operation is performed by taking the most general $d+2$ dimensional metric with null Killing vector

$$n^M = (1, \mathbf{0})\,, \qquad n_M = (0, n_\mu)\,, \tag{2.4}$$

which turns out to be of the form

$$G_{MN} = \begin{pmatrix} 0 & n_\nu \\ n_\mu & n_\mu A_\nu + n_\nu A_\mu + h_{\mu\nu} \end{pmatrix}, \qquad G^{MN} = \begin{pmatrix} A^2 - 2v\cdot A & v^\nu - h^{\nu\sigma}A_\sigma \\ v^\mu - h^{\mu\sigma}A_\sigma & h^{\mu\nu} \end{pmatrix}. \tag{2.5}$$

In order to parametrize all the degrees of freedom of a metric with the required isometry, we introduced the vector fields A_μ, v^μ and the semipositive-definite symmetric tensors $h_{\mu\nu}, h^{\mu\nu}$. Their interpretation as NC data will be clear soon.

We denote the determinant of the metric as

$$\sqrt{g} = \sqrt{-\det G_{AB}} = \sqrt{\det(h_{\mu\nu} + n_\mu n_\nu)}\,. \tag{2.6}$$

Being G_{MN} a non-degenerate metric on a pseudo-Riemannian manifold, we can define the usual Levi-Civita connection and we call $\mathscr{D}_M$ the covariant derivative associated to it.

The null reduction prescription also requires that any local field is decomposed as

$$\Phi(x^M) = \varphi(x^\mu) e^{imx^-}\,. \tag{2.7}$$

The quantities appearing in the decomposition of the metric (2.5) define the basic ingredients of a $d+1$ dimensional NC geometry: $n = n_\mu dx^\mu$ is a nowhere-vanishing one-form which locally gives the time direction, $h^{\mu\nu}$ is a semipositive definite symmetric tensor of rank d which satisfies the condition

$$n_\mu h^{\mu\nu} = 0 \tag{2.8}$$

and is interpreted as an inverse metric on spatial slices.

In analogy with the pseudo-Riemannian case, we would like to define a torsionless connection whose induced covariant derivative $\hat{D}_\mu$ preserves the constancy of the metric. In the case of NC geometry, a similar condition would be to require

$$\hat{D}_\mu n_\nu = 0\,, \qquad \hat{D}_\mu h^{\nu\rho} = 0\,. \tag{2.9}$$

A connection can be introduced by defining a velocity vector v^μ subject to the constraint

$$n_\mu v^\mu = 1\,, \tag{2.10}$$

and a covariant symmetric tensor $h_{\mu\nu}$ which satisfies

$$h^{\mu\rho} h_{\rho\nu} = \delta^\mu_\nu - v^\mu n_\nu \equiv P^\mu_\nu\,, \qquad h_{\mu\nu} v^\nu = 0\,, \tag{2.11}$$

where P^μ_ν is the projector onto spatial directions.

However, it turns out that the constancy of $(n_\mu, h^{\mu\nu})$ can be fulfilled only by introducing a non-vanishing torsion in the $d+1$ dimensional connection, and furthermore the covariant derivative is determined only up to a two-form F. More precisely, the Christoffel symbol can be taken to be

$$\hat{\Gamma}^\mu_{\nu\rho} = v^\mu \partial_\rho n_\nu + \frac{1}{2} h^{\mu\sigma}(\partial_\nu h_{\rho\sigma} + \partial_\rho h_{\nu\sigma} - \partial_\sigma h_{\nu\rho}) + h^{\mu\sigma} n_{(\nu} F_{\rho)\sigma}\,, \tag{2.12}$$

which has a purely temporal torsion. Moreover, it is not restrictive to take the two-form F to be close, which allows to locally define a gauge connection such that $F = dA$. This quantity enters the $d+2$ dimensional metric on the Lorentzian manifold and is naturally associated to the $U(1)$

mass or particle number, which is a conserved quantity in non-relativistic theories. The gauge transformations of the field A_μ are naturally interpreted from the $d+2$ dimensional point of view as additive reparametrizations along the null direction x^-.

The ambiguity in the definition of the connection is related to the fact that the velocity vector, the covariant spatial metric and the gauge connection are not uniquely defined. The following set of transformations (called Milne boosts) leaves the metric in the form[2] (2.5)

$$\begin{aligned} v'^\mu &= v^\mu + h^{\mu\nu}\psi_\nu \\ h'_{\mu\nu} &= h_{\mu\nu} - (n_\mu P^\rho_\nu + n_\nu P^\rho_\mu)\psi_\rho + n_\mu n_\nu h^{\rho\sigma}\psi_\rho\psi_\sigma\,, \\ A'_\mu &= A_\mu + P^\rho_\mu\psi_\rho - \frac{1}{2}n_\mu h^{\alpha\beta}\psi_\alpha\psi_\beta\,, \end{aligned} \tag{2.13}$$

where $\psi = \psi_\mu dx^\mu$ is a one-form parametrizing the transformation, while n_μ and $h^{\mu\nu}$ are invariant. There is not a convenient intrinsic $d+1$ dimensional way to build Milne boost-invariant quantities; the invariants that we can build by direct computation are

$$\begin{aligned} &v^\mu_A = v^\mu - h^{\mu\xi}A_\xi\,, \qquad (h_A)_{\mu\nu} = h_{\mu\nu} + A_\mu n_\nu + A_\nu n_\mu\,, \qquad \phi_A = A^2 - 2v\cdot A\,, \\ &(Q_A)_{\mu\nu\sigma} = (\partial_\mu(h_A)_{\nu\sigma} + \partial_\nu(h_A)_{\mu\sigma} - \partial_\sigma(h_A)_{\mu\nu})\,, \end{aligned} \tag{2.14}$$

where $A^2 = h^{\mu\nu}A_\mu A_\nu$ and $A\cdot v = v^\mu A_\mu$. The subscript A is a notation to identify the invariance of the object under Milne boosts.

It is not possible to find a $d+1$ dimensional connection which is invariant both under $U(1)$ gauge transformations and Milne boosts, but only under one of them. From the point of view of the relativistic parent, this is the statement that the Christoffel symbol is not invariant under reparametrizations along the null direction x^-, which represent the gauge variation under a local $U(1)$ transformation of the system. Moreover, it is important to observe that the Christoffel symbol in eq. (2.12) is not the Levi-Civita connection corresponding to the metric (2.5), which instead is torsionless and given by

$$\begin{aligned} &\Gamma^-_{--} = \Gamma^\mu_{--} = 0\,, \qquad \Gamma^-_{\mu-} = \frac{1}{2}v^\sigma_A\tilde{F}_{\mu\sigma}\,, \qquad \Gamma^\mu_{\nu-} = \frac{1}{2}h^{\mu\sigma}\tilde{F}_{\nu\sigma}\,, \\ &\Gamma^-_{\mu\nu} = \frac{1}{2}\left(\phi_A(\partial_\mu n_\nu + \partial_\nu n_\mu) + v^\sigma_A(Q_A)_{\mu\nu\sigma}\right)\,, \\ &\Gamma^\mu_{\nu\rho} = \frac{1}{2}\left(v^\mu_A(\partial_\nu n_\rho + \partial_\rho n_\nu) + h^{\mu\sigma}(Q_A)_{\nu\rho\sigma}\right)\,. \end{aligned} \tag{2.15}$$

In particular, the relation with the $d+1$ dimensional Cristopphel symbol is given by

$$\Gamma^\mu_{\nu\rho} = \hat{\Gamma}^\mu_{(\nu\rho)} + \frac{1}{2}h^{\mu\sigma}(Q_A)_{\nu\rho\sigma}\,, \tag{2.16}$$

while $\hat{\Gamma}^\mu_{[\nu\rho]}$ is not directly related to $\Gamma^\mu_{\nu\rho}$.

[2] Modified Milne transformation may also be considered, but then the null reduction trick can not be used (see e.g. [75]).

The frame fields defining the locally flat metric in $d+1$ dimensions can be derived as well from the $d+2$ dimensional relativistic framework. The tangent space in light-cone coordinates is equipped with the metric

$$G_{AB} = G^{AB} = \begin{pmatrix} 0 & 1 & 0 & \dots & 0 \\ 1 & 0 & 0 & \dots & 0 \\ 0 & 0 & 1 & \dots & 0 \\ \dots & \dots & \dots & \dots & \dots \\ 0 & 0 & 0 & 0 & 1 \end{pmatrix}, \tag{2.17}$$

and this induces the usual definition of the $d+2$ dimensional vielbein with the relations

$$\begin{aligned} G_{MN} &= e^{A}{}_{M} G_{AB} e^{B}{}_{N}, \qquad & G_{AB} &= e^{M}{}_{A} G_{MN} e^{N}{}_{B}, \\ e^{A}{}_{M} e^{M}{}_{B} &= \delta^{A}{}_{B}, \qquad & e^{M}{}_{A} e^{A}{}_{N} &= \delta^{M}{}_{N}. \end{aligned} \tag{2.18}$$

The corresponding $d+1$ dimensional vielbein defined by dimensional reduction is not unique, but we take the following convenient choice

$$e^{A}{}_{M} = \begin{pmatrix} e^{-}{}_{M} \\ e^{+}{}_{M} \\ e^{a}{}_{M} \end{pmatrix} = \begin{pmatrix} e^{-}{}_{-} & e^{-}{}_{\mu} \\ e^{+}{}_{-} & e^{+}{}_{\mu} \\ e^{a}{}_{-} & e^{a}{}_{\mu} \end{pmatrix} = \begin{pmatrix} 1 & A_{\mu} \\ 0 & n_{\mu} \\ \mathbf{0} & e^{a}{}_{\mu} \end{pmatrix}. \tag{2.19}$$

Using the consistency relations

$$e^{M}{}_{A} e^{B}{}_{M} = \delta_{A}{}^{B}, \qquad e^{A}{}_{M} e^{N}{}_{A} = \delta_{M}{}^{N}, \tag{2.20}$$

we can derive a simple expression for the inverse vielbein

$$e^{M}{}_{A} = \begin{pmatrix} e^{M}{}_{-} & e^{M}{}_{+} & e^{M}{}_{a} \end{pmatrix} = \begin{pmatrix} e^{-}{}_{-} & e^{-}{}_{+} & e^{-}{}_{a} \\ e^{\mu}{}_{-} & e^{\mu}{}_{+} & e^{\mu}{}_{a} \end{pmatrix} = \begin{pmatrix} 1 & -v^{\sigma} A_{\sigma} & -h^{\nu\sigma} A_{\sigma} e^{a}_{\nu} \\ \mathbf{0} & v^{\mu} & h^{\mu\nu} e^{a}_{\nu} \end{pmatrix}. \tag{2.21}$$

The previous construction of the Newton-Cartan geometry in $d+1$ dimensions from a relativistic parent allows to obtain a structure which is automatically invariant under

- Diffeomorphisms in the $d+1$ dimensional spacetime
- $U(1)$ gauge transformations
- Milne boosts

In fact, diffeomorphisms along the $d+1$ dimensions of the non-relativistic theory are obviously inherited from the diffeomorphisms of the higher dimensional theory, while the gauge transformations come from coordinate reparametrizations along the x^{-} direction. Furthermore, Milne boosts invariance is built-in from the choice of the metric (2.5).

For these reasons, it is convenient to build tensors and scalars starting using the null reduction: the non-relativistic symmetries are automatically implemented and the classification of terms entering the trace anomaly is easier and under control.

2.2 Null reduction of the Klein-Gordon action

We apply the null reduction prescription to the case of a relativistic free scalar in a curved background. The action with minimal coupling to gravity is given by

$$S = \int d^{d+2}x \sqrt{-\det G_{MN}} \left(-G^{MN}\partial_M\Phi^\dagger\partial_N\Phi - \xi R\Phi^\dagger\Phi\right) . \tag{2.22}$$

If we take the metric (2.5) and the decomposition of fields (2.7), we obtain the $d+1$ dimensional non-relativistic action

$$S = \int d^{d+1}x \sqrt{g} \left\{ imv^\mu \left(\varphi^\dagger D_t\varphi - D_\mu\varphi^\dagger\varphi\right) - h^{\mu\nu}D_\mu\varphi^\dagger D_\nu\varphi - \xi R\varphi^\dagger\varphi \right\} , \tag{2.23}$$

where the derivative is covariant only with respect to the gauge connection

$$D_\mu\varphi = \partial_\mu\varphi - imA_\mu\varphi . \tag{2.24}$$

We can get more a better understanding of the system by considering the case of flat space

$$n_\mu = (1,\mathbf{0}) , \quad h_{\mu\nu} = \mathrm{diag}(0,\mathbf{1}) , \quad v^\mu = (1,\mathbf{0}) \tag{2.25}$$

and $A_\mu = 0$, which brings the action to the form

$$S = \int d^{d+1}x \left(2im\varphi^\dagger\partial_t\varphi - |\partial_i\varphi|^2\right) = \int d^{d+1}x\, \varphi^\dagger \left(2im\partial_t + \partial_i^2\right)\varphi . \tag{2.26}$$

As expected, the Euler-Lagrange equations of motion are immediately identified with the Schrödinger equation for the free scalar field

$$i\partial_t\varphi = -\frac{1}{2m}\partial_i^2\varphi . \tag{2.27}$$

If we add a non-vanishing gauge field $A_\mu \neq 0$ to the system, the result is simply the action (2.26) with the minimal coupling replacement $\partial_\mu \to D_\mu$.

Finally, we consider the case where the gauge field is set to 0 and the background is curved. For future analysis it is convenient to write the action as a differential operator of a quadratic form using integration by parts to get

$$S = \int d^{d+1}x \sqrt{g}\,\varphi^\dagger \left\{ imv^\mu\partial_\mu\varphi + \frac{im\partial_\mu(\sqrt{g}v^\mu\varphi)}{\sqrt{g}} + \frac{\partial_\mu(\sqrt{g}h^{\mu\nu}\partial_\nu\varphi)}{\sqrt{g}} - \xi R\varphi \right\} . \tag{2.28}$$

2.3 Null reduction of the Dirac action

The way fermions are treated in Quantum Mechanics (QM) is very different from Quantum Field Theory (QFT): while in the latter case they satisfy the first-order Dirac equation (contrarily to the second-order Klein-Gordon equation), in the former case they satisfy the same Schrödinger equation as bosons. Moreover, properties such as spin are attached *by hands*, contrarily to the machinery of the Clifford algebra in the QFT treatment. This very different behaviour seems a consequence of the non-relativistic nature of QM, which describes theories at low energies and speeds, but we can see that it is instead a consequence of the framework of first quantization.

Following [72], it is possible to find a first-order differential equation for fermions inspired by the Dirac's method used for relativistic QFT. This procedure allows to derive from first principles the same result which is found from the $c \to \infty$ limit of the Dirac equation, where the Weyl spinors are recognized to split into an auxiliary and a dynamical doublet. While they are mixed in the Dirac equation, when integrating out the auxiliary Weyl fermion we obtain a single Schrödinger equation for the dynamical one.

In the spirit of this procedure, and following the null reduction prescription, we are led to consider the $d+2$ dimensional Dirac action as the starting point. The Dirac operator is expressed as

$$\not{D} = \gamma^M D_M = \gamma^A e_A^M D_M \,, \tag{2.29}$$

where the covariant derivative contains

$$D_M \Psi = \left(\partial_M + \frac{1}{4} \omega_{MAB} \gamma^{AB} \right) \Psi = \left(\partial_M + \frac{1}{8} \omega_{MAB} [\gamma^A, \gamma^B] \right) \Psi \,. \tag{2.30}$$

Conventions about the Dirac matrices in light-cone coordinates and the spin connection ω_{MAB} are summarized in Appendix A.

The Dirac action in curved spacetime is not uniquely defined, but there are various prescriptions which differ when the connection is torsionful. By taking the torsionless Levi-Civita connection in $d+2$ dimension, the Lagrangian can be made hermitian by means of partial integration, and it is not ambiguous to consider the action

$$S = \int d^4x \sqrt{g}\, i \bar{\Psi} \not{D} \Psi \,. \tag{2.31}$$

From now on, we will consider specifically the case of a null reduction from $3+1$ dimensions to get a $2+1$ dimensional non-relativistic theory. In order to perform the DLCQ technique, we take the metric (2.5) as the background and we specify the components of the Dirac spinor in $3+1$ dimensions

$$\Psi = \begin{pmatrix} \Psi_L \\ \Psi_R \end{pmatrix} . \tag{2.32}$$

Since we consider a massless Dirac action in $3+1$ dimensions, the Weyl spinors decouple and we can restrict our analysis to the action for the left-handed part

$$S_L = \int d^4x\sqrt{g}\,\mathscr{L}_W = \int d^4x\sqrt{g}\,i\Psi_L^\dagger\bar{\sigma}^A D_A\Psi_L\,. \tag{2.33}$$

This technicism allows to obtain the correct number of degrees of freedom to describe the non-relativistic fermion: indeed, the Dirac spinor in $2+1$ dimensions only contains 2 complex components as opposed to the 4 components of the higher-dimensional parent. In this way the dictionary of null reduction requires a decomposition of the relativistic field Ψ_L into a non-relativistic field times a phase along the compact direction

$$\Psi_L(x^M) = \begin{pmatrix}\xi(x^\mu)\\ \chi(x^\mu)\end{pmatrix} e^{imx^-}\,, \tag{2.34}$$

where ξ,χ are complex numbers.

We decompose the covariant derivative into the light-cone and the spatial directions

$$\begin{aligned}
D_{\underset{(A)}{-}} &= e^M_{\underset{(A)}{-}} D_M = \begin{pmatrix}1 & \mathbf{0}\end{pmatrix}\begin{pmatrix}D_{\underset{(M)}{-}}\\ D_\mu\end{pmatrix} = D_{\underset{(M)}{-}}\,,\\
D_{\underset{(A)}{+}} &= e^M_{\underset{(A)}{+}} D_M = \begin{pmatrix}-v^\sigma A_\sigma & v^\mu\end{pmatrix}\begin{pmatrix}D_{\underset{(M)}{-}}\\ D_\mu\end{pmatrix} = -v^\sigma A_\sigma D_{\underset{(M)}{-}} + v^\mu D_\mu\,,\\
D_a &= e^M_a D_M = \begin{pmatrix}-e^\sigma_a A_\sigma & e^\mu_a\end{pmatrix}\begin{pmatrix}D_{\underset{(M)}{-}}\\ D_\mu\end{pmatrix} = -e^\sigma_a A_\sigma D_{\underset{(M)}{-}} + e^\mu_a D_\mu\,.
\end{aligned} \tag{2.35}$$

In this way we decompose the sum in eq. (2.33) as

$$\begin{aligned}
\mathscr{L}_W = {} & ie^{-imx^-}\begin{pmatrix}\xi^\dagger & \chi^\dagger\end{pmatrix}\bar{\sigma}^- D_{\underset{(A)}{-}}\left[\begin{pmatrix}\xi\\ \chi\end{pmatrix}e^{imx^-}\right] + ie^{-imx^-}\begin{pmatrix}\xi^\dagger & \chi^\dagger\end{pmatrix}\bar{\sigma}^+ D_{\underset{(A)}{+}}\left[\begin{pmatrix}\xi\\ \chi\end{pmatrix}e^{imx^-}\right] +\\
& + ie^{-imx^-}\begin{pmatrix}\xi^\dagger & \chi^\dagger\end{pmatrix}\sigma^a e^M_a D_M\left[\begin{pmatrix}\xi\\ \chi\end{pmatrix}e^{imx^-}\right],
\end{aligned} \tag{2.36}$$

and the explicit expressions of the covariant derivatives give

$$\begin{aligned}
\mathscr{L}_W = {} & -\sqrt{2}m\xi^\dagger\xi - \sqrt{2}i\chi^\dagger\hat{D}_t\chi + i\chi^\dagger(\hat{D}_1+i\hat{D}_2)\xi + i\xi^\dagger(\hat{D}_1-i\hat{D}_2)\chi +\\
& + \frac{i}{4}\begin{pmatrix}\xi^\dagger & \chi^\dagger\end{pmatrix}(\bar{\sigma}^+ v^\mu + \sigma^a e^\mu_a)\omega_{\mu AB}\sigma^{AB}\begin{pmatrix}\xi\\ \chi\end{pmatrix}\\
& + \frac{i}{4}\begin{pmatrix}\xi^\dagger & \chi^\dagger\end{pmatrix}\left(\bar{\sigma}^- - v^\sigma A_\sigma\bar{\sigma}^+ - \sigma^a e^\sigma_a A_\sigma\right)\omega_{\underset{(M)}{-}AB}\sigma^{AB}\begin{pmatrix}\xi\\ \chi\end{pmatrix}.
\end{aligned} \tag{2.37}$$

In this formula we introduced derivatives which are covariant with respect to the local U(1) symmetry

$$\hat{D}_t = v^\mu \left(\partial_\mu - imA_\mu\right), \qquad \hat{D}_a = e^\mu_{\ a}\left(\partial_\mu - imA_\mu\right). \tag{2.38}$$

In order to write explicitly the last two lines of eq. (2.37), we need the use the precise expression of the components of the spin connection. In fact the sum implicitly contains a summation over spinorial objects, whose matricial content depends from the particular Pauli matrix we are summing over. Using the results in Appendix A we can re-write the Lagrangian in the compact form

$$\mathscr{L}_W = \begin{pmatrix}\xi^\dagger & \chi^\dagger\end{pmatrix}\begin{pmatrix}A & B\\ C & D\end{pmatrix}\begin{pmatrix}\xi\\ \chi\end{pmatrix}, \tag{2.39}$$

where

$$\begin{aligned} A &= -\sqrt{2}\left(m+\frac{1}{4}\tilde{F}_{\mu\nu}e^\mu_1 e^\nu_2\right),\\ B &= (e^\mu_1 - ie^\mu_2)(i\tilde{D}_\mu + \frac{i}{4}\tilde{F}_{\mu\nu}v^\nu), \qquad C = (e^\mu_1 + ie^\mu_2)(i\tilde{D}_\mu + i\frac{3}{4}\tilde{F}_{\mu\nu}v^\nu),\\ D &= \sqrt{2}\left[v^\mu(-i\tilde{D}_\mu - \frac{i}{4}h^{\rho\sigma}\partial_\mu h_{\rho\sigma}) - \frac{i}{2}(v^\mu v^\nu \partial_\mu n_\nu + \partial_\mu v^\mu) - \frac{1}{4}F_{\mu\nu}e^\mu_1 e^\nu_2\right]. \end{aligned} \tag{2.40}$$

Here $\tilde{D}_\mu$ denotes a covariant derivative which includes only the gauge and the curved space spin connection $\tilde{\omega}_{\mu ab}$ built with the spatial tetrad e^a_μ; this derivative acts on the matter fields ξ and χ as follows

$$\tilde{D}_\mu\xi = \left[\partial_\mu + \frac{i}{2}\tilde{\omega}_{\mu 12} - imA_\mu\right]\xi, \qquad \tilde{D}_\mu\chi = \left[\partial_\mu - \frac{i}{2}\tilde{\omega}_{\mu 12} - imA_\mu\right]\chi, \tag{2.41}$$

where

$$\tilde{\omega}_{\mu ab} = \frac{1}{2}\left(e^\nu_{\ a}\left(\partial_\mu e^b_{\ \nu} - \partial_\nu e^b_{\ \mu}\right) - e^\nu_{\ b}\left(\partial_\mu e^a_{\ \nu} - \partial_\nu e^a_{\ \mu}\right) - e^\nu_{\ a}e^\rho_{\ b}e^c_{\ \mu}\left(\partial_\nu e^c_{\ \rho} - \partial_\rho e^c_{\ \nu}\right)\right). \tag{2.42}$$

It is important to observe that the field ξ is auxiliary and can be integrated out by means of the Euler-Lagrange equations of motion

$$\xi = \frac{i(e^\mu_1 - ie^\mu_2)\left(\tilde{D}_\mu + \frac{1}{4}v^\nu\tilde{F}_{\mu\nu}\right)\chi}{\sqrt{2}\left(m + \frac{\tilde{F}_{\mu\nu}e^\mu_1 e^\nu_2}{4}\right)}. \tag{2.43}$$

Replacing it into the action in eq. (2.39), we could obtain a cumbersome Lagrangian written only in terms of χ. We can have a better understanding of the system by considering some limiting cases.

2.3.1 Flat spacetime

The simplest limit to consider is the case where the background is flat, described by eq. (2.25) plus $A_\mu = 0$. In this case the covariant derivative reduces to a simple partial derivative and the action for

the left-handed Weyl spinor becomes

$$\mathscr{L}_W = -\sqrt{2}m\xi^\dagger\xi - \sqrt{2}i\chi^\dagger\partial_t\chi + i\chi^\dagger(\partial_1 + i\partial_2)\xi + i\xi^\dagger(\partial_1 - i\partial_2)\chi\,. \tag{2.44}$$

The equations of motion are

$$\xi = \frac{i}{m}\frac{1}{\sqrt{2}}(\partial_1 - i\partial_2)\chi\,, \qquad \partial_t\chi = \frac{1}{\sqrt{2}}(\partial_1 + i\partial_2)\xi\,. \tag{2.45}$$

In particular, the auxiliary field ξ can be easily integrated out, giving the Schrödinger equation for the dynamical component χ, with action

$$S = \int d^3x \left(i\chi^\dagger\partial_t\chi - \frac{1}{2m}|\partial_i\chi|^2 \right). \tag{2.46}$$

The set of equations of motion and the Lagrangian obtained via null reduction from the $3+1$ dimensional right-handed Weyl spinor are analog to this result, giving another Schrödinger equation decoupled from the left-handed component.

2.3.2 Gyromagnetic ratio

The next limit that we consider is flat spacetime (2.25), plus a non-trivial gauge field $A_\mu \neq 0$ which accounts for a generic particle number background[3]. In this case the covariant derivative contains a gauge connection which arises from the presence of the non-trivial background gauge field in the metric (2.5). Specializing the general formulas in Appendix A to this case, we find that the non-vanishing components of the spin connection are

$$\omega_{++i} = -F_{0i} = -E_i\,, \qquad \omega_{i+j} = -\frac{1}{2}F_{ij} = -\frac{B}{2}\,, \qquad \omega_{0ij} = -\frac{1}{2}F_{ij} = -\frac{B}{2}\,. \tag{2.47}$$

The action for the dynamical field χ, obtained by integrating out the auxiliary component, is given by

$$S = \int d^3x \left[\frac{i}{2}\chi^\dagger \overleftrightarrow{\partial_t}\chi - \frac{1}{2m}\delta^{ij}(D_i\chi)^\dagger(D_j\chi) - \frac{1}{4}B\chi^\dagger\chi \right]. \tag{2.48}$$

This expression allows to extract the gyromagnetic ratio of a non-relativistic fermion. First of all, the analogous computation for the decoupled right-handed component gives as the only difference an opposite sign for the $B\chi^\dagger\chi$ coupling. Then the generic form of the gyromagnetic coupling in $2+1$ dimensions is

$$\mp g\frac{q}{4m}B\varphi^\dagger\varphi \tag{2.49}$$

[3] More correctly, this $U(1)$ symmetry in the presence of different species of fields ψ_i corresponds to the mass, because in the minimal coupling it enters the action as $-\sum_i m_i A_0|\psi_i|^2$, where m_i is the mass of the field ψ_i. In the presence of a single species, mass and particle number are proportional to each other. For simplicity, we refer to this $U(1)$ symmetry as particle number.

where q is the charge and the $\mp$ sign refers to left or right-handed spinor, respectively. Since in our conventions the charge associated to the particle number symmetry is $q = m$, we find a gyromagnetic ratio $g = 1$. This is consistent with the form of the Milne boost transformations which come from null reduction, which are valid for $g = 2s$ [25]: this is the simplest way in which Galilean covariance can be realized.

2.4 Non-relativistic Weyl invariance

The actions for the free non-relativistic bosons and fermions that we derived via null reduction are not only invariant under the Galilean group, but also under dilatations and special conformal transformations, which enlarge the symmetries to the Schrödinger group. While this is true in the limiting case of flat space, we expect that the system is also invariant under the local version of this group, obtained with the minimal coupling of the matter fields to a Newton-Cartan background.

In this generic situation, we need to define Weyl transformations for the objects in the curved geometry. In the Lifshitz case (1.9) we consider the variations

$$n_\mu \to e^{z\sigma} n_\mu \,, \qquad v^\mu \to e^{-z\sigma} v^\mu \,, \qquad A_\mu \to e^{(2-z)\sigma} A_\mu \,, \tag{2.50}$$

$$\sqrt{g} \to e^{(d+z)\sigma} \sqrt{g} \,, \qquad h_{\mu\nu} \to e^{2\sigma} h_{\mu\nu} \,, \qquad h^{\mu\nu} \to e^{-2\sigma} h^{\mu\nu} \,, \tag{2.51}$$

where $\sigma = \sigma(x^\mu)$ is a spacetime-dependent quantity.

In particular, the Schrödinger case is achieved when $z = 2$ with corresponding Weyl variations of the NC data given by

$$n_\mu \to e^{2\sigma} n_\mu \,, \qquad v^\mu \to e^{-2\sigma} v^\mu \,, \qquad h_{\mu\nu} \to e^{2\sigma} h_{\mu\nu} \qquad h^{\mu\nu} \to e^{-2\sigma} h^{\mu\nu} \,. \tag{2.52}$$

The action (2.23) for the free non-relativistic boson can be seen to be invariant under this set of transformation rules.

A Weyl transformation on the Newton-Cartan background is equivalent to a Weyl transformation in the extra-dimensional metric in eq. (2.5) which is independent from the x^- coordinate:

$$n^A D_A \sigma = 0 \,. \tag{2.53}$$

The transformations in the set (2.52) can also be derived from the null reduction method by requiring

$$G_{MN} \to e^{2\sigma} G_{MN} \,, \qquad G^{MN} \to e^{-2\sigma} G^{MN} \,, \qquad n^A \to n^A \,, \qquad n_A \to e^{2\sigma} n_A \,. \tag{2.54}$$

In fact, this transformation of the DLCQ metric is exactly the same which is required in the context of relativistic conformal transformations.

We can also find a corresponding set of variations for the frame fields

$$\begin{aligned} e^{-}_{M} &\to e^{-}_{M}\,, \qquad e^{+}_{M}\to e^{+}_{M}e^{2\sigma}\,, \qquad e^{a}_{M}\to e^{a}_{M}e^{\sigma} \\ e^{M}_{-} &\to e^{M}_{-}\,, \qquad e^{M}_{+}\to e^{M}_{+}e^{-2\sigma}\,, \qquad e^{M}_{a}\to e^{M}_{a}e^{-\sigma}\,, \end{aligned} \tag{2.55}$$

and consequently for the spin connection

$$\begin{aligned} \omega_{-ab} &\to \omega_{-ab}\,, \qquad \omega_{-+a}\to e^{-\sigma}(\omega_{-+a}+e^{\nu}_{a}\partial_{\nu}\sigma)\,, \qquad \omega_{\mu-a}\to e^{\sigma}(\omega_{\mu-a}+n_{\mu}e^{\nu}_{a}\partial_{\nu}\sigma)\,, \\ \omega_{\mu-+} &\to \omega_{\mu-+}-\partial_{\mu}\sigma+n_{\mu}v^{\nu}\partial_{\nu}\sigma\,, \qquad \omega_{\mu+a}\to e^{-\sigma}\left(\omega_{\mu+a}+\left(-v^{\nu}e^{a}_{\mu}+e^{\nu}_{a}A_{\mu}\right)\partial_{\nu}\sigma\right)\,, \\ \omega_{\mu ab} &\to \omega_{\mu ab}+\left(e^{a}_{\mu}e^{\nu}_{b}-e^{b}_{\mu}e^{\nu}_{a}\right)\partial_{\nu}\sigma\,. \end{aligned} \tag{2.56}$$

It is evident that the various components of the frame fields and of the spin connection change differently under Weyl transformations. A similar situation happens for the components of the left-handed Weyl spinor, contrarily to the relativistic case. The transformation of the (ξ,χ) components is as follows:

$$\xi\to e^{-2\sigma}\xi\,, \qquad \chi\to e^{-\sigma}\chi\,. \tag{2.57}$$

This can be derived from dimensional analysis in the flat case, see eq. (2.45): in units of length, $[\varphi]=-1$ and $[\chi]=-2$. In the case of a Dirac fermion

$$\Psi=\begin{pmatrix}\xi_{L}\\ \chi_{L}\\ \chi_{R}\\ \xi_{R}\end{pmatrix}\,, \qquad \text{length dimensions are} \qquad [\Psi]=\begin{pmatrix}-2\\ -1\\ -1\\ -2\end{pmatrix}\,. \tag{2.58}$$

The different length dimension of the components arises due to the particular behviour of the tetrads, and because one of them is auxiliary and the other is dynamical.

We note that this Weyl weight choice is crucial in order to assign to the term $\bar{\Psi}\Psi$ a well-defined Weyl weight. A conformal coupling term such as $R\bar{\Psi}\Psi$ would have mass dimension 5, spoiling conformal invariance.

It is possible to check that the action in eq. (2.37) for the non-relativistic free fermion is Weyl invariant, provided that eqs (2.57) and (2.43) are used. One can also verify that this is consistent with eq. (2.43): if we insert $\chi\to e^{-\sigma}\chi$, we indeed find that $\xi\to e^{-2\sigma}\xi$.

2.5 General classification of the non-relativistic trace anomaly

In this section we consider the problem of classifying the terms entering the trace anomaly for a Schrödinger-invariant field theory in 2+1 dimensions coupled to a NC geometry. We will briefly review the procedure to determine such classification and we will summarize the results found in the literature [15–18].

The general form of the trace anomaly on a curved background can be found by solving a cohomological problem. The following steps need to be applied:

1. We parametrized the most generic Weyl variation as

$$\delta_\sigma W = \int d^{d+1}x\sqrt{g}\,\sigma(x)\mathscr{A}(x)\,, \tag{2.59}$$

   where $\mathscr{A}$ is a scalar built from NC data which is invariant under the non-relativistic symmetries: diffeomorphisms, gauge transformations and Milne boosts.

2. We express the most general expression for $\mathscr{A}$ as a linear combination of a basis of independent terms.

3. We impose the Wess-Zumino consistency conditions

$$\Delta^{\rm WZ}_{\sigma_1\sigma_2} W = \delta_{\sigma_1(x)}\int d^4y\sqrt{-G}\,\mathscr{A}(y)\sigma_2(y) - \delta_{\sigma_2(x)}\int d^4y\sqrt{-G}\,\mathscr{A}(y)\sigma_1(y) = 0\,. \tag{2.60}$$

4. We eliminate from the basis the terms that are exact in the cohomology (*i.e.* they can be written as the Weyl variation of other terms in the basis).

The power of the null reduction method is that we can apply this procedure using the tensors in the relativistic parent theory, and the scalars built in this way automatically satisfy the invariances required in the point 1 of the previous procedure. While we can take various results from the 3+1 dimensional relativistic case[4], here the important difference stays in the additional vector n_M.

It turns out that the space of expressions with uniform scaling dimension and invariant under the symmetries of the non-relativistic theory can be divided into distinct sectors invariant under Weyl transformations. These sectors are distinguished by the number of appearances of n : all the terms with a fixed number of factors of n transform into each other under Weyl transformations. The cohomological problem can be studied separately for each sector.

The classification of the trace anomaly changes drastically if a causal structure on the NC geometry is required. This technically amounts to imposing the Frobenius condition on the one-form identifying the local time direction

$$n\wedge dn = 0\,, \tag{2.61}$$

which defines an integrable structure.

If Frobenius condition is applied, the possible scalars entering the anomaly collapse to only one sector, and then they compose a finite set. Unfortunately, the Euler density E_4 can be written as a linear combination of other DLCQ scalars, and type A anomalies disappear, precluding the existence of an $a-$theorem. The only independent term can be chosen to be the null reduction of the squared

[4]In fact the scalars built from the metric and the corresponding Levi-Civita connection are formally the same of the usual relativistic case. We only need to remark that curvature invariants secretely contain the NC data, since they appear in the metric used for the null reduction.

Weyl tensor, plus scheme-dependent scalars that can be eliminated with an appopriate choice of counterterms

$$\mathscr{A} = bW^2_{MNPQ} + \mathscr{A}_{\rm ct}\,. \tag{2.62}$$

If the Frobenius condition is not required, there are still infinite sectors and we can study them separately. There is a minimal sector without appearances of n which is the null reduction of the 3+1 dimensional relativistic case

$$\mathscr{A}^0 = aE_4 - cW^2_{MNPQ} + \mathscr{A}_{\rm ct}\,, \tag{2.63}$$

The coefficient of the Euler density is then a good candidate for a non-relativistic version of the $a-$theorem.

Instead it is possible to prove that the next sector with a single appearance of n has vanishing trace anomaly

$$\mathscr{A}^1 = 0\,. \tag{2.64}$$

The situation in the successive sectors is still not clear: by dimensional analysis, for each n_M we can add one extra DLCQ covariant derivatives[5] D_M. Examples of such terms which can enter the anomaly are

$$n^M D_M R_{NP} R^{NP}\,, \qquad R_{MNPQ} R^{MNPS} R^{Q}{}_{TSU} n^T n^U\,. \tag{2.65}$$

However, the cohomological problem in these sectors is not studied and then we do not know if type A anomalies appear.

2.6 Trace anomaly near a flat background

The general procedure for the classification of the trace anomaly allows to find a basis of curvature invariants, but does not identify the coefficients with which they appear in specific systems, in particular we do not know if some terms do not enter at all the trace anomaly. In principle, it is also possible that all the coefficients of the linear combination vanish and that the trace anomaly is exactly zero! In order to avoid or to investigate this possibility, we will study in chapter 3 the trace anomaly in specific cases with the heat kernel technique, a method which gives precisely the coefficients of the terms entering the trace anomaly. Tipically the heat kernel procedure is performed going nearby flat space; here we show how to treat variations of the background fields of the NC geometry.

Due to the conditions (2.8) and (2.10), arbitrary variations of the geometric data are not allowed but we can parametrize them with an arbitrary δn_μ, and the transverse perturbations δu^μ and $\delta\tilde{h}^{\mu\nu}$ such that

$$\delta u^\mu n_\mu = 0\,, \qquad \delta\tilde{h}^{\mu\nu} n_\nu = 0\,. \tag{2.66}$$

[5] Since the DLCQ Riemann tensor is the commutator of two covariant derivatives, two n_M are needed in order to buy a curvature

This means that the variation of the metric fields are

$$\delta n_\mu\,, \qquad \delta v^\mu = -v^\mu v^\alpha \delta n_\alpha + \delta u^\mu\,, \qquad \delta h^{\mu\nu} = -v^\mu \delta n^\nu - \delta n^\mu v^\nu - \delta\tilde{h}^{\mu\nu}\,. \tag{2.67}$$

If we specialize to a variation around flat space, which is the case of interest for the heat kernel expansion, these variations take the form

$$\begin{aligned} n_\mu &= (1+\delta n_0, \delta n_i)\,, \qquad v^\mu = (1-\delta n_0, \delta u_i)\,, \qquad \delta\tilde{h}^{0i} = 0\,, \\ h_{\mu\nu} &= \begin{pmatrix} 0 & -\delta u_i \\ -\delta u_i & \delta_{ij}+\delta\tilde{h}_{ij} \end{pmatrix}, \qquad h^{\mu\nu} = \begin{pmatrix} 0 & -\delta n_i \\ -\delta n_i & \delta_{ij}-\delta\tilde{h}_{ij} \end{pmatrix}, \end{aligned} \tag{2.68}$$

which can be written in terms of the parent metric as

$$\begin{aligned} G_{MN} &= \begin{pmatrix} 0 & 1+\delta n_0 & \delta n_i \\ 1+\delta n_0 & 2\delta A_0 & \delta A_i - \delta u_i \\ \delta n_i & \delta A_i - \delta u_i & \delta_{ij}+\delta\tilde{h}_{ij} \end{pmatrix}, \\ G^{MN} &= \begin{pmatrix} -2A_0 & 1-\delta n_0 & -\delta A_i + \delta u_i \\ 1-\delta n_0 & 0 & -\delta n_i \\ -\delta A_i + \delta u_i & -\delta n_i & \delta_{ij}+\delta\tilde{h}_{ij} \end{pmatrix}. \end{aligned} \tag{2.69}$$

These sources are used to define conserved currents, in particular the ones entering the energy-momentum tensor multiplet through the variation of the vacuum functional

$$\delta W = \int d^d x\sqrt{-g}\left(\frac{1}{2}T_{ij}\delta\tilde{h}_{ij} + j^\mu \delta A_\mu - \varepsilon^\mu \delta n_\mu - p_i \delta u_i\right), \tag{2.70}$$

where p_i is the momentum density, T_{ij} is the spatial stress tensor, $j^\mu = (j^0, j^i)$ contains the number density and current and $\varepsilon^\mu = (\varepsilon^0, \varepsilon^i)$ the energy density and current. The $U(1)$ number current is proportional to the momentum density[6].

This decomposition allows to find the Ward identities associated to the various symmetries of the non-relativistic theory. Particle number conservation implies the conservation of the $U(1)$ current

$$\langle \partial_\mu j^\mu \rangle = 0\,. \tag{2.71}$$

Associated to diffeomorphism invariance there are the conservation of the spatial stress tensor and of the energy current

$$\langle \partial_t p^j + \partial_i T^{ij} \rangle = 0\,, \quad \langle \partial_\mu \varepsilon^\mu \rangle = 0\,. \tag{2.72}$$

[6]This is a direct consequence of eq. (2.69), because only the combination $\delta A_i - \delta u_i$ enters the DLCQ metric

Finally, local Weyl transformations entail the Ward identity associated to the conservation of the scale current, which is found to be[7]

$$J_S^0 = p_i x^i - 2t\varepsilon^0\,, \quad J_S^i = x^j T^i{}_j - 2t\varepsilon^i\,, \quad \langle \partial_\mu J_S^\mu \rangle = 0\,. \tag{2.73}$$

By expanding explicitly the scale Ward identity we have

$$\langle \partial_\mu J_S^\mu \rangle = \langle T^i{}_i - 2\varepsilon^0 \rangle - 2t\langle \partial_\mu \varepsilon^\mu \rangle + x^j \langle \partial_t p_j + \partial_i T^i{}_j \rangle = 0\,. \tag{2.74}$$

Equation (2.74) is interesting, because it explicitly shows the relations intertwining between tracelessness of the energy-momentum tensor, conservation of the energy momentum tensor and scale invariance. A quantum violation of the scale symmetry manifests as a non conservation of the scale current J_S^μ which, in turn, is equivalent to a violation of the tracelessness condition $\langle T^i{}_i - 2\varepsilon^0 \rangle = 0$ only if the energy-momentum tensor does not have a diffeomorphism anomaly, *i.e.* only if the conditions (2.72) are satisfied. On the other hand, if the energy momentum tensor is not conserved at the quantum level, not only the trace anomaly, but also the diffeomorphism anomaly contribute to the scale anomaly.

If the diffeomorphisms ar chosen to be preserved[8], we can derive the Ward identity giving the tracelessness condition for the energy-momentum tensor by performing a Weyl variation nearby flat space

$$\delta W = \sigma G_{MN} \frac{\delta W}{\delta G_{MN}} = \sigma \left(\delta^{ij} \frac{\delta W}{\delta(\delta \tilde{h}_{ij})} + 2 \frac{\delta W}{\delta(\delta n_0)} \right) = \sigma (T^i_i - 2\varepsilon^0)\,, \tag{2.75}$$

which vanishes in the classical case or in flat space. In general the non-vanishing of this expression is the trace anomaly, which in $2+1$ dimensions for $z=2$ can be parametrized in terms of DLCQ quantities as

$$\Delta W = \int \sqrt{g} d^3x\, \sigma \left(-aE_4 + cW^2 + bR^2 + dD_A D^A R + eR^{AB}{}_{CD} R_{ABEF} \frac{\varepsilon^{CDEF}}{\sqrt{g}} \right) + \dots \tag{2.76}$$

Apart from the fact that we are performing a null reduction of the higher-dimensional tensors, the terms in parenthesis are exactly the same of the $3+1$ dimensional relativistic case, and a, c, e correspond to anomaly coefficients, while $b=0$ from the Wess-Zumino consistency conditions [76] and d can be removed by local counterterms. The dots in eq. (2.76) correspond to an infinite number of possible terms with a higher number of derivatives, which however belong to other Weyl sectors.

[7] Strictly speaking, the scale current has an additional term proportional to the scaling dimension Δ of the matter field. However, such term is a total derivative and can always be reabsorbed by a current redefinition.

[8] Since the diffeomorphisms are a gauge transformation, it is essential to preserve them in order to avoid the loss of unitarity in the theory.

Chapter 3

The heat kernel technique

Most of the content of this chapter appeared previously in [77, 78].

The heat kernel is a mathematical tool which has powerful applications in QFT to study the Casimir effect, effective actions, quantum anomalies and many other quantities. In this chapter we will start with a review of how the heat kernel can be used to renormalize the one-loop effective action and to extract quantum anomalies. Then we will treat how this procedure applies in the non-relativistic case, and we will use the technique to investigate the trace anomaly for a NC background in specific examples. The main references are [79–81].

3.1 General procedure

In this section we set up the general procedure to find the vacuum generating functional in curved space $W[J=0, g_{\mu\nu}]$ corresponding to the kinetic operator of a given Lagrangian action. This will be the starting point to derive a relation between the energy-momentum tensor and a set of coefficients coming from a series expansion of the so-called heat kernel operator. Ultimately, this leads to a precise way to compute the trace anomaly. In this section we review this procedure in the relativistic case by following the approach of [79].

3.1.1 The heat kernel and the zeta function operators

Definition 3.1. Given a n-dimensional Riemannian manifold $\mathscr{M}$ where is defined a self-adjoint and elliptic[1] differential operator $\mathscr{D}$, the heat kernel operator is defined as

$$K(\tau, \mathscr{D}) = \exp(-\tau\mathscr{D}) , \tag{3.1}$$

[1] An elliptic operator has at most a finite number of zero and negative modes.

and the zeta function of the operator $\mathscr{D}$ as

$$\zeta(s,\mathscr{D}) = \mathrm{Tr}(\mathscr{D}^{-s})\,. \tag{3.2}$$

The zeta function and the heat kernel operators are related by a Mellin transformation via the Euler Gamma function

$$\zeta(s,\mathscr{D}) = \Gamma(s)^{-1}\int_0^\infty d\tau\,\tau^{s-1}\mathrm{Tr}\left[K(\tau,\mathscr{D})\right]\,. \tag{3.3}$$

This relation can be inverted giving

$$\mathrm{Tr}\left[K(\tau,\mathscr{D})\right] = \frac{1}{2\pi i}\int ds\,\tau^{-s}\Gamma(s)\zeta(s,\mathscr{D})\,, \tag{3.4}$$

where the integration contour encircles all the poles of the integrand.

If $\mathscr{M}$ is a manifold without boundaries, there exists an asymptothic expansion of the trace of the heat kernel operator which takes the form

$$\mathrm{Tr}\left[K(\tau,\mathscr{D})\right] = \sum_{k=0}^{\infty}\tau^{\frac{k-n}{2}}a_k(\mathscr{D})\,, \tag{3.5}$$

where the a_k are called Seeley-De Witt coefficients. This set of coefficients will play a fundamental role in determining the trace anomaly, because they can be locally computed in most physical cases in terms of the volume and of boundary integrals of local invariants.

Using this series expansion inside the integral transformation (3.4), we find a representation of the Seleey-De Witt coefficients in terms of the zeta function

$$a_k(\mathscr{D}) = \mathrm{Res}_{s=\frac{n-k}{2}}\left[\Gamma(s)\zeta(s,\mathscr{D})\right]\,, \tag{3.6}$$

with the particular case

$$a_n(\mathscr{D}) = \zeta(0,\mathscr{D})\,. \tag{3.7}$$

3.1.2 Renormalization of the effective action

Let's turn to the physical part of the problem. We consider a QFT for a generic field ϕ with generating functional

$$Z[J] = e^{-W[J]} = \int \mathscr{D}\phi\,\exp\left(-S[\phi,J]\right)\,. \tag{3.8}$$

The heat kernel method is most suited for the investigation of one-loop properties of a system, and as such we take an approximation where we expand the action up to second order in the quantum fluctuations of the field

$$S[\phi,J] = S_{\mathrm{cl}} + \langle\phi,J\rangle + \langle\phi,\mathscr{D}\phi\rangle + \mathscr{O}(\phi^3)\,, \tag{3.9}$$

where $S_{\rm cl}$ is the action on the classical background and the bracket $\langle \dots \rangle$ denotes an inner product in the space of quantum fields. For example, the inner product involving a real scalar field φ is

$$\langle \varphi J \rangle = \int_{\mathscr{M}} d^n x \sqrt{g}\, \varphi(x) J(x) \,. \tag{3.10}$$

The linear term in the expansion (3.9) contains both a contribution from external sources and the first variation of the action, the latter piece vanishing on the classical equations of motion. The differential operator $\mathscr{D}$ modulates the quadratic quantum fluctuations of the action.

Within the gaussian approximation (3.9), the path integral (3.8) can be solved exactly. In the specific case of a real scalar field the result is

$$Z_{\rm scalar}[J] = e^{-S_{\rm cl}} \left[\det(\mathscr{D})\right]^{-\frac{1}{2}} \exp\left(\frac{1}{4} J \mathscr{D}^{-1} J\right) , \tag{3.11}$$

while for other theories containing complex scalars, Dirac spinors or other fields the result usually involves different powers of the functional determinant of the differential operator $\mathscr{D}$. From now on, we will use the numerical factors referred to the case of a real scalar field, while the other aspects of the derivation will be completely general.

The part of the gaussian expansion (3.9) involving the differential operator $\mathscr{D}$ contributes to the so-called one-loop effective action

$$W_{\rm eff} = \frac{1}{2} \log\left(\det \mathscr{D}\right) . \tag{3.12}$$

There exists an integral representation of the logarithm which relates the one-loop effective action to the heat kernel. Given a generic positive eigenvalue λ of the differential operator[2] $\mathscr{D}$, we have

$$\log \lambda = -\int_0^\infty \frac{d\tau}{\tau} e^{-\tau\lambda} \,. \tag{3.13}$$

This relation holds up to an infinite constant which, being independent from λ, we will ignore. Using the identity $\log\left(\det \mathscr{D}\right) = \mathrm{Tr}\left(\log \mathscr{D}\right)$, we can extend the previous equation to the trace of the heat kernel operator, finding

$$W_{\rm eff} = -\frac{1}{2} \int_0^\infty \frac{d\tau}{\tau} \mathrm{Tr}\left[K(\tau, \mathscr{D})\right] . \tag{3.14}$$

As it happens for a particular eigenvalue λ, this identity is formally true up to an infinite constant. In order to regularize the effective action, we consider a shift of the power in the denominator

$$W_{\rm reg}(s) = -\frac{1}{2} \mu^{2s} \int_0^\infty \frac{d\tau}{\tau^{1-s}} \mathrm{Tr}\left[K(\tau, \mathscr{D})\right] , \tag{3.15}$$

where μ is a mass scale introduced to account for the different dimensions of the integrand with respect to the case $s = 0$. Using the inverse Mellin transformation (3.4), the regularized effective

[2] Since the operator is required to be elliptic, there exists at most a finite number of non-positive modes.

action can be expressed as

$$W_{\text{reg}}(s) = -\frac{1}{2}\mu^{2s}\Gamma(s)\zeta(s,\mathscr{D})\,, \tag{3.16}$$

from which the name *zeta function regularization*. The Laurent expansion of the Euler Gamma function around 0

$$\Gamma(s) = \frac{1}{s} - \gamma_E + \mathscr{O}(s) \tag{3.17}$$

allows to determine

$$W_{\text{reg}}(s) = -\frac{1}{2}\left(\frac{1}{s} - \gamma_E + \log\mu^2\right)\zeta(0,\mathscr{D}) - \frac{1}{2}\zeta'(0,\mathscr{D}) + \mathscr{O}(s)\,, \tag{3.18}$$

where $f' \equiv \frac{d}{ds}f$. This shows that the divergence of the one-loop effective action arises due to a simple pole located at $s = 0$, and precisely this contribution gives a divergence in the Seeley-De Witt coefficient $a_n(\mathscr{D})$ via eq. (3.7). This result requires a renormalization procedure which eliminates the divergent part, giving the renormalized effective action as the remaining part at $s = 0$, *i.e.*

$$W^{\text{ren}} = -\frac{1}{2}\zeta'(0,\mathscr{D}) - \frac{1}{2}\log(\tilde{\mu}^2)\zeta(0,\mathscr{D})\,, \tag{3.19}$$

where $\tilde{\mu}^2 = e^{-\gamma_E}\mu^2$.

3.1.3 Relation with the trace anomaly

The energy-momentum tensor of a QFT coupled to a curved background is defined as

$$T_{\mu\nu} = \frac{2}{\sqrt{g}}\frac{\delta W}{\delta g^{\mu\nu}}\,. \tag{3.20}$$

Let's consider a conformal transformation

$$g_{\mu\nu} \to e^{2\sigma(x)}g_{\mu\nu}\,, \tag{3.21}$$

its infinitesimal version allows to express the variation of the effective action under this change of the metric as

$$\delta W = \frac{1}{2}\int_{\mathscr{M}} d^n x\sqrt{g}\,T^{\mu\nu}\delta g_{\mu\nu} = -\int_{\mathscr{M}} d^n x\sqrt{g}\,\sigma(x)T^{\mu}_{\mu}\,. \tag{3.22}$$

This result clearly shows that the invariance of a theory under conformal transformations can be expressed as the vanishing of the trace of the energy-momentum tensor. The opposite case, when $T^{\mu}_{\mu} \neq 0$, signals the quantum breaking of the conformal symmetry and goes under the name of *trace anomaly*.

Our final aim is to relate the trace anomaly to the Seeley-de Witt coefficients. We start with a general variation of the zeta function operator

$$\delta\zeta(s,\mathscr{D}) = -s\text{Tr}\left[(\delta\mathscr{D})\mathscr{D}^{-s-1}\right]\,. \tag{3.23}$$

If the classical action is conformally invariant, the differential operator is conformally covariant and then transforms under a Weyl variation as[3]

$$\mathscr{D} \to e^{-2\sigma(x)}\mathscr{D}\,. \tag{3.24}$$

In this way, the variation of the zeta function under a conformal transformation is

$$\delta\zeta(s,\mathscr{D}) = 2s\sigma(x)\mathrm{Tr}\mathscr{D}^{-s} = 2s\sigma(x)\zeta(s,\mathscr{D})\,, \tag{3.25}$$

and this induces a change of the one-loop renormalized effective action (3.19) given by

$$\delta W_{\rm ren} = -\sigma(x)\zeta(0,\mathscr{D}) = -\sigma(x)a_n(\mathscr{D}) = -\int_{\mathscr{M}} d^n x\,\sqrt{g}\,\sigma a_n(x,\mathscr{D})\,. \tag{3.26}$$

Comparing with eq. (3.22) we obtain

$$T^{\mu}_{\mu}(x) = a_n(x,\mathscr{D})\,. \tag{3.27}$$

Stated in this way, the problem to determine the trace anomaly is reduced to the computation of the Seeley-De Witt coefficient $a_n(x,\mathscr{D})$.

3.1.4 Computation of the Seeley-De Witt coefficients

We restrict to a class of second order operators of the Laplace type, *i.e.* that can be represented as

$$\mathscr{D} = -\left(g^{\mu\nu}\partial_\mu\partial_\nu + a^\mu\partial_\mu + b\right) \tag{3.28}$$

with an appropriate choice of the matrix valued functions a^μ, b. The last expression can be further decomposed as a perturbation of a reference operator $\mathscr{D}_0$ as

$$\mathscr{D} = \mathscr{D}_0 + \delta\mathscr{D}\,, \tag{3.29}$$

where a convenient choice is $\mathscr{D}_0 = -\Box$, when expanding the metric around flat space as

$$g_{\mu\nu} = \delta_{\mu\nu} + h_{\mu\nu}\,. \tag{3.30}$$

In order to study the heat kernel of the differential operator $\mathscr{D}$ defined on the curved manifold $\mathscr{M}$, it is convenient to work with an inner product which does not involve the determinant of the metric in

[3] This assertion is not so simple to derive as it may appear, due to the classical conformal invariance of the problem. In fact, the relation is strictly speaking true only after a similarity transformation $\mathscr{D} \to e^{\alpha\sigma(x)}\mathscr{D}e^{-\alpha\sigma(x)}$ which leaves the functional determinant invariant. A careful treatment of this aspect will be done in the specific computation of the diffeomorphism anomaly, to which the same method applies.

the measure. This requirement leads to a normalization of the eigenstates given by

$$\langle xt|x't'\rangle_g = \frac{\delta(x-x')\delta(t-t')}{\sqrt{g}}\,, \tag{3.31}$$

and to the definition of another differential operator

$$O = g^{1/4}(x)\,(\mathscr{D}_0 + \delta\mathscr{D})\,g^{-1/4}(x) = -\,(\Box + V)\,, \tag{3.32}$$

where g is the determinant of the metric. The last decomposition of the new hermitian operator O in terms of a perturbation of flat space is always possible going around a locally inertial frame. An important implication of this choice for the inner product and the Hilbert space where the operator O lives is that the expansion giving the Seeley-De Witt coefficients takes a factor in the determinant of the metric

$$\mathrm{Tr}\,[K(\tau,O)] = \sum_{k=0}^{\infty} \tau^{\frac{k-n}{2}} a_k(O) = \sum_{k=0}^{\infty} \sqrt{g}\,\tau^{\frac{k-n}{2}} a_k(\mathscr{D}) = \frac{\sqrt{g}}{\tau^{n/2}}\left[1 + a_2(\mathscr{D})\tau + a_4(\mathscr{D})\tau^2 + \mathscr{O}(\tau^3)\right]. \tag{3.33}$$

We find the implications of this perturbative expansion on the heat kernel operator. Given the requirements of $\mathscr{D}$ to be self-adjoint and elliptic, the heat kernel is analytic and can then be Taylor-expanded around $\tau = 0$, giving

$$K(\tau) = \sum_{i=0}^{\infty} K_i(\tau)\,, \tag{3.34}$$

where $K_n(\tau)$ is an operator of n-th order in the perturbation V. By construction, the heat kernel of such a differential operator solves the exact differential equation

$$\frac{dK}{d\tau} = (\Box + V)K\,. \tag{3.35}$$

The assumption that the deviation from flat metric and the potential are small translates into the fact that we can solve the differential equation order by order and we can truncate the series. The leading term is

$$\frac{dK_0}{d\tau} = \triangle K_0\,, \tag{3.36}$$

while the first-order term is

$$\frac{dK_1}{d\tau} = \triangle K_1 + V K_0\,. \tag{3.37}$$

Remembering that the initial condition is $K(\tau) = \mathbf{1}$, we infer the initial condition for the 0-th and 1-st order of the heat kernel expansion, which are $K_0(\tau) = \mathbf{1}$ and $K_1(\tau) = 0$. Thus the formal solution of the equation for K_0 is

$$K_0(\tau) = \exp(\tau\Box)\,. \tag{3.38}$$

The equation for the first-order term can be solved using the method of variation of constants by searching solutions of the form

$$K_1(\tau) = K_0(\tau)C(\tau)\,. \tag{3.39}$$

Putting this trial function in eq. (3.37) gives

$$K_0(\tau)\frac{dC(\tau)}{d\tau} = VK_0(\tau)\,, \tag{3.40}$$

whose solution is

$$C(\tau) = \int_0^\tau d\tau' K_0^{-1}(\tau')V K_0(\tau')\,. \tag{3.41}$$

In order to avoid using the inverse of the heat kernel at zero-th order to appear in the solution, we observe that the solution for $K_0(\tau)$ satisfies the relation

$$K_0(\tau)K_0(\tau') = K_0(\tau+\tau')\,. \tag{3.42}$$

We can in particular choose the proper times $\tau+\tau'=0$, so that $K_0(0)=\mathbf{1}$ and we derive

$$K_0^{-1}(\tau) = K_0(-\tau)\,. \tag{3.43}$$

This allows to write the final result for $K_1(\tau)$ as

$$K_1(\tau) = \int_0^\tau d\tau' K_0(\tau-\tau')V K_0(\tau')\,. \tag{3.44}$$

The procedure can be applied recursively order by order in the perturbative expansion. The result for the i-th order of the series is

$$K_i(\tau) = \int_0^\tau d\tau_i \int_0^{\tau_i} d\tau_{i-1}\cdots\int_0^{\tau_2} d\tau_1\, K_0(\tau-\tau_i)V K_0(\tau_i-\tau_{i-1})V\ldots K_0(\tau_2-\tau_1)VK_0(\tau_1)\,. \tag{3.45}$$

Using this perturbative expansion, we can determine the Seeley-De Witt coefficients by means of eq. (3.5) order by order in V. In particular, the a_n coefficient gives the trace anomaly.

Here we put a remark: using this series expansion we find the expression of the quantum anomaly up to a chosen order in the parameter of the expansion. However, in the case of the trace anomaly, we know that the exact expression must be a scalar under diffeomorphisms. Having this hint, we will interpret the perturbative results in terms of the curvature invariants, and then we will infer that the expression obtained up to the chosen order of the expansion is valid at all orders.

3.1.5 Heat kernel in flat space

The zero-th order term of the heat kernel expansion refers to the flat space solution, which can be solved analytically. In configuration space we have

$$\langle x|K_0(\tau)|y\rangle = \langle x|e^{\tau\triangle}|y\rangle = e^{\tau\triangle_x}\delta(x-y)\,. \tag{3.46}$$

If we replace the Delta function with its integral representation

$$\delta(x-y) = \int \frac{d^n k}{(2\pi)^n}\, e^{ik(x-y)}\,, \tag{3.47}$$

we find

$$e^{\tau\Box_x}\delta(x-y) = e^{\tau\Box_x}\int \frac{d^n k}{(2\pi)^n}\, e^{ik(x-y)} = \int \frac{d^n k}{(2\pi)^n}\, e^{-\tau k^2 + ik(x-y)}\,. \tag{3.48}$$

Since the final expression is a Gaussian integral, we can directly compute it finding

$$G_0(x,y,\tau) = \langle x|K_0(\tau)|y\rangle = \frac{1}{(4\pi\tau)^{n/2}}\exp\left[-\frac{(x-y)^2}{4\tau}\right]\,. \tag{3.49}$$

This is simply the Green function of the heat kernel equation in n dimensions. In particular it contributes to the trace via the expression

$$G_0(x,x,\tau) = \langle x|K_0(\tau)|x\rangle = \frac{1}{(4\pi\tau)^{n/2}}\,. \tag{3.50}$$

Putting this exact solution into the Dyson expansion (3.45), we can find the perturbative corrections order by order in V.

3.2 Non-relativistic heat kernel

The derivation of the heat kernel technique in section 3.1 assumes the existence of a differential operator of the Laplace type which we can expand as in eq. (3.28).

What happens in the non-relativistic case? Is it always possible to express a Galilean-invariant action as an hermitian and elliptic operator, and expand with respect to a well-defined flat operator? The first problem to face is that Euclidean space is not well-defined in the non-relativistic case, and then we need to give a prescription for a consistent way to perform the analogous of a Wick rotation. We consider as an example the action for a Galilean-invariant free scalar in $d+1$ dimensions coupled to a NC gravity with $A_\mu = 0$, see eq. (2.28). The analog of the Wick rotation in this case would require to send

$$t \to -it_E\,, \qquad m \to im_E\,, \tag{3.51}$$

according to the prescription of [81]. In the following, we will omit the subscript E referring to Euclidean space. The equivalent prescription to apply in curved space is to send

$$v^\mu \to i v^\mu\,, \qquad m \to im\,, \qquad n_\mu \to -i n_\mu\,, \qquad \sqrt{g} \to i\sqrt{g}\,. \tag{3.52}$$

In the previous section we were able to consider a local inertial frame to expand the differential operator as in eq. (3.29). In the non-relativistic case, the Schrödinger operator in Euclidean space around which we expand the solution is not an elliptic operator, being defined as

$$-2im\partial_t + \partial_i^2\,. \tag{3.53}$$

The only possible positive-definite operator that we can build out of it arises from the interpretation

$$\triangle_E \equiv -2m\sqrt{-\partial_t^2} + \partial_i^2\,, \qquad \mathscr{D}_0 = -\triangle_E \tag{3.54}$$

where we only take the positive branch cut of the square root. Using the rules (3.52), we obtain an Euclidean version for the non-relativistic free scalar given by

$$S_E = \int d^{d+1}x\sqrt{g}\,\varphi^\dagger \left\{ m v^\mu \sqrt{-\partial_\mu^2}\varphi + \frac{m\sqrt{-\partial_\mu^2}(\sqrt{g}v^\mu\varphi)}{\sqrt{g}} - \frac{\partial_\mu(\sqrt{g}h^{\mu\nu}\partial_\nu\varphi)}{\sqrt{g}} + \xi R\varphi \right\}. \tag{3.55}$$

Expanding the differential operator around flat space, it can be written as

$$\mathscr{D} = -\triangle_E + \delta\mathscr{D} \quad \Rightarrow \quad O = g^{1/4}(x)\,\mathscr{D}\,g^{-1/4}(x) = -(\triangle_E + V)\,. \tag{3.56}$$

Given this decomposition, the perturbative expansion works exactly in the same way of the relativistic case.

The Euclidean prescription that we chose in eq. (3.54) deserves more comments. First of all, the heat kernel procedure is well-defined only when an hermitian and elliptic operator is used [79]. Our prescription (which was introduced in [81]) is the only possible way to define an operator which such requirements starting from the real time Schrödinger one, which contains only a single partial derivative of time. While it is true that this procedure changes the spectrum of the theory, it seems to us a prescription similar to the way in which a Dirac fermion is treated in the relativistic case. In fact, in that situation the Dirac operator by itself is not elliptic, and the standard way to proceed is to evaluate the heat kernel for the squared operator $\not{D}^2$, which is instead of the Laplace type and has a positive spectrum. At the end, the Binet theorem is used and the square root of the result is extracted. Our procedure for the non-relativistic case appears in spirit the same. We remark that the results given in the following subsections are consistent with [82], where the Fujikawa technique is used, without the necessity to perform a Euclidean continuation. A different approach with the heat kernel computation is considered in [83], where the final result is proportional to the Dirac delta function of

the mass of the non-relativistic particle. We disagree with their result, in particular we point out that their Euclidean prescription for the Schrödinger operator defines a parabolic operator instead of an elliptic one, and then the corresponding heat kernel operator is not well-defined.

3.2.1 Flat space

We compute the zero-th order contribution to the heat kernel coming from the flat space Schrödinger operator. We can write the Euclidean version in eq. (3.54) as a sum of hermitian and elliptic operators via the integral expansion [81]

$$e^{-2m\sqrt{-\partial_t^2}} = \int_0^\infty d\sigma \frac{m}{\sqrt{\pi}} \frac{1}{\sigma^{3/2}} e^{-\frac{m^2}{\sigma}} e^{-\sigma(-\partial_t^2)}\,, \tag{3.57}$$

in such a way that we find

$$G_{-\triangle_t}(t,t',\tau) = \langle t|e^{-2m\tau\sqrt{-\partial_t^2}}|t'\rangle = \int_0^\infty d\sigma \frac{m}{2\pi}\frac{\tau}{\sigma^{3/2}} \exp\left[-\frac{4\tau^2m^2+(t-t')^2}{4\sigma}\right] = \frac{m\tau}{2\pi}\frac{1}{m^2\tau^2+\frac{(t-t')^2}{4}}\,. \tag{3.58}$$

The spatial part of the flat heat kernel factorizes and is the same of the relativistic case. Putting the results together, the flat non-relativistic heat kernel in $d+1$ dimensions becomes

$$G_{-\triangle_E}(x,t,x',t',\tau) = \langle x,t|e^{\tau\triangle_E}|x',t'\rangle = \frac{m\tau}{2\pi}\frac{1}{m^2\tau^2+\frac{(t-t')^2}{4}}\frac{1}{(4\pi\tau)^{d/2}}\exp\left[-\frac{(x-x')^2}{4\tau}\right]\,. \tag{3.59}$$

In particular, the trace of the heat kernel operator is

$$\mathrm{Tr}\,K(-\triangle_E,\tau) = \langle x,t|e^{\tau\triangle_E}|x,t\rangle = \frac{2}{m(4\pi\tau)^{d/2}}\,. \tag{3.60}$$

It is interesting to compare this expression with the corresponding one (3.50) in the relativistic case. A comparison shows that the Schrödinger operator in $d+1$ dimensions feels the same spectral dimension

$$d_O = -2\frac{\partial \log \mathrm{Tr}\,K_{\mathscr{O}}(\tau)}{\partial \log \tau} \tag{3.61}$$

as the Laplace operator in $d+2$ dimensions. This is a pleasant result in the light of the null reduction procedure, which relates the Schrödinger group with the conformal group in one higher dimension.

When performing the heat kernel expansion in a $d+1$ dimensional non-relativistic background, we will find in the next Section a behaviour of kind

$$\begin{aligned}\mathrm{Tr}\left[K(\tau,O)\right] &= \frac{1}{\tau^{d/2+1}}\left[a_0(O)+a_2(O)\tau+a_4(O)\tau^2+\mathscr{O}(\tau^3)\right] = \\ &= \frac{\sqrt{g}}{\tau^{d/2+1}}\left[a_0(\mathscr{D})+a_2(\mathscr{D})\tau+a_4(\mathscr{D})\tau^2+\mathscr{O}(\tau^3)\right]\,.\end{aligned} \tag{3.62}$$

Due to the spectral dimension (3.61), we will need to take the $a_4(O)$ coefficient to find the trace anomaly in $2+1$ dimensions.

3.2.2 Heat kernel expansion

It turns out that the operator $O = g^{1/4}\mathscr{D}g^{-1/4}$ entering the heat kernel expansion for a non-relativistic free scalar and fermion can be put into the form

$$\begin{aligned}\langle x,t|O|x',t'\rangle =&\langle x,t|\Big[\triangle_E \mathbf{1} + P(x,t)\delta(x-x')\delta(t-t') + S(x,t)\sqrt{-\partial_t^2}\delta(x-x')\delta(t-t')+\\ &+Q_i(x,t)\,\partial_i\delta(x-x')\delta(t-t')\Big]|x',t'\rangle\,.\end{aligned} \tag{3.63}$$

At the first order the Dyson series is

$$K_1(\tau) = \mathrm{tr}\int_0^\tau d\tau'\,\langle x,t|e^{(\tau-\tau')\triangle_E}V(x,t)e^{\tau'\triangle_E}|x',t'\rangle\,, \tag{3.64}$$

where here the trace is only evaluated on the internal indices of the differential operator (such as spinorial ones). According to eq. (3.63), we can decompose the expression as

$$\begin{aligned}K_1(\tau) = K_{1P}(\tau)+K_{1S}(\tau)+K_{1Q_i}(\tau) = \mathrm{tr}\int_0^\tau d\tau'\,\langle xt|e^{(\tau-\tau')\triangle_E}P(x,t)e^{\tau'\triangle_E}|x't'\rangle+\\ +\mathrm{tr}\int_0^\tau d\tau'\,\langle xt|e^{(\tau-\tau')\triangle_E}S(x,t)\sqrt{-\partial_t^2}e^{\tau'\triangle_E}|x't'\rangle+\mathrm{tr}\int_0^\tau d\tau'\,\langle xt|e^{(\tau-\tau')\triangle_E}Q_i(x,t)\partial_i e^{\tau'\triangle}|x't'\rangle\,.\end{aligned} \tag{3.65}$$

These integrals are explicitly computed in Appendix B.1 for time-independent operators and the result is

$$\mathrm{Tr}\,K_{1P}(\tau) = \frac{2}{m(4\pi\tau)^{d/2+1}}\left(\tau P(x)+\frac{1}{6}\tau^2\partial_x^2 P(x)+\mathscr{O}(\tau^3)\right), \tag{3.66}$$

$$\mathrm{Tr}\,K_{1S}(\tau) = \frac{2}{m(4\pi\tau)^{d/2+1}}\,\mathrm{tr}\left(\frac{S}{2m}+\frac{\tau}{12m}\partial_i^2 S+\frac{\tau^2}{120m}\partial_i^4 S+\mathscr{O}(\tau^3)\right), \tag{3.67}$$

$$\mathrm{Tr}\,K_{1Q_i}(\tau) = \frac{2}{m(4\pi\tau)^{d/2+1}}\,\mathrm{tr}\left(-\frac{\tau}{2}\partial_i Q_i-\frac{\tau^2}{12}\partial_i\partial_k^2 Q_i+\mathscr{O}(\tau^3)\right). \tag{3.68}$$

At the second order the heat kernel expansion is

$$K_2(s) = \mathrm{tr}\int_0^\tau d\tau'\int_0^{\tau'} d\tau''\,\langle x,t|e^{(\tau-\tau')\triangle_E}V(x,t)e^{(\tau'-\tau'')\triangle_E}V(x,t)e^{\tau''\triangle_E}|x',t'\rangle\,. \tag{3.69}$$

K_2 splits into the sum of several contributions:

$$K_2(\tau) = \sum_X K_{2X}(\tau) = \tag{3.70}$$

$$= K_{2PP}(\tau)+K_{2SS}(\tau)+K_{2PS}(\tau)+K_{2SP}(\tau)+K_{2Q_iaj}(\tau)+K_{2Q_iP}(\tau)+K_{2PQ_i}(\tau)+K_{2Q_iS}(\tau)+K_{2SQ_i}(\tau)\,.$$

Their expressions are computed in Appendix B.2 for time-independent operators and they are given by

$$\mathrm{Tr}\,K_{2PP} = \frac{2}{m(4\pi\tau)^{d/2+1}}\mathrm{tr}\left(\frac{\tau^2}{2}P(x)^2+\mathscr{O}(\tau^3)\right), \tag{3.71}$$

$$\begin{aligned}\mathrm{Tr}\,K_{2SS} =& \frac{2}{m(4\pi\tau)^{d/2+1}}\mathrm{tr}\left(\frac{S^2}{4m^2}+\frac{\tau}{12m^2}S\partial^2 S+\frac{\tau}{24m^2}\partial_k S\partial_k S+\frac{\tau^2}{120m^2}S\partial^4 S+\right.\\ &\left.+\frac{\tau^2}{144m^2}\partial^2 S\partial^2 S+\frac{\tau^2}{60m^2}\partial_i\partial^2 S\partial_i S+\frac{\tau^2}{180m^2}\partial_{ij}S\partial_{ij}S+\mathscr{O}(\tau^3)\right),\end{aligned} \tag{3.72}$$

$$\mathrm{Tr}\,K_{2PS} = \tilde{K}_{2SP} = \frac{1}{m(4\pi\tau)^{d/2+1}}\mathrm{tr}\left(\frac{\tau}{2m}SP+\frac{\tau^2}{12m}S\partial^2 P+\frac{\tau^2}{12m}\partial^2 SP+\frac{\tau^2}{12m}\partial_i S\partial_i P+\mathscr{O}(\tau^3)\right), \tag{3.73}$$

$$\begin{aligned}\mathrm{Tr}\,K_{2Q_jQ_i} =& \frac{2}{m(4\pi\tau)^{d/2+1}}\mathrm{tr}\left[-\frac{\tau}{4}Q_iQ_i-\frac{\tau^2}{24}(\partial_j Q_i)(\partial_i a_j)\right.\\ &\left.+\frac{\tau^2}{8}(\partial_i Q_i)(\partial_j a_j)-\frac{\tau^2}{12}Q_i(\partial^2 Q_i)-\frac{\tau^2}{24}(\partial_i a_j)^2+\mathscr{O}(\tau^3)\right],\end{aligned} \tag{3.74}$$

$$\mathrm{Tr}\,K_{2Q_iP} = \frac{2}{m(4\pi\tau)^{d/2+1}}\mathrm{tr}\left(-\frac{\tau^2}{3}P(\partial_i Q_i)-\frac{\tau^2}{6}(\partial_i P)Q_i+\mathscr{O}(\tau^3)\right), \tag{3.75}$$

$$\mathrm{Tr}\,K_{2PQ_i} = \frac{2}{m(4\pi\tau)^{d/2+1}}\mathrm{tr}\left(\frac{\tau^2}{6}Q_i(\partial_i P)-\frac{\tau^2}{6}(\partial_i Q_i)P+\mathscr{O}(\tau^3)\right), \tag{3.76}$$

$$\begin{aligned}\mathrm{Tr}\,K_{2Q_iS} =& \frac{2}{m(4\pi\tau)^{d/2+1}}\mathrm{tr}\left[-\frac{\tau}{24m^2}\left(S\partial_k^2 S+\frac{1}{2}(\partial_k S)^2\right)+\right.\\ &\left.-\frac{\tau^2}{80m^2}\left(\frac{1}{2}S\partial_k^2\partial_j^2 S+\frac{7}{12}(\partial_k^2 S)^2+\frac{13}{12}\partial_k S(\partial_k\partial_j^2 S)+\frac{1}{3}(\partial_k\partial_j S)^2\right)+\mathscr{O}(\tau^3)\right],\end{aligned} \tag{3.77}$$

$$\begin{aligned}\mathrm{Tr}\,K_{2SQ_i} =& \frac{2}{m(4\pi\tau)^{d/2+1}}\mathrm{tr}\left[\frac{\tau}{48m^2}\left((\partial_k S)^2-S\partial_k^2 S\right)+\right.\\ &\left.+\frac{\tau^2}{80m^2}\left(-\frac{1}{3}S\partial_k^2\partial_j^2 S-\frac{1}{4}(\partial_k^2 S)^2+\frac{1}{4}\partial_k S(\partial_k\partial_j^2 S)+\frac{1}{3}(\partial_k\partial_j S)^2\right)+\mathscr{O}(\tau^3)\right].\end{aligned} \tag{3.78}$$

3.2.3 A specific perturbation of flat space

We consider a specific perurbation of $2+1$ dimensional flat space which will be the reference background for the computation of the heat kernel for non-relativistic free scalars and fermions. It is described by the conditions

$$n_\mu = \left(\frac{1}{1-\eta(x^i)},0,0\right), \qquad v^\mu = \left(1-\eta(x^i),0,0\right), \qquad h_{ij}=\delta_{ij}, \qquad A_\mu = 0, \tag{3.79}$$

which gives a constraint on the spatial part of the frame fields

$$e_i^a = e_a^i = \delta_a^i. \tag{3.80}$$

Notice that we consider a time-independent background, as it is sufficient to find non-trivial curvature invariants appearing in the trace anomaly.

The determinant of the metric is

$$\sqrt{g} = \frac{1}{1-\eta(x^i)}\,. \tag{3.81}$$

The non-vanishing components of the spin connection and Cristoffel symbols are:

$$\begin{aligned} &\omega_{\underset{(M)}{-}+a} = \frac{1}{2}\frac{\partial_a\eta}{1-\eta}\,, \qquad \omega_{\mu\underset{(A)(A)}{-+}} = -\frac{1}{2}\delta_{\mu i}\frac{\partial_i\eta}{1-\eta}\,, \quad \omega_{\mu\underset{(A)}{-}a} = \frac{1}{2}\delta_{\mu+}\frac{\partial_a\eta}{(1-\eta)^2}\,, \\ &\Gamma^{-}_{\mu-} = \frac{1}{2}\delta_{\mu i}\frac{\partial_i\eta}{1-\eta}\,, \quad \Gamma^{\rho}_{\mu-} = -\frac{1}{2}\delta_{\mu+}\delta^{\rho i}\frac{\partial_i\eta}{(1-\eta)^2}\,, \quad \Gamma^{\rho}_{\mu\nu} = \frac{1}{2}\delta^{\rho+}\delta_{\mu+}\delta_{\nu i}\frac{\partial_i\eta}{1-\eta}\,. \end{aligned} \tag{3.82}$$

Using eq. (3.79) , we compute the Ricci scalar

$$R = -2\partial_i^2\eta - 2\eta\,\partial_i^2\eta - \frac{7}{2}\partial_i\eta\,\partial_i\eta + \mathscr{O}(\eta^3)\,. \tag{3.83}$$

The dimension 4 curvature invariants are given up to second order in the perturbation parameter η by

$$\begin{aligned} R^2 &= 4(\partial_i^2\eta)^2 + \mathscr{O}(\eta^3)\,, \qquad W^2_{ABCD} = \tfrac{1}{3}(\partial_i^2\eta)^2 + \mathscr{O}(\eta^3)\,, \qquad E_4 = 2(\partial_i^2\eta)^2 - 2\partial_{ij}\eta\,\partial_{ij}\eta + \mathscr{O}(\eta^3)\,, \\ D_A D^A R &= -2\partial_i^2\partial_j^2\eta - 2(\partial_i^2\eta)^2 - 2\eta\,\partial_i^2\partial_j^2\eta - 13\partial_k\eta\,\partial_k\partial_i^2\eta - 7\partial_{ij}\eta\,\partial_{ij}\eta + \mathscr{O}(\eta^3)\,. \end{aligned} \tag{3.84}$$

In the next section, we will compute the heat kernel expansion and the Seeley-De Witt coefficients in terms of the curvature invariants.

3.3 Trace anomaly in specific examples

3.3.1 Trace anomaly for a non-relativistic free scalar

The differential operator $\mathscr{D}_{\rm bos}$ to consider for a non-relativistic free scalar coupled to NC gravity is given in eq. (3.55). From this expression we find that the functions appearing in eq. (3.63) for the specific background (3.79) are given by

$$S(x) = 2m\eta\,, \qquad P(x) = -\left(\frac{\partial_i^2\eta}{2} + \frac{1}{2}\eta\,\partial_i^2\eta + \frac{3}{4}(\partial_i\eta)^2\right) + \xi\left(2\partial_i^2\eta + 2\eta\,\partial_i^2\eta + \frac{7}{2}(\partial_i\eta)^2\right), \tag{3.85}$$

and $Q_i(x) = 0$. Putting these expressions inside the first and second order heat kernel expansion given in eqs. (3.66)-(3.68) and in eqs. (3.71)-(3.78), we obtain the $a_4(\mathscr{D}_{\rm bos})$ coefficient in $2+1$ dimensions:

$$\begin{aligned} a_4(O_{\rm bos}) = \sqrt{g}\,a_4(\mathscr{D}_{\rm bos}) = \frac{1}{8m\pi^2}\Bigg[&\frac{7-180\xi+720\xi^2}{360}(\partial^2\eta)^2 + \frac{210\xi-41}{180}(\partial_{ij}\eta)^2 - \frac{1-5\xi}{15}\partial^4\eta \\ &-\frac{2(1-5\xi)}{15}\eta\,\partial^4\eta - \frac{13}{30}(1-5\xi)(\partial_i\eta)(\partial_i\partial^2\eta) + \mathscr{O}(\eta^3)\Bigg]\,. \end{aligned} \tag{3.86}$$

Using the leading order expansions (3.83) and (3.84), we are finally able to re-write the Seeley-De Witt coefficient in terms of the curvature invariants finding the trace anomaly as

$$\mathscr{A}_{\rm bos} = a_4(\mathscr{D}_{\rm bos}) = \frac{1}{8m\pi^2}\left[-\frac{1}{360}E_4 + \frac{3}{360}W^2 + \frac{1}{2}\left(\xi - \frac{1}{6}\right)^2 R^2 + \frac{1-5\xi}{30}D^2R\right]. \tag{3.87}$$

3.3.2 Trace anomaly for a non-relativistic free fermion

In the fermionic case there are two main differences with respect to the free scalar: the path integral contains a Berezin integration and the Dirac operator $\not{D}$ is not elliptic after Wick rotation, even in the relativistic framework. The first change simply influences the sign of the functional determinant. In fact, in the bosonic case the effective action is

$$e^{iW} = \int \mathscr{D}\varphi^\dagger\, \mathscr{D}\varphi\; e^{i\int d^dx\, \varphi^\dagger \mathscr{D}_{\rm bos}\varphi}, \tag{3.88}$$

whose solution is

$$iW_{\rm bos} = -\log\det(\mathscr{D}_{\rm bos}). \tag{3.89}$$

In the fermionic case, the vacuum functional is instead

$$e^{iW} = \int \mathscr{D}\bar\psi\, \mathscr{D}\psi\; e^{i\int d^dx\, \bar\psi \not{D}\psi}, \tag{3.90}$$

and the anticommuting nature of the spinorial objects gives an additional minus sign

$$iW_{\rm ferm} = \log\det(\not{D}). \tag{3.91}$$

While this procedure would in principle work, the fact that the Dirac operator is not elliptic forbids the possibility to apply the heat kernel method to this differential operator. The problem is solved by studying the square of the Dirac operator $\not{D}^2$, which is instead both hermitian and elliptic after Wick rotation. In fact, this operator is also of the Laplace type because it can be written as (see e.g. [84], [85]):

$$\left(i\not{D}\right)^2 = -\Box + \frac{1}{4}R, \qquad \Box = D_A D^A. \tag{3.92}$$

At the level of the functional determinant, to recover the original differential operator we need to extract the square root, which simply gives a factor of $1/2$ in the functional determinant

$$iW_{\rm ferm} = \frac{1}{2}\log\det(\not{D}^2). \tag{3.93}$$

The same trick applies to the non-relativistic case, where we perform the null reduction of the differential operator (3.92). The result in the background (3.79), after applying the rules for the

Euclidean space formulation

$$t \to -it\,, \qquad \partial_t \to i\partial_t\,, \qquad m \to im\,, \tag{3.94}$$

is the differential operator

$$\begin{aligned}
& g^{1/4}\left(\Box - \frac{1}{4}R\right)_E g^{-1/4}\Psi = \\
= \;& \left[-2im\mathbf{1} + 2im\eta\,\mathbf{1} + \frac{i}{2}(\partial_a\eta)\gamma^{+a}\right]\partial_t\Psi + \left[-\frac{1}{2}(\partial_a\eta)\gamma^{-+} - \frac{1}{2}\eta(\partial_a\eta)\gamma^{-+}\right]\partial_a\Psi + \\
+ \;& \left[\frac{1}{8}(\partial_a\eta)^2\mathbf{1} - \frac{1}{4}\partial^2\eta\,\gamma^{-+} - \frac{1}{4}\eta(\partial^2\eta)\gamma^{-+} - \frac{1}{4}(\partial_a\eta)^2\gamma^{-+} - \frac{1}{2}m(\partial_a\eta)\gamma^{-a} - \frac{1}{2}m\eta(\partial_a\eta)\gamma^{-a}\right]\Psi + \\
+ \;& \left[\frac{1}{16}(\partial_a\eta)^2\mathbf{1} + \frac{1}{16}(\partial_a\eta)(\partial_b\eta)\{\gamma^{-a},\gamma^{+b}\}\right]\Psi + \partial^2\Psi\,.
\end{aligned} \tag{3.95}$$

This expression can be put in the form (3.63) with the identifications

$$\begin{aligned}
P(x) &= \frac{3}{16}(\partial_i\eta)^2\mathbf{1} - \frac{1}{4}(\partial^2\eta)\gamma^{-+} - \frac{1}{4}\eta(\partial^2\eta)\gamma^{-+} - \frac{1}{4}(\partial_i\eta)^2\gamma^{-+} \\
&\quad - \frac{1}{2}m(\partial_i\eta)\gamma^{-i} - \frac{1}{2}m\eta(\partial_i\eta)\gamma^{-i} + \frac{1}{16}(\partial_i\eta)(\partial_j\eta)\{\gamma^{-i},\gamma^{-j}\}\,, \\
S(x) &= 2m\eta\,\mathbf{1} + \frac{1}{2}(\partial_i\eta)\gamma^{+i}\,, \\
Q_i(x) &= -\frac{1}{2}(\partial_i\eta)\gamma^{-+} - \frac{1}{2}\eta(\partial_i\eta)\gamma^{-+}\,.
\end{aligned} \tag{3.96}$$

In particular, more explicitly the matrix content is given by

$$P(x) = \begin{pmatrix} P_{11}(x) & 0 & 0 & 0 \\ P_{21}(x) & P_{22}(x) & 0 & 0 \\ 0 & 0 & P_{22}(x) & P_{32}(x) \\ 0 & 0 & 0 & P_{11}(x) \end{pmatrix}, \tag{3.97}$$

where

$$\begin{aligned}
P_{11}(x) &= \frac{5}{16}(\partial_i\eta)^2 + \frac{1}{4}(\partial^2\eta) + \frac{1}{4}\eta(\partial^2\eta)\,, \\
P_{22}(x) &= -\frac{3}{16}(\partial_i\eta)^2 - \frac{1}{4}(\partial^2\eta) - \frac{1}{4}\eta(\partial^2\eta)\,, \\
P_{21}(x) &= \frac{\sqrt{2}}{2}m\left[(\partial_1 + i\partial_2)\eta + \eta(\partial_1 + i\partial_2)\eta\right], \\
P_{32}(x) &= \frac{\sqrt{2}}{2}m\left[(-\partial_1 + i\partial_2)\eta + \eta(-\partial_1 + i\partial_2)\eta\right].
\end{aligned} \tag{3.98}$$

Moreover

$$S(x) = \begin{pmatrix} S_{11}(x) & S_{12}(x) & 0 & 0 \\ 0 & S_{11}(x) & 0 & 0 \\ 0 & 0 & S_{11}(x) & 0 \\ 0 & 0 & S_{43}(x) & S_{11}(x) \end{pmatrix}, \tag{3.99}$$

where

$$S_{11}(x) = 2m\eta\,, \qquad S_{12}(x) = \frac{\sqrt{2}}{2}(\partial_1 - i\partial_2)\eta\,, \qquad S_{43}(x) = -\frac{\sqrt{2}}{2}(\partial_1 + i\partial_2)\eta\,. \tag{3.100}$$

Finally

$$Q_i(x) = Q_{11}(x) \begin{pmatrix} 1 & 0 & 0 & 0 \\ 0 & -1 & 0 & 0 \\ 0 & 0 & -1 & 0 \\ 0 & 0 & 0 & 1 \end{pmatrix}, \qquad Q_{11}(x) = \frac{1}{2}(\partial_i\eta) + \frac{1}{2}\eta(\partial_i\eta)\,. \tag{3.101}$$

The perturbative expansion works as in the bosonic case, apart from an additional factor in the flat space heat kernel coming from the trace over the spinorial indices of the operators. This gives

$$\mathrm{Tr}\, K_\triangle(s) = \mathrm{Tr}\langle xt|e^{\tau\triangle\mathbf{1}}|xt\rangle = \frac{2}{m(4\pi\tau)^{d/2+1}}\,\mathrm{Tr}(\mathbf{1}) = \frac{8}{m(4\pi\tau)^{d/2+1}}\,. \tag{3.102}$$

The formulae (3.66)-(3.68) and (3.71)-(3.78) still apply and we obtain after several computations that in $2+1$ dimensions

$$\sqrt{g}a_4(\not{D}_E^2) = \frac{2}{m(4\pi)^2}\left[\frac{1}{15}\partial^4\eta + \frac{2}{15}\eta(\partial^4\eta) + \frac{13}{30}(\partial_i\eta)(\partial_i\partial^2\eta) + \frac{1}{9}(\partial^2\eta)^2 + \frac{31}{180}(\partial_{ij}\eta)^2 + \mathscr{O}(\eta^3)\right], \tag{3.103}$$

which is recognized to be

$$a_4(\not{D}_E^2) = \frac{1}{8m\pi^2}\left(\frac{11}{360}E_4 - \frac{1}{20}W^2 - \frac{1}{30}D^2R\right). \tag{3.104}$$

The trace anomaly is finally given by

$$\mathscr{A}_{\mathrm{ferm}} = -\frac{1}{2}a_4(\not{D}_E^2)\,. \tag{3.105}$$

3.4 Trace anomaly with particle number background

The background (3.79) is rich enough to allow the computation of non-vanishing curvature invariants, but on the other hand it hides the presence of many terms which can enter the trace anomaly and depend from the gauge field. In particular, in [82] it was shown by means of the Fujikawa technique

in a NC background with a non-vanishing particle number that the trace anomaly was not $U(1)$ gauge invariant.

In order to investigate these issues, we consider a NC background whose data are

$$n_\mu = (1,\mathbf{0})\,, \qquad v^\mu = (1,\mathbf{0})\,, \qquad h_{ij} = \delta_{ij}\,, \qquad A_\mu = (A_0(t,x^i),A_i(t,x^i))\,, \tag{3.106}$$

which in terms of the higher-dimensional metric give

$$G_{MN} = \begin{pmatrix} 0 & 1 & 0 & 0 \\ 1 & 2A_0 & A_1 & A_2 \\ 0 & A_1 & 1 & 0 \\ 0 & A_2 & 0 & 1 \end{pmatrix}, \qquad G^{MN} = \begin{pmatrix} -2A_0 + A_iA_i & 1 & -A_1 & -A_2 \\ 1 & 0 & 0 & 0 \\ -A_1 & 0 & 1 & 0 \\ -A_2 & 0 & 0 & 1 \end{pmatrix}, \tag{3.107}$$

with vielbein

$$e^A_{\ M} = \begin{pmatrix} 1 & A_0 & A_1 & A_2 \\ 0 & 1 & 0 & 0 \\ 0 & 0 & 1 & 0 \\ 0 & 0 & 0 & 1 \end{pmatrix}, \qquad e^M_{\ A} = \begin{pmatrix} 1 & -A_0 & -A_1 & -A_2 \\ 0 & 1 & 0 & 0 \\ 0 & 0 & 1 & 0 \\ 0 & 0 & 0 & 1 \end{pmatrix}. \tag{3.108}$$

In this case the metric is flat apart from the contribution from the gauge connection. This greatly simplifies the spin connection, whose only non-vanishing components are

$$\omega_{++i} = -F_{0i}\,, \qquad \omega_{+ij} = -\frac{1}{2}F_{ij}\,, \qquad \omega_{i+j} = -\frac{1}{2}F_{ij}\,, \tag{3.109}$$

while the non-vanishing components of the Christoffel symbol are

$$\Gamma^-_{\mu\nu} = \frac{1}{2}(v_A)^\sigma (Q_A)_{\mu\nu\sigma}\,, \qquad \Gamma^\rho_{\mu\nu} = \frac{1}{2}h^{\rho\sigma}(Q_A)_{\mu\nu\sigma}\,, \tag{3.110}$$

In this notation, $F = dA$ is the usual field strength while the other quantities are Milne-boost invariants defined in eq. (2.14).

The perturbative expansion of the heat kernel applies to the differential operators computed on this background as well, but now the gauge field is considered to be time-dependent. This requires a generalization of the insertion operators which is performed in Appendices B.3 and B.4, but surprisingly the result is that the formal expression is unchanged and given again by eqs. (3.66)-(3.68) and (3.71)-(3.78).

3.4.1 Boson

The action (2.23) for a Galilean-invariant scalar field reduces on the background (3.106) to

$$S = \int d^3x \left[2im\varphi^\dagger\partial_t\varphi + \varphi^\dagger\partial_i^2\varphi - 2imA_i\varphi^\dagger\partial_i\varphi + \left(2m^2A_0 - m^2A_iA_i - im\partial_iA_i\right)\varphi^\dagger\varphi\right]. \tag{3.111}$$

In order to get the Euclidean space version of this functional, we need to perform a rotation of the gauge field according to[4]

$$A_0 \to A_0 \qquad A_i \to -iA_i\,, \tag{3.112}$$

which gives the imaginary time action

$$S_E = -\int d^3x\,\varphi^\dagger\left[\triangle - 2imA_i\partial_i - 2m^2A_0 - m^2A_iA_i - im(\partial_iA_i)\right]\varphi\,. \tag{3.113}$$

The differential operator in parenthesis is naturally splitted as

$$P(t,x^i) = -2m^2A_0 - m^2A_iA_i - im(\partial_iA_i)\,, \quad S(t,x^i) = 0\,, \quad Q_i(t,x^i) = -2imA_i\,. \tag{3.114}$$

In particular, all insertions containing at least one factor of $S(t,x^i)$ trivially vanish. Summing all the contributions to the a_4 Seeley-De Witt coefficient, we find

$$\mathscr{A}_{\rm bos} = a_4(\mathscr{D}_{\rm bos}) = -\frac{m}{8\pi^2}\left(\frac{1}{3}\partial^2A_0 + \frac{1}{6}B^2 - 2m^2A_0^2 + \mathscr{O}(A_\mu^3)\right), \tag{3.115}$$

where $B = F_{12}$.

3.4.2 Fermion

Similar steps can be followed for the null reduction of the Dirac spinor, whose differential operator in the imaginary time space in the background (3.106) is

$$\not{D}_E^2\Psi = \triangle\Psi - 2m^2A_0\Psi - m^2A_kA_k\Psi - im(\partial_iA_i)\Psi - 2imA_i(\partial_i\Psi) + \tag{3.116}$$

$$-mF_{i0}\gamma^{+i}\Psi - \frac{1}{4}imF_{ij}\gamma^{ij}\Psi + \frac{1}{2}mA_iF_{ij}\gamma^{+j}\Psi + \frac{1}{2}iF_{ij}\gamma^{+j}(\partial_i\Psi) + \frac{1}{4}i(\partial_iF_{ij})\gamma^{+j}\Psi\,.$$

In this way we identify

$$P(t,x^i) = \left[-2m^2A_0 - m^2A_kA_k - im(\partial_iA_i)\right]\mathbf{1} - mF_{i0}\gamma^{+i} - \frac{1}{4}imF_{ij}\gamma^{ij} + \frac{1}{2}mA_iF_{ij}\gamma^{+j} + \frac{1}{4}i(\partial_iF_{ij})\gamma^{+j}\,, \tag{3.117}$$

$$S(t,x^i) = 0\,, \qquad Q_i(t,x^i) = (-2imA_i)\mathbf{1} + \frac{1}{2}iF_{ij}\gamma^{+j}\,, \tag{3.118}$$

[4]The unconventional redefinition of the gauge field in the imaginary time formalism is required by consistency with $[D_\mu, D_\nu] = -imF_{\mu\nu}$ and the prescription $m \to im$. The imaginary mass is required in order to get a positive definite euclidean action.

where the explicit Dirac matrices are

$$\gamma^{+1} = \begin{pmatrix} 0 & \sqrt{2} & 0 & 0 \\ 0 & 0 & 0 & 0 \\ 0 & 0 & 0 & 0 \\ 0 & 0 & -\sqrt{2} & 0 \end{pmatrix}, \; \gamma^{+2} = \begin{pmatrix} 0 & -\sqrt{2}i & 0 & 0 \\ 0 & 0 & 0 & 0 \\ 0 & 0 & 0 & 0 \\ 0 & 0 & -\sqrt{2}i & 0 \end{pmatrix}, \; \gamma^{12} = \begin{pmatrix} -i & 0 & 0 & 0 \\ 0 & i & 0 & 0 \\ 0 & 0 & -i & 0 \\ 0 & 0 & 0 & i \end{pmatrix}. \tag{3.119}$$

From these expressions we extract again the trace anomaly finding

$$a_4(\not{D}_E^2) = -\frac{m}{48\pi^2}B^2 - \frac{m}{6\pi^2}\partial^2 A_0 + \frac{m^3}{\pi^2}A_0^2 + \mathscr{O}(A_\mu^3). \tag{3.120}$$

The trace of the stress-energy tensor is finally given by

$$\mathscr{A}_{\text{ferm}} = -\frac{1}{2}a_4(\not{D}_E^2) = \frac{m}{12\pi^2}\partial^2 A_0 - \frac{m^3}{2\pi^2}A_0^2 + \frac{m}{96\pi^2}B^2 + \mathscr{O}(A_\mu^3). \tag{3.121}$$

3.5 Diffeomorphism anomaly

The heat kernel technique allows not only to compute the trace anomaly corresponding to a given differential operator, but also any other quantum anomaly using the same ζ-function regularization introduced in section 3.1.2. The key point is to investigate the variation

$$\delta\zeta(s,\mathscr{D}) = -s\,\text{Tr}\left((\delta\mathscr{D})\mathscr{D}^{-s-1}\right) \tag{3.122}$$

under the classical symmetry whose quantum anomaly we want to compute.

For simplicity, we are interested to study the diffeomorphism anomaly for a non-relativistic free scalar, whose associated Euclidean differential operator is

$$\mathscr{D}\varphi = imv^\mu D_\mu\varphi + \frac{im}{\sqrt{g}}D_\mu\left(\sqrt{g}v^\mu\varphi\right) - \frac{1}{\sqrt{g}}D_\mu\left(\sqrt{g}h^{\mu\nu}D_\nu\varphi\right). \tag{3.123}$$

We specialize again to the flat background with generic gauge field, in which case the differential operator becomes

$$\mathscr{D}_0 = 2im\partial_0 - \partial_i^2 + 2m^2A_0 + m^2A_iA_i + 2imA_i\partial_i + im(\partial_iA_i). \tag{3.124}$$

Its variation under diffeomorphisms is

$$\begin{aligned}\delta\mathscr{D}_0 \;=\; & -2im(\partial_0\varepsilon^\mu)\partial_\mu + 2(\partial_i\varepsilon^\mu)\partial_i\partial_\mu + (\partial_i^2\varepsilon^\mu)\partial_\mu + 2m^2\varepsilon^\mu(\partial_\mu A_0) \\ & + 2im\varepsilon^\mu(\partial_\mu A_i)\partial_i - 2imA_i(\partial_i\varepsilon^\mu)\partial_\mu + im\varepsilon^\mu(\partial_i\partial_\mu A_i) + 2m^2A_i\varepsilon^\mu(\partial_\mu A_i). \end{aligned} \tag{3.125}$$

Using these expressions inside eq. (3.122), we would be able to find after some steps the corresponding diffeomorphism anomaly from the heat kernel expansion. Before proceeding with the calculation, it is convenient to perform a trick. We notice that eq. (3.122) is a trace, and as such it is invariant under the similarity transformation

$$\zeta(s,\tilde{\mathscr{D}}) = \zeta(s,\mathscr{D}) \qquad \text{if} \quad \tilde{\mathscr{D}} = e^{\hat{O}}\mathscr{D}e^{-\hat{O}}, \tag{3.126}$$

because the operators $\mathscr{D}$ and $\tilde{\mathscr{D}}$ have the same functional determinant.

In particular, when dealing with diffeomorphisms, it is convenient to consider

$$\hat{O} = \alpha\xi^{\mu}\partial_{\mu}\,, \tag{3.127}$$

with α a real coefficient and ξ^{μ} transforming under diffeomorphisms as $\delta\xi^{\mu} = \varepsilon^{\mu}$.

In this way we obtain

$$\begin{aligned}\tilde{\mathscr{D}}_0 = e^{\alpha\xi^{\mu}\partial_{\mu}}\mathscr{D}_0 e^{-\alpha\xi^{\nu}\partial_{\nu}} = \mathscr{D}_0 &- 2im\alpha(\partial_0\xi^{\mu})\partial_{\mu} + 2\alpha(\partial_i\xi^{\mu})\partial_i\partial_{\mu} + \alpha(\partial_i^2\xi^{\mu})\partial_{\mu} \\ &+ 2m^2\alpha\xi^{\mu}(\partial_{\mu}A_0) + 2m^2\alpha A_i\xi^{\mu}(\partial_{\mu}A_i) + 2im\alpha\xi^{\mu}(\partial_{\mu}A_i)\partial_i \\ &+ im\alpha\xi^{\mu}(\partial_{\mu}\partial_i A_i) - 2im\alpha A_i(\partial_i\xi^{\mu})\partial_{\mu} + \mathscr{O}(\xi^2)\,.\end{aligned} \tag{3.128}$$

Using eq. (3.125) and setting $\alpha = -1$, we obtain $\delta\tilde{\mathscr{D}}_0 = 0$, which in turn implies $\delta W^{\text{ren}} = 0$, and therefore there is no gravitational anomaly

$$\langle\partial_{\mu}T^{\mu}_{\nu}\rangle = 0\,. \tag{3.129}$$

3.6 Comments and discussion

It is interesting to compare the results for the non-relativistic complex scalar and the fermion among themselves and with the $3+1$ dimensional relativistic parents. The general structure of the trace anomaly is

$$\mathscr{A} = \frac{1}{360(4\pi^2)}\left(-aE_4 + cW^2_{MNPQ} + bR^2 + dD^2R\right) + \dots\,, \tag{3.130}$$

where the coefficients for the cases of interest are reported in the table below. The dots refer to the possible terms in the other sectors of the non-relativistic trace anomaly and to the possible $U(1)$ gauge and Milne-boost violating terms, which we comment later.

First of all, we stress that the curvature invariants entering the trace anomaly are computed in $3+1$ dimensions in the relativistic case, while they are null reduced to $2+1$ dimensions in the non-relativistic one. In particular, in the latter case they can be expressed only in terms of NC geometric data, without referring in any way to higher-dimensional quantities. In the bosonic case, the parameter ξ is the coupling with the Ricci scalar, which both in the conformal and in the Schrödinger cases turns out to be $\xi = 1/6$. If ξ assumes this value, we observe that the b coefficient vanishes both for

Spin	**a**	**c**	**b**	**d**
0 (relativistic real scalar)	1	3	$180\left(\xi-\frac{1}{6}\right)^2$	$12\left(5\xi-1\right)$
0 (non-rel. complex scalar)	$\frac{2}{m}$	$\frac{6}{m}$	$\frac{360}{m}\left(\xi-\frac{1}{6}\right)^2$	$\frac{24}{m}\left(5\xi-1\right)$
$\frac{1}{2}$ (relativistic Dirac)	11	18	0	12
$\frac{1}{2}$ (non-rel. fermion)	$\frac{11}{m}$	$\frac{18}{m}$	0	$\frac{12}{m}$

Table 3.1: Coefficients of the trace anomaly for free fields with various spins.

the scalar and the fermionic cases, because the R^2 term is forbidden by Wess-Zumino consistency conditions. The coefficient d is instead non-vanishing but refers to the curvature invariant D^2R, which is scheme-dependent and then less interesting because it does not contain universal informations of the RG flow. Finally, the a,c coefficients are scheme-independent anomalies and the first one is a candidate for a non-relativistic version of the a-theorem.

The comparison with the relativistic parent shows that the coefficients are the same, apart from an overall normalization $1/m$ depending only from the $U(1)$ mass of the non-relativistic particle[5]. A natural guess for an a-theorem in the case where the only degrees of freedom involved in the physical system are scalars and spin $1/2$ fermions would be

$$a_{\rm UV} \propto \sum_{\rm scalars}^{\rm UV} \frac{1}{m} + \frac{11}{2} \sum_{\rm fermions}^{\rm UV} \frac{1}{m} \geq \sum_{\rm scalars}^{\rm IR} \frac{1}{m} + \frac{11}{2} \sum_{\rm fermions}^{\rm IR} \frac{1}{m} \propto a_{\rm IR}\,. \tag{3.131}$$

In Galilean-invariant theories the mass of a bound state is equal to the sum of the masses of the elementary constituents: no bound-state contribution is present as in the relativistic case. The $1/m$ dependence may give a quantitative formulation to the physical intuition that bound states should form in the IR: as energy is added, bound states tend to be broken.

Now we comment on the additional terms found in eqs. (3.115) and (3.121) when a particle number background is turned on. First of all, we observe that the terms entering the trace anomaly are the same for the bosonic and the fermionic case, which confirms that the structure of the expression is universal. In both cases, the result is not invariant either under Milne boosts nor under gauge transformations. Since there is a strong relation between these symmetries[6], it is not surprising that the violation of one of them entails the violation of the other.

As was done in the case with background (3.79), we should try to express the resulting anomaly as a combination of terms which are invariant under the non-relativistic symmetries, but since two of them are violated, we should at least try to obtain a diffeomorphism-invariant combination. A possibility is that the terms containing only the temporal component of the gauge field A_0 arise from

[5]The scalar field also differs for a factor of 2 because in the relativistic case we put the result for a real field, while the Galilean case necessarily requires a complex field, due to the $U(1)$ mass conservation.

[6]In the Bargmann algebra, the commutator of the momentum and a boost is the particle number generator.

the combination $v^\mu A_\mu$, which is a scalar and has the correct scaling dimension. In this way, the term

$$\partial^2 A_0 = \partial^2 (v^\mu A_\mu) \tag{3.132}$$

can be reabsorbed by a local counterterm proportional to $Rv^\mu A_\mu$ in the vacuum functional. This is not possible for the term $A_0^2 = (v^\mu A_\mu)^2$, which is instead a genuine type B anomaly.

Both in the free scalar and free fermion examples, the field A_0 plays the role of an external chemical potential for the particle number J_0; in the multiple species case, J_0 plays the role of mass density. Moreover, studying geodesics in a NC background, one sees that A_0 can also be identified as the Newtonian gravitational potential. On physical ground one would expect mass conservation in an external gravitational field. On the other hand, the breaking of gauge invariance in eqs. (3.115) and (3.121) may hint a violation of the conservation of the $U(1)$ current, which would not be consistent with the physical intuition. For these reasons, we think that this topic deserves further future investigations to understand the precise mechanism responsible for these results.

Chapter 4

Non-relativistic Supersymmetry

The work in this chapter has previously appeared in [86].

Anomalies are a powerful tool to investigate dualities and non-trivial properties of a physical system, such as the irreversibility properties of the RG flow controlled by the trace anomaly which we studied in chapters 2, 3. In this context, another powerful tool which allows to investigate dualities and to obtain non-perturbative results is Supersymmetry (SUSY), an invariance which rotates bosons into fermions and viceversa. In the relativistic case, SUSY gives strong constraints on the quantum corrections of physical theories, giving rise to the non-renormalization theorem and many other exact results [31, 32].

In the previous chapters we introduced the group of symmetries for non-relativistic systems and we observed that many interesting results about the irreversibility of the RG flow could be investigated for these systems. Similarly, it is interesting to understand if some exact results coming from the SUSY invariance can be inherited from the relativistic case, and if the intertwining with the Schrödinger group can give even further restrictions on the quantum corrections of such systems.

The study of such systems can also be interesting from the point of view of holography: in fact, most of the examples where AdS/CFT correspondence is verified are supersymmetric. SUSY may allow to gain control on non-relativistic holography and suggest the way to build explicit top-down examples.

Furthermore, we know that non-relativistic systems are well understood from the point of view of experimental realizations: we may hope to find some hints to understand if SUSY is a fundamental invariance that is broken at low energies, if it arises at low energies as an enhanced symmetry or if it plays any other important role in high energy physics.

SUSY extensions of the Galilean algebra were first introduced in 3+1 dimensions [41], where two super-Galilean algebras were constructed, $\mathscr{S}_1\mathscr{G}$ which includes a single two-component spinorial supercharge and $\mathscr{S}_2\mathscr{G}$, which contains two supercharges. There are various ways to find such gradations of the Galilean algebra. One method consists in performing the Inönü-Wigner contraction

of the $\mathcal{N}=1$ and $\mathcal{N}=2$ Super-Poincaré algebras in the $c\to\infty$ limit[1]. On the other hand, $\mathscr{S}_2\mathscr{G}$ can be obtained performing a null reduction of the super-Poincarè algebra in 4+1 dimensions. It turns out that $\mathscr{S}_1\mathscr{G}\subset\mathscr{S}_2\mathscr{G}$.

In this chapter we will apply the DLCQ prescription to build a theory with $\mathscr{S}_2\mathscr{G}$ invariance in $2+1$ dimensions, obtained from the $3+1$ dimensional $\mathcal{N}=1$ relativistic Wess-Zumino model. We will show that a non-vanishing superpotential is allowed only when considering at least two species of chiral fields and in this context we will investigate the renormalization properties of this Galilean Wess-Zumino model in order to compare with the relativistic non-renormalization theorem. We anticipate the remarkable UV properties of this model:

- like the relativistic parent, the model is renormalizable and the superpotential term does not acquire quantum corrections,
- unlike the relativistic parent, there is strong evidence that the whole renormalization of the two-point function is just at one loop (we check this claim explicitly up to four loops and discuss in general higher orders). This remarkable property is due to the $U(1)$ symmetry associated to the non-relativistic particle number conservation, which constrains the number of diagrams at a given perturbative order. Moreover, the causal structure strongly reduces the number of non-vanishing diagrams.

As a consequence of these two properties, we will build a set of selection rules which will simplify the analysis of the allowed quantum corrections.

4.1 Non-relativistic supersymmetry algebra

We start with the graded generalization of the Galilean algebra in $2+1$ dimensions containing two complex supercharges, which leads to the invariance under the $\mathscr{S}_2\mathscr{G}$ group. The algebra is[2]

$$\begin{aligned}
&[P_j,K_k]=i\delta_{jk}M\,,\qquad [H,K_j]=iP_j\,,\\
&[P_j,J]=-i\varepsilon_{jk}P_k\,,\qquad [K_j,J]=-i\varepsilon_{jk}K_k\,,\qquad\qquad j,k=1,2
\end{aligned}\tag{4.1}$$

$$\begin{aligned}
&[Q,J]=\tfrac{1}{2}Q\,,\qquad \{Q,Q^\dagger\}=\sqrt{2}M\,,\\
&[\tilde{Q},J]=-\tfrac{1}{2}\tilde{Q}\,,\quad [\tilde{Q},K_1-iK_2]=-iQ\,,\quad \{\tilde{Q},\tilde{Q}^\dagger\}=\sqrt{2}H\,,\\
&\{Q,\tilde{Q}^\dagger\}=-(P_1-iP_2)\,,\quad \{\tilde{Q},Q^\dagger\}=-(P_1+iP_2)\,.
\end{aligned}\tag{4.2}$$

[1] When performing this procedure, divergent expressions in the speed of light appear and we need to introduce some subtraction terms via a chemical potential and by appropriately rescaling the fields [12].

[2] We remark that in the model we are going to consider, the presence of an R-symmetry is not necessary in the algebra. In fact, in the upcoming non-perturbative proof on the non-renormalization theorem (see sections 4.2.3, 4.4.5), we will need to assume that the theory in the UV after promoting the couplings to background superfields will possess a $U(1)_R$ symmetry, but nothing is required on the original model. Since in all the evaluations for the Galilean WZ model the grassmannian part of the superfields and of the supercharges is unaffected, this requirement is analog with the same argument applied in the relativistic case.

Here P_j are the spatial components of the momentum, K_j are the generators of Galilean boosts, J is the planar angular momentum and $Q, \tilde{Q}$ are the two complex supercharges. The central charge M corresponds to the mass or particle number conservation[3].

The $\mathscr{S}_2\mathscr{G}$ algebra can be obtained in different ways. We can start with the non-relativistic Galilean algebra, add two supercharges and impose consistency conditions (this was done in $3+1$ dimensions [41]). Alternatively, we can perform the Inönü-Wigner contraction of the $2+1$ dimensional super-Poincarè algebra in the $c \to \infty$ limit [87]. Finally, it can be obtained by null reduction of $\mathscr{N}=1$ super-Poincaré in $3+1$ dimensions. We will follow the last approach, since it is the most convenient for constructing the non-relativistic $\mathscr{N}=2$ superspace.

4.1.1 Null reduction from the $\mathscr{N}=1$ SUSY algebra in $3+1$ dimensions

In order to perform the null reduction of the $\mathscr{N}=1$ SUSY algebra in $3+1$ dimensions, we introduce light-cone coordinates in the parent theory in such a way that the spacetime is parametrized by

$$x^M = (x^-, x^+, x^1, x^2) \equiv (x^-, x^\mu) \qquad x^\pm = \frac{x^3 \pm x^0}{\sqrt{2}}. \tag{4.3}$$

In flat Minkowski space, the DLCQ method is realized by compactifying x^- on a small circle of radius R. For convenience, we rescale $x^- \to x^-/R$ in such a way that the rescaled coordinate is adimensional, and consequently we also rescale $x^+ \to R x^+$ in order for the metric tensor to be dimensionless.

It is well known that the bosonic part of the super-Poincaré algebra reduces to the Bargmann algebra (4.1) by identifying some components of the linear and angular momenta with the central charge and the boost operator [13, 14]. The fermionic part of the algebra requires to consider the relativistic anticommutator $\{\mathscr{Q}_\alpha, \bar{\mathscr{Q}}_{\dot\beta}\} = i\sigma^M_{\alpha\dot\beta}\partial_M$ and write the r.h.s. in terms of light-cone derivatives[4] $\partial_\pm = \frac{1}{\sqrt{2}}(\partial_3 \pm \partial_0)$

$$\{\mathscr{Q}, \bar{\mathscr{Q}}\} = i \begin{pmatrix} \sqrt{2}\partial_+ & \partial_1 - i\partial_2 \\ \partial_1 + i\partial_2 & -\sqrt{2}\partial_- \end{pmatrix}. \tag{4.4}$$

We also require that any local function of the spacetime coordinates is decomposed into a non-relativistic field plus a phase according to eq. (2.7), m being the dimensionless parameter associated to the $U(1)$ mass conservation. In this way we have a dictionary for the spacetime derivatives

$$\partial_+ \to \partial_t\,, \qquad \partial_- \to im\,. \tag{4.5}$$

In addition, we interpret the two-components complex Weyl spinors in 3+1 dimensions as complex Grassmann scalars in 2+1 dimensions, according to the identification $\mathscr{Q}_\alpha \to Q_\alpha$, $\bar{\mathscr{Q}}_{\dot\beta} \to Q^\dagger_\beta$.

[3] When we consider the coupling with a curved NC background, this is the responsibile for the appeareance of the $U(1)$ gauge field in the metric data.

[4] For conventions on four-dimensional spinors and light-cone coordinates, see appendix A.

Combining all these rules we obtain the algebra

$$\begin{aligned} &\{Q_1, Q_1^\dagger\} = \sqrt{2} i \partial_t = \sqrt{2} H\,, && \{Q_1, Q_2^\dagger\} = i(\partial_1 - i\partial_2) = -(P_1 - iP_2)\,, \\ &\{Q_2, Q_1^\dagger\} = i(\partial_1 + i\partial_2) = -(P_1 + iP_2)\,, && \{Q_2, Q_2^\dagger\} = -\sqrt{2} i \partial_- = \sqrt{2} m\,, \end{aligned} \tag{4.6}$$

which is identical to (4.2) upon the identifications[5]

$$Q_1 = \tilde{Q}\,, \qquad Q_1^\dagger = \tilde{Q}^\dagger\,, \qquad Q_2 = Q\,, \qquad Q_2^\dagger = Q^\dagger\,, \tag{4.7}$$

and m with the eigeinvalue of the U(1) generator M.

It is instructive to look at the similar case of a Kaluza-Klein reduction from $3+1$ dimensional $\mathcal{N}=1$ SUSY algebra to the $2+1$ dimensional $\mathcal{N}=2$ SUSY algebra. In this case we start from the same anticommutation rules $\{\mathcal{Q}_\alpha, \bar{\mathcal{Q}}_{\dot\beta}\} = -\sigma^M_{\alpha\dot\beta} P_M$, but we compactify along the x^3 direction with momentum $p_3 \equiv Z$. The result is [88]

$$\{\mathcal{Q}_\alpha, \mathcal{Q}_\beta^\dagger\} = -\sigma^\mu_{\alpha\beta} P_\mu + i\varepsilon_{\alpha\beta} Z \tag{4.8}$$

where $\mu = 0,1,2$ and Z plays the role of a central term. This expression is very similar to the one found in the non-relativistic case, eq. (4.6) with m playing the role of a central charge. However, while in the relativistic reduction a central term appears in the fermionic part of the algebra when we reduce the number of dimensions, in the non-relativistic case the central charge is produced already in the bosonic sector (without requiring any SUSY extension) and accounts for the physical fact that in non-relativistic theories the particle number is a conserved quantity.

4.1.2 Non-relativistic superspace

In the context of relativistic QFT, the superfield formulation is a nice tool which allows to build actions and quantities automatically invariant under the SUSY transformations. In this context, fields belonging to the same multiplet are organized in a unique superfield, and the spacetime coordinates are supplemented by additional Grassmann coordinates which compose the superspace. We want to apply this technique to the $\mathcal{N}=2$ non-relativistic superspace by applying the null reduction to the $\mathcal{N}=1$ formulation in $3+1$ dimensions. The non-relativistic superspace was first introduced in four dimensions [43, 44], whereas previous constructions in three dimensions based on different techniques can be found in [46, 89].

[5] We note that identification (4.7) is required to obtain the correct anticommutators $\{Q, Q^\dagger\}$ and $\{\tilde{Q}, \tilde{Q}^\dagger\}$, but it interchanges $(P_1 + iP_2)$ and $(P_1 - iP_2)$ in the mixed anticommutators. This is simply due to the fact that we chose x^- as the compact light-cone coordinate. Had we chosen x^+ we would have obtained exactly the algebra in (4.2). Since having $(P_1 + iP_2)$ and $(P_1 - iP_2)$ interchanged does not affect our construction, we take x^- as the compact direction being this a more conventional choice in the literature.

We start with the set of superspace coordinates $(x^M, \theta^\alpha, \bar\theta^{\dot\alpha})$ and we take the explicit realization of the super-Poincaré algebra in terms of the following supercharges[6]

$$\mathscr{Q}_\alpha = i\frac{\partial}{\partial\theta^\alpha} - \frac{1}{2}\bar\theta^{\dot\beta}\partial_{\alpha\dot\beta}\,, \qquad \bar{\mathscr{Q}}_{\dot\alpha} = -i\frac{\partial}{\partial\bar\theta^{\dot\alpha}} + \frac{1}{2}\theta^\beta\partial_{\beta\dot\alpha} \tag{4.9}$$

and SUSY covariant derivatives

$$\mathscr{D}_\alpha = \frac{\partial}{\partial\theta^\alpha} - \frac{i}{2}\bar\theta^{\dot\beta}\partial_{\alpha\dot\beta}\,, \qquad \bar{\mathscr{D}}_{\dot\alpha} = \frac{\partial}{\partial\bar\theta^{\dot\alpha}} - \frac{i}{2}\theta^\beta\partial_{\beta\dot\alpha}\,, \tag{4.10}$$

which act on local superfields $\Psi(x^M, \theta^\alpha, \bar\theta^{\dot\alpha})$.

The $\mathscr{N} = 2$ non-relativistic superspace in 2+1 dimensions can be obtained with a suitable generalization of the null reduction prescription that we used to treat separately bosons and fermions in chapter 2, and to obtain the algebra in the previous section. We consider light-cone coordinates and rewrite $\partial_{\alpha\dot\beta} = \sigma^M_{\alpha\dot\beta}\partial_M$ in (4.9, 4.10) in terms of $\partial_\pm, \partial_1, \partial_2$. Since supersymmetry requires each field component of a multiplet to be an eigenfunction of the ∂_- operator with the same eigenvalue m, the reduction can be done directly at the level of superfields, by requiring a decomposition of the fields as

$$\Psi(x^M, \theta^\alpha, \bar\theta^{\dot\alpha}) = e^{imx^-}\tilde\Psi(x^+ \equiv t, x^i, \theta^\alpha, (\theta^\alpha)^\dagger)\,. \tag{4.11}$$

Acting on these superfields with supercharges and covariant derivatives (4.9, 4.10) rewritten in terms of light-cone derivatives, and performing the identification $\partial_+ \equiv \partial_t$ and $\partial_- \equiv iM$ (with eigenvalue m), we obtain[7]

$$\begin{cases} Q_1 = i\frac{\partial}{\partial\theta^1} - \frac{1}{2}\bar\theta^2(\partial_1 - i\partial_2) - \frac{1}{\sqrt2}\bar\theta^1\partial_t \\ \bar Q_1 = -i\frac{\partial}{\partial\bar\theta^1} + \frac{1}{2}\theta^2(\partial_1 + i\partial_2) + \frac{1}{\sqrt2}\theta^1\partial_t \\ Q_2 = i\frac{\partial}{\partial\theta^2} - \frac{1}{2}\bar\theta^1(\partial_1 + i\partial_2) - \frac{i}{\sqrt2}\bar\theta^2 M \\ \bar Q_2 = -i\frac{\partial}{\partial\bar\theta^2} + \frac{1}{2}\theta^1(\partial_1 - i\partial_2) - \frac{i}{\sqrt2}\theta^2 M \end{cases} \qquad \begin{cases} D_1 = \frac{\partial}{\partial\theta^1} - \frac{i}{2}\bar\theta^2(\partial_1 - i\partial_2) - \frac{i}{\sqrt2}\bar\theta^1\partial_t \\ \bar D_1 = \frac{\partial}{\partial\bar\theta^1} - \frac{i}{2}\theta^2(\partial_1 + i\partial_2) - \frac{i}{\sqrt2}\theta^1\partial_t \\ D_2 = \frac{\partial}{\partial\theta^2} - \frac{i}{2}\bar\theta^1(\partial_1 + i\partial_2) - \frac{1}{\sqrt2}\bar\theta^2 M \\ \bar D_2 = \frac{\partial}{\partial\bar\theta^2} - \frac{i}{2}\theta^1(\partial_1 - i\partial_2) - \frac{1}{\sqrt2}\theta^2 M\,. \end{cases} \tag{4.12}$$

These operators realize a representation of the non-relativistic algebra (4.2) and can be interpreted as the supercharges and the covariant derivatives of a three-dimensional $\mathscr{N} = 2$ superspace described by coordinates $(t, x^1, x^2, \theta^1, \theta^2, \bar\theta^1, \bar\theta^2)$. Correspondingly, the functions $\tilde\Psi$ in (4.11) are three-dimensional $\mathscr{N} = 2$ superfields realizing a representation of the non-relativistic SUSY algebra[8].

We point out that the non-relativistic superspace and the corresponding supercharges could be alternatively constructed by quotienting the SUSY extension of the Bargmann algebra by the subgroup

[6] Superspace conventions are discussed in Appendix A.

[7] From now on we rename $(\theta^\alpha)^\dagger \equiv \bar\theta^\alpha$ and similarly for the other grassmannian quantities.

[8] While the structure of the non-relativistic supercharges may suggest the appearance of an interesting complex structure, we did not find any useful consequence of their particular form. In fact, the dependence from $z = x^1 + ix^2$ and $\bar z = x^1 - ix^2$ does not seem separable, and we did not find any remarkable holomorphic dependence among the relevant objects of the theory. The change of variables $(x^1, x^2) \to (z, \bar z)$ seems only a useful computational way to gather the spatial dependence, but does not play a meaningful role in the supergraph formulation.

of spatial rotations and Galilean boosts, in analogy with the construction of the relativistic superspace as the quotient super-Poincaré$/SO(1,3)$. However, we used the null reduction method for convenience because it refers to the quotient algebra already found in $3+1$ dimensions, and the analogy with this case is also helpful in view of the investigation of the renormalization pattern of the model and of the holomorphic properties of the superpotential.

As in the relativistic case, imposing suitable constraints we can reduce the number of superfield components and realize irreducible representations of the superalgebra. In particular, we are interested in the construction of (anti)chiral superfields. These can be obtained either by null reduction of the four-dimensional (anti)chiral superfields, $\bar{\mathscr{D}}_{\dot{\alpha}}\Sigma = 0$ ($\mathscr{D}_\alpha\bar{\Sigma} = 0$), or directly in three-dimensional superspace by imposing

$$\bar{D}_\alpha\Sigma = 0, \qquad\qquad D_\alpha\bar{\Sigma} = 0 \tag{4.13}$$

where the covariant derivatives are given in (4.12).

Defining coordinates

$$x^\mu_{L,R} = x^\mu \mp i\theta^\alpha(\bar{\sigma}^\mu)_{\alpha\beta}\bar{\theta}^\beta \qquad\qquad \mu = +,1,2 \tag{4.14}$$

which satisfy $\bar{D}_\alpha x^\mu_L = 0, D_\alpha x^\mu_R = 0$, the (anti)chiral superfields have the following expansion

$$\Sigma(x^\mu_L,\theta^\alpha) = \varphi(x^\mu_L) + \theta^\alpha\tilde{\psi}_\alpha(x^\mu_L) - \theta^2 F(x^\mu_L) \tag{4.15}$$

$$\bar{\Sigma}(x^\mu_R,\bar{\theta}^\beta) = \bar{\varphi}(x^\mu_R) + \bar{\theta}_\gamma\tilde{\bar{\psi}}^\gamma(x^\mu_R) - \bar{\theta}^2\bar{F}(x^\mu_R) \tag{4.16}$$

We are now ready to build automatically SUSY-invariant actions using the Berezin integration on spinorial coordinates. In the relativistic setting, we can define for a generic superfield Ψ the term

$$\int d^4x d^4\theta\,\Psi = \int d^4x\,\mathscr{D}^2\bar{\mathscr{D}}^2\Psi\Big|_{\theta=\bar{\theta}=0} \tag{4.17}$$

with covariant derivatives given in (4.10). Performing the null reduction and extracting the x^- dependence of the superfield by setting $\Psi = e^{imx^-}\tilde{\Psi}$, we obtain the prescription for the Berezin integrals in the non-relativistic superspace

$$\begin{aligned}&\int d^4x d^4\theta\,\Psi = \int d^4x\,\mathscr{D}^2\bar{\mathscr{D}}^2\Psi\Big|_{\theta=\bar{\theta}=0} \longrightarrow \\ &\int d^3x D^2\bar{D}^2\tilde{\Psi}\Big|_{\theta=\bar{\theta}=0} \times \frac{1}{2\pi}\int_0^{2\pi} dx^-\,e^{imx^-} \equiv \int d^3x d^4\theta\,\tilde{\Psi} \times \frac{1}{2\pi}\int_0^{2\pi} dx^-\,e^{imx^-}\end{aligned} \tag{4.18}$$

where in the r.h.s. $d^3x \equiv dt\,dx^1dx^2$ and the spinorial derivatives are the ones in eq. (4.12). It is immediate to observe that whenever $m \neq 0$ we obtain a trivial reduction due to the x^- integral. Non-vanishing expressions arise only if the super-integrand Ψ is uncharged respect to the mass generator. In the construction of SUSY invariant actions this is equivalent to require the action to be invariant under one extra global U(1) symmetry [44]. This immediately shows that a superpotential term is

admitted in non-relativistic theories only when at least two species of chiral superfields are considered in the matter content.

4.2 Review of the relativistic Wess-Zumino model

In this Section we will briefly review the renormalization properties of the $3+1$ dimensional relativistic Wess-Zumino (WZ) model. In particular, we will set up the conventions for the study of the system both in superspace and component formulation, and we will recall the supergraph technique, which is very useful to simplify the computation of the quantum corrections. The same techniques will be adopted in the non-relativistic context in the next section.

The classical action [90] is given by

$$S = \int d^4x d^4\theta\, \bar{\Sigma}\Sigma + \int d^4x d^2\theta \left(\frac{m}{2}\Sigma^2 + \frac{\lambda}{3!}\Sigma^3\right) + \text{h.c.} \tag{4.19}$$

and describes the dynamics of the field components of a chiral superfield $\Sigma = (\phi, \psi, F)$. In anticipation of the non-relativistic case, we focus on the massless model $m = 0$, which is simpler to study but is general enough to find interesting results. With this choice, the model is classically scale invariant (λ is a dimensionless coupling).

When using the explicit decomposition of the chiral superfield into its components via eq. (A.18), the action becomes

$$S = \int d^4x \Big[-\partial^M \bar{\phi}\, \partial_M \phi + i\bar{\psi}\bar{\sigma}^M \partial_M \psi + \bar{F}F + \left(3\lambda F\phi^2 - 3\lambda\, \psi^\alpha \psi_\alpha \phi + \text{h.c.}\right) \Big] . \tag{4.20}$$

This is manifestly invariant under $\mathscr{N} = 1$ SUSY transformations

$$\delta_\varepsilon \Sigma = \left[i\varepsilon^\alpha \mathscr{Q}_\alpha + i\bar{\varepsilon}_{\dot{\alpha}} \bar{\mathscr{Q}}^{\dot{\alpha}}, \Sigma \right] , \tag{4.21}$$

which in component form read

$$\begin{cases} \delta_\varepsilon \phi = -\varepsilon^\alpha \psi_\alpha \\ \delta_\varepsilon \psi_\alpha = i\bar{\varepsilon}^{\dot{\alpha}} (\partial_{\alpha\dot{\alpha}} \phi) + \varepsilon_\alpha F \\ \delta_\varepsilon F = -i\bar{\varepsilon}^{\dot{\alpha}} \partial_{\alpha\dot{\alpha}} \psi^\alpha . \end{cases} \tag{4.22}$$

4.2.1 Renormalization in superspace

The quantization of the theory is performed by considering the generating functional

$$Z[J, \bar{J}] = \int \mathscr{D}\Sigma\, \mathscr{D}\bar{\Sigma} \exp\left\{ i \left(S + \int d^2\theta\, J\Sigma + \int d^2\bar{\theta}\, \bar{J}\bar{\Sigma} \right) \right\} , \tag{4.23}$$

where $J, \bar{J}$ are chiral and anti-chiral superfields acting as sources, respectively. Since they are constrained by the requirement of being annihilated by half of the supercharges, when performing the functional differentiation we need to require that

$$\frac{\delta J(z_i)}{\delta J(z_j)} = \bar{\mathscr{D}}^2\, \delta^{(8)}(z_i - z_j)\,, \qquad \frac{\delta \bar{J}(z_i)}{\delta \bar{J}(z_j)} = \mathscr{D}^2\, \delta^{(8)}(z_i - z_j)\,, \tag{4.24}$$

where $z \equiv (x^M, \theta^\alpha, \bar{\theta}^{\dot{\alpha}})$ and $\delta^{(8)}(z_i - z_j) \equiv \delta^{(4)}(x_i - x_j)\delta^{(2)}(\theta_i - \theta_j)\delta^{(2)}(\bar{\theta}_i - \bar{\theta}_j)$. The constraints are responsible for the appearance of the covariant derivatives., which will play an important role in the manipulations of the perturbative computations.

The superfield formulation is not only useful to write automatically SUSY-invariant actions and find the SUSY variation of the fields, but also to perform the computation of quantum corrections. In fact, it turns out that the Feynman diagrams can be collected and organized in a systematic way by associating Feynman rules directly to the superfields. Only when performing the algebra of covariant derivatives (D-algebra), they reduce to ordinary graphs for the component fields. The super-Feynman rules for the massless WZ model are [91]

- Superfield propagator

$$\langle \Sigma(z_i)\bar{\Sigma}(z_j)\rangle = \frac{1}{\Box}\,\delta^{(8)}(z_i - z_j) \;\longrightarrow\; \langle \Sigma(p)\bar{\Sigma}(-p)\rangle = -\frac{1}{p^2}\,\delta^{(4)}(\theta_i - \theta_j)\,. \tag{4.25}$$

- Vertices. The are read directly from the interacting Lagrangian: the massless WZ model contains only cubic vertices with chiral or anti-chiral superfields. The rule (4.24) implies that we assign a factor of $\bar{\mathscr{D}}^2$ ($\mathscr{D}^2$) to every internal line exiting from a chiral (anti-chiral) vertex. Moreover, we use one of these factors to complete a chiral (anti-chiral) integral at the vertex, in such a way that we only have $\int d^4\theta$ integrals at each vertex.

At this point, we perform the D-algebra: we get rid of the integration along the Grassmann variables using the spinorial delta functions in order to reach a result given by a local function of $(\theta, \bar{\theta})$ integrated in a single $d^4\theta$. In order to obtain such a local function, we need to take into account the residual covariant derivatives $\mathscr{D}$'s or $\bar{\mathscr{D}}$'s acting on the internal lines and use the identities (we call for convenience $\delta_{ij} \equiv \delta^{(2)}(\theta_i - \theta_j)\,\delta^{(2)}(\bar{\theta}_i - \bar{\theta}_j)$)

$$\delta_{ij}\delta_{ij} = 0\,, \qquad \delta_{ij}\mathscr{D}^\alpha\delta_{ij} = 0\,, \qquad \delta_{ij}\mathscr{D}^2\delta_{ij} = 0\,, \qquad \delta_{ij}\mathscr{D}^\alpha\bar{\mathscr{D}}^{\dot{\alpha}}\delta_{ij} = 0\,, \qquad \delta_{ij}\mathscr{D}^\alpha\bar{\mathscr{D}}^2\delta_{ij} = 0\,,$$

$$\delta_{ij}\mathscr{D}^\alpha\bar{\mathscr{D}}^2\mathscr{D}^\beta\delta_{ij} = -\varepsilon^{\alpha\beta}\delta_{ij}\,, \qquad \delta_{ij}\mathscr{D}^2\bar{\mathscr{D}}^2\delta_{ij} = \delta_{ij}\bar{\mathscr{D}}^2\mathscr{D}^2\delta_{ij} = \delta_{ij}\frac{\mathscr{D}^\alpha\bar{\mathscr{D}}^2\mathscr{D}_\alpha}{2}\delta_{ij} = \delta_{ij}\,. \tag{4.26}$$

A careful analysis reveals that the D-algebra method must be applied until we reach a configuration in which exactly two $\mathscr{D}$'s and two $\bar{\mathscr{D}}$'s survive in each loop. This amounts to integrate by parts spinorial derivatives at the vertices and trade products of them with space-time derivatives through commutation

rules like

$$[\mathscr{D}^\alpha, \bar{\mathscr{D}}^2] = i\partial^{\alpha\dot{\alpha}}\bar{\mathscr{D}}_{\dot{\alpha}}\,, \quad [\bar{\mathscr{D}}^{\dot{\alpha}}, \mathscr{D}^2] = -i\partial^{\alpha\dot{\alpha}}\mathscr{D}_\alpha\,, \quad \mathscr{D}^2\bar{\mathscr{D}}^2\mathscr{D}^2 = \Box\mathscr{D}^2\,, \quad \bar{\mathscr{D}}^2\mathscr{D}^2\bar{\mathscr{D}}^2 = \Box\bar{\mathscr{D}}^2\,. \tag{4.27}$$

Every configuration in which a loop ends up containing less than $2\mathscr{D}$'s $+2\bar{\mathscr{D}}$'s must be discarded, while the configurations with exactly two $\mathscr{D}$'s plus two $\bar{\mathscr{D}}$'s have a non-vanishing Grassmann integration and give a local expression in the spinorial coordinates.

In this way, a supergraph is reduced to a sum of ordinary Feynman diagrams. As usual, in momentum space these correspond to integrals over loop momenta, with momentum conservation at each vertex. In general UV and IR divergences arise, and suitable regularizations are required in order to perform the integrals. At the end of the calculation, going back to configuration space we obtain contributions that are given by local functions of the superspace coordinates integrated in $d^4x d^4\theta$.

The WZ model is renormalizable by power counting. The D-algebra method described above immediately tells us that the only quantum corrections of the theory arise in the form of non-chiral superspace integrals, which by construction can only contribute to the kinetic part of the effective action, but not to the superpotential term. This is the perturbative proof of the non-renormalization theorem for the superpotential of the WZ model [31].

This fact does not mean that the coupling constant does not renormalize, instead it inherits a non-trivial behaviour only as a consequence of the wavefunction renormalization. Concretely, we have

$$\mathscr{L} = \int d^4\theta\,(\bar{\Sigma}\Sigma) + \int d^2\theta\,(\lambda\Sigma^3) \to \mathscr{L}_{\text{ren}} = \int d^4\theta\, Z_\Sigma(\bar{\Sigma}\Sigma) + \int d^2\theta\, Z_\lambda Z_\Sigma^{3/2}(\lambda\Sigma^3)\,, \tag{4.28}$$

but the absence of chiral divergences implies

$$Z_\lambda Z_\Sigma^{3/2} = 1 \implies Z_\lambda = Z_\Sigma^{-3/2}\,. \tag{4.29}$$

4.2.2 Renormalization in components

In view of the comparison with the non-relativistic case, where up to now most of the literature has used the components field formalism, it is instructive to show how the perturbative computations occur in components.

The Feynman rules can be read from the action (4.20), where the only difference with the usual QFT formulation is the presence of auxiliary fields with 2-point function $\langle F\bar{F}\rangle = 1$. The scalar and fermionic propagator are the ordinary ones[9]. A direct inspection of the interacting action immediately gives the vertices, which are only cubic. The study of ordinary Feynman diagrams gives a renormalized Lagrangian of the form

$$\mathscr{L}_{\text{ren}} = -Z\,\partial^M\bar{\phi}\,\partial_M\phi + iZ\bar{\psi}\bar{\sigma}^M\partial_M\psi + Z\bar{F}F + \left(3\lambda Z_\lambda Z^{3/2}F\phi^2 + 3\lambda Z_\lambda Z^{3/2}\psi^\alpha\psi_\alpha\phi + \text{h.c.}\right) \tag{4.30}$$

[9] The propagators can also be obtained by reducing the super-propagator (4.25) in components.

where we have used the SUSY condition $Z_\phi = Z_\psi = Z_F \equiv Z$. In this way, the non-renormalization theorem still leads to condition (4.29). In fact, since we have not eliminated the auxiliary field F, this is nothing but a trivial rephrasing of the superspace approach.

On the other hand, a different way to proceed is to integrate out all the auxiliary fields and retain only the dynamical ones. In this case we use the equations of motion of F, which are algebraic relations, and we perform again the perturbative analysis. Taking into acount the non-renormalization condition (4.29), it turns out that the renormalized action for the dynamical fields reads

$$\mathscr{L}_{\text{ren}} = -Z\partial^M\bar{\phi}\,\partial_M\phi + iZ\bar{\psi}\bar{\sigma}^M\partial_M\psi + \left(3\lambda\,\psi^\alpha\psi_\alpha\phi - 9Z^{-1}|\lambda|^2|\phi|^4 + \text{h.c.}\right) \tag{4.31}$$

We observe that renormalization in component fields formulation is more subtle: while the cubic vertex is still non-renormalized, the quartic term instead renormalizes non-trivially, due the wavefunction renormalization. Even if the non-renormalization theorem is still at work, this procedure shows that quantum corrections to the vertices may arise in the component field formulation containing only dynamical fields.

4.2.3 The non-renormalization theorem

The holomorphicity of the superpotential is a powerful constraint which forces all quantum corrections to vanish. At perturbative level, superspace techniques provide a straightforward proof, as we have just recalled. The non-perturbative derivation of this result comes instead from an argument due to Seiberg [32], which we reviewed in the introduction 1.2.

This classical argument can be extended, following [92], to the case of a generic superpotential W giving the action

$$S = \int d^4x\,d^4\theta\,\bar{\Sigma}_a\Sigma_a + \int d^4x\,d^2\theta\,W(\Sigma_a) + \text{h.c.} \tag{4.32}$$

We introduce one extra chiral superfield Y, whose scalar part is set to 1 to recover the original action, whereas the spinorial and auxiliary components vanish identically. A consistent assignment of R-charges for the superfields appearing in the action is $R(\Sigma_a) = 0$ and $R(Y) = 2$. Upon quantization, the kinetic part of the action will be in general modified by the wave function renormalization, which we parametrize with the introduction of real superfields Z_{ab} in the following way

$$\tilde{S} = \int d^4x\,d^4\theta\,Z_{ab}\bar{\Sigma}_a\Sigma_b + \int d^4x\,d^2\theta\,Y\,W(\Sigma_a) + \text{h.c.} \tag{4.33}$$

Assuming that the regularization procedure does not spoil SUSY, the Wilsonian effective action at a given scale λ is of the form

$$\tilde{S}_\lambda = \int d^4x\,d^4\theta\,K(\bar{\Sigma}_a\Sigma_a, Z_{ab}, Y, \bar{Y}, \mathscr{D}) + \int d^4x\,d^2\theta\,W_\lambda(\Sigma_a, Y) + \text{h.c.} \tag{4.34}$$

Then R-invariance and holomorphicity of the superpotential force W_λ to be of the form

$$W_\lambda(\Sigma_a, Y) = Y\, W_\lambda(\Sigma_a) \tag{4.35}$$

Taking the weak coupling limit $Y \to 0$, the only contribution to the superpotential is a tree-level vertex, and therefore we find $W_\lambda(\Sigma_a) = W(\Sigma_a)$.

4.3 The non-relativistic Wess-Zumino model

We use the superfield formalism introduced in Section 4.1.2 to investigate the renormalization properties of the non-relativistic counterpart of the WZ model. First of all, we find the Galilean-invariant version of the WZ model by applying the null reduction prescription for Berezin integration (4.18) to the action in (4.19).

Using the decomposition of the superfields as $\Sigma = e^{imx^-}\Phi$, we immediately observe that while the canonical Kahler potential survives the reduction being U(1) neutral, the holomorphic superpotential has charge 3 and is killed by the x^- integration. The only way-out to obtain an interacting non-relativistic scalar model is then to introduce at least two species of superfields with different m charges, and trigger them in such a way that also the superpotential turns out to be neutral.

The minimal non-trivial case is the null reduction of the $3+1$ dimensional relativistic WZ model with two massless fields described by the action

$$S = \int d^4x d^4\theta \left(\bar\Sigma_1\Sigma_1 + \bar\Sigma_2\Sigma_2\right) + g\int d^4x d^2\theta\, \Sigma_1^2\Sigma_2 + \text{h.c.} \tag{4.36}$$

with the decomposition

$$\Sigma_1(x^M, \theta, \bar\theta) = \Phi_1(x^\mu, \theta, \bar\theta)\, e^{imx^-}, \qquad \Sigma_2(x^M, \theta, \bar\theta) = \Phi_2(x^\mu, \theta, \bar\theta)\, e^{-2imx^-} \tag{4.37}$$

which ensures that the superpotential is neutral under the $U(1)$ mass generator. We will refer to these superfields as belonging to sector 1 and 2, respectively.

The null-reduced action simply becomes

$$S = \int d^3x d^4\theta \left(\bar\Phi_1\Phi_1 + \bar\Phi_2\Phi_2\right) + g\int d^3x d^2\theta\, \Phi_1^2\Phi_2 + \text{h.c.} \tag{4.38}$$

Using the definitions in eq. (4.3) and below, it is clear that in the non-relativistic case the time coordinate has twice the dimensions of the spatial ones. In this way, the superfields have still mass dimension one and the coupling g is dimensionless. Therefore the model shares classical scale invariance with its relativistic parent. Moreover, the formulation with superfields obtained from the null reduction of $\mathcal{N} = 1$ relativistic ones assures that the $2+1$ dimensional action is invariant under $\mathcal{N} = 2$ non-relativistic SUSY.

4.3.1 Expansion of the action in components

In order to compare with the standard approach in the literature, we put the action to the component formalism. We start with the null reduction of the kinetic part, since it reveals some non-trivial features. Applying the prescription for the Berezin integration (4.18) we can write

$$S_{kin} = \int d^3x \left[\bar{D}^2\bar{\Sigma}_a D^2\Sigma_a + \bar{D}_\alpha\bar{\Sigma}_a\,\bar{D}^\alpha D^2\Sigma_a + \bar{\Sigma}_a\bar{D}^2D^2\Sigma_a\right], \tag{4.39}$$

where the non-relativistic covariant derivatives are given in eq. (4.12) and $a = 1,2$ labels the two sectors of superfields.

We define the theta expansion of the Wess-Zumino chiral superfields as (here θ^1,θ^2 indicate components 1 and 2 of the θ^α spinor)

$$\begin{aligned}\Sigma_1 &= \varphi_1 + \theta^1\xi_1 + \theta^2 2^{\frac{1}{4}}\sqrt{m}\,\chi_1 - \frac{1}{2}\theta^\alpha\theta_\alpha F_1\,,\\ \Sigma_2 &= \varphi_2 + \theta^1\xi_2 + \theta^2 i2^{\frac{1}{4}}\sqrt{2m}\,\chi_2 - \frac{1}{2}\theta^\alpha\theta_\alpha F_2\,,\end{aligned} \tag{4.40}$$

where a convenient rescaling of the grassmannian fields has been implemented in order to have the standard normalization of the kinetic terms, with φ_a and χ_a sharing the same dimensions. Using these conventions we obtain

$$\begin{aligned}S_{kin} = \int d^3x \,\big[&2im\bar{\varphi}_1(\partial_t\varphi_1) + \bar{\varphi}_1\partial_i^2\varphi_1 - 4im\bar{\varphi}_2(\partial_t\varphi_2) + \bar{\varphi}_2\partial_i^2\varphi_2 + \bar{F}_1F_1 + \bar{F}_2F_2\\ &+\sqrt{2}m\bar{\xi}_1\xi_1 + 2im\bar{\chi}_1(\partial_t\chi_1) - 2^{\frac{1}{4}}i\sqrt{m}\,\bar{\xi}_1(\partial_1 - i\partial_2)\chi_1 - 2^{\frac{1}{4}}i\sqrt{m}\bar{\chi}_1(\partial_1 + i\partial_2)\xi_1\\ &-2\sqrt{2}m\bar{\xi}_2\xi_2 + 4im\bar{\chi}_2(\partial_t\chi_2) + 2^{\frac{1}{4}}\sqrt{2m}\,\bar{\xi}_2(\partial_1 - i\partial_2)\chi_2 - 2^{\frac{1}{4}}\sqrt{2m}\bar{\chi}_2(\partial_1 + i\partial_2)\xi_2\Big]\,.\end{aligned} \tag{4.41}$$

Integrating out the auxiliary fields $F_{1,2}$ and $\xi_{1,2}$ we find

$$\begin{aligned}S_{kin} = \int d^3x \,\big[&2im\bar{\varphi}_1\partial_t\varphi_1 + \bar{\varphi}_1\partial_i^2\varphi_1 - 4im\bar{\varphi}_2\partial_t\varphi_2 + \bar{\varphi}_2\partial_i^2\varphi_2\\ &+2im\bar{\chi}_1\partial_t\chi_1 + \bar{\chi}_1\partial_i^2\chi_1 + 4im\bar{\chi}_2\partial_t\chi_2 - \bar{\chi}_2\partial_i^2\chi_2\big]\,,\end{aligned} \tag{4.42}$$

where $\varphi_{1,2}$ and $\chi_{1,2}$ are the dynamical non-relativistic scalar and fermion fields, respectively.

If we Fourier-transform both the scalar and fermion fields

$$\varphi(x^\mu) = \int \frac{d\omega\,d^2k}{(2\pi)^3}\,a(\vec{k})e^{-i(\omega t - \vec{k}\cdot\vec{x})}\,, \tag{4.43}$$

the free equations of motion lead to the following dispersion relations

$$\omega_1 = \frac{\vec{k_1}^2}{2m}\,, \qquad\qquad \omega_2 = -\frac{\vec{k_2}^2}{4m}\,. \tag{4.44}$$

The wrong sign for the energy of fields in sector 2 is due to U(1) invariance, which forces to assign a negative eigenvalue to the mass operator for Φ_2 in the decomposition (4.37).

The problem can be avoided if we integrate by parts the derivatives in sector 2

$$\begin{aligned} S_{kin} = \int d^3x \, \big[& 2im\bar{\varphi}_1 \partial_t \varphi_1 + \bar{\varphi}_1 \partial_i^2 \varphi_1 + 4im\varphi_2 \partial_t \bar{\varphi}_2 + \varphi_2 \partial_i^2 \bar{\varphi}_2 \\ & + 2im\bar{\chi}_1 \partial_t \chi_1 + \bar{\chi}_1 \partial_i^2 \chi_1 + 4im\chi_2 \partial_t \bar{\chi}_2 + \chi_2 \partial_i^2 \bar{\chi}_2 \big] \, , \end{aligned} \tag{4.45}$$

and we interchange the roles of φ_2 with $\bar{\varphi}_2$, and of χ_2 with $\bar{\chi}_2$. This operation is equivalent to reversing the role of creation and annihilation operators. From the point of view of the superfield formulation, this is equivalent to interchanging all the components of Φ_2 with the components of $\bar{\Phi}_2$, without affecting the chirality property of the superfield itself (the Grassmann coordinates entering the superfield are not modified in this exchange). From now on we will call Φ_2 the chiral superfield whose components[10] are $(\bar{\varphi}_2, \bar{\xi}_2, \bar{\chi}_2, \bar{F}_2)$, while the antichiral $\bar{\Phi}_2$ has components $(\varphi_2, \xi_2, \chi_2, F_2)$, and assign positive mass $2m$ to Φ_2.

The component form of the interacting part of the action can be similarly obtained by means of the standard superspace manipulations combined with the Berezin integration (4.18). After performing the redefinition of the fields and adding the contribution from the interacting part of the Lagrangian, we obtain

$$\begin{aligned} S = \int d^3x \, \Big[& 2im\bar{\varphi}_1 \partial_t \varphi_1 + \bar{\varphi}_1 \partial_i^2 \varphi_1 + 4im\bar{\varphi}_2 \partial_t \varphi_2 + \bar{\varphi}_2 \partial_i^2 \varphi_2 \\ & + 2im\bar{\chi}_1 \partial_t \chi_1 + \bar{\chi}_1 \partial_i^2 \chi_1 + 4im\bar{\chi}_2 \partial_t \chi_2 + \bar{\chi}_2 \partial_i^2 \chi_2 - 4|g|^2 |\varphi_1 \varphi_2|^2 - |g|^2 |\varphi_1|^4 \\ & - ig \left(\sqrt{2} \varphi_1 \chi_1 (\partial_1 - i\partial_2) \bar{\chi}_2 - 2\bar{\varphi}_2 \chi_1 (\partial_1 - i\partial_2) \chi_1 + 2\sqrt{2} \varphi_1 ((\partial_1 - i\partial_2)\chi_1) \bar{\chi}_2 \right) + \text{h.c.} \\ & + 2|g|^2 \left(-|\varphi_1|^2 \bar{\chi}_1 \chi_1 - 4|\varphi_1|^2 \bar{\chi}_2 \chi_2 + 2|\varphi_2|^2 \bar{\chi}_1 \chi_1 + 2\sqrt{2} \varphi_1 \varphi_2 \bar{\chi}_1 \bar{\chi}_2 + 2\sqrt{2} \bar{\varphi}_1 \bar{\varphi}_2 \chi_2 \chi_1 \right) \Big] . \end{aligned} \tag{4.46}$$

In component field formulation, there are standard quartic scalar interactions together with cubic derivative interactions, similar to the interacting part of a non-supersymmetric $1+1$ dimensional Galilean model recently studied in [93].

An alternative way to derive this action is to consider the null reduction of the component field formulation of the relativistic $3+1$ dimensional WZ model, where the auxiliary fields are integrated out. In other words, the elimination of the non-dynamical fields from the action commute with the DLCQ.

[10] For details about the null reduction of non-relativistic fermions, see Appendix A.

4.4 Quantum corrections in superspace

We study the renormalization properties of the model in eq. (4.38) by means of the superfield formalism[11]. As in the relativistic case, this procedure turns out to be very convenient to consider the contributions from various fields inside a unique supergraph.

First of all, we will collect the super-Feynman rules for the propagators and the vertices of the theory from the null reduction of the corresponding ones in the relativistic parent[12] found in Section 4.2. Moreover, we will show how the non-relativistic properties of the theory strongly constrain the form of the supergraphs accounting for the quantum corrections of the theory. A crucial role is played by the $U(1)$ symmetry associated to the mass central charge M, which implies that the particle number has to be conserved at each vertex and the only non-vanishing Green functions are the ones whose external particle numbers add up to zero. The other fundamental property will be the causal structure of the inverse non-relativistic propagator, which is linear in the energy instead of quadratic as it happens in the relativistic case.

4.4.1 Super-Feynman and selection rules

The $U(1)$ particle conservation at each vertex can be implemented in a graphical way by associating to each propagator line a flow depicted with an arrow: a single one for the superfield Φ_1 with mass m, and a double one for Φ_2 with mass $2m$. Consequently, the super-Feynman rules in the non-relativisitic $\mathcal{N}=2$ superspace are:

- Superfield propagators. The null reduction simply acts as the replacement $\Box \to 2iM\,\partial_t + \partial_i^2$, with $M = m$ or $2m$ in the propagators of the relativistic parent (4.25). In momentum space, this is equivalent to send $-p^2 \to 2M\omega - \vec{p}^{\,2}$. The result is

$$\langle \Phi_1(\omega,\vec{p})\bar{\Phi}_1(-\omega,-\vec{p})\rangle = i\frac{\delta^{(4)}(\theta_1-\theta_2)}{2m\omega-\vec{p}^{\,2}+i\varepsilon}\,, \quad \langle \bar{\Phi}_2(\omega,\vec{p})\Phi_2(-\omega,-\vec{p})\rangle = i\frac{\delta^{(4)}(\theta_1-\theta_2)}{4m\omega-\vec{p}^{\,2}+i\varepsilon} \tag{4.47}$$

  The dimensional analysis of the denominator works correctly when remembering that the energy dimensions in the Galilean setting are taken to be

$$[\omega] = E^2\,, \qquad [\vec{k}] = E\,, \qquad [m] = E^0\,, \tag{4.48}$$

  since we rescaled the x^- direction as $x^- \to x^-/R$ and the time direction as $x^+ \to Rx^+$, being R the radius of the circle along the compact null direction. The propagators for both sectors have a retarded $i\varepsilon$ prescription which follows the order of fields shown in fig. 4.1, where the

[11] The computation in component field formalism is performed in Appendix C.

[12] As usual, these Feynman rules can be taken as well directly from the null reduced non-relativistic action (4.38).

exchange of particles with anti-particles in sector 2 is manifest from the reversed order of the fields with respect to sector 1. [13]

- Vertices. There are no subtleties in the non-relativistic limit and they are cubic vertices containing only chiral or anti-chiral superfields. The particle number conservation at each vertex translates into the condition that the numbers of entering and exiting arrows have to match (see fig. 4.1).

Figure 4.1: Propagators and vertices in superspace.

What are the changes in the D-algebra procedure with respect to the relativistic case? The null reduction does not affect the grassmannian part of the superspace, which means that the rules (4.24) for the sources in the path integral still hold we have to count one extra $\bar{D}^2$ (D^2) for each chiral (anti-chiral) superfield entering or exiting a vertex, and use one of these factors at each vertex to complete the chiral integral to a $\int d^4\theta$ one. The only important difference is that in the present case the grassmannian derivatives are the non-relativistic ones in (4.12). Every other step of the D-algebra that applies in the relativistic case can be performed as in Section 4.2.1 in order to reduce the supergraph to a combination of ordinary Feynman graphs for functions that are local in $(\theta,\bar{\theta})$. The identities (4.26), which immediately rule out all the diagrams without enough covariant derivatives running along the lines of the graph, still hold with the change $D,\bar{D}\to\mathscr{D},\bar{\mathscr{D}}$. The rules (4.27) require instead the application of the DLCQ prescription and become (see eqs. (A.27, A.29) in Appendix A for more details)

$$
\begin{aligned}
&[D^\alpha,\bar{D}^2]=\sqrt{2}M\bar{D}_1\delta_1^\alpha+i(\bar{\sigma}^\mu)^{\alpha\beta}\partial_\mu\bar{D}_\beta\,,\quad [\bar{D}^\alpha,D^2]=-\sqrt{2}MD_1\delta_1^\alpha-i(\bar{\sigma}^\mu)^{\alpha\beta}\partial_\mu D_\beta\,,\\
&D^2\bar{D}^2D^2=(2iM\partial_t+\partial_i^2)D^2\,,\qquad\qquad \bar{D}^2D^2\bar{D}^2=(2iM\partial_t+\partial_i^2)\bar{D}^2
\end{aligned}
\tag{4.50}
$$

[13] In configuration space the $i\varepsilon$ prescription translates into a retarded prescription for the propagator. In fact, the Fourier transform of (4.47) reads ($M=m$ or $2m$)

$$
D(\vec{x},t)=\int\frac{d^2p\,d\omega}{(2\pi)^3}i\frac{\delta^{(4)}(\theta_1-\theta_2)}{2M\,\omega-\vec{p}^2+i\varepsilon}\,e^{-i(\omega t-\vec{p}\cdot\vec{x})}=-\frac{i\Theta(t)}{4\pi t}e^{i\frac{M\vec{x}^2}{2t}}\,\delta^{(4)}(\theta_1-\theta_2)
\tag{4.49}
$$

where Θ is the Heaviside function. We will see that the appearance of the step function (a consequence of the linearity of the inverse propagator with respect to energy) will play a fundamental role in the determination of the renormalization properties of the model.

where $\mu \in \{+,1,2\}$.

Since the only kind of interactions appearing in the superpotential are cubic as in the relativistic case, the possible topologies of supergraphs that can be built with the rules at our disposal are the same of the ordinary WZ model (in particular, they were studied *e.g.* in [94], [95]). In addition, there are certain selection rules which can be derived by the non-relativistic properties of the theory and that drastically reduce the number of non-vanishing diagrams.

We start analyzing the consequences of the retarded nature of the non-relativistic propagator. The linearity in the energy ω implies that

Selection rule 4.4.1. *Arrows inside a Feynman diagram cannot form a closed loop.*

This can be easily seen to be a consequence of the residue theorem in momentum space and is better illustrated with an example. We consider the quantum correction to the self-energy of the superpropagator in sector 1, as depicted in fig. 4.2.

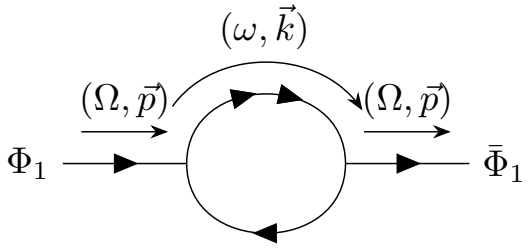

Figure 4.2: One-loop correction to the self-energy of the Φ_1 superfield.

The contribution to the effective action from this diagram is[14]

$$i\Gamma_1^{(2)}(\Phi_1,\bar{\Phi}_1) = 4|g|^2 \int d^4\theta \, \frac{d\omega\, d^2k}{(2\pi)^3} \, \frac{\Phi_1(\Omega,\vec{p},\theta)\bar{\Phi}_1(\Omega,\vec{p},\theta)}{\left[4m\omega - \vec{k}^2 + i\varepsilon\right]\left[2m(\omega-\Omega) - (\vec{k}-\vec{p})^2 + i\varepsilon\right]} \,. \tag{4.51}$$

The integral in ω is convergent and can be performed *e.g.* by means of the residue theorem. The poles of the integrand are located in

$$\omega^{(1)} = \frac{\vec{k}^2}{4m} - i\varepsilon \,, \qquad \omega^{(2)} = \Omega + \frac{(\vec{k}-\vec{p})^2}{2m} - i\varepsilon \,, \tag{4.52}$$

and in particular are both in the lower-half complex plane, so that we can close the integration contour in the upper half-plane, obtaining

$$\Gamma_1^{(2)}(\Phi_1,\bar{\Phi}_1) = 0 \,. \tag{4.53}$$

Analogously, in configuration space, the vanishing of the two-point function arises from the product of two Heaviside functions with opposite arguments, which would have support only in one point. By normal ordering, we choose to put this contribution to zero [96].

[14] We denote the effective action with a subscript referring to the sector to which the superfield belongs, and with a superscript referring to the number of external lines to attach to the diagram.

This argument can be generalized to the case where the analitic structure of the integrand in momentum space is given by a set of simple poles located from the same side of the complex plane in ω. In particular, this analitic structure corresponds from the diagrammatic point of view to a disposition of the arrows where they form a closed loop, which is the statement of the selection rule 4.4.1. On the other hand, we need to be careful on the convergence conditions of the integral: the rule relies on the possibility to apply the residue theorem to perform the $\omega-$integration, which in turn requires the integrand to be sufficiently decreasing at infinity for applying Jordan's lemma. The behaviour of the propagators should guarantee that this is always the case, but the D-algebra procedure can in principle spoil the convergence due to extra ω factors coming from the commutation rules (4.50). As it will be discussed in Section 4.4.2, this never happens and then selection rule 4.4.1 is true even before performing D-algebra.

We stated that the supergraphs which we can build with the super-Feynman rules are in principle the same of the relativistic case, having the same building blocks (the propagators and the vertices are graphically are the same). However, after imposing the stringent constraints provided by selection rule 4.4.1, the number of allowed diagrams drastically reduce. For example, an immediate consequence is that at one loop, one-particle irreducible diagrams with two external lines admit only one non-vanishing configuration, given in fig. 4.3(a). This rule is true also when the diagram is part of a bigger graph. As a consequence, the topology shown in fig. 4.3(b) is always forbidden, when the number of horizontal lines is bigger than two.

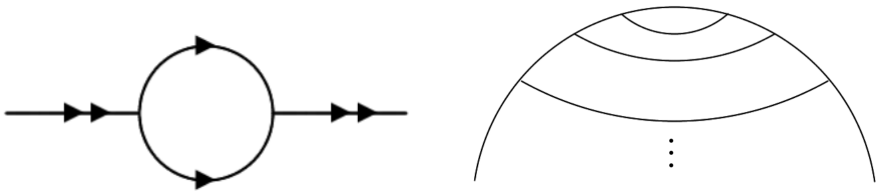

(a) (b)

Figure 4.3: Configurations allowed (a) and forbidden (b) by selection rule 4.4.1.

Further selection rules can be obtained from the application of the particle number conservation:

Selection rule 4.4.2. *The (sub)diagrams appearing in fig. 4.4 are forbidden by particle number conservation. Configuration* (e) *is forbidden only for an even number of horizontal lines on the right side of the vertical line.*

In order to prove the previous rule, the following procedure is applied:

- Consider a particular diagram obtained by using as building blocks propagators and 3-point vertices
- Draw all the possible configurations of arrows that can be assigned to the lines

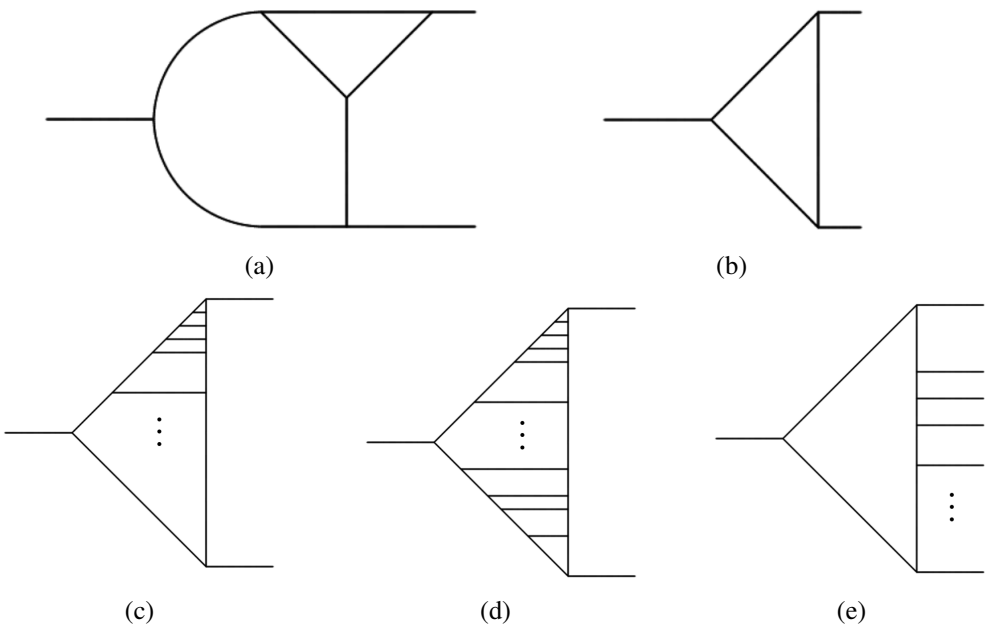

Figure 4.4: Set of vanishing (sub)diagrams due to particle number conservation. In (e) the number of horizontal lines on the right side is required to be even.

- Check that particle number is conserved at every vertex (the number of entering and exiting arrows must be the same).

If there is no way to assign the arrows consistently at each vertex, then the diagram is forbidden and must be discarded.

As an example, we consider diagram 4.4(a) for which all possible configurations of arrows are drawn in fig. 4.5. It can be seen that in all the configurations we cannot consistently assign arrows in the top right vertex.

4.4.2 Renormalizability of the theory

We study the renormalizability of the model by considering the superficial degree of divergence of a generic supergraph with L loops, $E = E_C + E_A$ external lines, P internal propagators and $V = V_C + V_A$ vertices, where the C and A subscripts stand for chiral and anti-chiral, respectively.

A connected graph satisfies the topological constraint

$$L = P - V + 1\,. \tag{4.54}$$

In addition, the fact that all the vertices of the theory are cubic implies that the relation $E + 2P = 3V$ also holds. Combined with the previous constraint, this leads to

$$P = E + 3L - 3\,. \tag{4.55}$$

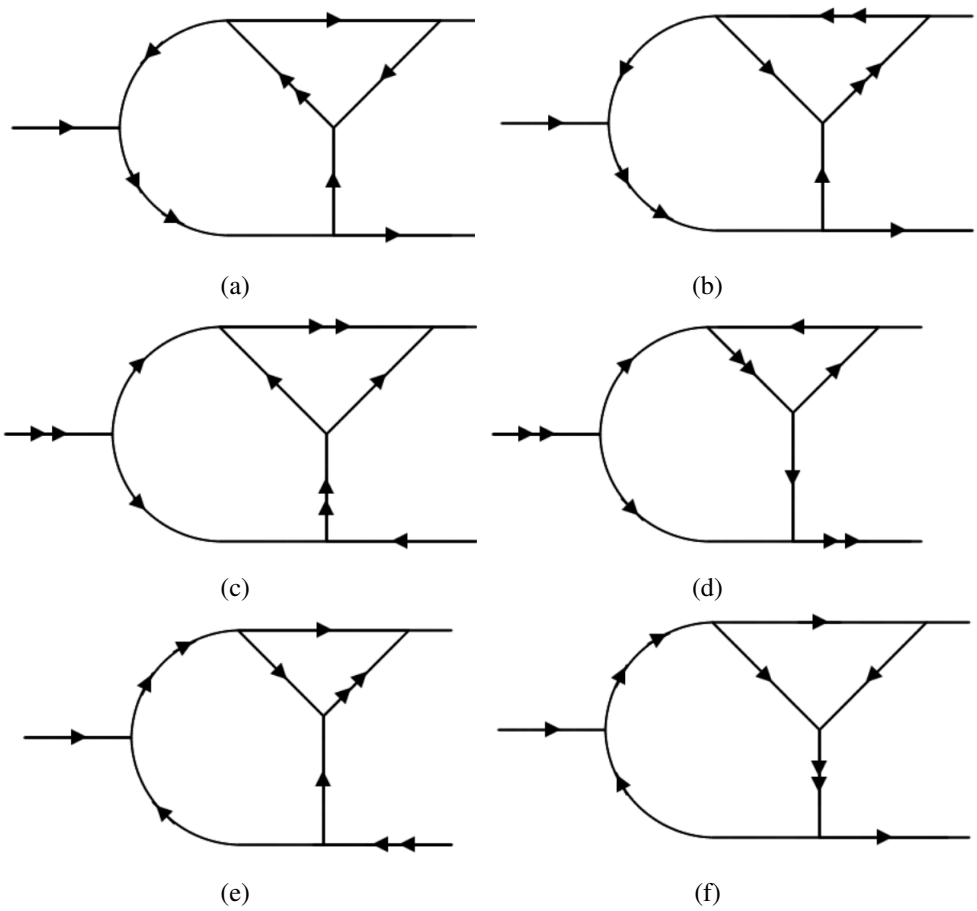

Figure 4.5: All possible configurations of arrows in an example of subdiagram. All of them are forbidden by particle number conservation at the upper right vertex.

Since the Galilean model comes from the null reduction of a massless WZ model, the propagator necessarily connects a chiral superfield with an anti-chiral one. This requires the following relations to be true:

$$3V_A = P + E_A\,, \qquad 3V_C = P + E_C\,. \tag{4.56}$$

We consider the ingredients composing the integrand of a 1PI supergraph with these properties. There is a product of P super-propagators (4.47) times factors of covariant derivatives $D, \bar{D}$ acting on the grassmannian delta functions. The precise counting is:

- One factor of $(\bar{D}^2)^2$ associated to each internal chiral vertex
- One factor of D^2 associated to each internal anti-chiral vertex
- One factor of $\bar{D}^2$ for each chiral vertex with an external line attached
- One factor of D^2 for each anti-chiral vertex with an external line attached.

The total number of covariant derivatives is then

$$(D^2)^{2V_A-E_A}(\bar{D}^2)^{2V_C-E_C} \tag{4.57}$$

On the other hand, D-algebra requires one factor $D^2\bar{D}^2$ coming from each loop in order to contract the integral to a point in the $(\theta,\bar{\theta})$ space. This implies that in non-vanishing diagrams the remaining derivatives

$$(D^2)^{2V_A-E_A-L}(\bar{D}^2)^{2V_C-E_C-L} \tag{4.58}$$

are traded with powers of loop momenta, according to the D-algebra procedure explained in section 4.2.1.

The constraints (4.56) allow to express the total factor of covariant derivatives acting on the supergraph as

$$(D^2\bar{D}^2)^{\frac{2}{3}P-L}(D^2)^{-\frac{E_A}{3}}(\bar{D}^2)^{-\frac{E_C}{3}} \tag{4.59}$$

In addition to this factor, the diagram contains by assumption a set of P propagators $1/\triangle$ with $\triangle \equiv 2M\omega - \vec{k}^2$, times L integrations on the loop variables. Looking at the superficial degree of divergence of the integral, the worst case occurs when identities (4.50) can be used to trade $D^2\bar{D}^2$ with $\triangle$, which then cancel internal propagators. The corresponding integral reads

$$\int d\omega_1 d^2k_1 \ldots d\omega_L d^2k_L \frac{(D^2)^{-\frac{E_A}{3}}(\bar{D}^2)^{-\frac{E_C}{3}}}{\triangle^{L+\frac{P}{3}}} = \int d\omega_1 d^2k_1 \ldots d\omega_L d^2k_L \frac{(D^2)^{-\frac{E_A}{3}}(\bar{D}^2)^{-\frac{E_C}{3}}}{\triangle^{2L+\frac{E}{3}-1}}, \tag{4.60}$$

where in the last step eq. (4.55) has been used.

The worst case for the convergence of the integral is a supergraph with $E_A = E_C = E/2$ where the remaining covariant derivatives also combine into inverse propagators. In this case the diagram schematically contributes as

$$\int d\omega_1 d^2k_1 \ldots d\omega_L d^2k_L \frac{1}{\triangle^{2L+\frac{E}{2}-1}} \tag{4.61}$$

The superficial degree of divergence is $\delta = 2-E$. It is always negative for $E \geq 3$ and the corresponding integrals give finite contributions. For self-energy diagrams ($E = 2$) logarithmic divergences arise, which can be subtracted by wave-function renormalization.

The more problematic case for convergence is $E = 1$, which needs a careful treatment. The prototype for such case is a 1-loop diagram of the form

$$\int \frac{d\omega\, d^2k}{2M\omega - \vec{k}^2 + i\varepsilon} \tag{4.62}$$

After performing the ω-integration, we can use dimensional regularization to compute the $\vec{k}$ integral. The result is zero since the integral is dimensionful and cannot depend on any possible scale. This shows that the non-relativistic WZ model is renormalizable.

While the check of renormalizability ensures that we can regularize the divergences coming from quantum corrections with a finite number of counterterms, in view of the application of the selection rule 4.4.1, the non-relativistic case requires a further property to prove: the loop integrals on $\omega_1,\dots,\omega_L$ are separately convergent. This can happen only if the integrand converges at least like $1/\omega_i^2$ for a given ω_i-integration.

Let's then consider a generic loop L_i inside the supergraph containing P_i propagators. It is crucial that the inverse Galilean propagator is linear in the energy, because this information combined with the energy conservation at each vertex ensures that the P_i propagators provide a power $1/\omega_i^{P_i}$. Since in a loop we always have $P_i \geq 2$ (tadpoles are zero due to the previous argument), the convergence of the ω_i-integral is guaranteed, as long as there are no ω_i powers at the numerator. Problems of convergence can arise if ω_i factors appear at the numerator fro D-algebra manipulations, but in the worst situation D-derivatives produce factors which cancel completely some propagators, contracting points in momentum space. In any case, this process leads to a loop with at least two propagators, which is sufficient to ensure the convergence of the integral. Moreover we observe that adjacent loops which in the relativistic case would lead to overlapping divergences, have an even better convergence in ω.

In conclusion, all the energy integrals are convergent, they do not need to be regularized and we can compute them in the complex plane by using the residue theorem. This property allows to apply selection rule 4.4.1 to a given supergraph without worrying of D-algebra manipulations.

4.4.3 Loop corrections to the self-energy

Having at disposal the power of the selection rules coming from the properties of the non-relativistic model, we study the quantum corrections to the Galilean WZ model (4.38) by means of the supergraph formalism. Due to the analysis in the previous section on the convergence of integrals along the energy variable, only integrals involving the spatial momentum need to be regularized and we choose the prescription of dimensional regularization with the minimal subtraction scheme.

In this way, we work in $d = 2-\varepsilon$ dimensions and we introduce a mass scale μ to keep the coupling constant g dimensionless. We define renormalized quantities

$$\begin{cases} \Phi_a = Z_a^{-1/2}\,\Phi_a^{(B)} = \left(1-\frac{1}{2}\delta_a\right)\Phi_a^{(B)} & a=1,2 \\ g = \mu^{-\varepsilon} Z_g^{-1}\, g^{(B)} = \mu^{-\varepsilon}(1-\delta_g) g^{(B)} \end{cases} \tag{4.63}$$

and determine counterterms proportional to δ_a, δ_g

$$\mathscr{L}_{\text{ren}} + \int d^4\theta\, \left(\delta_1 \bar{\Phi}_1\Phi_1 + \delta_2\bar{\Phi}_2\Phi_2\right) + \int d^2\theta\, \left[\mu^{\varepsilon} g\left(\delta_g+\delta_1+\frac{1}{2}\delta_2\right)\Phi_1^2\Phi_2\right] + \text{h.c.} \tag{4.64}$$

to cancel UV divergences.

In this section we investigate the quantum corrections to the self-energy: only 1PI diagrams are considered. We follow this strategy:

- Draw all the possible topologies of 1PI supergraphs at a given loop order
- Assign arrows to the lines of the diagram consistently with particle number conservation
- Check if there is any part of the diagram where the arrows form a close loop, and discard the diagram if this happens
- Apply D-algebra to find if the grassmannian nature of the amplitude forbids the diagram
- Perform the remaining integral with the usual techniques, *e.g* with dimensional regularization

One loop

We start with the 1PI diagrams contributing to the quantum corrections of the self-energy of the superfield in sector 1. The selection rule 4.4.1 applies, and immediately tells us that there are no possible configurations: the only admitted diagram would be the one depicted in Fig. 4.2, but we already showed that this vanishes by means of the residue theorem. As a consequence,

$$\delta_1^{(1\text{loop})} = 0 \tag{4.65}$$

For the one-loop self-energy in sector 2 we find, instead, that there is an allowed diagram, depicted in fig. 4.6.

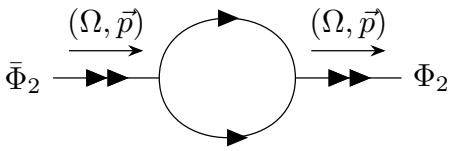

Figure 4.6: One-loop correction to the self-energy of Φ_2.

After performing the D-algebra, the corresponding contribution reads

$$i\Gamma_2^{(2)}(\Phi_2,\bar{\Phi}_2) = 2|g|^2 \int d^4\theta \, \frac{d\omega\, d^2k}{(2\pi)^3} \, \frac{\Phi_2(\Omega,\vec{p},\theta)\bar{\Phi}_2(\Omega,\vec{p},\theta)}{\left[2m\omega - \vec{k}^2 + i\varepsilon\right]\left[2m(\Omega-\omega) - (\vec{p}-\vec{k})^2 + i\varepsilon\right]} \,. \tag{4.66}$$

The crucial difference with the computations in sector 1 is the fact that the arrows of particle number and momenta are directed in the same way, and then the poles of the integrand are located in both sides of the complex plane

$$\omega^{(1)} = \frac{\vec{k}^2}{4\tilde{m}} - i\varepsilon \,, \qquad \omega^{(2)} = \Omega - \frac{(\vec{k}-\vec{p})^2}{2\tilde{m}} + i\varepsilon \,. \tag{4.67}$$

In this way the integral is non-vanishing and since the ω-integral is convergent, we can apply the residue theorem to obtain

$$\Gamma_2^{(2)}(\Phi_2,\bar{\Phi}_2) = -\frac{|g|^2}{m}\int d^4\theta\,\Phi_2(\Omega,\vec{p},\theta)\bar{\Phi}_2(\Omega,\vec{p},\theta)\int\frac{d^2k}{(2\pi)^2}\frac{1}{2m\Omega-\vec{k}^2-(\vec{p}-\vec{k})^2+i\varepsilon}\,. \tag{4.68}$$

The two-dimensional momentum integral can be now performed using dimensional regularization. In generic spatial dimensions d there exists a region in complex plane where the integral is convergent and we can translate the integration variable as

$$\vec{l}=\vec{k}-\frac{\vec{p}}{2}\Rightarrow d\vec{l}=d\vec{k}\,, \tag{4.69}$$

giving

$$\Gamma_2^{(2)}(\phi_2,\bar{\phi}_2) = \frac{2|g|^2}{(2\pi)^2}\int d^4\theta\,\phi_2(\Omega,\vec{p},\theta)\bar{\phi}_2(\Omega,\vec{p},\theta)\frac{2\pi^{d/2}}{\Gamma(d/2)}\int_0^\infty dl\,\frac{l^{d-1}}{l^2-m\Omega+\frac{\vec{p}^2}{4}}\,. \tag{4.70}$$

Focusing on its divergent part we obtain

$$\Gamma_2^{(2)}(\Phi_2,\bar{\Phi}_2)\to\frac{|g|^2}{4\pi m}\frac{1}{\varepsilon}\int d^4\theta\,\Phi_2(\Omega,\vec{p},\theta)\bar{\Phi}_2(\Omega,\vec{p},\theta)\,. \tag{4.71}$$

In the minimal subtraction scheme this leads to the counterterm

$$\delta_2^{(1\text{loop})} = -\frac{|g|^2}{4\pi m}\frac{1}{\varepsilon}\,. \tag{4.72}$$

Two loops

It turns out that the selection rules 4.4.1 and 4.4.2 are sufficient to rule out every two-loop corrections to the self-energy. In particular, looking at the two possible two-loop topologies of diagrams depicted in fig. 4.7, it is easy to realize that no consistent assignments of arrows exist, or they vanish due to circulating arrows in a loop.

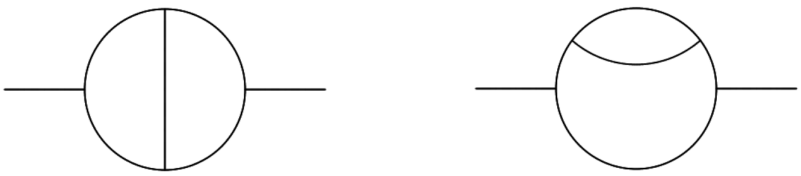

Figure 4.7: Topologies of possible two-loop corrections to the self-energies.

Three loops

At three loops, the classification is richer and the possible cases in the relativistic setting are given in [94], where the three-loop β function was computed.

In the non-relativistic case selection rules 4.4.1 and 4.4.2 discard almost all possible configurations, leading only to one non-trivial type of diagram, the non-planar one depicted in fig. 4.8. However, looking at all possible assignments of arrows we conclude that there is always a circulating loop, which entails a vanishing result according to selection rule 4.4.1. Therefore, there are no three-loop corrections to the self-energies of both superfields.

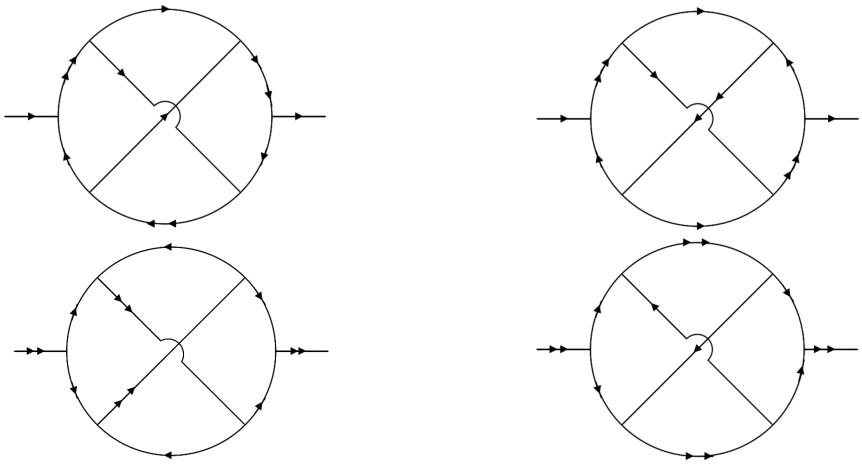

Figure 4.8: Non-trivial three-loop corrections to the self-energies. We depict all possible assignments of arrows in the lines.

Four loops

At four loops we take the classification of all the topologies in the relativistic case from [95], where the β-function for the relativistic WZ model was computed.

Following the same strategy of lower loops, we find few non-trivial diagrams listed in fig. 4.9(a)-(c). The first two graphs contain as a subgraph the non-planar three-loop diagram already discussed, and then we discard them by similar arguments to the three-loop case. The remaining case (c) allows for various configurations of arrows depicted in fig. 4.10(a)-(d), but all of them contain at least one subgraph where the arrows form a close loop. This implies that the diagram does not give any quantum correction to the self-energy.

Higher loops

Up to four loops we have found that non-vanishing quantum corrections to the self-energy appear only in sector 2 and only at one loop. Triggered by these results, the natural question which arises is

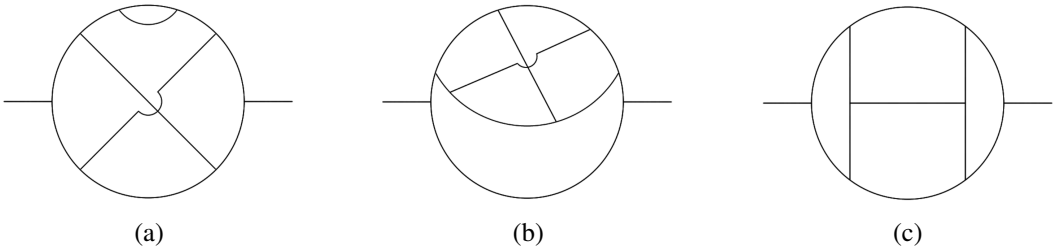

Figure 4.9: Non-trivial quantum corrections to the self-energy at four loops.

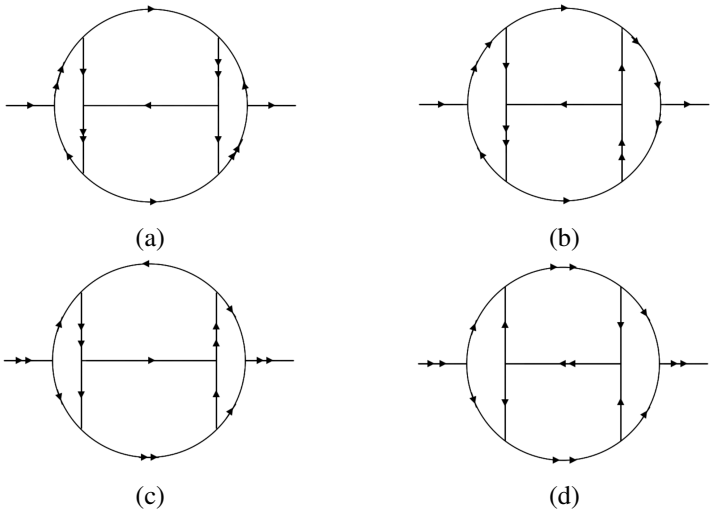

Figure 4.10: Allowed assignments of arrows to the lines of diagram (c) in Fig. 4.9.

whether the same pattern repeats at any loop order or we should expect non-vanishing contributions at higher loops.

A deeper understanding of the problem can be found by applying the strategy followed at lower loops to find recursive configurations of diagrams that vanish, and possibly rule out every graph that it is possible to draw. First of all, every diagram containing the stuctures in fig. 4.4 as a subgraph vanish by means of selection rule 4.4.2.

If we further apply selection rule 4.4.1, we can find among the set of allowed configurations other structures that vanish, depicted in fig. 4.11. This is also true for all the diagrams that can be obtained by gluing different structures among the previous set.

Although these topologies cover a vast number of diagrams, they are not exhaustive and in principle we cannot exclude the appearance of possible non-vanishing contributions from more general configurations, like the one in fig. 4.12. Nonetheless, based on the experience gained up to four loops, we expect that when the numbers of loops increases it becomes more and more difficult to realize configurations of arrows without closed loops. Therefore, we can quite safely conjecture that the self-energy of the Φ_1 superfield is not corrected at quantum level, while the one for Φ_2 is one-loop exact.

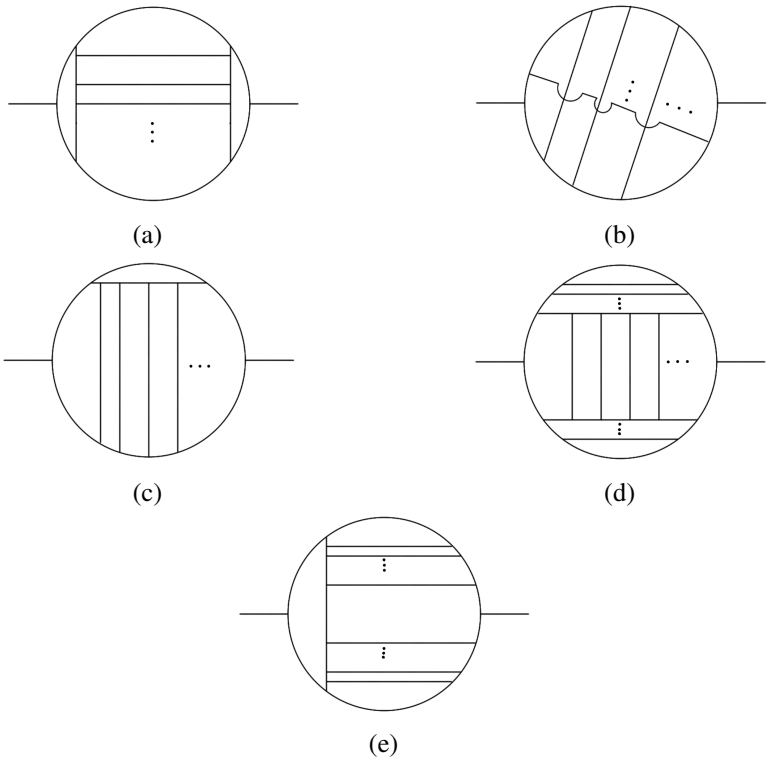

Figure 4.11: Non-trivial vanishing quantum corrections to self-energies at generic loop level.

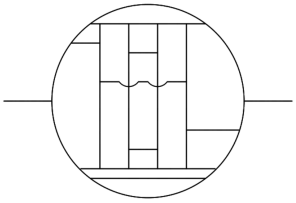

Figure 4.12: General self-energy diagram.

Independently of the validity of this conjecture, there are various things that we learned from the study of quantum corrections to the self-energy in the non-relativistic case. First of all, it is evident that the computation is simpler than the relativistic parent $\mathscr{N} = 1$ theory in 3+1 dimensions, because the selection rules greatly increase the number of vanishing contributions. In fact, in the relativistic case the kinetic term acquires UV divergent corrections at any loop order, while in the non-relativistic case there are contributions coming only from the one-loop computation. In particular, this shows that at quantum level the non-relativistic three-dimensional $\mathscr{N} = 2$ WZ model cannot be obtained simply from null reduction of the four-dimensional relativistic model.

4.4.4 Loop corrections to the vertices

The discussion in section 4.4.2 shows that UV divergent contributions should not arise from any diagram with three or more external legs. Moreover, the grassmannian nature of the superspace, not being affected by the null reduction, does not allow the production of any chiral integral at the perturbative level. This means that the perturbartive non-renormalization theorem for the superpotential should still work, giving the constraint

$$\delta_g + \delta_1 + \frac{1}{2}\delta_2 = 0 \quad \Rightarrow \quad \delta_g^{(1\text{loop})} = \frac{|g|^2}{8\pi m}\frac{1}{\varepsilon}\,. \tag{4.73}$$

In this section we will study the case of the 1PI quantum corrections to the three-point vertex, both to investigate how the selection rules restrict the number of possible quantum corrections for configurations with three external fields, and to provide further evidence of the previous statements.

As in the relativistic case, at one-loop there is no way to draw any three-point diagram as long as the model is massless.

At two loops the only supergraph allowed by particle number conservation is the one in fig. 4.13, where all possible configurations of arrows have been depicted. In all the configurations we see that a circulating loop of arrows appears, thus this diagram is ruled out by selection rule 4.4.1.

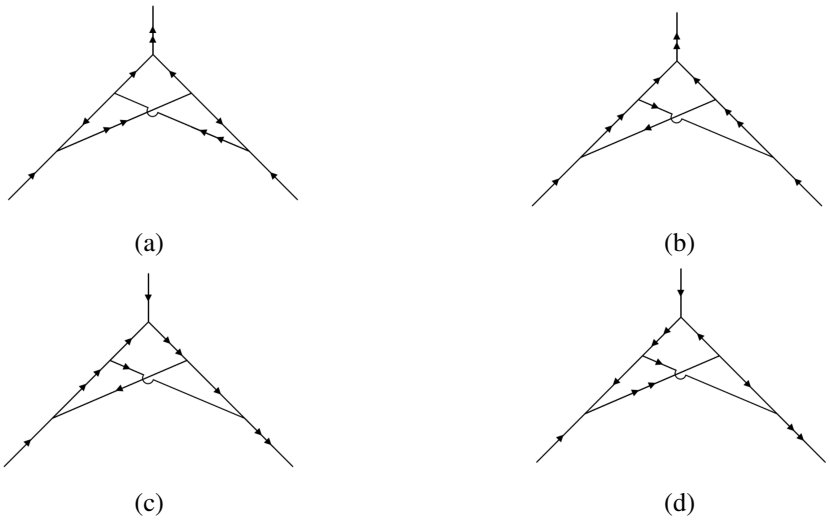

Figure 4.13: Two-loop 1PI diagram for the three-point vertex. We depicted all the configurations of arrows associated to the lines.

Since this is a configuration where the number of chiral and anti-chiral vertices is different, the factors of covariant derivatives are not only used to simplify propagators, but the application of the D-algebra (4.50) gives additional powers of momenta at the numerator which might affect the convergence of the ω integrations. In order to show that there is enough regularity to guarantee the convergence of the ω integral, we analyze the diagram in more details. For instance, focusing on the arrow configuration 4.13(d), the result of D-algebra is given in fig. 4.14.

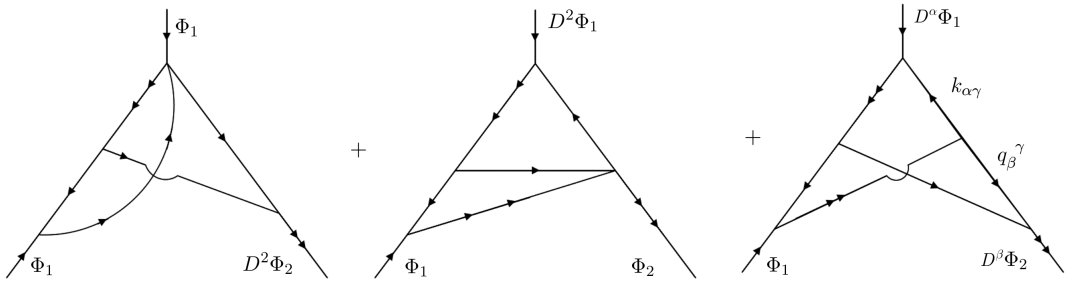

Figure 4.14: Diagrams resulting from the D-algebra reduction of diagram 4.13(d).

In the first two diagrams the covariant derivatives act on the external fields or they are responsible for the simplification of some propagators. In fact, there are some effective 4-point vertices due to Dirac δ-functions arising in this way. In both cases we are left with a loop containing three propagators whose arrows form a closed loop, and then there is enough regularity to apply the Jordan's lemma and conclude that they vanish.

Due to the structure of the external covariant derivatives, the only relevant contribution from the third diagram in fig. 4.14 is proportional to

$$\begin{aligned}\int \frac{d\omega_q d^2q}{(2\pi)^3}\frac{d\omega_k d^2k}{(2\pi)^3}\,\varepsilon_{\alpha\beta}\left(m(\omega_k+\omega_q)+\vec{k}\cdot\vec{q}\right)\frac{1}{2m\omega_k-\vec{k}^2+i\varepsilon}\frac{1}{4m(\omega_{p_1}+\omega_k)-(\vec{p}_1+\vec{k})^2+i\varepsilon}\\ \times\frac{1}{2m(\omega_k+\omega_q-\omega_{p_2})-(\vec{k}+\vec{q}-\vec{p}_2)^2+i\varepsilon}\frac{1}{4m(\omega_k+\omega_q)-(\vec{k}+\vec{q})^2+i\varepsilon}\\ \times\frac{1}{2m\omega_q-\vec{q}^2+i\varepsilon}\frac{1}{2m(\omega_{p_1}+\omega_{p_2}-\omega_q)-(\vec{p}_1+\vec{p}_2-\vec{q})^2+i\varepsilon}\end{aligned} \tag{4.74}$$

where momenta $(\omega_{p_a},\vec{p}_a)$, $a=1,2$ refer to the external Φ_1,Φ_2 particles. At the numerator we have used the null reduction of the 4d expression $k_{\alpha\dot\alpha}\,q_\beta^{\dot\alpha}=(\sigma^M)_{\alpha\dot\alpha}(\sigma^N)_\beta{}^{\dot\alpha}k_M q_N$.

If we now focus on the ω_k integration, we see that in the region of large ω_k the worst integrand goes as $1/\omega_k^3$. This allows to apply Jordan's lemma and compute the integral by residue theorem. Since all the poles are on the same side of the complex plane the result is zero.

The same pattern occurs for the other configurations of arrows in fig. 4.13(a)-(c). This provides a check of selection rule 4.4.1 in this particular case.

Extending the analysis of quantum corrections of the three-point vertex at higher loops, again we find that in the non-relativistic model the number of (finite) quantum contributions is drastically reduced compared to the relativistic case.

4.4.5 Non-relativistic non-renormalization theorem

There is an ever stronger support to the absence of quantum corrections to the three-point vertex: we argue that it is possible to inherit the non-renormalization theorem from the relativistic parent theory.

We consider a generic Galilean WZ model for n chiral superfields

$$S = \int d^3x d^2\theta d^2\bar{\theta}\,\bar{\Phi}_a\Phi_a + g\int d^3x d^2\theta\, W(\Phi_a) + \text{h.c.} \tag{4.75}$$

obtained by null reduction of the relativistic one in eq. (4.32).

The same argument used in the relativistic case can be adapted here in order to rule out quantum corrections to the F-term. As in eq. (4.33) we can introduce one extra chiral superfield Y multiplying the superpotential, which can be set equal to 1 in order to reproduce eq. (4.75), together with wave function renormalization superfields Z_{ab}

$$\tilde{S} = \int d^3x d^4\theta\, Z_{ab}\bar{\Phi}_a\Phi_b + \int d^3x d^2\theta\, Y\, W(\Phi_a) + \text{h.c.} \tag{4.76}$$

Since the non-relativistic limit via null reduction technique does not affect the grassmannian part of the superfields in the action, R-symmetry works in the same way as in the relativistic case. Therefore, as in the relativistic case, we assign R-charges $R(\Phi_a) = 0$ and $R(Y) = 2$.

The regularization that we used, which corresponds to first performing the regular ω-integrals and then the $\vec{k}$-integrals in dimensional regularization, preserves SUSY[15]. Therefore, the Wilsonian effective action at a given scale λ will have the following general structure

$$\tilde{S}_\lambda = \int d^3x d^4\theta\, K(\bar{\Phi}_a\Phi_a, Z_{ab}, Y, \bar{Y}, D) + \int d^3x d^2\theta\, W_\lambda(\Phi_a, Y) \tag{4.77}$$

R-invariance and holomorphicity of the superpotential, combined with the weak coupling limit, give as in the relativistic case $W_\lambda = Y\,W(\Phi_a)$.

4.5 Comments and discussion

We have seen many interesting properties from the investigation of the null reduction of the $3+1$ dimensional WZ model. The non-renormalization theorem is inherited because the DLCQ method does not affect the grassmannian part of the superfields and SUSY is preserved after quantization, which allow to import both the perturbative and the non-perturbative formulations of the theorem.

More surprisingly, the properties of the model coming from the Galilean invariance of the problem produce many interesting results. Combining the retarded nature of the propagator with the mass conservation, we found a set of selection rules which eliminate from the study of quantum corrections a lot of supergraphs which are instead allowed in the relativistic parent theory. As a result, the contributions to the self-energy vanish up to four loops, except for a one-loop diagram for the superfield Φ_2.

Extending the investigation to higher loops we have provided strong evidence that the combination of the non-renormalization properties of the F-terms and the selection rules, in particular the vanishing

[15] The fact that our regularization scheme preserves SUSY can also be seen at the level of components fields, see Appendix C, where we find consistent results from the quantum corrections of the various fields.

of loop diagrams whose arrows form a closed loop, sup- presses Galilean UV divergences in a very efficient way and makes the model one-loop exact. This remarkable property is not shared by the relativistic parent theory, and then we have strong evidence that the non-relativistic limit and the quantization of a theory do not commute: we cannot obtain the Galilean WZ model at quantum level simply by null-reducing the quantum relativistic one. This observation points in the same direction of the fact that the non-relativistic trace anomaly studied in chapters 2, 3 is not simply the null reduction of the relativistic ones.

The result we have found is reminiscent of relativistic gauge theories with extended SUSY, like for instance the relativistic $\mathcal{N} = 2$ SYM in 3+1 dimensions. In that case extended supersymmetry constrains the corrections to the Kähler potential to be related to the F-terms, which are protected by the non-renormalization theorem. In the non-relativistic model discussed in this paper, instead the protection of the Kähler potential is related to the $U(1)$ charge conservation at each vertex, which in many diagrammatic contributions constrains arrows to form a closed loop, so leading to a vanishing integral. It would be interesting to investigate if a common hidden mechanism exists, which is responsible of the similar mild UV behavior of these two rather different classes of theories.

The Galilean WZ model that we investigated is classically scale invariant, but not quantum mechanically. In fact, choosing for simplicity the case where the coupling constant g is real, we find from the non-renormalization theorem and the one-loop exactness of the self-energy that the beta function is given by

$$\beta_g = \frac{dg}{d\log\mu} = \frac{g^3}{4\pi m} \tag{4.78}$$

and the theory is infrared free at low energies, like the model studied in [96]. It is interesting to observe that the result in ref. [96] is also exact, but for different reasons: in that model there are only scalar fields with quartic interaction, and the non-relativistic invariance forbids any self-energy correction, while the contributions to the vertex can be resummed.

Part II

Complexity

Chapter 5

Complexity for warped AdS black holes

The work in this chapter has previously appeared in [97, 98].

In the first part of this thesis we focused on QFT aspects concerning the investigation of the trace anomaly and the renormalization properties of Galilean-invariant systems. In this context, there was recently much interest in the investigation of a particular kind of models with non-relativistic invariance, called Warped Conformal Field Theories (WCFTs) and studied in $1+1$ dimensions. These are local field theories invariant under translations and chiral dilatations[1]

$$x^{\pm} \to x^{\pm} + c^{\pm}\,, \qquad x^{-} \to \lambda x^{-}\,, \tag{5.1}$$

where $\lambda, c^{\pm}$ are constants. If we require unitarity, locality and a spectrum bounded from below of the dilatation operator, this symmetry enhances to an infinite-dimensional group which can be either the conventional conformal group or a Virasoro times a Kac-Moody algebra, which give the warped conformal case [99]. The global subgroup in the latter case is $SL(2,\mathbb{R}) \times U(1)$.

General classifications of quantum anomalies can be performed for this class of theories [64]: the computation requires to couple the system to an appropriate background, which turns out to be the NC geometry introduced in section 2.1. On this background Weyl invariance can be defined and it is possible to interpret WCFTs as Lifshitz field theories with dynamical exponent $z = \infty$.

As for the trace anomaly, we can hope to compute the quantum anomalies for explicit models realizing the warped symmetry, but it turns out that there are very few examples of such models, and moreover they are all on the edge of non-locality: there is an infinite number of exactly marginal operators which are non-local along one of the coordinates in the 1+1 dimensional spacetime. For these reasons, it may be convenient to investigate the quantum anomalies and other aspects of these theories from a different point of view, *i.e.* using holography. In fact, it was conjectured that WCFTs are dual to a non-trivial deformation of AdS_3 which only preserves the isometries $SL(2,\mathbb{R}) \times U(1)$, called warped AdS_3 spacetime [63, 64, 100–102]. First of all, the set of symmetries of this spacetime

[1] We label the two coordinates as $x^{\pm}$, which is the common choice in the literature. Despite the name, these are not light-cone coordinates.

matches with the field theory side. Secondly, the entanglement entropy was studied in this context and an analog of the Cardy formula was found [63]. Entanglement entropy in this context has been studied by several authors [103–107].

There are various reasons to study WCFTs and their holographic dual. First of all, from the theoretical point of view, it is interesting to consider a non-relativistic conformal field theory with an infinite dimensional symmetry group. Since in the relativistic case the constraints given by the Virasoro algebra and the holomorphic structure of the symmetry group are so powerful to give remarkable results, we may hope to find similar phenomena in this case as well. Secondly, it is thought that WCFT techniques can be applied in condensed matter systems like the Potts model, because they show an anisotropic scaling [108]. The investigation of the field theory side is also useful to study higher spin theories. In fact, these models require to consider all kind of conserved currents on equal footing, a treatment that can be obtained in the WCFT context. This approach turns out to be useful to understand the modular properties of partition functions for such theories [109, 110]. From the point of view of holography, extremal rotating black holes have a near horizon which is topologically $AdS_3 \times S^2$ in 3+1 dimensions. This structure leads to a simplifications of low-energy S-matrix elements and is conjectured to be dual to a CFT (Kerr/CFT correspondence). In particular, when going at fixed polar angle in this configuration, we precisely find a $WAdS_3$ structure. We then think that an analysis of WAdS/WCFT correspondence can also shed light on properties of extremal rotating black holes.

In this chapter we continue the investigation of non-local quantities from the gravity side by studying the computational complexity, which recently was proposed to describe the time evolution of the Einstein-Rosen Bridge (ERB) of a BH [56, 57]. In the Complexity=Volume (CV) conjecture, complexity is proportional to the volume of a maximal codimension-one slice anchored at the boundary

$$C_V \sim \frac{\mathrm{Max}(V)}{Gl}\,. \tag{5.2}$$

In this expression l is a length scale which depends from the holographic setting we are considering. The precise proportionality factor also depends from the specific BH.

In the Complexity=Action (CA) conjecture, complexity is proportional to the gravitational action evaluated in the Wheeler-De Witt (WDW) patch, *i.e.* the bulk domain of dependence of the extremal slice

$$C_A = \frac{I}{\pi\hbar}\,. \tag{5.3}$$

Holographic complexity has been recently studied by many groups in various asymptotically AdS gravity backgrounds, see *e.g.* [58, 111–122]. In the context of warped AdS, previous studies were performed in [123, 124].

In order to test the holographic proposals by Susskind, we will study both the CV and the CA conjectures for BHs in Warped AdS_3 seen as a solution of Einstein gravity coupled to electromagnetism with Chern-Simons term.

We point out that while this computation can provide important hints for the matching of complexity with the field theory side of the duality, the precise definition of complexity in QFT has yet to be completely understood. Here we briefly review the state of the art of this problem[2].

A promising approach is based on Nielsen's geometric formalism, which involves the search for geodesics in the space of unitary evolutions [125–128]. The idea is to consider a quantum circuit model in order to obtain the target state $|\psi_T\rangle$ starting from a simple reference state $|\psi_R\rangle$ via the application of a unitary operator such that

$$|\psi_T\rangle = U|\psi_R\rangle\,, \tag{5.4}$$

where U is built with a set of simple elementary gates. The unitary operator can be synthesized by means of an Hamiltonian such that

$$U = \vec{\mathscr{P}} \exp\left[\int_0^1 dt\, H(t)\right], \tag{5.5}$$

where

$$H(t) = \sum_I Y^I(t) M_I\,. \tag{5.6}$$

In the previous expressions $\vec{\mathscr{P}}$ is the path ordering such that the Hamiltonian at earlier times is applied to the first state (*i.e.* the circuit is built starting from the right), M_I is a set of generalized Pauli matrices and Y^I are control functions which specify the tangent vector to a trajectory in the space of unitaries, given by

$$U(t) = \vec{\mathscr{P}} \exp\left[\int_0^t dt'\, H(t')\right]. \tag{5.7}$$

The boundary conditions on such trajectories are $U(0) = \mathbf{1}$ and $U(1) = U$, *i.e.* we start from the reference state and we end up with the target state as in eq. (5.4). In order to give a measure of the difficulty to perform a path in the space of unitary, we have to define a cost function

$$\mathscr{D}(U(t)) = \int_0^1 dt\, F\left(U(t), \dot{U}(t)\right), \tag{5.8}$$

where the minimum corresponds to the optimal circuit, thus providing the definition of complexity. The minimal requirements for a reasonable cost function imposed by Nielsen correspond to define (5.8) as a length functional for a Finsler manifold, which is a particular class of differentiable manifolds where a concept of distance can be introduced. In this context, the problem to find the optimal circuit corresponds to finding the length of geodesics in this particular geometry.

When considering free field theories, it is possible to regularize the theory by placing it on a lattice, which reduces the computation of complexity to the case of a set of harmonic oscillators. Progress

[2]The reader interested only in the holographic approach to complexity can directly skip to section 5.1.

with this approach has been made in computing the complexity for a set of harmonic oscillators for the preparation of Gaussian states, while the computation is challenging for more general states.

Another approach from the field theory side is based on building a path in the space of states, where the distance is determined using the Fubini-Study metric on the space of the normalized states [129]. In this case we define a path as

$$|\psi(\sigma)\rangle = U(\sigma)|\psi_R\rangle\,, \tag{5.9}$$

with

$$U(\sigma) = \vec{\mathscr{P}} \exp\left[-i\int_{s_i}^{\sigma} ds\, G(s)\right]. \tag{5.10}$$

In this context, s parametrizes the progress along a path in the space of states starting from s_i and ending at s_f, with $\sigma \in [s_i, s_f]$, while $G(s)$ is a generator taken from an elementary set of hermitian operators. The Fubini-Study line element is then defined to be

$$ds^2 = d\sigma^2\left(|\partial_\sigma|\psi(\sigma)\rangle|^2 - |\langle\psi(\sigma)|\partial_\sigma|\psi(\sigma)\rangle|^2\right). \tag{5.11}$$

The complexity is found by computing the geodesics corresponding to this geometry. Even using this technique, most of the results are formulated for Gaussian states.

We conclude the review of field theory definitions of complexity with an approach slightly different from the previous ones, being based on a path integral optimization process [130–132]. Consider a QFT defined in Euclidean spacetime $\mathbb{R}^d$ with coordinates denoted as (x,z), being x the vector referring to the spatial dimensions $\mathbb{R}^{d-1}$ and $z = -\tau$ the opposite of Eucidean time, which is interpreted to be the radial coordinate of AdS_{d+1} in the holographic picture. The reference state can be considered to be the vacuum computed as a path integral over the spatial directions and $\varepsilon < z < \infty$, where ε is a UV cutoff:

$$\psi_{g_0,\lambda_0}[\phi(x)] = \int \prod_x \prod_{\varepsilon<z<\infty} \mathscr{D}\phi(x,z)\, e^{-S_{g_0,\lambda_0}[\phi]} \prod_x \delta\left(\phi(x,\varepsilon) - \phi(x)\right). \tag{5.12}$$

In this definition g_0 is the flat space metric where the integration is performed

$$ds^2 = \frac{dx^2 + dz^2}{\varepsilon^2}\,, \tag{5.13}$$

while λ_0 is a general label for the coupling constants of the QFT with action $S_{g_0,\lambda_0}[\phi]$. The optimization process consists in letting the metric and the coupling constants to vary with the space coordinates $g(x,z), \lambda(x,z)$ with boundary conditions

$$g(x,\varepsilon) = g_0\,, \qquad \lambda(x,\varepsilon) = \lambda_0\,. \tag{5.14}$$

In this way, the general path integral defining a state is

$$\psi_{g(x,z),\lambda(x,z)}[\phi(x)] = \int \prod_x \prod_{\varepsilon<z<\infty} \mathscr{D}\phi(x,z)\, e^{-S_{g(x,z),\lambda(x,z)}[\phi]} \prod_x \delta\left(\phi(x,\varepsilon)-\phi(x)\right). \tag{5.15}$$

Of course this state differs from (5.12) in a non-trivial way, but it is possible to fine tune $g(x,z),\lambda(x,z)$ in order to find particular configurations such that

$$\psi_{g(x,z),\lambda(x,z)}[\phi(x)] = e^{N[g,\lambda]-N[g_0,\lambda_0]}\, \psi_{g_0,\lambda_0}[\phi(x)]. \tag{5.16}$$

If this is possible, it means that the wave-functions describe the same quantum state. The optimization procedure consists in minimizing the functional $N[g,\lambda]$ appearing in the exponential, and this minimum value corresponds to complexity. It turns out that most of the results obtained with this approach are limited to $d=2$ dimensions, where the functional can be related to the Liouville action.

Given the previous approaches to complexity from the field theory side, we understand how much is important to have computations from the gravitational side in order to have some feelings for the results to compare, and to understand which of the previous proposals should be taken to define complexity. We start testing the holographic conjectures by Susskind for black holes in warped AdS_3 spacetime.

5.1 Black holes in Warped AdS

We consider BHs in a spacetime with Warped AdS_3 asymptotic [133, 134, 100], which are interpreted to be dual to a boundary WCFT at finite temperature. The metric is given by

$$\frac{ds^2}{l^2} = dt^2 + \frac{dr^2}{(\nu^2+3)(r-r_+)(r-r_-)} + \left(2\nu r - \sqrt{r_+ r_-(\nu^2+3)}\right) dt d\theta + \frac{r}{4}\Psi d\theta^2, \tag{5.17}$$

$$\Psi(r) = 3(\nu^2-1)r + (\nu^2+3)(r_++r_-) - 4\nu\sqrt{r_+r_-(\nu^2+3)}. \tag{5.18}$$

We introduce the quantity $\tilde{r}_0$ as

$$\tilde{r}_0 = \max(0,\rho_0), \qquad \rho_0 = \frac{4\nu\sqrt{r_+r_-(\nu^2+3)} - (\nu^2+3)(r_++r_-)}{3(\nu^2-1)}, \tag{5.19}$$

where $\Psi(\rho_0)=0$. The range of coordinates is $r\in[\tilde{r}_0,\infty), t\in(-\infty,\infty)$ and $\theta\in[0,2\pi]$ with the identification $\theta\sim\theta+2\pi$. We denote with r_-, r_+ the inner and outer horizons, respectively. They satisfy $r_-\le r_+$ and the particular case $r_-=r_+=0$ corresponds to empty warped AdS_3 spacetime in Poincaré patch with timelike boundary parametrized by (t,θ). The parameter ν is related to the left and right central charges of the boundary WCFTs, which in Einstein gravity are [101]

$$c_L = c_R = \frac{12 l \nu^2}{G(\nu^2+3)^{3/2}}. \tag{5.20}$$

Ordinary AdS_3 spacetime can be seen as a fibration of the real line over AdS_2, but if a warping factor multiplies the fiber metric we obtain a spacetime whose asympthotic changes from $SL(2,\mathbb{R})_L \times SL(2,\mathbb{R})_R$ to $SL(2,\mathbb{R})_L \times U(1)_R$. This warping is parametrized by ν and it is such that for $\nu = 1$ the Banados-Teitelboim-Zanelli (BTZ) black hole [135, 136] is recovered. In fact, in this case the change of coordinates

$$r = \bar{r}^2\,, \qquad t = \frac{\sqrt{r_+} - \sqrt{r_-}}{l^2}\bar{t}\,, \qquad \theta = \frac{l\bar{\theta} - \bar{t}}{l^2(\sqrt{r_+} - \sqrt{r_-})}\,, \qquad r_\pm = \bar{r}_\pm^2 \tag{5.21}$$

brings the metric to the standard BTZ form

$$ds^2 = -\frac{\bar{r}^2 - \bar{r}_+^2 - \bar{r}_-^2}{l^2}d\bar{t}^2 + \frac{l^2\bar{r}^2}{(\bar{r}^2 - \bar{r}_+^2)(\bar{r}^2 - \bar{r}_-^2)}d\bar{r}^2 - 2\frac{\bar{r}_+\bar{r}_-}{l}d\bar{t}d\bar{\theta} + \bar{r}^2 d\bar{\theta}^2\,. \tag{5.22}$$

For $\nu^2 < 1$ the solution is pathological because it has closed time-like curves. For $\nu^2 > 1$ the solution is not sick and can be realized as an exact vacuum solution of Topologically Massive Gravity (TMG) [133, 134], New Massive Gravity (NMG) [137] and also general linear combinations of the two mass terms [138]. We restrict our analysis to the case of positive ν. So at the end we will consider just the case $\nu \geq 1$.

Strictly speaking, the relation between area and entropy holds just in Einstein gravity: if we consider higher order corrections to the gravitational entropy, we have to use the Wald entropy formula [139] instead of the geometrical area law. So the CV conjecture should be directly applicable just to Einstein gravity and should be appropriately modified in order to take into account higher order corrections in the gravitational action. A proposal for such correction has been put forward in [140, 141]. The CA conjecture can also be generalized to the case of higher derivatives corrections to the gravitational action, see e.g. [142, 123, 143].

As far as we know, there is no known non-pathological matter content in field theory supporting stretched warped BHs in Einstein gravity [101]. However, they can be obtained as solutions to a perfect fluid stress tensor with spacelike quadrivelocity [144]. Alternatively they can arise as a solution of Chern-Simons-Maxwell electrodynamics coupled to Einstein gravity [145, 146], but a wrong sign for the kinetic Maxwell term is required in order to have solutions with no closed time-like curves (which corresponds to $\nu^2 \geq 1$). Moreover, warped BH can arise in string theory constructions, e.g. [147–149]. In the following we take a pragmatical approach: we suppose that a consistent realization of stretched warped BHs in Einstein gravity exists, and we investigate the CV conjecture.

We will use for concreteness the model studied in [145, 146], which is Chern-Simons-Maxwell electrodynamics coupled to Einstein gravity. In order to have solutions without closed time-like curves, a wrong sign for the kinetic Maxwell term is needed. Solutions with positive Maxwell kinetic energy have $\nu^2 < 1$ and correspond to Gödel spacetimes. We will see that the CA conjecture is so solid that can survive to an unphysical action with ghosts.

5.1.1 Conserved charges and thermodynamics

In order to get a physical understanding of the computation of complexity, we need to find the conserved charges and the thermodynamics quantities of the BH. Since we are studying the implications of taking the warped BH as a solution of Einstein gravity, the entropy is simply given by the area law

$$S = S_+ = \frac{l\pi}{4G}(2\nu r_+ - \sqrt{r_+ r_-(\nu^2+3)}), \tag{5.23}$$

while the Hawking temperature[3] and angular momentum are given by [100]:

$$T = \frac{\nu^2+3}{4\pi l}\frac{r_+ - r_-}{2\nu r_+ - \sqrt{(\nu^2+3)r_+ r_-}}, \qquad \Omega = \frac{2}{(2\nu r_+ - \sqrt{(\nu^2+3)r_+ r_-})l}. \tag{5.24}$$

At least formally, it is possible to associate an entropy via the area law to the surface corresponding to the inner horizon as

$$S_- = \frac{l\pi}{4G}(\sqrt{r_+ r_-(\nu^2+3)} - 2\nu r_-). \tag{5.25}$$

Following [150, 151], the existence of a holographic dual implies a quantization condition on the product of inner and outer entropies, which in turn must be proportional to the conserved charges of the black hole which are quantized. Since the angular momentum is the only quantized conserved charge, we obtain $J = S_- S_+ f(\nu)$, where $f(\nu)$ is a so far arbitrary function which will be fixed by thermodynamics.

Imposing that the resulting dM is an exact differential, the function $f(\nu)$ is fixed and allows to solve for both the conserved charges:

$$M = \frac{1}{16G}(\nu^2+3)\left((r_- + r_+) - \frac{\sqrt{r_+ r_-(\nu^2+3)}}{\nu}\right), \tag{5.26}$$

$$J = \frac{l}{32G}(\nu^2+3)\left(\frac{r_- r_+(3+5\nu^2)}{2\nu} - (r_+ + r_-)\sqrt{(3+\nu^2)r_+ r_-}\right). \tag{5.27}$$

Another approach to find these conserved charges is described in Appendix D.1.

5.1.2 Null coordinates and causal structure

In order to compute the CV and CA conjectures for this class of BHs, we need to know the causal structure of spacetime: this allows to depict extremal surfaces anchored at the boundaries and to build the WDW patch where the gravitational action will be computed. In particular, the Penrose diagram is a useful tool to easily understand the causal properties of spacetime and to visualize these structures.

[3] As in the standard AdS case, the Hawking temperature can be found by requiring the metric does not contain conical singularities after Wick rotating the t coordinate.

We start by finding null coordinates. The expression of the metric (5.17) in Arnowitt-Deser-Misner (ADM) form is:

$$ds^2 = -N^2 dt^2 + \frac{l^4 dr^2}{4R^2 N^2} + l^2 R^2 (d\theta + N^\theta dt)^2 \,, \tag{5.28}$$

where

$$R^2 = \frac{r}{4}\Psi \,, \qquad N^2 = \frac{l^2(\nu^2+3)(r-r_+)(r-r_-)}{4R^2} \,, \qquad N^\theta = \frac{2\nu r - \sqrt{r_+ r_- (\nu^2+3)}}{2R^2} \,. \tag{5.29}$$

We consider a set of null geodesics which satisfy $(d\theta + N^\theta dt) = 0$; then a positive-definite term in the metric (5.28) saturates to zero, and the null geodesics are given by the constant u and v trajectories [152]

$$du = dt - \frac{l^2}{2RN^2} dr \,, \qquad dv = dt + \frac{l^2}{2RN^2} dr \,. \tag{5.30}$$

These are the normal one-forms to the WDW null surfaces

$$dv = v_\alpha dx^\alpha \,, \qquad du = u_\alpha dx^\alpha \,. \tag{5.31}$$

Moreover, the integral curves of u^α and v^α are null geodesics in the affine parameterization, *i.e.*

$$u^\alpha D_\alpha u^\beta = 0 \,, \qquad v^\alpha D_\alpha v^\beta = 0 \,, \tag{5.32}$$

where D_α is the covariant derivative.

Direct integration of them allows to define Eddington-Finkelstein coordinates as

$$u = t - r^*(r) \,, \qquad v = t + r^*(r) \,, \tag{5.33}$$

where the tortoise coordinate r^* is given by

$$r^*(r) = \int^r \frac{dr'}{f(r')} \,, \qquad f(r) = \frac{2RN^2}{l^2} = \frac{(\nu^2+3)(r-r_-)(r-r_+)}{\sqrt{r\Psi(r)}} \,. \tag{5.34}$$

Integrating eq. (5.34), r^* can be explicitly found [152]; for $r_+ \neq r_-$ the explicit expression is

$$\begin{aligned} r^*(r) = & \frac{\sqrt{3(\nu^2-1)}}{(\nu^2+3)} \left\{ \frac{\sqrt{r_+(r_+-\rho_0)}}{r_+-r_-} \log\left(\frac{|r-r_+|}{\left(\sqrt{r}\sqrt{r_+-\rho_0} + \sqrt{r-\rho_0}\sqrt{r_+}\right)^2} \right) \right. \\ & \left. - \frac{\sqrt{r_-(r_--\rho_0)}}{r_+-r_-} \log\left(\frac{|r-r_-|}{\left(\sqrt{r}\sqrt{r_--\rho_0} + \sqrt{r-\rho_0}\sqrt{r_-}\right)^2} \right) + 2\log(\sqrt{r}+\sqrt{r-\rho_0}) \right\} \,, \end{aligned} \tag{5.35}$$

where ρ_0 was defined in eq. (5.19).

The non-rotating case is defined by the condition $J = 0$, and corresponds to the following values:

$$r_- = 0\,, \qquad \frac{r_+}{r_-} = \frac{4\nu^2}{\nu^2+3}\,. \tag{5.36}$$

The two values in eq (5.36) can be mapped among each other by an isometry [152], then we will always consider the case $r_- = 0, r_+ = r_h$ for simplicity when referring to the non-rotating case. Curiously enough, in this case the Penrose diagram is the same as the ones for the Schwarzchild BH in 3+1 dimensions [152]. In the rotating case, for generic (r_+, r_-), the Penrose diagram is the same as the one of the Reissner-Nordström BH (see figs. 7 and 8 of [152]). The extremal limit corresponds to $r_+ = r_-$; in this case temperature is zero and there is no thermofield double: the Penrose diagram has just one boundary.

In light of the conjectured WAdS/WCFT duality, it is puzzling that the spacetime has a Minkwoskian asymptotic, because it is not completely clear where the boundary theory should live. We point out that in our computation we will always require the existence of a UV cutoff Λ which induces a timelike boundary where we can think that the QFT lives. When taking the limit $\Lambda \to \infty$, the timelike boundary goes to a single point in the Penrose diagram, where there is the future timelike infinity[4]. A similar issue arises when we will build the WDW patch for this black hole: we discuss in more details how we treat the problem in section 6.3.1.

5.1.3 An explicit realization in Einstein gravity

In view of the computation of the CA conjecture, we need to take a specific theory supporting warped BHs as a solution of Einstein gravity. For concreteness we will use a model introduced in [145], where the matter content is a Chern-Simons $U(1)$ gauge field. In order to find absence of closed time-like curves ($\nu^2 \geq 1$), a ghost-like kinetic Maxwell term is needed. We will see that the CA conjecture seems solid enough to survive to unphysical matter contents which include ghosts, giving a physical result consistent with expectations about complexity from quantum information.

We consider Einstein gravity in $2+1$ dimensions with a negative cosmological constant, coupled to a $U(1)$ gauge field with both Maxwell and Chern-Simons terms

$$I_{\mathscr{V}} = \frac{1}{16\pi G}\int_{\mathscr{V}} d^3x \left\{\sqrt{-g}\left[\left(R+\frac{2}{L^2}\right) - \frac{\kappa}{4}F_{\mu\nu}F^{\mu\nu}\right] - \frac{\alpha}{2}\varepsilon^{\mu\nu\rho}A_\mu F_{\nu\rho}\right\} = \int_{\mathscr{V}} d^3x\sqrt{-g}\,\mathscr{L}\,, \tag{5.37}$$

where $\varepsilon^{\mu\nu\rho}$ is the Levi-Civita tensorial density. Here we put a coefficient $\kappa = \pm 1$ in front of the Maxwell kinetic term

The equations of motion for the gauge field are

$$D_\mu F^{\alpha\mu} = -\frac{\alpha}{\kappa}\frac{\varepsilon^{\alpha\nu\rho}}{\sqrt{g}}F_{\nu\rho}\,, \tag{5.38}$$

[4] We remind that the Penrose diagram for 2+1 dimensional WAdS contains at each point a factor of S^1, so that the future timelike infinity is not actually a single point.

while the Einstein equations are

$$G_{\mu\nu} - \frac{1}{L^2} g_{\mu\nu} = \frac{\kappa}{2} T_{\mu\nu}\,, \qquad T_{\mu\nu} = F_{\mu\alpha} F_{\nu}{}^{\alpha} - \frac{1}{4} g_{\mu\nu} F^{\alpha\beta} F_{\alpha\beta}\,. \tag{5.39}$$

We consider the set of coordinates (r,t,θ) where the metric assumes the form (5.17), and we choose a gauge motivated by the ansatz from [145]:

$$A = a dt + (b + cr) d\theta\,, \qquad F = c\, dr \wedge d\theta\,, \tag{5.40}$$

where $\{a,b,c\}$ is a set of constants. Thus, the Maxwell equations give:

$$\alpha = \kappa \frac{\nu}{l}\,. \tag{5.41}$$

From the Einstein equations, we get, independently from (r_+, r_-):

$$L = l \sqrt{\frac{2}{3-\nu^2}}\,, \qquad c = \pm l \sqrt{\frac{3}{2} \frac{1-\nu^2}{\kappa}}\,. \tag{5.42}$$

The second equation shows that there is conflict between absence of closed time-like curves and the presence of ghosts ($\kappa = -1$).

The gauge parameter a is not constrained by the equations of motion, but the action depends explicitly on a through the Chern-Simons term. The value of a is important to properly define the mass M as a conserved charge [146]. Formally, only for the value

$$a = \frac{l}{\nu} \sqrt{\frac{3}{2}} \sqrt{\nu^2 - 1}\,. \tag{5.43}$$

the mass is associated to the Killing vector $\partial/\partial t$ and it does not depend on the $U(1)$ gauge transformations. For this value, the action density reads:

$$16\pi G \sqrt{-g}\, \mathscr{L} = -\frac{l}{2}(\nu^2 + 3) \equiv \mathscr{I}\,. \tag{5.44}$$

The comparison with the solution of [145] is discussed in appendix D.1.

5.2 Complexity=Volume

5.2.1 Einstein-Rosen bridge

The Penrose diagram for the non-rotating case is shown in figure 5.1, with some lines at constant r and t. Both in the rotating and non-rotating cases, for $r \to \infty$, the asymptotic behavior of $r^*(r)$ is

$$r^*(r) \approx \frac{3\sqrt{\nu^2 - 1}}{\nu^2 + 3} \log r \equiv C \log r\,. \tag{5.45}$$

So we should first fix a cutoff surface at $r = \Lambda$ to make our calculations finite. The WDW surface is bounded by lines with constant values of v and u, which in the Penrose diagram correspond to 45 degrees lines.

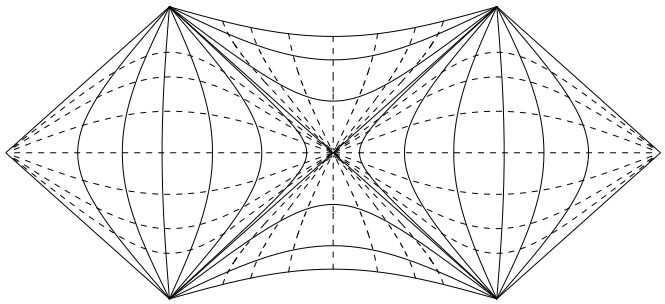

Figure 5.1: Constant r lines (solid) and constant t lines (dashed) of the Penrose diagram in the non-rotating case.

On the left and right boundaries, the time coordinate t diverges to $\pm\infty$ in the upper and lower sides, respectively. From eqs. (5.33), a change of cutoff from Λ_1 to Λ_2 implies a constant shift in the time coordinate by $C \log \frac{\Lambda_2}{\Lambda_1}$. For $\nu = 1$ we recover the AdS asymptotic, $r^*(\infty)$ is finite and no shift is needed; the Penrose diagram in this case is different and is the standard one of the BTZ black hole.

As done in [54, 56] for the AdS and the flat cases, we consider an extremal codimension-one bulk surface extending between the left and the right side of the Kruskal diagram; we denote the times at the left and right sides as t_L, t_R, respectively. The dual thermofield double state has the following form:

$$|\Psi_{TFD}\rangle \propto \sum_n e^{-E_n\beta/2 - iE_n(t_L+t_R)} |E_n\rangle_R |E_n\rangle_L \,, \tag{5.46}$$

where $|E_n\rangle_{L,R}$ refer to the energy eigenstates of left and right boundary theories, β is the inverse temperature. The usual time translation symmetry in Schwarzschild coordinates corresponds to a forward time translation on the right side and a backward translation on the left one [55], *i.e.*

$$t_L \to t_L + \Delta t \,, \qquad t_R \to t_R - \Delta t \,. \tag{5.47}$$

This corresponds to the invariance of the thermofield double state under the evolution described by the Hamiltonian $H = H_L - H_R$ in the associated couple of entangled WCFTs. If instead we take time running forward on both the copies of the boundaries, we introduce some genuine time dependence in the problem [153] and the volume of the maximal slice will depend on time [56]. We will then consider the symmetric case with equal boundary times

$$t_L = t_R = t_b/2 \,. \tag{5.48}$$

In order to regularize the divergences, the times at the left and right boundaries are evaluated at the cutoff surface $r = \Lambda$.

5.2.2 Null coordinates for the computation of the Volume

In Section 5.1.2 we already introduced a set of null geodesics, but it turns out that there is a similar coordinate system that is convenient to study the volume of the Einstein-Rosen bridge anchored at the boundary.

We have the following conserved quantities along geodesics:

$$\begin{aligned} K &= 2\dot{t} + \left(2\nu r - \sqrt{r_+ r_-(\nu^2+3)}\right)\dot{\theta}\,, \\ P &= \left(2\nu r - \sqrt{r_+ r_-(\nu^2+3)}\right)\dot{t} + \frac{r}{2}\Psi(r)\,, \end{aligned} \tag{5.49}$$

where dots denote derivatives with respect to the geodesic affine parameter.

All the null geodesics that can be found in the spacetime are parametrized by these conserved quantities. By taking the particular choice $P = 0$ with generic K we find precisely the set of null coordinates defined in Section 5.1.2. In this case we take instead the special value $K = 0$ with generic P, getting a particular set of geodesics satisfying

$$\dot{t} = \frac{P\left(2\nu r - \sqrt{r_+ r_-(\nu^2+3)}\right)}{(\nu^2+3)(r-r_-)(r-r_+)}\,, \qquad \dot{\theta} = -\frac{2P}{(\nu^2+3)(r-r_-)(r-r_+)}\,, \qquad \dot{r} = \pm P\,. \tag{5.50}$$

These geodesics can be used to introduce null coordinates which are regular at the horizon.

The infalling geodesics correspond to

$$\frac{d\theta}{dr} = \frac{2}{(\nu^2+3)(r-r_-)(r-r_+)}\,, \qquad \frac{dt}{dr} = -\frac{2\nu r - \sqrt{r_+ r_-(\nu^2+3)}}{(\nu^2+3)(r-r_-)(r-r_+)}\,, \tag{5.51}$$

and allow to define Eddington-Finkelstein coordinates (w, θ_w) such that

$$dw = dt + \frac{2\nu r - \sqrt{r_+ r_-(\nu^2+3)}}{(\nu^2+3)(r-r_-)(r-r_+)}dr\,, \qquad d\theta_w = d\theta - \frac{2}{(\nu^2+3)(r-r_-)(r-r_+)}dr\,. \tag{5.52}$$

The finite expression for the coordinate change is[5]

$$w = t + \tilde{r}(r)\,, \qquad \theta_w = \theta - \frac{2}{(\nu^2+3)(r_+-r_-)}\log\left|\frac{r-r_+}{r-r_-}\right|\,, \tag{5.53}$$

[5] We called the null coordinate and the associated tortoise coordinate as $w, \tilde{r}(r)$ to distinguish them from the names $v, r^*(r)$ used for the quantities defined in section 5.1.2. However, they are defined with the same spirit, the only difference being the particular choice of the parameters K, P in the conserved quantities (5.49) along a null geodesic.

where

$$\tilde{r}(r) = \frac{2\nu r_+ - \sqrt{r_+ r_-(\nu^2+3)}}{(\nu^2+3)(r_+ - r_-)} \log|r - r_+| - \frac{2\nu r_- - \sqrt{r_+ r_-(\nu^2+3)}}{(\nu^2+3)(r_+ - r_-)} \log|r - r_-| \,. \tag{5.54}$$

In terms of these coordinates, the metric becomes

$$\frac{ds^2}{l^2} = dw^2 - dr d\theta_w + \left(2\nu r - \sqrt{r_+ r_-(\nu^2+3)}\right) dw d\theta_w + \frac{r}{4}\Psi(r) d\theta_w^2 \,. \tag{5.55}$$

5.2.3 Computation of the Volume in the non-rotating case

In this section we will compute the volume of the ERB as a function of time [56]. We first study the non-rotating case, setting $r_+ = r_h$ and $r_- = 0$ in the metric with coordinates (5.55).

The minimal volume is chosen along the $0 \le \theta_w \le 2\pi$ coordinate, and with profile functions $w(\lambda)$, $r(\lambda)$, written in terms of a parameter λ. The volume integral will run from $\lambda_{\min}$ to $\lambda_{\max}$, with associated radii $r_{\min}$ and $r_{\max}$:

$$V = 2\cdot 2\pi \int_{\lambda_{\min}}^{\lambda_{\max}} d\lambda\, l^2 \sqrt{\frac{\dot{w}^2 r}{4}\left[3(\nu^2-1)r + (\nu^2+3)r_h\right] - \left(\dot{w} r \nu - \frac{\dot{r}}{2}\right)^2} = 4\pi \int d\lambda\, \mathscr{L}(r, \dot{r}, \dot{w}) \,. \tag{5.56}$$

The factor 2 takes into account the two sides of the Kruskal extension, the 2π is the result of the integration in θ_w and the dots denote derivatives with respect to λ. The radius $r_{\max}$ plays the role of an ultraviolet cutoff; we will take the limit $r_{\max} \to \infty$ at the end of the calculation. The conserved quantity from translational invariance in w gives

$$E = \frac{1}{l^2}\frac{\partial \mathscr{L}}{\partial \dot{w}} = \frac{\frac{\nu^2+3}{4}\dot{w} r (r_h - r) + \frac{\nu r \dot{r}}{2}}{\sqrt{\frac{\dot{w}^2 r}{4}\left[3(\nu^2-1)r + (\nu^2+3)r_h\right] - \left(\dot{w} r \nu - \frac{\dot{r}}{2}\right)^2}} \,. \tag{5.57}$$

We use the reparametrization symmetry for λ in such a way that $V = 4\pi l^2 \int d\lambda$, which implies

$$\frac{\dot{w}^2 r}{4}\left[3(\nu^2-1)r + (\nu^2+3)r_h\right] - \left(\dot{w} r \nu - \frac{\dot{r}}{2}\right)^2 = 1 \,, \qquad E = \frac{\nu^2+3}{4}\dot{w} r (r_h - r) + \frac{\nu r \dot{r}}{2} \,. \tag{5.58}$$

We can then solve for $\dot{r}, \dot{w}$:

$$\dot{r} = 2\sqrt{\frac{4E^2 + (\nu^2+3)\, r\,(r - r_h)}{r\,(3\,(\nu^2-1)\,r + (\nu^2+3)\, r_h)}} \,, \qquad \dot{w} = \frac{4}{(\nu^2+3)(r_h - r)}\left(\frac{E}{r} - \frac{\nu}{2}\dot{r}\right) \,, \tag{5.59}$$

where we took λ in the direction of increasing r. These equations can be solved numerically; some example of solutions, plotted in the Penrose diagram, are shown in figure 5.2.

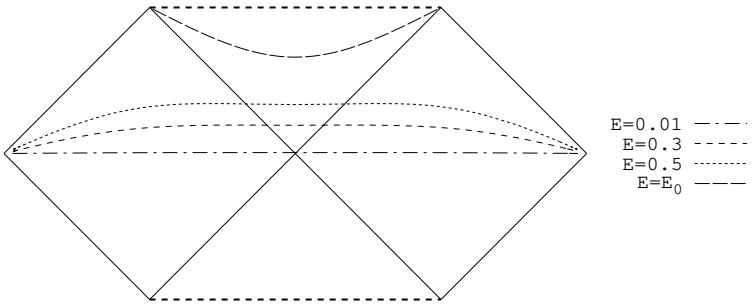

Figure 5.2: Solutions to eqs. (5.59) for the non-rotating case, plotted in a Penrose diagram, for $\nu = 2.5$ and $r_h = 1$. The $E = E_0$ line, which sits at constant $r_{\rm min} = \frac{r_h}{2}$, corresponds to the large t_b limit.

The minimum radius $r_{\rm min}$ is a solution of $\dot{r} = 0$:

$$r_{\rm min}^2 - r_h r_{\rm min} + \frac{4E^2}{(3+\nu^2)} = 0\,, \qquad r_{\rm min} = \frac{r_h}{2}\left(1 \pm \sqrt{1 - \frac{16E^2}{r_h^2(3+\nu^2)}}\right), \tag{5.60}$$

where the physical solution relevant for holographic complexity is the one with the + sign. Conventionally, $t_b = 0$ corresponds to $E = 0$ and $r_{\rm min} = r_h$. The $t_b \to \infty$ limit, instead, corresponds to coincident roots for $r_{\rm min}$ in eq. (5.60), i.e. $E \to \frac{r_h}{4}\sqrt{\nu^2+3}$ and $r_{\rm min} = \frac{r_h}{2}$. The minimal value of the radial coordinate is inside the black hole horizon $\frac{r_h}{2} \le r_{\rm min} \le r_h$.

The volume can be written as an integral over tha radial coordinate

$$V = 4\pi l^2 \int \frac{dr}{\dot{r}} = 2\pi l^2 \int_{r_{\rm min}}^{r_{\rm max}} \sqrt{\frac{r\left(3\left(\nu^2-1\right)r + \left(\nu^2+3\right)r_h\right)}{4E^2 + \left(\nu^2+3\right)r\left(r-r_h\right)}}\,dr\,. \tag{5.61}$$

Here we use a trick similar to the AdS case [113]. We consider the difference of w coordinates

$$\begin{aligned} w(r_{\rm max}) - w(r_{\rm min}) &= \int_{r_{\rm min}}^{r_{\rm max}} dr \frac{\dot{w}}{\dot{r}} \\ &= \int_{r_{\rm min}}^{r_{\rm max}} dr \left[\frac{2}{(\nu^2+3)(r_h - r)}\left(\frac{E}{r}\sqrt{\frac{r\left(3\left(\nu^2-1\right)r + \left(\nu^2+3\right)r_h\right)}{4E^2 + \left(\nu^2+3\right)r\left(r-r_h\right)}} - \nu\right)\right]. \end{aligned} \tag{5.62}$$

Note that this integral is not divergent for $r \to r_h$. The volume can then be written as follows:

$$\begin{aligned} \frac{V}{4\pi l^2} &= E\left(w(r_{\rm max}) - w(r_{\rm min})\right) + \int_{r_{\rm min}}^{r_{\rm max}} dr \left\{\frac{2\nu E}{(\nu^2+3)(r_h - r)}\right. \\ &\quad \left. - \frac{\sqrt{r\left[4E^2 - r(r_h - r)(\nu^2+3)\right]\left[(\nu^2+3)r_h + 3r(\nu^2-1)\right]}}{2(\nu^2+3)r(r_h - r)}\right\}. \end{aligned} \tag{5.63}$$

It is important to emphasize that

$$\lim_{r_{\max}\to\infty} w(r_{\max}) - \tilde{r}(r_{\max}) = t_R \tag{5.64}$$

is finite and can be identified with the time on the right boundary. In the limit $r_{\max} \to \infty$, we can use the explicit expression

$$w(r_{\max}) - w(r_{\min}) = t_R + \tilde{r}(r_{\max}) - \tilde{r}(r_{\min}) \,, \tag{5.65}$$

obtained specializing eq. (5.53) with the values

$$w(r_{\max}) = t_R + \tilde{r}(r_{\max}) \,, \qquad w(r_{\min}) = \tilde{r}(r_{\min}) \,. \tag{5.66}$$

In fact, we have $t = 0$ at $r = r_{\min}$ by symmetry considerations.

Taking into account that both E and $r_{\min}$ depend on t_R (see eq. (5.60) for the relation among $r_{\min}$ and E), the time derivative of eq. (5.63) gives, after several cancellations among terms, the result

$$\frac{1}{2l}\frac{dV}{dt_R} = \frac{dV}{d\tau} = 2\pi l E \,, \tag{5.67}$$

where $\tau = l\, t_b = 2l\, t_R$. At large τ, E approaches to the constant $E_0 = \frac{r_h}{4}\sqrt{\nu^2+3}$. Computing the constant of motion E in eq. (5.57) for the particular value $r = r_{\min}$ shows that $E > 0$ for $\tau > 0$ (corresponding to $\dot{w} > 0$) and $E < 0$ for $\tau < 0$ (corresponding to $\dot{w} < 0$). Numerical calculations with the full time dependence can be obtained by expressing τ in terms of E using eqs. (5.62-5.65), are shown in figure 5.3. For $\nu = 1$ the results in [56], [113] are recovered, under the change of variables in eq. (5.21).

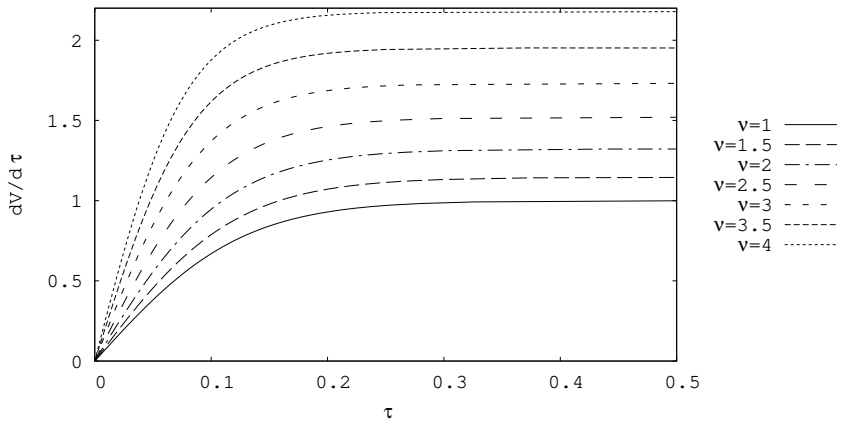

Figure 5.3: Time dependence of $\frac{dV}{d\tau}$ in units of πl, for $r_h = 1$ and various values of the warping parameter ν.

5.2.4 Computation of the Volume in the rotating case

The procedure to compute the volume in the rotating case is similar to the non-rotating black hole, then we will be very schematic. The volume functional using the metric in the coordinates (5.55) is written as

$$V = 4\pi \int_{\lambda_{\min}}^{\lambda_{\max}} d\lambda\, l^2 \sqrt{\frac{r\dot{w}^2}{4}\Psi - \left(\frac{\dot{w}}{2}\left(2\nu r - \sqrt{r_+ r_-(\nu^2+3)}\right) - \frac{\dot{r}}{2}\right)^2} = 4\pi \int d\lambda\, \mathscr{L}(r,\dot{r},\dot{w})\,, \quad (5.68)$$

where we used the axial symmetry to put the codimension-one surface along the θ_w direction. As before, there is a conserved quantity because the variable w is cyclic

$$E = \frac{1}{l^2}\frac{\partial \mathscr{L}}{\partial \dot{w}} = \frac{\frac{r\dot{w}}{4}\Psi - \left(\frac{\dot{w}}{2}\left(2\nu r - \sqrt{r_+ r_-(\nu^2+3)}\right) - \frac{\dot{r}}{2}\right)\frac{1}{2}\left(2\nu r - \sqrt{r_+ r_-(\nu^2+3)}\right)}{\sqrt{\frac{r\dot{w}^2}{4}\Psi - \left(\frac{\dot{w}}{2}\left(2\nu r - \sqrt{r_+ r_-(\nu^2+3)}\right) - \frac{\dot{r}}{2}\right)^2}}\,. \quad (5.69)$$

The expression greatly simplifies choosing a parametrization for λ such that $V = 4\pi l^2 \int d\lambda$, which corresponds to set

$$\frac{r\dot{w}^2}{4}\Psi - \left(\frac{\dot{w}}{2}\left(2\nu r - \sqrt{r_+ r_-(\nu^2+3)}\right) - \frac{\dot{r}}{2}\right)^2 = 1\,, \quad (5.70)$$

finding

$$E = -\frac{\nu^2+3}{4}\dot{w}(r-r_-)(r-r_+) + \frac{\dot{r}}{4}\left(2\nu r - \sqrt{r_+ r_-(\nu^2+3)}\right)\,. \quad (5.71)$$

Solving eqs. (5.70, 5.71), we obtain the inverse expressions

$$\dot{r} = 2\sqrt{\frac{4E^2 + (\nu^2+3)(r-r_-)(r-r_+)}{\left(2\nu r - \sqrt{r_+ r_-(\nu^2+3)}\right)^2 - (\nu^2+3)(r-r_-)(r-r_+)}}\,, \quad (5.72)$$

$$\begin{aligned}\dot{w} \;&= \frac{2}{(\nu^2+3)(r-r_-)(r-r_+)} \\ &\left[\frac{\sqrt{4E^2 + (\nu^2+3)(r-r_-)(r-r_+)}\left(2\nu r - \sqrt{r_+ r_-(\nu^2+3)}\right)}{\sqrt{\left(2\nu r - \sqrt{r_+ r_-(\nu^2+3)}\right)^2 - (\nu^2+3)(r-r_-)(r-r_+)}} - 2E\right]\,,\end{aligned} \quad (5.73)$$

which will be used later to conveniently express the volume functional in terms of the conserved quantity. The minimum value $r_{\min}$ of the radial coordinate is obtained by solving $\dot{r} = 0$:

$$r_{\min} = \frac{r_+ + r_-}{2}\left(1 \pm \sqrt{1 - \frac{16E^2}{(\nu^2+3)(r_+ + r_-)^2}}\right)\,. \quad (5.74)$$

As in the non-rotating case, the physical solution relevant for holographic complexity is the one with the + sign. Conventionally, $t_b = 0$ corresponds to $E = 0$ and $r_{\min} = r_+ + r_-$. The $t_b \to \infty$ limit corresponds to $E \to \frac{(r_+ - r_-)}{4}\sqrt{\nu^2+3}$ and $r_{\min} = \frac{r_+ + r_-}{2}$.

The volume expressed as an integral over the radial coordinate becomes

$$V = 2\pi l^2 \int_{r_{\min}}^{r_{\max}} dr \sqrt{\frac{\left(2\nu r - \sqrt{r_+ r_-(\nu^2+3)}\right)^2 - (\nu^2+3)(r-r_-)(r-r_+)}{4E^2 + (\nu^2+3)(r-r_-)(r-r_+)}}\,, \tag{5.75}$$

while the difference between the extermal values of the null coordinates is

$$w(r_{\max}) - w(r_{\min}) = \int_{r_{\min}}^{r_{\max}} dr \frac{1}{(\nu^2+3)(r-r_-)(r-r_+)} \left[\left(2\nu r - \sqrt{r_+ r_-(\nu^2+3)}\right) \right.$$
$$\left. -2E\sqrt{\frac{\left(2\nu r - \sqrt{r_+ r_-(\nu^2+3)}\right)^2 - (\nu^2+3)(r-r_-)(r-r_+)}{4E^2 + (\nu^2+3)(r-r_-)(r-r_+)}} \right]. \tag{5.76}$$

As in the non-rotating case, the symmetry of the configuration sets $t = 0$ at $r = r_{\min}$, giving the simple result

$$w(r_{\max}) - w(r_{\min}) = t_R + \tilde{r}(r_{\max}) - \tilde{r}(r_{\min})\,. \tag{5.77}$$

This will be used again to find the time derivative of the volume in terms of the conserved quantity along the surface. In order to do that, we consider the relation (obtained by direct computation)

$$\begin{aligned} \frac{V}{4\pi l^2} \;=\; & \int_{r_{\min}}^{r_{\max}} dr \left[\frac{\sqrt{4E^2 + (\nu^2+3)(r-r_-)(r-r_+)}}{2(\nu^2+3)(r-r_-)(r-r_+)} \right. \\ & \sqrt{\left(2\nu r - \sqrt{r_+ r_-(\nu^2+3)}\right)^2 - (\nu^2+3)(r-r_-)(r-r_+)} \\ & \left. -E\frac{2\nu r - \sqrt{r_+ r_-(\nu^2+3)}}{(\nu^2+3)(r-r_-)(r-r_+)} \right] + E(w(r_{\max}) - w(r_{\min}))\,. \end{aligned} \tag{5.78}$$

Using the previous definitions and simplifying the expression, we formally obtain the same result of the non-rotating case

$$\frac{dV}{d\tau} = 2\pi l E\,, \tag{5.79}$$

where $\tau = l\, t_b = 2l\, t_R$. At large τ, E approaches the constant value

$$E_0 = \frac{(r_+ - r_-)}{4}\sqrt{\nu^2+3}\,. \tag{5.80}$$

Numerical calculation are shown in figure 5.4. As a consistency check, putting $\nu = 1$ for the BTZ case, we obtain

$$\lim_{\tau\to\infty} \frac{dV}{d\tau} = \pi l (r_+ - r_-)\,, \tag{5.81}$$

which is the same result found in standard coordinates on the Poincaré patch when we perform the change of variables (5.21).

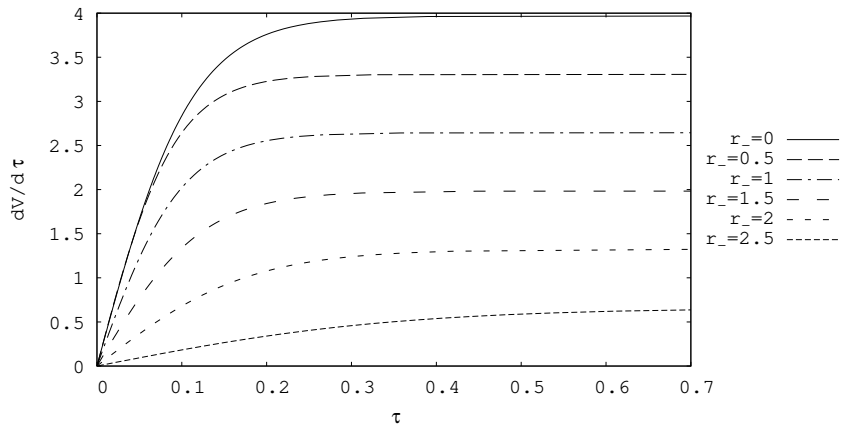

Figure 5.4: Time dependence of $\frac{dV}{d\tau}$ in units of πl, for $r_+ = 3$, $\nu = 2$ and several values of r_-. For other values of ν the plots are qualitatively similar.

The late time limit of the maximal volume slices can be found also in a simpler way, as in [56]. In this limit, we expect that the maximal volume slice sits at constant r, due to translation invariance in time[6]. We can then consider volume slices at a constant $r = \hat{r}$. Extremizing the volume from the metric in eq. (5.17), we find that the only possible maximal constant-r slice sits at

$$\hat{r} = \frac{r_+ + r_-}{2}\,. \tag{5.82}$$

Inserting this value back in the volume functional, we recover eq. (5.79) with $E = E_0$.

The late time result can be written in terms of the Bekenstein-Hawking entropy and the Hawking temperature by observing that for the WAdS BH solutions in Einstein gravity the following identity is true

$$TS = \frac{(r_+ - r_-)(3+\nu^2)}{16G}\,. \tag{5.83}$$

In this way the late time volume growth is

$$\lim_{\tau\to\infty}\frac{dV}{d\tau} = \frac{\pi l}{2}(r_+ - r_-)\sqrt{3+\nu^2} = TS\frac{8\pi G l}{\sqrt{3+\nu^2}}\,. \tag{5.84}$$

5.3 Complexity=Action

The action of the WDW patch has several contributions, which can be summarized as [58]

$$I = I_{\mathscr{V}} + I_{\mathscr{B}} + I_{\mathscr{J}} + I_{\rm ct}\,. \tag{5.85}$$

[6]Besides time translation invariance, the configuration is also symmetric with respect to the angular direction, which means that the only coordinate remaining is the radial direction.

In this formula $I_{\mathscr{V}}$ refers to the Einstein-Hilbert action in the bulk, $I_{\mathscr{B}}$ to the codimension-one boundaries (timelike, spacelike or null) and $I_{\mathscr{J}}$ to the codimension-two joints coming from intersections of other boundaries. The contribution $I_{\rm ct}$ is a counterterm to be added in order to ensure the reparameterization invariance of the action, which cancels the ambiguities in the action arising from the normalization of null normals.

The bulk action integrand $\sqrt{g}\mathscr{L}$ in eq. (5.37) evaluated on the background defined in eqs. (5.17) and (5.40) is constant and independent from the parameters (r_+, r_-):

$$I_{\mathscr{V}} = \int dr dt d\theta \frac{\mathscr{I}}{16\pi G}, \qquad \mathscr{I} = -\frac{l}{2}(v^2+3) + \frac{\kappa c^2}{l} - \alpha a c. \tag{5.86}$$

In particular, the quantity $\mathscr{I}$ is the same introduced in eq. (5.44) , but without using the gauge choice $a = \frac{l}{v}\sqrt{\frac{3}{2}}\sqrt{v^2-1}$ which makes the conserved charges of the black hole well-defined. We will perform this further simplification later.

The boundary terms contain two kind of contributions

$$I_{\mathscr{B}} = I_{\rm GHY} + I_{\mathscr{N}}, \tag{5.87}$$

where $I_{\rm GHY}$ refers to spacelike or timelike boundaries (Gibbons-Hawking-York (GHY) term), while $I_{\mathscr{N}}$ is the contribution for null boundaries. The GHY term is given by

$$I_{\rm GHY} = \frac{\varepsilon}{8\pi G}\int_{\mathscr{B}} d^2x \sqrt{|h|}\, K, \tag{5.88}$$

where $\mathscr{B}$ is the appropriate boundary, h the induced metric, K the extrinsic curvature and ε is equal to $+1$ if the boundary is timelike and -1 if it is spacelike. It is well-known that the GHY term must be added to the Einstein-Hilber action in order to make the variational problem well-defined.

The new term appearing in the treatment of the action in the WDW patch refers to the null surface boundaries and is given by [154, 155, 58]

$$I_{\mathscr{N}} = \frac{1}{8\pi G}\int_{\mathscr{B}} \tilde{\kappa} d\lambda dS, \tag{5.89}$$

where λ parameterizes the null direction of the surface, dS is the area element of the spatial cross-section orthogonal to the null direction and $\tilde{\kappa}$ is the acceleration measuring the failure of λ to be an affine parameter: if we denote by k^α the null generator, $\tilde{\kappa}$ is defined by the relation: $k^\mu D_\mu k^\alpha = \tilde{\kappa} k^\alpha$. It turns out that the contribution to the action $I_{\mathscr{N}}$ is not reparameterization-invariant [155, 58] and it can be set to zero using an affine parameterization for the null direction of the boundary [58].

In the case of joints between spacelike and timelike surfaces, this contribution was studied in [156]. The analysis for joints between a null surface and either a timelike, spacelike or another null surface were recently studied in [58]. In the CA calculations done in the next sections, we will use

these null joints contributions several times:

$$I_{\mathscr{J}} = \frac{1}{8\pi G}\int_{\Sigma} d\theta \sqrt{\sigma}\,\mathfrak{a}\,, \tag{5.90}$$

where σ_{ab} is the induced metric over the joint (in this case, it is 1-dimensional) and $\mathfrak{a}$ depends on the kind of joint, but it is chosen in such a way that the action is additive when inserting new boundaries inside a given region of spacetime. Let us denote with k^{α} the future directed null normal to a null surface (which is also tangent to the surface), n_{α} the normal to a spacelike surface and s_{α} the normal to a timelike surface, both directed outwards the volume of interest. In the case of the intersection between two null surfaces with normals k_1^{α} and k_2^{α} the integrand is given by

$$\mathfrak{a} = \eta \log\left|\frac{k_1\cdot k_2}{2}\right|, \tag{5.91}$$

while in the case of intersection of a null surface with normal k^{α} and a spacelike surface with normal n_{α} (or a timelike surface with normal s_{α}):

$$\mathfrak{a} = \eta \log|k\cdot n|\,, \qquad \mathfrak{a} = \eta \log|k\cdot s|\,. \tag{5.92}$$

In eqs. (5.91-5.92) we set $\eta = +1$ if the joint lies in past of the spacetime volume of interest, and $\eta = -1$ if the joint lies in the future of the relevant region. Note that eqs. (5.91) and (5.92) are ambiguous because of the normalization of the null normal k^{α}. This ambiguity is related to the boundary term on the null surfaces and does not affect the late-time limit of the complexity, but just the finite-time behavior[7]. As discussed in [113], we will partially fix this ambiguity by requiring that the null vector k^{μ} have constant scalar product with the boundary time killing vector $\partial/\partial t$.

The following counterterm [58] must be added to the boundary term of null boundaries, in order to make the action invariant under reparameterization

$$I_{\rm ct} = \frac{1}{8\pi G}\int d\theta\, d\lambda\, \sqrt{\sigma}\,\Theta \log|\tilde{L}\Theta|\,, \tag{5.93}$$

where λ is the affine parameter of the null geodesics which delimit the boundary, and

$$\Theta = D_{\alpha}k^{\alpha} = \frac{1}{\sqrt{\sigma}}\frac{\partial\sqrt{\sigma}}{\partial\lambda} \tag{5.94}$$

is the expansion of the congruence of null geodesics on the hypersurface. The parameter $\tilde{L}$ appearing in eq. (5.93) is an arbitrary length scale which is needed for dimensional reasons, whose physical meaning is so far obscure.

[7] These ambiguities could be related to various ambiguities of the dual circuit complexity of the quantum state, such as the choice of the reference state, the specific set of elementary gates and the amount of tolerance that one introduces to describe the accuracy with which the final state should be constructed.

5.3.1 Computation of the action in the non-rotating case

The Penrose diagrams with the WDW patch associated to the boundary region for the non-rotating case are shown in figures 5.5 and 5.6. We choose without loss of generality the symmetric configuration $t_L = t_R = \frac{t_b}{2}$.

A difference between the volume and action conjectures is that the extremal surface goes very deep inside the horizon but stays away from curvature singularities, while the WDW patch reaches the singularities of the black hole. For this reason, we need both a IR cutoff ε_0 and a UV cutoff Λ. We will see that the time derivative of the action is independent from both of them, and moreover the curvature singularities do not give any problem or divergence during the computation.

The structure of the WDW patch in the non-rotating case changes with time: at early times it looks like in figure 5.5, while at late times like in figure 5.6. In particular, there exists a critical time t_C such that the bottom vertex of the patch touches the past singularity. This is given by

$$t_C = 2(r^*_\Lambda - r^*(0))\,, \tag{5.95}$$

where $r^*_\Lambda \equiv r^*(\Lambda)$. We will separate the calculation of the action in two cases. At the end we will express the results in terms of

$$\tau = l(t_b - t_C)\,, \tag{5.96}$$

which is the boundary time rescaled with the AdS radius l for dimensional purposes and with the origin translated at the critical time t_C.

Initial times $t_b < t_C$

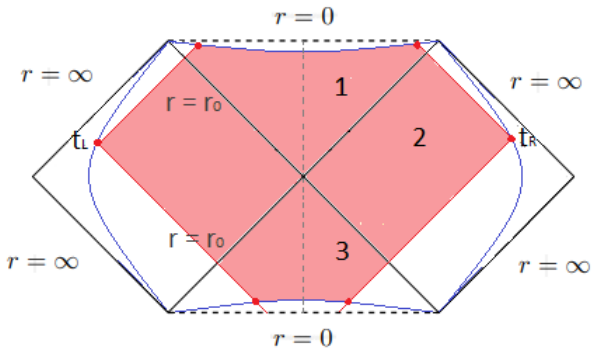

Figure 5.5: Penrose diagram for the non-rotating BH, with the WDW patch for $t_b < t_C$. In this picture we called the horizon radius r_0.

Bulk contributions: We decompose the WDW patch into three regions and we use the symmetry of the configuration to write the bulk action as

$$I_{\mathscr{V}} = 2\left(I^1_{\mathscr{V}} + I^2_{\mathscr{V}} + I^3_{\mathscr{V}}\right), \tag{5.97}$$

where

$$\begin{aligned} I^1_{\mathscr{V}} &= \frac{\mathscr{J}}{16\pi G}\int_0^{2\pi} d\theta \int_{\varepsilon_0}^{r_h} dr \int_0^{v-r^*(r)} dt = \frac{\mathscr{J}}{8G}\int_{\varepsilon_0}^{r_h} dr \left(\frac{t_b}{2} + r^*_\Lambda - r^*(r)\right), \\ I^2_{\mathscr{V}} &= \frac{\mathscr{J}}{16\pi G}\int_0^{2\pi} d\theta \int_{r_h}^{\Lambda} dr \int_{u+r^*(r)}^{v-r^*(r)} dt = \frac{\mathscr{J}}{4G}\int_{r_h}^{\Lambda} dr\,(r^*_\Lambda - r^*(r)), \\ I^3_{\mathscr{V}} &= \frac{\mathscr{J}}{16\pi G}\int_0^{2\pi} d\theta \int_{\varepsilon_0}^{r_h} dr \int_{u+r^*(r)}^{0} dt = \frac{\mathscr{J}}{8G}\int_{\varepsilon_0}^{r_h} dr \left(-\frac{t_b}{2} + r^*_\Lambda - r^*(r)\right). \end{aligned} \tag{5.98}$$

Summing all the contributions, we get the result

$$I_{\mathscr{V}} = \frac{\mathscr{J}}{2G}\int_{\varepsilon_0}^{\Lambda} dr\,(r^*_\Lambda - r^*(r)) \equiv I^0_{\mathscr{V}}. \tag{5.99}$$

This contribution is time-independent.

GHY surface contributions: The constant r surface, inside the horizon, is a spacelike surface whose induced metric in the $x^i = (t,\theta)$ coordinates reads:

$$h_{ij} = l^2\begin{pmatrix} 1 & \nu r \\ \nu r & \frac{r}{4}\Psi(r) \end{pmatrix}, \qquad \sqrt{h} = \frac{l^2}{2}\sqrt{(\nu^2+3)r(r_h-r)}. \tag{5.100}$$

The normal vector to these slices is

$$n^\mu = \left(0, -\frac{1}{l}\sqrt{(\nu^2+3)r(r_h-r)}, 0\right), \qquad n^\alpha n_\alpha = -1, \tag{5.101}$$

and the extrinsic curvature is

$$K = \frac{1}{2l}\sqrt{\nu^2+3}\,\frac{2r-r_h}{\sqrt{r(r_h-r)}}. \tag{5.102}$$

In the GHY term we then set $\varepsilon = -1$ because the surface is spacelike. We now have all the ingredients to compute the two contributions to the GHY term coming from the regions near the past and future singularities:

$$I^1_{\rm GHY} = -\frac{(\nu^2+3)l}{16G}\left[(2r-r_h)\left(\frac{t_b}{2} + r^*_\Lambda - r^*(r)\right)\right]_{r=\varepsilon_0}, \tag{5.103}$$

$$I^2_{\rm GHY} = -\frac{(\nu^2+3)l}{16G}\left[(2r-r_h)\left(-\frac{t_b}{2} + r^*_\Lambda - r^*(r)\right)\right]_{r=\varepsilon_0}. \tag{5.104}$$

Consequently, the total GHY contribution is

$$I_{\rm GHY} = 2\left(I^1_{\rm GHY} + I^2_{\rm GHY}\right) = -\frac{(v^2+3)l}{4G}\left[(2r-r_h)\left(r^*_\Lambda - r^*(r)\right)\right]_{r=\varepsilon_0} \equiv I^0_{\rm GHY}\,, \tag{5.105}$$

which is time-independent.

Joint contributions: There are four joints between null and spacelike surfaces at $r=\varepsilon_0$ (nearby the future and past singularities) and two joints at $r=\Lambda$. The normal to the constant r spacelike surfaces is n^α given by eq. (5.101), while the normal to the lightlike surfaces are u^α, v^α from eq. (5.31). From eq. (5.92), the four joint contributions nearby the singularities vanish in the limit $\varepsilon_0 \to 0$, while the two joint contributions nearby the UV cutoff are time-independent (see eq. 5.91).

Total: Summing all the terms coming from the bulk, the boundary and the joint contributions, we find that the action of the WDW patch is time-independent.

Later times $t_b > t_C$

After the critical time t_C, the WDW patch moves and the lower vertex of the diagram does not reach the past singularity (see figure 5.6). This vertex is defined via the relation

$$\frac{t_b}{2} - r^*_\Lambda + r^*(r_m) = 0\,. \tag{5.106}$$

The evaluation of the null joint contributions will require the computation of the time derivative of the tortoise coordinate, which is done by differentiating eq. (5.106):

$$\frac{dr_m}{dt_b} = -\frac{1}{2}\left(\frac{dr^*(r_m)}{dr_m}\right)^{-1}\,. \tag{5.107}$$

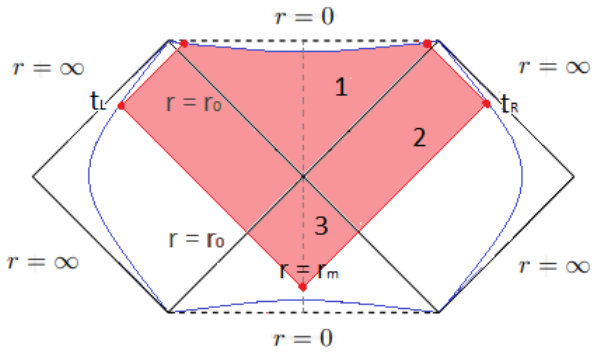

Figure 5.6: Penrose diagram for the non-rotating BH, with the WDW patch for $t_b > t_C$. In this picture we called the horizon radius r_0.

Bulk contributions: The bulk action is the same of the case $t_b < t_C$, apart from the last contribution which becomes

$$I^3_{\mathscr{V}}(t_b > t_C) = \frac{\mathscr{J}}{16\pi G}\int_0^{2\pi} d\theta \int_{r_m}^{r_h} dr \int_{u+r^*(r)}^{0} dt = \frac{\mathscr{J}}{8G}\int_{r_m}^{r_h} dr \left(-\frac{t_b}{2} + r^*_\Lambda - r^*(r)\right). \tag{5.108}$$

We can re-write this contribution in the following way:

$$I^3_{\mathscr{V}}(t_b > t_C) = I^3_{\mathscr{V}}(t_b < t_C) + \frac{\mathscr{J}}{8G}\int_{\varepsilon_0}^{r_m} dr \left(\frac{t_b}{2} - r^*_\Lambda + r^*(r)\right). \tag{5.109}$$

Since the other contributions to the bulk action are unchanged, the total result is

$$I_{\mathscr{V}}(t_b > t_C) = I^0_{\mathscr{V}} + \frac{\mathscr{J}}{4G}\int_{\varepsilon_0}^{r_m} dr \left(\frac{t_b}{2} - r^*_\Lambda + r^*(r)\right), \tag{5.110}$$

the first term being time-independent. Then the time derivative of the bulk action is

$$\frac{dI_{\mathscr{V}}}{dt_b}(t_b > t_C) = \frac{\mathscr{J}}{8G} r_m = \frac{1}{8G}\left[-\frac{l}{2}(\nu^2+3) + \frac{\kappa c^2}{l} - \alpha a c\right] r_m, \tag{5.111}$$

where the defining relation (5.106) is used in order to obtain a vanishing contribution from the upper integration extreme.

GHY surface contributions: After the critical time t_C we only have a contribution from the future singularity, because the lower part of the WDW patch does not reach the past singularity. We are only left with

$$I_{\text{GHY}} = 2I^1_{\text{GHY}} = -\frac{(\nu^2+3)l}{8G}\left[(2r - r_h)\left(\frac{t_b}{2} + r^*_\Lambda - r^*(r)\right)\right]_{r=\varepsilon_0}, \tag{5.112}$$

which is time-dependent. The time derivative of this term gives

$$\lim_{\varepsilon_0 \to 0} \frac{dI_{\text{GHY}}}{dt_b}(t_b > t_C) = \frac{(\nu^2+3)l}{16G} r_h. \tag{5.113}$$

Joint contributions: Following the same procedure of the case $t_b < t_C$, we find that the null joints at the UV cutoff give time-independent contributions, while the joint at the future singularity gives a vanishing result. The contribution from the remaining null-null joint between u^α and v^α at $r = r_m$ is instead time-dependent, because r_m is function of time (see eq. (5.107)). We find that this contribution to the action is given by eq. (5.90), with $\mathfrak{a}$ defined in eq. (5.91):

$$\mathfrak{a} = \log\left|A^2 \frac{u^\alpha v_\alpha}{2}\right| = \log\left|A^2 \frac{1}{l^2}\frac{\Psi(r)}{(\nu^2+3)(r-r_h)}\right|. \tag{5.114}$$

The normalization factor A^2 corresponds to an ambiguity in the contribution to the action due to the null joint [58], because the normalization of the two null normals u^α and v^α which delimitate the

WDW patch is in principle not fixed by the metric. The action contribution from eq. (5.114), evaluated for $r = r_m$, gives

$$I_{\mathscr{J}} = -\frac{l}{4G}\sqrt{\frac{r_m}{4}\Psi(r_m)}\log\left|\frac{l^2}{A^2}\frac{(\nu^2+3)(r_m-r_h)}{\Psi(r_m)}\right|, \tag{5.115}$$

whose time derivatives is

$$\begin{aligned}\frac{dI_{\mathscr{J}}}{dt_b} =& -\frac{l}{16G}\frac{dr_m}{dt_b}\frac{6(\nu^2-1)r_m+(\nu^2+3)r_h}{\sqrt{r_m\left[3(\nu^2-1)r_m+(\nu^2+3)r_h\right]}}\log\left|\frac{l^2}{A^2}\frac{(\nu^2+3)(r_m-r_h)}{\Psi(r_m)}\right| + \\ &-\frac{l}{8G}\frac{dr_m}{dt_b}\frac{4\nu^2 r_h\sqrt{r_m\left[3(\nu^2-1)r_m+(\nu^2+3)r_h\right]}}{(r_m-r_h)\left(3r_m(\nu^2-1)+(\nu^2+3)r_h\right)}.\end{aligned} \tag{5.116}$$

Inserting eq. (5.107) we obtain a further simplification:

$$\begin{aligned}\frac{dI_{\mathscr{J}}}{dt_b} =& \frac{l}{32G}\frac{(\nu^2+3)(r_m-r_h)\left(6(\nu^2-1)r_m+(\nu^2+3)r_h\right)}{3(\nu^2-1)r_m+(\nu^2+3)r_h}\log\left|\frac{l^2}{A^2}\frac{(\nu^2+3)(r_m-r_h)}{\Psi(r_m)}\right| + \\ &+\frac{l}{16G}\frac{4\nu^2(\nu^2+3)r_m r_h}{3r_m(\nu^2-1)+(\nu^2+3)r_h}.\end{aligned} \tag{5.117}$$

Total: The total time derivative of the action is finally given by

$$\begin{aligned}\frac{dI}{dt_b} =& \frac{1}{8G}\left[-\frac{l}{2}(\nu^2+3)+\frac{\kappa c^2}{l}-\alpha ac\right]r_m+\frac{(\nu^2+3)l}{16G}r_h+\frac{l}{16G}\frac{4\nu^2(\nu^2+3)r_m r_h}{3r_m(\nu^2-1)+(\nu^2+3)r_h} \\ &+\frac{l}{32G}\frac{(\nu^2+3)(r_m-r_h)\left(6(\nu^2-1)r_m+(\nu^2+3)r_h\right)}{3(\nu^2-1)r_m+(\nu^2+3)r_h}\log\left|\frac{l^2}{A^2}\frac{(\nu^2+3)(r_m-r_h)}{\Psi(r_m)}\right|.\end{aligned} \tag{5.118}$$

We can now perform the late time limit of the previous rate. In this limit $r_m \to r_h$, which implies that the term in the second line vanishes and we find:

$$\lim_{t_b\to\infty}\frac{dI}{dt_b} = \frac{(\nu^2+3)l}{16G}r_h+\frac{1}{8G}\left(\frac{\kappa}{l}c^2-\alpha ac\right)r_h. \tag{5.119}$$

Note that the general result (5.118) depends on A^2, while its late time limit does not. Using the value of a given in eq. (5.43), we can now evaluate the combination appearing in the rate of the action

$$\frac{\kappa}{l}c^2-\alpha ac = 0, \tag{5.120}$$

finding

$$\lim_{t_b\to\infty}\frac{1}{l}\frac{dI}{dt_b} = \lim_{\tau\to\infty}\frac{dI}{d\tau} = \frac{\nu^2+3}{16G}r_h = M = TS. \tag{5.121}$$

This late-time results can also be recovered using the approach by [57] (see Appendix D.2 for details).

Numerical plots of the time dependence of the action rate (5.118) for different values of ν are shown in figure 5.7. The same qualitative structure as for the AdS case [113] is found; in particular the growth rate of the action is a decreasing function at late times. As in [113], the late-time limit then overshoots the asymptotic rate, which was previously believed [57] to be associated to an universal

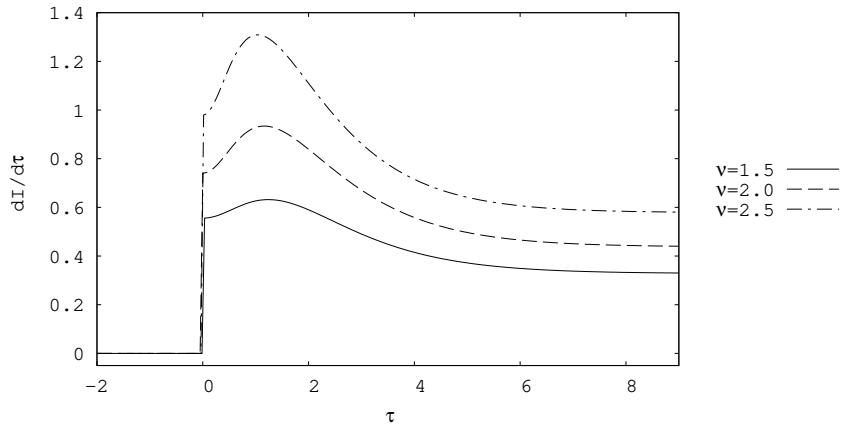

Figure 5.7: Time dependence of the WDW action in the non-rotating case for different values of ν. We set $G = 1$, $l = 1$, $r_h = 1$ and $A = 2$. The critical time t_C corresponds to $\tau = 0$.

upper bound, conjectured by Lloyd [157]. There is some dependence at finite time on the parameter A, see figure 5.8; this is a feature also of the AdS case [58, 112, 113]. The late-time limit is instead independent from A.

5.3.2 Computation of the action in the rotating case

In the rotating case (see figure 5.9) we do not need to distinguish between initial and later times, because in this case the form of the WDW patch is the same at any time and the complexity is already non-vanishing at initial times. We define $\tau = l\, t_b$. We call r_{m1}, r_{m2} the null joints referring respectively to the top and bottom vertices of the spacetime region of interest. Due to the structure of the Penrose diagram in the rotating case (similar to the 3+1 dimensional diagram for a Reissner-Nordstrom black hole), we do not have boundaries contributing to the GHY term.

The definition of the null joints in terms of the tortoise coordinates are:

$$\frac{t_b}{2} + r^*_\Lambda - r^*(r_{m1}) = 0\,, \qquad \frac{t_b}{2} - r^*_\Lambda + r^*(r_{m2}) = 0\,. \tag{5.122}$$

It will be useful to differentiate with respect to time these expressions to find

$$\frac{dr_{m1}}{dt_b} = \frac{1}{2}\left(\frac{dr^*}{dr_{m1}}\right)^{-1}, \qquad \frac{dr_{m2}}{dt_b} = -\frac{1}{2}\left(\frac{dr^*}{dr_{m2}}\right)^{-1}. \tag{5.123}$$

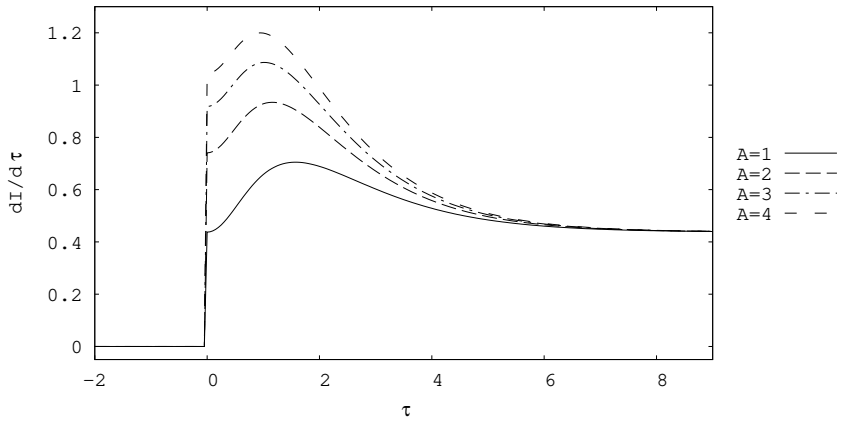

Figure 5.8: Time dependence of the WDW action in the non-rotating case for different values of the parameter A. We set $G=1$, $l=1$, $r_h=1$ and $\nu=2$.

Bulk contributions: We can still split the WDW patch into three regions covering only the right half of the diagram, which contribute as

$$\begin{aligned} I^1_{\mathscr{V}} &= \frac{\mathscr{I}}{8G}\int_{r_{m1}}^{r_+} dr\left(\frac{t_b}{2}+r^*_\Lambda-r^*(r)\right), \qquad I^2_{\mathscr{V}}=\frac{\mathscr{I}}{4G}\int_{r_+}^{\Lambda} dr\,(r^*_\Lambda-r^*(r))\,, \\ I^3_{\mathscr{V}} &= \frac{\mathscr{I}}{8G}\int_{r_{m2}}^{r_+} dr\left(-\frac{t_b}{2}+r^*_\Lambda-r^*(r)\right). \end{aligned} \tag{5.124}$$

The whole bulk contribution then amounts to

$$\begin{aligned} I_{\mathscr{V}} &= \frac{\mathscr{I}}{2G}\int_{r_+}^{\Lambda} dr\,(r^*_\Lambda-r^*(r))+ \\ &+ \frac{\mathscr{I}}{4G}\left[\int_{r_{m1}}^{r_+} dr\left(\frac{t_b}{2}+r^*_\Lambda-r^*(r)\right)+\int_{r_+}^{r_{m2}} dr\left(\frac{t_b}{2}-r^*_\Lambda+r^*(r)\right)\right]. \end{aligned} \tag{5.125}$$

The rate of the bulk action is

$$\frac{dI_{\mathscr{V}}}{dt_b}=\frac{\mathscr{I}}{8G}(r_{m2}-r_{m1})\,, \tag{5.126}$$

where the relations (5.122) are used to obtain a vanishing result when differentiating the endpoints of integration. The result simplifies when performing the late time limit, when $r_{m1}\to r_+$ and $r_{m2}\to r_-$, and the bulk action time-derivative becomes

$$\lim_{t_b\to\infty}\frac{dI_{\mathscr{V}}}{dt_b}=-\frac{(\nu^2+3)l}{16G}(r_+-r_-)+\frac{1}{8G}\left(\frac{\kappa}{l}c^2-\alpha ac\right)(r_+-r_-)\,. \tag{5.127}$$

Null joint contributions: As in the non-rotating case, the joints at $r=\Lambda$ give a time-independent contribution, and then they are not of interest to find the rate of complexity. We have two time-dependent contributions coming from the top and bottom joints.

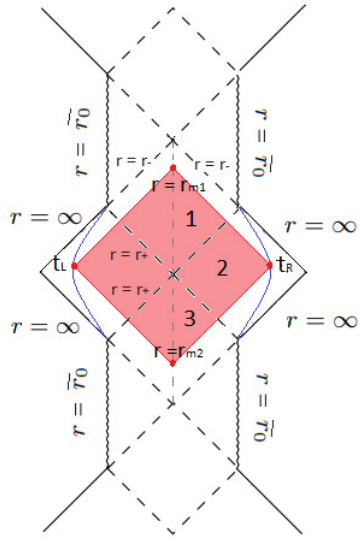

Figure 5.9: Penrose diagram for the WDW patch in the rotating case.

As a function of r, these contributions are proportional to:

$$\mathfrak{a} = \eta \log\left|A^2 \frac{1}{2} u^\alpha v_\alpha\right| = \eta \log\left|\frac{A^2}{l^2} \frac{r\Psi(r)}{(\nu^2+3)(r-r_-)(r-r_+)}\right| . \tag{5.128}$$

For both $r = r_{m1}$ and $r = r_{m2}$ we have to insert $\eta_1 = -1$.

The action of each joint is

$$I^k_{\mathscr{J}} = -\frac{1}{4G}\sqrt{\frac{r_k}{4}\Psi(r_k)}\log\left|\frac{l^2}{A^2}F(r_k)\right| , \qquad F(r_k) \equiv \frac{(\nu^2+3)(r_k-r_-)(r_k-r_+)}{r_k\Psi(r_k)} , \tag{5.129}$$

and the corresponding time derivative is

$$\begin{aligned}\frac{dI^k_{\mathscr{J}}}{dt_b} = -\frac{l}{8G}\frac{dr_k}{dt_b}\Bigg\{ &\sqrt{r_k\Psi(r_k)}\frac{d}{dr_k}\left(\log\left|\frac{l^2}{A^2}F(r_k)\right|\right) + \\ &+\frac{1}{2}\frac{6(\nu^2-1)r_k + (\nu^2+3)(r_+ + r_-) - 4\nu\sqrt{(\nu^2+3)r_+ r_-}}{\sqrt{r_k\Psi(r_k)}}\log\left|\frac{l^2}{A^2}F(r_k)\right|\Bigg\} .\end{aligned} \tag{5.130}$$

Using eqs. (5.123) in the previous expression, it is possible to find the complete time dependence of the null contributions. Since the expression is rather cumbersome, we only write the late-time limit

$$\lim_{t_b\to\infty}\frac{dI^k_{\mathscr{J}}}{dt_b} = \frac{(\nu^2+3)l}{16G}(r_+ - r_-) , \qquad k = 1,2 . \tag{5.131}$$

Total: Summing all the previous asymptotic expressions, the late-time limit of the action growth is given by

$$\lim_{t_b\to\infty}\frac{dI}{dt_b}=\frac{(v^2+3)l}{16G}(r_+-r_-)-\frac{1}{8G}\left(\frac{\kappa}{l}c^2-\alpha ac\right)(r_+-r_-)\,. \tag{5.132}$$

Taking into account eq. (5.43) we finally find

$$\lim_{t_b\to\infty}\frac{1}{l}\frac{dI}{dt_b}=\lim_{\tau\to\infty}\frac{dI}{d\tau}=\frac{(v^2+3)}{16G}(r_+-r_-)=TS\,. \tag{5.133}$$

The late-time limit can be recovered also with the methods introduced in [57] and the results agree; details of the explicit calculation can be found in appendix D.2.

5.3.3 Adding the counterterm

In eq. (5.85) we included in the gravitational action a counterterm accounting for the reparametrization invariance of the result, but so far we did not include it in the computation. The reason is that it does not play an important role in this specific case. In fact, we observe from eq. (5.93) that the expression contains an arbitrary length scale $\tilde{L}$ which introduces another ambiguity in the action! While adding the counterterm eliminates the parameter A related to the ambiguity in giving a normalization for the null normals, and renders the action invariant under reparametrizations, on the other hand there is no way to fix a priori the value of the scale $\tilde{L}$. In this way, the various graphs depicted in fig. 5.8 are simply substituted by analogous graphs where the free parameter is the value associated to the counterterm length $\tilde{L}$. On the other hand, the late time result was independent from the ambiguity in the normalization of null normals, and the same can be proven to be true about the dependence from the length scale $\tilde{L}$ after adding the counterterm.

From this discussion it seems that adding or not the counterterm does not change anything meaninginful in the action, and then its role appears to be insignificant. However, we will see in chapters 6 and 7 that it will play a role in determining the sub/super-additivity properties of the subregion action, and that will introduce only the length scale $\tilde{L}$ in exchange of all the ambiguous parameters related to null normals when multiple null surfaces are considered in the geometric set-up. Moreover the role of the counterterm was found to play an important role in time-dependent configurations [117, 118].

5.3.4 Comments and discussion

There are some expectations about computational complexity which we can check with the late time volume and action rates in eqs. (5.84) and (5.133), which we report here for convenience

$$\lim_{\tau\to\infty}\frac{dV}{d\tau}=TS\frac{8\pi Gl}{\sqrt{3+v^2}}\,,\qquad \lim_{\tau\to\infty}\frac{dI}{d\tau}=TS\,, \tag{5.134}$$

$$TS=\frac{(r_+-r_-)(3+v^2)}{16G}\,. \tag{5.135}$$

In [56] it has been proposed that the asymptotic rate of increase of complexity should be proportional to the product of temperature times entropy

$$\frac{dC}{d\tau} \simeq TS. \tag{5.136}$$

The main motivation comes from the fact that complexity growth rate is an extensive quantity which has the dimensions of an energy, and which should vanish for a static object as an extremal BH. Moreover, the authors of [111] proposed the following bound for the complexity growth rate:

$$\frac{dC}{d\tau} \lesssim [(M-\Omega J-\Phi Q)_+ - (M-\Omega J-\Phi Q)_-]\,, \tag{5.137}$$

where $\pm$ indicate that the corresponding values of the quantities are computed at the outer and inner horizons. With suitable units for complexity, the bound (5.137) seems to be saturated in several cases.

For WAdS BHs, the angular velocities computed on the inner and outer horizons are:

$$\Omega_+ = \frac{2}{l(2\nu r_+ - \sqrt{(\nu^2+3)r_+r_-})}\,, \qquad \Omega_- = \frac{2}{l(2\nu r_- - \sqrt{(\nu^2+3)r_+r_-})}\,. \tag{5.138}$$

If we use the values of mass and angular momentum in eqs. (5.26)-(5.27), we find that

$$(M-\Omega_+ J)-(M-\Omega_- J) = \frac{(r_+-r_-)(3+\nu^2)}{16G} = TS. \tag{5.139}$$

For the purpose of the case studied in this paper, the saturation of the bound in eq. (5.137) is equivalent to eq. (5.136). Since both the volume and the action rate for late times are proportional to the product TS, we satisfy all the previous requirements: in particular, they both vanishes in the extremal case $r_+ = r_-$.

In asymptotically AdS$_D$ spacetime, we have that the coefficient of proportionality between complexity and volume [54] is usually taken as

$$C = (D-1)\frac{V}{Gl}\,, \tag{5.140}$$

and the late-time rate of growth of the volume is

$$\lim_{\tau\to\infty}\frac{dV}{d\tau} = \frac{8\pi Gl}{D-1}TS. \tag{5.141}$$

For comparison, in the case of flat spacetime BHs,

$$\lim_{\tau\to\infty}\frac{dV}{d\tau} \approx \frac{Gr_h}{D-3}TS\,, \tag{5.142}$$

where r_h is the horizon radius ($\approx$ refer to a neglected order one prefactor [54]). Consequently, the proportionality coefficient between the late time rate of growth of the volume and TS depends on the kind of asymptotic of the spacetime.

In order to compare with the AdS_3 case, we can write the rate of growth of the volume in WAdS as

$$\frac{dV}{d\tau} \to ST\, 4\pi Gl\, \eta\,, \qquad \eta = \frac{2}{\sqrt{3+\nu^2}}\,. \tag{5.143}$$

We may interpret the details of this result in distinct ways, depending on the exact holographic dictionary that we may conjecture between volume and complexity. For example, it could be that complexity approaches at late time to $\eta\, TS$ (note that $\eta \leq 1$ if we impose $\nu^2 \geq 1$); if this is true, warping would make complexity rate decreases. On the other hand, it could also be that in spaces with WAdS asymptotic the holographic dictionary between complexity and volume is changed by some non-trivial function of the warping parameter ν; for example, if we would have that

$$C = \frac{2}{Gl\eta} V\,, \tag{5.144}$$

the asymptotic complexity increase rate would be still TS for every ν. The investigation of Complexity=Action conjecture suggests that the latter possibility may be preferrable.

We notice that in the case of the action computation, the only terms which contribute are the bulk and the joints, while in the non-rotating case there is also a surface GHY contribution. Although the details of the calculation are quite different, the final result is a continuous function of the parameters of the solution (r_+, r_-). A curious feature of the non-rotating case is that there exists an initial time period ($t < t_c$) in which complexity is constant; this is the same as in the AdS case [113].

Chapter 6

Subregion complexity for warped AdS black holes

The work in this chapter has previously appeared in [158].

By analogy with entanglement entropy, an interesting further extension of the CV and CA conjectures consists in the case where the physical state is mixed, *i.e.* we consider a subregion of the full boundary. In this case, it is well known that the information properties of the subregion on the boundary are encoded in some extremal slices in the bulk, *i.e.* the Ryu-Takayanagi (RT) and the Hubeny-Rangamani-Takayanagi (HRT) surfaces for the static and time-dependent cases, respectively. Moreover, a bulk region which naturally encodes all the informations coming from a subsystem on the boundary is the entanglement wedge, defined as the bulk domain of dependence of the spacetime region bounded by the RT surface and the subregion on the boundary [159].

There are two proposals which naturally generalize the CV and CA conjectures for mixed states [65]:

- The CV requires to compute the spacetime volume of an extremal codimension-one surface anchored at the boundary and bounded by the RT (HRT) surface for a static (time-dependent) configuration. We will denote as $\mathscr{C}_V$ such quantity.
- The CA requires to compute the gravitational action in the domain given by the intersection between the WDW patch and the entanglement wedge. We will denote this quantity as $\mathscr{C}_A$.

Subregion complexity has been recently studied by many authors, *e.g.* [160–171].

The investigation of the two conjectures for mixed states can give additional hints on which of them is preferrable, and may also help to identify a correct quantity to match from the field theory side. Various notions of complexity exist from an analysis of tensor networks [163]:

- Purification complexity $\mathscr{C}_P$, which can be defined as the minimal number of gates needed to transform the initial pure state (plus some ancillary external qubits) into a purification of the mixed state ρ.

- Spectrum complexity $\mathscr{C}_S$, which can be defined as the minimal number of operations needed to prepare a mixed state ρ_{spec} with the same spectrum as ρ.

- Basis complexity $\mathscr{C}_B$, which can be defined as the minimum number of gates needed to prepare ρ from ρ_{spec}.

The previous definitions are pictorially represented in fig. 6.1. The spectrum complexity does not reduce to complexity when computed on pure states, and so it is not a good candidate as a field theory dual of CV or CA. Instead both $\mathscr{C}_P$ and $\mathscr{C}_B$ might be in principle reasonable candidates as duals of holographic complexities. These issues were recently investigated by [163–165, 172].

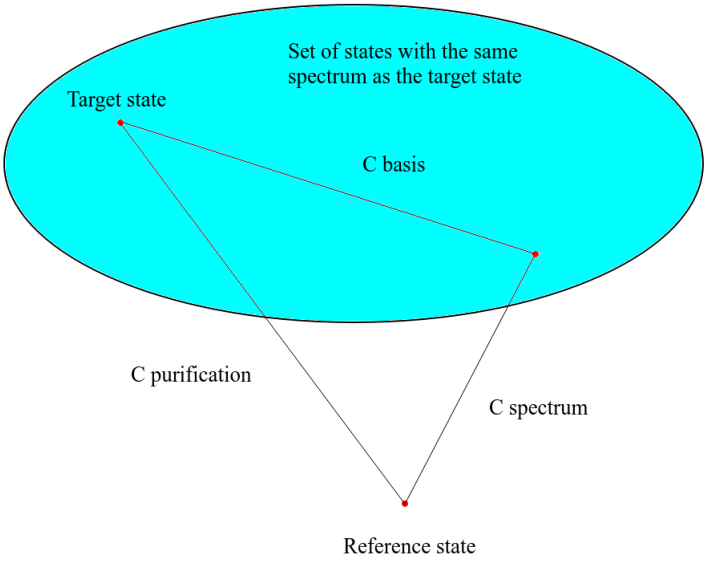

Figure 6.1: Various definitions of subsystem complexity: basis, spectrum and purification. The coloured area represents the states with the same spectrum as the target state ρ, in particular the one which is reached with the least number of operations is ρ_{spec} and gives the spectrum complexity.

There are some interesting properties that we can investigate for the subregion complexity: structure of UV divergencies, sub/superadditivity and temperature dependence. The first aspect can be useful for the matching from the field theory side. In this context, it is also interesting to understand if logarithmic or constant pieces arise, which usually contain universal informations in the case of the entanglement entropy.

The sub/superadditivity properties can be matched with the various definitions of computational complexity proposed from the tensor network analysis. In particular, it was conjectured in [163] that $\mathscr{C}_P$ should be subadditive for the left L and right R factors of the thermofield double state TD. An analog guess was made about superadditivity of $\mathscr{C}_B$.

The volume complexity $\mathscr{C}_V$ is in general superadditive because the volume is always a positive-definite quantity: given two regions A,B and their union, we have

$$\mathscr{C}_V(A\cup B)\geq\mathscr{C}_V(A)+\mathscr{C}_V(B)\,. \tag{6.1}$$

In the special case where the theormofield (TD) double state is considered at vanishing boundary time t_b and the subregions are chosen to be the left (L) and right (R) boundaries separately, this inequality saturates:

$$\mathscr{C}_V(TD,t_b=0)=\mathscr{C}_V(L)+\mathscr{C}_V(R)\,. \tag{6.2}$$

The situation is less clear when the action is considered, because it is not positive-definite. An interesting technical point which arises in the CA conjecture is due to an arbitrary length scale $\tilde{L}$ which appears in the counterterm needed to make the action reparameterization invariant [58]. Depending on the choice of $\tilde{L}$, for the AdS neutral black hole, one can get either [164] that CA is superadditive or subadditive for the L,R sides of the thermofield double.

The investigation of the temperature dependence leads to the conclusion that $\mathscr{C}_B$ decreases with temperature T and approaches zero for $T\to\infty$, while $\mathscr{C}_P$ should not have strong dependence on T. As studied in [163, 164], for the AdS neutral black hole the behaviour of subsystem action complexity as a function of temperature also depends on $\tilde{L}$.

Following the analysis started in chapter 5, here we compute the divergences of subregion complexity for the left and right factors of the thermofield double state, in the case of black holes in asymptotically warped AdS_3 spacetimes. We investigate the temperature dependence of subregion complexity in each of the conjectures and the sub/superadditivity properties of the CA conjecture.

The configuration that we consider is a the particular subregion identified by only one of the two boundaries of the spacetime (left L or right R). In this case the computations can be performed analitically and the RT surface degenerates to the bifurcation surface, which implies that the associated subregion complexity refers only to the part of the volume (action) external to the horizon. The study of sub/superadditivity in this set up coincides with the investigation of the sign of the complexity internal to the horizon, because we have to study the condition (*e.g.* in the case of superadditivity)

$$\mathscr{C}(TD,t_b=0)-(\mathscr{C}(L)+\mathscr{C}(R))\geq 0\Rightarrow\mathscr{C}_{\text{ext}}-\mathscr{C}_{\text{out}}=\mathscr{C}_{\text{int}}\geq 0\,. \tag{6.3}$$

6.1 Subregion Complexity=Volume

In this section we compute the divergences of the volume complexity at $t_b=0$ for the generic rotating black hole[1]. The time dependence of the volume studied in section 5.2 tells us that the complexity is a monotonically increasing quantity, and then its minimum is obtained in the case $t_b=0$.

[1] We have seen during the computation of the Complexity=Volume conjecture in section 5.2 that the limit $r_-\to 0$ is smooth, despite the radical change of the Penrose diagram in the two cases. For this reason, we will focus immediately on the general rotating situation, and we put the non-rotating limit in Appendix D.3.3 as a check that everything works well.

In this configuration, the extremal surface is a constant $t=0$ bulk slice, connecting the two $t_L=0$ and $t_R=0$ regions on the left and right boundaries. The RT surface is a line at a constant value of the radial coordinate $r=r_+$. We denote by $V(L)$ the volume of the codimension-one extremal surface anchored at the entire left boundary of the spacetime, and by $V(R)$ the corresponding volume for the right boundary. The symmetry of the problem implies that the subregion complexity on the two boundaries separately is the same, and then

$$V_{\text{ext}} = V(L)+V(R) = 2V(L)\,. \tag{6.4}$$

The volume can be computed directly from the determinant of the induced metric on the $t=0$ slice

$$\begin{aligned} V(L) &= 2\pi l^2 \int_{r_+}^{\Lambda} dr\, G(r)\,, \\ G(r) &= \sqrt{\frac{r\left(3(\nu^2-1)r+(\nu^2+3)(r_++r_-)-4\nu\sqrt{r_+r_-(\nu^2+3)}\right)}{4(\nu^2+3)(r-r_-)(r-r_+)}}\,, \end{aligned} \tag{6.5}$$

where Λ is an UV cutoff. We investigate the possible divergences of the integral, which are near the outer horizon or near to the cutoff surface. When $r\to r_+$, the function $G(r)$ can be approximated as

$$G(r) = \frac{g}{\sqrt{r-r_+}} + \mathscr{O}\left(\sqrt{r-r_+}\right)\,, \quad g = \sqrt{\frac{r_+\left(4\nu^2 r_+ +(\nu^2+3)r_- -4\nu\sqrt{r_+r_-(\nu^2+3)}\right)}{4(\nu^2+3)(r_+-r_-)}}\,. \tag{6.6}$$

Then the contribution to the volume coming from the region nearby the outer horizon is not divergent, because we obtain

$$2\pi l^2 \int_{r_+}^{r_++\varepsilon} dr\, G(r) \approx 2\pi l^2 \int_{r_+}^{r_++\varepsilon} dr\, \frac{g}{\sqrt{r-r_+}} \approx 4\pi l^2 g\sqrt{\varepsilon}\,. \tag{6.7}$$

At $r\to\infty$, the function $G(r)$ can be expanded as

$$G(r) = \sqrt{\frac{3(\nu^2-1)}{4(\nu^2+3)}} + \frac{\nu\left(\nu(r_++r_-)-\sqrt{r_+r_-(\nu^2+3)}\right)}{\sqrt{3(\nu^2-1)(\nu^2+3)}}\frac{1}{r} + \mathscr{O}\left(\frac{1}{r^2}\right)\,. \tag{6.8}$$

Upon integration, the first two terms give rise to a linear and a logarithmic divergences. Consequently, the divergence of the volume is

$$V(L) = \pi l^2\sqrt{\frac{3(\nu^2-1)}{\nu^2+3}}\Lambda + \frac{32\pi G l^2\nu^2}{(\nu^2+3)^{3/2}\sqrt{3(\nu^2-1)}}M\log\Lambda + \mathscr{O}\left(\Lambda^0\right)\,. \tag{6.9}$$

Interestingly, the logarithmically divergent term is proportional to the mass M.

6.2 Subregion Complexity=Action

The Penrose diagram and the WDW patch corresponding to the case

$$t_b = t_L = t_R = 0\,, \tag{6.10}$$

which by symmetry argument corresponds to the minimum of the action, are depicted in fig. 6.2, where we have also drawn the surfaces at constant radius $r = \Lambda$ taken as the UV cutoff. We call r_{m1}, r_{m2} the null joints referring respectively to the top and bottom vertices of the spacetime region of interest. The definition of the null joints in terms of the tortoise coordinates are

$$\frac{t_b}{2} + r^*_\Lambda - r^*(r_{m1}) = 0\,, \qquad \frac{t_b}{2} - r^*_\Lambda + r^*(r_{m2}) = 0\,, \tag{6.11}$$

where $r^*_\Lambda \equiv r^*(\Lambda)$. At $t_b = 0$, we get

$$r^*_\Lambda = r^*(r_{m1}) = r^*(r_{m2}) \equiv r^*(r_m)\,, \tag{6.12}$$

and the configuration is symmetric, so the future and past interior actions are the same.

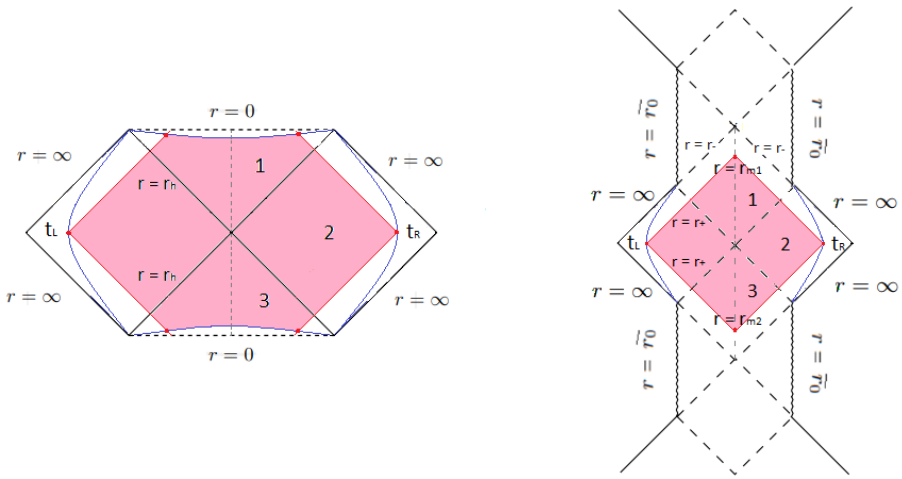

Figure 6.2: Penrose diagram and WDW patch at $t_b = 0$ for the non-rotating (left) and rotating (right) black holes.

In this section we compute the divergences of the total action of the WDW patch at $t_b = 0$ in the rotating case. The calculation for the non-rotating case involves slightly different details which are sketched in appendix D.3.1; as expected, the result reproduces the $r_- \to 0$ limit of the rotating case.

The conditions (5.122) cannot be solved analitically; we then consider a series expansion to obtain a closed form for r_m. Both at $r = \Lambda \to \infty$ and at $r \to r_-$ the function $r^*(r)$ diverges to $+\infty$, so we study the behaviour around these points:

- Nearby $r \approx r_-$, we find

$$r^*(r_m) = -\frac{\sqrt{3(\nu^2-1)}}{\nu^2+3}\tilde{A}\log|r_m - r_-| + \tilde{B} + \mathcal{O}(r_m - r_-)\,, \tag{6.13}$$

  where $\tilde{B}$ is a constant and

$$\tilde{A} = \frac{\sqrt{r_-\Psi(r_-)}}{(r_+ - r_-)\sqrt{3(\nu^2-1)}} > 0\,. \tag{6.14}$$

- Around $r = \Lambda$,

$$r^*_\Lambda = \frac{\sqrt{3(\nu^2-1)}}{\nu^2+3}\log\Lambda + \tilde{C} + \mathcal{O}(\Lambda^{-1})\,, \tag{6.15}$$

  where $\tilde{C}$ is the finite piece of order Λ^0 .

Consequently, eq. (6.12) gives:

$$r_m - r_- \approx \Lambda^{-1/\tilde{A}} \exp\left[\frac{(\tilde{B}-\tilde{C})(\nu^2+3)}{\tilde{A}\sqrt{3(\nu^2-1)}}\right]. \tag{6.16}$$

We study the contributions to the gravitational action given in eq. (5.85), computed in the relevant spacetime region corresponding to this case, focusing on the divergent terms.

Interior bulk term: The interior bulk term can be obtained from eq. (5.124) and it is written as

$$I^{\text{int}}_{\mathscr{V}} = 2(I^1_{\mathscr{V}} + I^3_{\mathscr{V}}) = -\frac{l}{4G}(\nu^2+3)\left[(r_+ - r_m)r^*_\Lambda - \int_{r_m}^{r_+} dr\, r^*(r)\right]. \tag{6.17}$$

The last integral in eq. (6.17) is finite, because the function $r^*(r)$ has integrable singularities around $r = r_-, r_+$. The divergent part of the internal bulk action therefore comes only from the divergence of the tortoise coordinate near the boundary and the result is

$$I^{\text{int}}_{\mathscr{V}} = -\frac{l}{4G}\sqrt{3(\nu^2-1)}(r_+ - r_-)\log\Lambda + \mathcal{O}(\Lambda^0)\,. \tag{6.18}$$

External bulk term: The external part of the bulk term, taken from eq. (5.124), is given by

$$I^{\text{ext}}_{\mathscr{V}} = 2I^2_{\mathscr{V}} = -\frac{l}{4G}(\nu^2+3)\int_{r_+}^{\Lambda} dr\,(r^*_\Lambda - r^*(r))\,. \tag{6.19}$$

In this case the divergence structure is richer: there are some contributions coming from the constant term r^*_Λ multiplied by the integration range, and in addition we have another contribution from the integral of the tortoise coordinate near infinity. In both cases, we need to consider the behaviour of $r^*(r)$ near infinity

$$r^*(r) = \alpha\log(4r) + \beta + \frac{\gamma}{r} + \mathcal{O}(r^{-2})\,, \tag{6.20}$$

where

$$\begin{aligned}\beta &= -2\frac{\sqrt{r_+\Psi(r_+)}\log\left(\sqrt{r_+}+\sqrt{r_+-\rho_0}\right)-\sqrt{r_-\Psi(r_-)}\log\left(\sqrt{r_-}+\sqrt{r_--\rho_0}\right)}{(\nu^2+3)(r_+-r_-)}\,,\\ \alpha &= \frac{\sqrt{3(\nu^2-1)}}{\nu^2+3}\,,\qquad \gamma=\frac{\sqrt{3(\nu^2-1)}}{2(\nu^2+3)}\left(\rho_0-2r_+-2r_-\right).\end{aligned} \tag{6.21}$$

The divergences of (6.19) then are

$$\begin{aligned}I^{\text{ext}}_{\mathscr{V}} &= \frac{l}{4G}(\nu^2+3)\left[-\alpha\Lambda+(\alpha r_++\gamma)\log\Lambda\right]+\mathscr{O}(\Lambda^0)\\ &= -\Lambda\frac{l}{4G}\sqrt{3(\nu^2-1)}+\frac{l}{8G}\sqrt{3(\nu^2-1)}(\rho_0-2r_-)(\log\Lambda)+\mathscr{O}(\Lambda^0)\,.\end{aligned} \tag{6.22}$$

Joint terms: The action evaluated on the WDW patch has four joint contributions: two on the cutoff surface $r=\Lambda$ and two in the region inside the black and white hole, coming from the top and bottom vertices. They can all be directly evaluated from eq. (5.90). The joint inside the black hole, located at $r=r_m$, gives the following contribution:

$$\begin{aligned}I^{r_m}_{\mathscr{J}} &= -\frac{l}{8G}\sqrt{r_m\Psi(r_m)}\log\left|\frac{l^2}{A^2}\frac{\left(\nu^2+3\right)\left(r_m-r_-\right)\left(r_m-r_+\right)}{r_m\Psi(r_m)}\right|=\\ &= \frac{l}{8G}\sqrt{3\left(\nu^2-1\right)}\left(r_+-r_-\right)\log\Lambda+\mathscr{O}\left(\Lambda^0\right).\end{aligned} \tag{6.23}$$

The joint nearby the cutoff surface gives:

$$\begin{aligned}I^{\Lambda}_{\mathscr{J}} &= \frac{l}{8G}\sqrt{\Lambda\Psi\left(\Lambda\right)}\log\left|\frac{l^2}{A^2}\frac{\left(\nu^2+3\right)\left(\Lambda-r_-\right)\left(\Lambda-r_+\right)}{\Lambda\Psi\left(\Lambda\right)}\right|=\\ &= \Lambda\frac{l}{8G}\sqrt{3\left(\nu^2-1\right)}\log\left|\frac{l^2}{A^2}\frac{\nu^2+3}{3\left(\nu^2-1\right)}\right|+\mathscr{O}\left(\Lambda^0\right).\end{aligned} \tag{6.24}$$

Summing the contributions of the four joints[2], we find

$$I^{\text{tot}}_{\mathscr{J}}=\Lambda\frac{l}{4G}\sqrt{3\left(\nu^2-1\right)}\log\left|\frac{l^2}{A^2}\frac{\nu^2+3}{3\left(\nu^2-1\right)}\right|+\frac{l}{4G}\sqrt{3\left(\nu^2-1\right)}\left(r_+-r_-\right)\log\Lambda+\mathscr{O}\left(\Lambda^0\right). \tag{6.25}$$

Counterterm: The WDW patch is bounded by four codimension-one null surfaces; they are all the same by symmetry, and so from (5.93) we find

$$I_{\text{ct}}=\frac{l}{4G}\int_{r_m}^{\Lambda}dr\,\frac{\partial_r(r\Psi(r))}{\sqrt{r\Psi(r)}}\log\left|\frac{2A\tilde{L}}{l^2}\frac{\partial_r(r\Psi(r))}{4\sqrt{r\Psi(r)}}\right|. \tag{6.26}$$

[2]Here we put a symmetry factor of 2 in the previous computations of the joints due to the symmetry of the configuration.

Since $\Psi(r)$ is linear in r, the only divergence comes from the region near $r=\Lambda$, giving

$$I_{\rm ct}=\Lambda\frac{l}{4G}\sqrt{3\left(\nu^2-1\right)}\log\left|\frac{\tilde{L}^2A^2}{l^4}3\left(\nu^2-1\right)\right|+\mathscr{O}\left(\Lambda^0\right). \tag{6.27}$$

Total action: Summing all the contributions, the divergences of the total action are

$$I_{\rm tot}=\frac{l}{4G}\sqrt{3(\nu^2-1)}\Lambda\left(\log\left(\frac{\tilde{L}^2}{l^2}(\nu^2+3)\right)-1\right)+(\log\Lambda)\frac{l}{4G}\sqrt{3(\nu^2-1)}\left(\frac{\rho_0}{2}-r_-\right), \tag{6.28}$$

where ρ_0 was defined in eq. (5.19). As expected, the divergent contribution in the counterterm cancels the dependence on the ambiguous normalization constant A appearing in the divergent contribution of the joints.

6.2.1 Action of internal region and subregion complexity

Now we focus on the divergence structure of the external action, which in the subregion action prescription corresponds to the complexity associated to one of the boundaries of the spacetime. We will see that this investigation will not only provide a classification of the UV divergences, but will also be sufficient to find the sub/superadditivity properties of the action, giving also an interesting temperature behaviour. The external bulk term was already identified in eq. (6.22).

Joint terms: In the interior of the black hole, there are four contributions of the form (5.90), which are all in principle divergent because the function $f(r)$ defined in eq. (5.34) satisfies $f(r_+)=f(r_-)=0$. There are other four joints inside the white hole. As in the AdS case [163], due to the signs $\eta=\pm1$ of each joint, these divergences will partially cancel each other.

It is useful to introduce the Kruskal coordinates (U,V) defined for $r>r_-$ as in [152]

$$\begin{aligned} U &= \mathrm{sgn}(r-r_+)\,e^{b_*(r^*(r)-t)}=\mathrm{sgn}(r-r_+)\,e^{-b_*u}, \\ V &= e^{b_*(r^*(r)+t)}=e^{b_*v}, \end{aligned} \tag{6.29}$$

where

$$b_*=\frac{f'(r_+)}{2}=\frac{(\nu^2+3)(r_+-r_-)}{2\sqrt{r_+\Psi(r_+)}}. \tag{6.30}$$

These coordinates satisfy the relation

$$\log|UV|=2b_*r^*(r)=f'(r_+)r^*(r) \tag{6.31}$$

which is useful to simplify expressions involving the joints. Note that, since $r_*\to-\infty$ when $r\to r_+$, the external horizon corresponds to $U=0$ (black hole horizon for the right boundary) and $V=0$ (white hole horizon for the right boundary).

Let us consider a contribution coming from sums of joints nearby the horizon. We follow the prescription given in [163], introducing the regulators $\varepsilon_U,\varepsilon_V$ to move the joints off the horizon by an

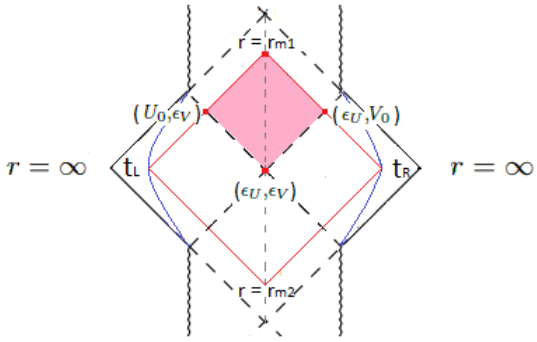

Figure 6.3: Joint terms needed for the action of the black hole interior.

infinitesimal quantity. For instance, if we evaluate the sum of the contributions of two terms with the same $V=\varepsilon_V$, from eq. (5.90), we find a term proportional to

$$\begin{aligned}\log\left|\frac{l^2}{A^2}\frac{f(r_{U_1,\varepsilon_V})}{2R(r_+)}\right|-\log\left|\frac{l^2}{A^2}\frac{f(r_{U_2,\varepsilon_V})}{2R(r_+)}\right|=\int_{r_{U_2,\varepsilon_V}}^{r_{U_1,\varepsilon_V}}\frac{dr}{f(r)}f'(r)\approx f'(r_+)\int_{r_{U_2,\varepsilon_V}}^{r_{U_1,\varepsilon_V}}\frac{dr}{f(r)}=\\ =f'(r_+)\left[r^*(r_{U_1,\varepsilon_V})-r^*(r_{U_2,\varepsilon_V})\right]=\log|U_1\varepsilon_V|-\log|U_2\varepsilon_V|=\log\left|\frac{U_1}{U_2}\right|,\end{aligned}\tag{6.32}$$

where in the last steps we simplified the result by means of eq. (6.31).

This expression tells us that in the limit $\varepsilon_V\to 0$, the difference of joints at the horizon is regular and the divergences coming from each term separately cancel. We could perform the same trick exchanging the $U\leftrightarrow V$ coordinates, since the previous manipulations are symmetric under this transformation. Combining these two results, one can conclude that

$$\log\left|\frac{l^2}{A^2}\frac{f(r_{U,V)}}{2R(r_+)}\right|=\log|UV|+F(r_+),\tag{6.33}$$

where the function $F(r)$ is regular at the horizon and is given by

$$F(r)=\log\left|\frac{l^2}{A^2}\frac{f(r)}{2R(r)}\right|-f'(r_+)r^*(r).\tag{6.34}$$

There are four joint contributions inside the black hole and four inside the white hole; by symmetry they are the same and the total contribution is twice the ones of the black hole:

$$\begin{aligned}I^{\text{int}}_{\mathscr{J}}=&-2\times\frac{l}{4G}\sqrt{\frac{r_+}{4}\Psi(r_+)}\left[\log\left|\frac{l^2}{A^2}\frac{f(r_{\varepsilon_U,\varepsilon_V})}{2R(r_+)}\right|-\log\left|\frac{l^2}{A^2}\frac{f(r_{U_0,\varepsilon_V})}{2R(r_+)}\right|-\log\left|\frac{l^2}{A^2}\frac{f(r_{\varepsilon_U,V_0})}{2R(r_+)}\right|\right]\\ &-2\times\frac{l}{4G}\sqrt{\frac{r_m}{4}\Psi(r_m)}\log\left|\frac{l^2}{A^2}\frac{f(r_m)}{2R(r_m)}\right|.\end{aligned}\tag{6.35}$$

Thus, using the relations (6.31) and (6.33), this expression simplifies to

$$\begin{aligned} I^{\text{int}}_{\mathscr{J}} &= \frac{l}{4G}\sqrt{r_+\Psi(r_+)}\,[2b_* r^*_\Lambda + F(r_+)] - \frac{l}{4G}\sqrt{r_m\Psi(r_m)}\log\left|\frac{l^2}{A^2}\frac{f(r_m)}{2R(r_m)}\right| \\ &= \frac{l}{2G}\sqrt{3(\nu^2-1)}(r_+ - r_-)\log\Lambda + \mathscr{O}(\Lambda^0)\,. \end{aligned} \tag{6.36}$$

Counterterms: The possible dependences from the UV cutoff can arise only from the $r = r_m$ endpoint of integration. However, putting the expansion (6.16) inside the counterterm, we find that no divergent pieces appear.

Internal and external action: Putting together all the terms contributing to the interior action in the rotating case, we find that the divergent part is

$$I^{\text{int}} = \frac{l}{4G}\sqrt{3(\nu^2-1)}(r_+ - r_-)\log\Lambda + \mathscr{O}(\Lambda^0)\,. \tag{6.37}$$

Subtracting this expression from eq. (6.28), we find the divergences of the external action, which correspond to the subsystem complexity:

$$I^{\text{ext}} = \frac{l}{4G}\sqrt{3(\nu^2-1)}\Lambda\left(\log\left(\frac{\tilde{L}^2}{l^2}(\nu^2+3)\right) - 1\right) + (\log\Lambda)\frac{l}{4G}\sqrt{3(\nu^2-1)}\left(\frac{\rho_0}{2} - r_+\right). \tag{6.38}$$

6.3 Comments and discussion

6.3.1 Regularization of the WDW patch

In AdS one can consider two different regularizations [65] for the CA conjecture (see figure 6.4):

- The edge of the WDW can end on the asymptotic AdS boundary (regularization A).
- The edge of the WDW patch can end on the regulator surface (regularization B).

The two regularizations give the same complexity rate at large times. In asymptotically AdS spaces, if one introduces appropriate counterterms in regularization A one can reproduce the same results as in regularization B [173, 174].

In WAdS the structure of the Penrose diagram is radically different from AdS, and it resembles instead the one of asymptotically Minkowski space: the right corner of the Penrose diagram corresponds to $r \to \infty$ and arbitrary t (spacelike infinity). The 45 degrees boundaries correspond to the future null infinity and past null infinity (see figure 6.5).

In all the previous works on the CA conjectures in WAdS [123, 124], regularization B was implicitly used. This approach gives the expected result for the complexity rate at late time $\dot{\mathscr{C}}_A \propto TS$ in the case of Einstein gravity, see eq. (5.133). We used as well this regularization in the previous section to compute subregion action complexity.

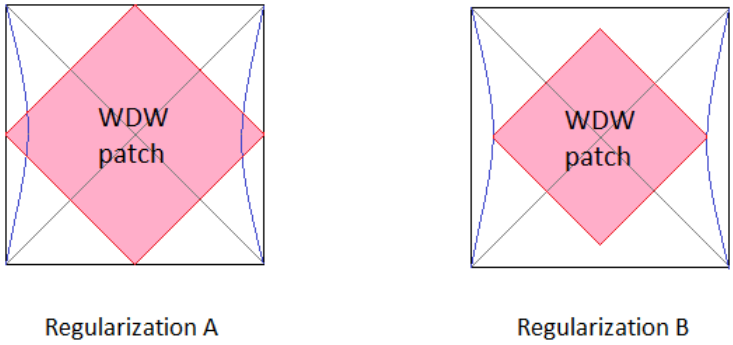

Figure 6.4: Two different regularizations can be chosen for the action of the WDW patch for black holes in AdS (here for illustrative purpose we show the case of non-rotating black hole in asymptotically AdS spacetime).

It is not straightforward to generalise regularization A to the case of WAdS, because then the corner of the WDW patch would be located at the spacelike infinity point for all values of the time. This would give the unphysical result that complexity is time-independent.

If in regularization B we sent the UV cutoff to infinity, we would find that the WDW patch includes all the interior of the black hole. This is the same part of the Penrose diagram which gives the linear growth of complexity at large time; so sending the cutoff to infinity is equivalent to sending the time to infinity with finite cutoff, which gives a divergent internal action. This explains why the action of the internal part of the WDW is UV divergent in WAdS, while it is finite in AdS.

6.3.2 Role of the counterterm

Following [58], we inserted in the gravitational action a counterterm of kind (5.93) which is needed in order to maintain reparameterization invariance in presence of null boundaries. This term is not necessarily unique.

Let us borrow some notation from [58]. We consider a null hypersurface defined by the function $\Phi(x^\alpha) = 0$. The hypersurface can be described by parametric equations $x^\mu(\lambda, \theta^A)$, where λ is the affine null parameter and θ^A is constant on each null generator on the surface. The vectors

$$k^\mu = \frac{\partial x^\mu}{\partial \lambda}, \qquad e^\mu_A = \frac{\partial x^\mu}{\partial \theta^A} \tag{6.39}$$

are tangent to the surface, while k^α is the null normal to the surface. Let us denote by

$$\sigma_{AB} = g_{\alpha\beta} e^\alpha_A e^\beta_B \tag{6.40}$$

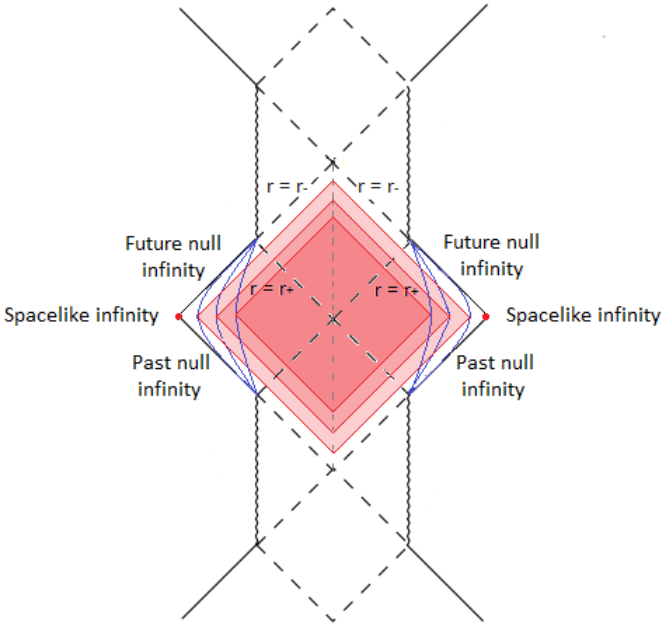

Figure 6.5: In WAdS the causal structure resemble the one of asymptotically Minkowski spacetime. Regularization A would give a WDW patch with a corner which is located at the spacelike infinity, and so would give a time-independent complexity. Moreover, the WDW patch in regularization B covers the entire black hole interior in the limit of infinite cutoff Λ.

the induced metric on the transverse directions θ_A. Also, one can introduce the following tensor

$$B_{AB} = e_A^\alpha e_B^\beta D_\alpha k_\beta \,, \tag{6.41}$$

which describes the behaviour of the congruence of null generators.

In principle, as discussed in the Appendix B of [58], in presence of null boundaries we can also allow for Lagrangians depending on combinations of the Riemann tensor $\hat{R}_{ABCD}$ computed from the transverse induced metric σ_{AB}. Moreover, contributions containing the tensor B_{AB} are also allowed. A priori we could have a counterterm of the type

$$\mathscr{L}_{\rm ct}(\hat{R}, \hat{R}_{AB}, \hat{R}_{ABCD}, B_{AB}, \Theta) \,, \tag{6.42}$$

where we should require that the total action is reparametrization-invariant. Dramatic restrictions arise from the fact that we are working in 3 dimensions, which means that the null surfaces are 2-dimensional and that the induced metric σ_{AB} is 1-dimensional. This implies that

$$\hat{R}_{ABCD} = 0 \,, \qquad \hat{R}_{AB} = 0 \,, \qquad \hat{R} = 0 \,, \qquad B_{AB} = \frac{1}{2}\Theta\,\sigma_{AB} \,, \tag{6.43}$$

and then there is no space for curvature terms other than the geodesic expansion parameter Θ, which we already considered for the counterterm (5.93).

6.3.3 Structure of divergences

For the BTZ black hole, the only divergence in the holographic subregion complexity is linear in the cutoff Λ. In WAdS_3, we found that the two versions of holographic subregion complexity have all a linear and a logarithmic divergence in Λ. The coefficient of the linear divergence, as in the BTZ case, can be positive or negative depending on the counterterm parameter $\tilde{L}$. The coefficient of the logarithmic divergence is independent of $\tilde{L}$; it is instead a function of the black holes parameters (r_+, r_-), or equivalently of (T, J). In each of the two versions, the logarithmic divergence of the subregion complexity is proportional to a different quantity:

- In the CA conjecture, eq. (6.38) gives a result proportional to $K_A = \frac{\rho_0}{2} - r_+$, with a positive coefficient.

- In the CV conjecture, eq. (6.9) gives a term proportional to the mass M, with a positive coefficent.

6.3.4 Sub/superadditivity

In AdS black holes the internal action I^{int} at $t_b = 0$ is finite [164, 163] and has a sign which depends on the choice of the counterterm parameter $\tilde{L}$. In turn, depending from the sign of I^{int}, the action subregion complexity can be sub/superadditive. Instead, in WAdS_3 the interior action I^{int} is always positive and independent of the counterterm length scale; as a consequence, $\mathscr{C}_A$ subregion complexity of the left and right side of the thermofield double is superadditive. Moreover, I^{int} is proportional to the product of temperature and entropy of the black hole:

$$I^{\text{int}} = \frac{4\sqrt{3(\nu^2-1)}}{\nu^2+3}\, l\, T S \log\Lambda + \mathscr{O}(\Lambda^0)\,. \tag{6.44}$$

By construction, $\mathscr{C}_V$ is superadditive and saturates superadditivity (6.2) for the left and right side of thermofield double at $t_b = 0$.

6.3.5 Temperature behaviour

For neutral black holes in AdS, subregion $\mathscr{C}_A$ has different properties depending on the regularization parameter $\tilde{L}$. For $\tilde{L} \ll l$, C_A increases with temperature, whereas, for $\tilde{L} \gg l$, $\mathscr{C}_A$ decreases with temperature. Instead, for neutral black holes in AdS, subregion $\mathscr{C}_V$ is an increasing powerlike function of temperature [112] (for AdS_3, actually, it is independent of temperature).

In WAdS$_3$, the leading dependence on temperature of the subsystem complexity is in the $\log\Lambda$ terms. To this purpose we introduce

$$C_J = \frac{\partial M}{\partial T}\Big|_J, \qquad C_A = \frac{\partial K_A}{\partial T}\Big|_J, \tag{6.45}$$

which are explicitly computed in Appendix D.4. C_J is the specific heat at constant J. We note that the scale r_+ factorises from the quantities (6.45), then it is convenient to introduce

$$\varepsilon = r_-/r_+, \qquad 0 \le \varepsilon < 1\,, \tag{6.46}$$

and to study the sign of (6.45) as a function of (ε, ν). Let us define (see figure 6.6)

$$\text{Region A}: \qquad 0 < \varepsilon < \frac{\nu^2+3}{4\nu^2} \tag{6.47}$$

$$\text{Region B}: \qquad \frac{\nu^2+3}{4\nu^2} < \varepsilon < 1\,. \tag{6.48}$$

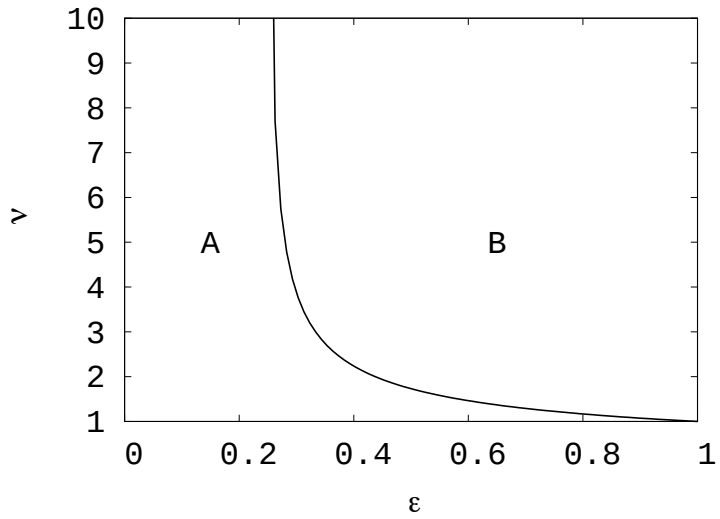

Figure 6.6: Regions A and B in (ε, ν) plane.

The angular momentum J is negative in region A and positive in region B, while it vanishes along the two curves

$$\varepsilon = 0 \qquad \text{and} \qquad \varepsilon = \frac{\nu^2+3}{4\nu^2}\,. \tag{6.49}$$

It is interesting that the two quantities (C_J, C_A) change sign in regions A,B:

- C_J is positive in region B and negative in region A.
- C_A is negative in region B and positive in region A.

As a consequence, in the region where $C_J > 0$, subregion $\mathscr{C}_V$ at constant J increases with temperature while $\mathscr{C}_A$ decreases. In the thermodynamically unstable region where $C_J < 0$, subregion $\mathscr{C}_V$ decreases with temperature while $\mathscr{C}_A$ increases.

Chapter 7

Subregion action complexity of the BTZ black hole

The work in this chapter has previously appeared in [175].

In chapters 5 and 6 we investigated various aspects of complexity: we obtained the time evolution of complexity for both the volume and action conjectures, we studied their divergence structure, we observed that they are both superadditive and we studied the temperature behaviour. The task of these computations was to obtain some informations for the putative field theory side of WAdS/WCFT correspondence, but we also had in mind to compare the warped case with the traditional AdS case, in order to find some universal aspects of the conjectures.

While in the general case volume and action differ from the transient behaviour of complexity for intermediate times, but they agree at late times, we observed that subregion complexity helps in finding situations where the two conjectures lead to different results. Motivated by this observation, we find important to search for other examples where the holographic computation discriminates between the two proposals. Some of them were already considered in the literature, *e.g.* by studying defects [114] or time-dependent backgrounds [117, 118].

In this chapter we consider the subregion complexity for asymptotically AdS_3 spacetime with a generic subsystem on the boundary, *i.e.* without restricting to the particular case where the subregion is taken to be one of the disconnected boundaries of the eternal black hole, which was studied in [163]. The volume case was considered in previous works [160, 162], and will be reviewed for comparison with the action computation later.

In this chapter we will find the following analytic result for the subregion complexity of a segment of length l in the BTZ black hole background:

$$\mathscr{C}_A^{\mathrm{BTZ}} = \frac{l}{\varepsilon}\frac{c}{6\pi^2}\log\left(\frac{\tilde{L}}{L}\right) - \log\left(\frac{2\tilde{L}}{L}\right)\frac{S^{\mathrm{BTZ}}}{\pi^2} + \frac{1}{24}c\,, \tag{7.1}$$

where $\tilde{L}$ is the counterterm length scale, ε is the UV cutoff, c the CFT central charge and S^{BTZ} the Ryu-Takayanagi (RT) entanglement entropy of the segment subregion. This shows a direct connection at equilibrium, in the case of the one segment subregion, between action complexity and entropy. This expression is also valid for the particular case of AdS_3, which was previously studied in [65, 114].

One may wonder if such a simple connection between subregion complexity and entanglement entropy is valid also for more general subsystems. For this reason, we compute action complexity in the case of a two segments subregion in AdS_3. This quantity has again a linear divergence proportional to the total size of the region and a logarithmic divergence proportional to the divergent part of the entropy. However, if the separation between the two disjoint segments is small, there is no straightforward relation between the finite part of complexity and entropy, as we will derive in eq. (7.91).

7.1 Subregion complexity for a segment in AdS_3

It is useful to review the AdS_3 calculation [65, 114, 128] to set up the notation and the procedure, and as a warm-up for the more complicated BTZ case. We consider the Einstein-Hilbert action with negative cosmological constant in $2+1$ dimensions

$$S = \frac{1}{16\pi G}\int\left(R+\frac{2}{L^2}\right)\sqrt{-g}\,d^3x\,, \tag{7.2}$$

which has as a solution AdS_3 spacetime, whose metric in Poincaré coordinates reads

$$ds^2 = \frac{L^2}{z^2}\left(-dt^2+dz^2+dx^2\right). \tag{7.3}$$

The AdS curvature is $R=-6/L^2$ and L is the AdS length. The central charge of the dual conformal field theory is related to the bulk quantities via the expression

$$c = \frac{3L}{2G}\,. \tag{7.4}$$

Two common regularizations [65] are used in the CA conjecture (see figure 6.4):

- Regularization A: the WDW patch is built starting from the boundary $z=0$ of the spacetime and a cutoff is then introduced at $z=\varepsilon$.
- Regularization B: the WDW patch is built from the surface $z=\varepsilon$.

As for the warped case, we will use in the main text the regularization B, while the comparison with regularization A is discussed in Appendix D.5.

We consider a subregion on the boundary given by a strip of length l and for convenience we take $x\in\left[-\frac{l}{2},\frac{l}{2}\right]$, at the constant time slice $t=0$. This choice is possible due to the translation invariance of the set-up along these directions. The geometry relevant to the computation of action complexity is the

intersection between the entanglement wedge [159] of the subregion with the WDW patch [176, 57], see figure 7.1. Notice that among the various boundary terms involving the null surfaces, there is a codimension-three joint coming from the intersection between the WDW patch, the entanglement wedge and the boundary at $z = 0, x = \pm l/2$. This kind of joint exists only in regularization B and can a priori give a non-vanishing contribution. Since we will check that regularization A gives a similar result for the subregion action in Appendix D.5, we believe that this joint at most shifts the action by an overall constant.

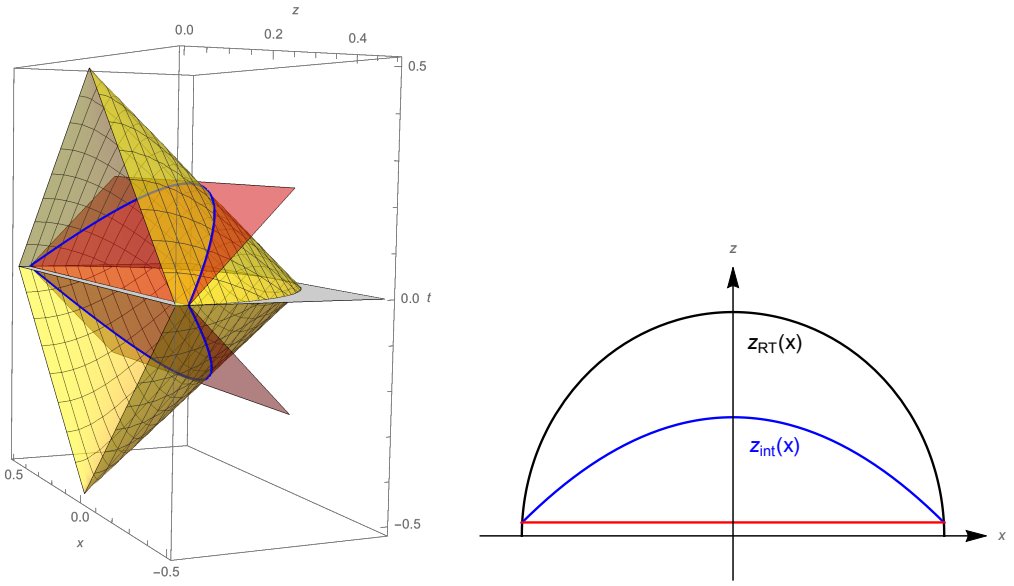

Figure 7.1: Left: Intersection of WDW patch with entanglement wedge in the (x,z,t) space. The boundary of the entanglement wedge is in yellow, while the boundary of the WDW patch is in red. Right: intersections in the (x,z) plane, with z_{RT} in black, z_{int} in blue and the cutoff $z = \varepsilon$ in red.

We use regularization B with a cutoff a $z = \varepsilon$ and we consider all the ingredients describing the boundaries of the spacetime region of interest. The RT surface is given by the space-like geodesic

$$t = 0\,, \qquad z^2 + x^2 = \left(\frac{l}{2}\right)^2\,, \tag{7.5}$$

which is a circle of radius $l/2$. A useful alternative parametrization of the curve is

$$z_{RT} = \sqrt{\left(\frac{l}{2}\right)^2 - x^2}\,. \tag{7.6}$$

The entanglement wedge is a cone whose null boundaries are parameterized by

$$t_{\rm EW} = \pm\left(\frac{l}{2} - \sqrt{z^2 + x^2}\right)\,. \tag{7.7}$$

The boundaries of the WDW patch, which are attached to the regulator surface, are described by the equations

$$t_{\rm WDW} = \pm(z-\varepsilon)\,. \tag{7.8}$$

In order to split the bulk term and to compute the joint contributions, we need to find the intersection curve between the null boundary of the WDW patch and the one of the entanglement wedge, parametrized by

$$z_{\rm int} = \frac{(l+2\varepsilon)^2-4x^2}{4(l+2\varepsilon)} \qquad \text{or} \qquad x_{\rm int} = \frac{1}{2}\sqrt{(l+2\varepsilon)(l-4z+2\varepsilon)}\,. \tag{7.9}$$

The introduction of the UV cutoff surface for the radial coordinate z induces a constraint on the values that the transverse coordinate can assume. In particular, the maximal one corresponds to the x coordinate of the RT surface evaluated at the cutoff, *i.e.*

$$x_{\rm max} \equiv x_{\rm RT}(z=\varepsilon) = \sqrt{\left(\frac{l}{2}\right)^2-\varepsilon^2}\,. \tag{7.10}$$

This shift from $x = l/2$ is necessary for a correct regularization of the on-shell action. We remind the contributions to the action

$$I = I_{\mathscr{V}} + I_{\mathscr{N}} + I_{\rm ct} + I_{\mathscr{J}}\,, \tag{7.11}$$

where $I_{\mathscr{V}}$ is the bulk term (see eq. 7.2), $I_{\mathscr{N}}$ the null boundary term (see (7.16)), $I_{\rm ct}$ the counterterm (7.20) and $I_{\mathscr{J}}$ the null joint contribution (7.23).

In the following computations there will be various symmetry factors induced by the fact that we consider for most of the terms only the region $x>0, t>0$. We will include all of these factors when giving the total bulk, joint and counterterm expressions. In all the computations of this chapter it will be understood that the results are given up to the finite term, namely we omit $\mathscr{O}(\varepsilon)$ contributions, which vanish in the limit $\varepsilon \to 0$.

7.1.1 Bulk term

The curvature is constant and so the Einstein-Hilbert term (7.2) is proportional to the spacetime volume. We can split the bulk contribution in two parts, based on the intersection between the WDW patch and the entanglement wedge, which we parametrize with the function $z_{int}(x)$. In the first region the WDW patch is subtended by the entanglement wedge. Consequently, we integrate along time $0 \le t \le t_{\rm WDW}(z)$, then the radial direction along $\varepsilon \le z \le z_{\rm int}(x)$, and finally along the coordinate $0 \le x \le x_{\rm max}$:

$$I^1_{\mathscr{V}} = -\frac{L}{4\pi G}\int_0^{x_{max}} dx \int_\varepsilon^{z_{int}} dz \int_0^{t_{WDW}} dt\, \frac{1}{z^3} \tag{7.12}$$

In the second region the entanglement wedge is under the WDW patch, then the integration involves the endpoints $0 \leq t \leq t_{\rm EW}(z,x), z_{\rm int}(x) \leq z \leq z_{\rm RT}(x)$ and finally $0 \leq x \leq x_{\rm max}$:

$$I^2_{\mathscr{V}} = -\frac{L}{4\pi G}\int_0^{x_{max}} dx \int_{z_{int}}^{z_{RT}} dz \int_0^{t_{EW}} dt\, \frac{1}{z^3} \tag{7.13}$$

A direct evaluation of the integrals gives:

$$\begin{aligned} I^1_{\mathscr{V}} &= -\frac{L}{16\pi G}\frac{l}{\varepsilon} - \frac{L}{4\pi G}\log\left(\frac{\varepsilon}{l}\right) - \frac{L}{8\pi G}\,. \\ I^2_{\mathscr{V}} &= \frac{L}{8\pi G}\log\left(\frac{\varepsilon}{l}\right) + \frac{L(\pi^2+8)}{64\pi G}\,. \end{aligned} \tag{7.14}$$

The total result of the bulk action is:

$$I^{\rm AdS}_{\mathscr{V}} = 4(I^1_{\mathscr{V}} + I^2_{\mathscr{V}}) = -\frac{L}{4\pi G}\frac{l}{\varepsilon} + \frac{L}{2\pi G}\log\left(\frac{l}{\varepsilon}\right) + \frac{L\pi}{16G}\,. \tag{7.15}$$

7.1.2 Null boundary counterterms

A hypersurface described by the scalar equation $\Phi(x^a) = 0$ has a normal vector $k_a = -\partial_a\Phi$. If the hypersurface is null, $k_a k^a = 0$ and then it can be shown [177] that the hypersurface is generated by null geodesics, which have k^α as a tangent vector.

In correspondence of a null boundary, the following term appears in the action

$$I_{\mathscr{N}} = \int dS\, d\lambda\, \sqrt{\sigma}\kappa\,, \tag{7.16}$$

where λ is the geodesic parameter, S the transverse spatial directions, σ is the determinant of the induced metric on S and κ is defined by the geodesic equation

$$k^\mu D_\mu k^\alpha = \kappa k^\alpha\,. \tag{7.17}$$

In our case, the null normals to the WDW patch and the entanglement wedge are given respectively by the following one-forms:

$$\mathbf{k}^\pm = \alpha\,(\pm dt - dz)\,, \qquad \mathbf{w}^\pm = \beta\left(\pm dt + \frac{z dz}{\sqrt{z^2+x^2}} + \frac{x dx}{\sqrt{z^2+x^2}}\right), \tag{7.18}$$

where α, β are arbitrary constants that will cancel in the final result. We denote by $(k^\pm)^\mu$ and $(w^\pm)^\mu$ the corresponding vectors. It can be checked that they correspond to an affine parametrization of their null surfaces, i.e.

$$(k^\pm)^\mu D_\mu (k^\pm)^\alpha = 0\,, \qquad (w^\pm)^\mu D_\mu (w^\pm)^\alpha = 0\,. \tag{7.19}$$

The term (7.16) vanishes in our calculation because we used an affine parameterization, see eq. (7.19).

We still need to include the contribution from the counterterm, which ensures the reparameterization invariance of the action:

$$I_{\rm ct} = \frac{1}{8\pi G}\int d\lambda\, dS\,\sqrt{\sigma}\,\Theta\log\left|\tilde{L}\Theta\right|\,, \tag{7.20}$$

where Θ is the expansion scalar of the boundary geodesics and $\tilde{L}$ is an arbitrary scale. If an affine parameterization is used, the following result holds [177]:

$$\Theta = D_\mu k^\mu\,. \tag{7.21}$$

We can then evaluate eq. (7.20) on each boundary:

- The counterterm on the entanglement wedge boundary vanishes because $\Theta = 0$. This agrees with the calculations in [159].

- For the boundary of the WDW patch we obtain:

$$\begin{aligned} I_{\rm ct}^{\rm WDW} &= -\frac{L}{2\pi G}\int_0^{x_{\rm max}} dx\int_\varepsilon^{z_{\rm int}}\frac{dz}{z^2}\log\left|\alpha\frac{\tilde{L}z}{L^2}\right| \\ &= \frac{L}{4\pi G}\frac{l}{\varepsilon}\left[1+\log\left(\alpha\frac{\tilde{L}\varepsilon}{L^2}\right)\right]+\frac{L}{4\pi G}\log\left(\frac{\varepsilon}{l}\right)\log\left(\alpha^2\frac{\varepsilon l\tilde{L}^2}{L^4}\right) \\ &+ \frac{L}{2\pi G}\log\left(\frac{\varepsilon}{l}\right)+\frac{L\pi}{12G}\,. \end{aligned} \tag{7.22}$$

7.1.3 Joint terms

The contribution to the gravitational action coming from a codimension-two joint, given by intersection of two codimension-one null surfaces [58], is

$$I_{\mathscr{J}} = \frac{\eta}{8\pi G}\int dx\sqrt{\sigma}\log\left|\frac{\mathbf{a_1}\cdot\mathbf{a_2}}{2}\right| \tag{7.23}$$

where σ is the induced metric determinant on the codimension-two surface, $\mathbf{a_1}$ and $\mathbf{a_2}$ are the null normals to the two intersecting codimension-one null surfaces and $\eta = \pm 1$ depending from the orientation of the normals to the surface. The four joints give the following contributions:

- The joint at the UV cutoff $z = \varepsilon$ is characterized by the data

$$\sqrt{\sigma} = \frac{L}{\varepsilon}\,, \qquad \log\left|\frac{\mathbf{k}^-\cdot\mathbf{k}^+}{2}\right| = \log\left|\alpha^2\frac{\varepsilon^2}{L^2}\right|\,, \tag{7.24}$$

  and then from the general expression (7.23) we find

$$I_{\mathscr{J}}^{\rm cutoff} = -\frac{L}{4\pi G}\frac{l}{\varepsilon}\log\left(\alpha\frac{\varepsilon}{L}\right)\,. \tag{7.25}$$

- The joint coming from the intersection of the regions with $t > 0$ and $t < 0$ of the entanglement wedge corresponds to the RT surface and is described by

$$\sqrt{\sigma} = \frac{2lL}{l^2 - 4x^2}, \qquad \log\left|\frac{\mathbf{w}^+ \cdot \mathbf{w}^-}{2}\right| = \log\left|\beta^2 \frac{l^2 - 4x^2}{4L^2}\right|, \tag{7.26}$$

  which gives

$$I^{\mathrm{RT}}_{\mathscr{J}} = \frac{L}{4\pi G} \log\left(\frac{\varepsilon}{l}\right) \log\left(\frac{\beta^2 \varepsilon l}{L^2}\right) + \frac{L\pi}{48G}. \tag{7.27}$$

- The last two joint terms come from the intersections between the null boundaries of the WDW patch and the ones of the entanglement wedge:

$$\sqrt{\sigma} = \frac{4L(l+2\varepsilon)}{(l-2x+2\varepsilon)(l+2x+2\varepsilon)}, \tag{7.28}$$

$$\log\left|\frac{\mathbf{k}^+ \cdot \mathbf{w}^+}{2}\right| = \log\left|\frac{(l-2x+2\varepsilon)(l+2x+2\varepsilon)}{4L(4x^2+(l+2\varepsilon)^2)}\right|^2. \tag{7.29}$$

  Therefore they evaluate to

$$I^{\mathrm{int}}_{\mathscr{J}} = -\frac{L}{2\pi G} \log\left(\frac{\varepsilon}{l}\right) \log\left(\frac{\alpha\beta}{2} \frac{\varepsilon l}{L^2}\right) - \frac{5\pi L}{48G}. \tag{7.30}$$

Summing all the joint contributions we find

$$I^{\mathrm{tot}}_{\mathscr{J}} = -\frac{L}{4\pi G} \frac{l}{\varepsilon} \log\left(\alpha \frac{\varepsilon}{L}\right) + \frac{L}{4\pi G} \log\left(\frac{\varepsilon}{l}\right) \log\left(\frac{4L^2}{\alpha^2 \varepsilon l}\right) - \frac{\pi L}{12G}. \tag{7.31}$$

Note that the dependence on the normalization constant β of the normals cancels in (7.31); this is due to the fact that the null surfaces which have the RT surface as boundaries have vanishing expansion parameter Θ. Also, when summing the joint term (7.31) with the counterterm contribution (7.22) the double logarithmic terms cancel and the dependence on α disappears.

7.1.4 Complexity

Summing all the contributions, the action complexity is:

$$\mathscr{C}_A^{\mathrm{AdS}} = \frac{I^{\mathrm{AdS}}_{\mathrm{tot}}}{\pi} = \frac{c}{3\pi^2} \left\{ \frac{l}{2\varepsilon} \log\left(\frac{\tilde{L}}{L}\right) - \log\left(\frac{2\tilde{L}}{L}\right) \log\left(\frac{l}{\varepsilon}\right) + \frac{\pi^2}{8} \right\}. \tag{7.32}$$

The calculations is in agreement with [128]. In the expression for the complexity we recognize a term proportional to the entanglement entropy of the segment:

$$S^{\mathrm{AdS}} = \frac{c}{3} \log\left(\frac{l}{\varepsilon}\right). \tag{7.33}$$

This suggests that the complexity for a single interval has a leading divergence proportional to the length of the subregion on the boundary, a subleading divergence proportional to the entanglement entropy and a constant finite piece. We test this expression for the BTZ case in the next section.

7.2 Subregion complexity for a segment in the BTZ black hole

We consider the metric of the planar BTZ black hole in $2+1$ dimensions with non-compact coordinates (t,z,x)

$$ds^2 = \frac{L^2}{z^2}\left(-f dt^2 + \frac{dz^2}{f} + dx^2\right), \qquad f = 1 - \left(\frac{z}{z_h}\right)^2, \tag{7.34}$$

where L is the AdS radius and z_h is the position of the horizon. The mass, temperature and entropy are:

$$M = \frac{L^2}{8Gz_h^2}, \qquad T = \frac{1}{2\pi z_h}, \qquad S = \frac{\pi L^2}{2Gz_h}. \tag{7.35}$$

The geometry needed to evaluate the subregion complexity for a segment is shown in figure 7.2

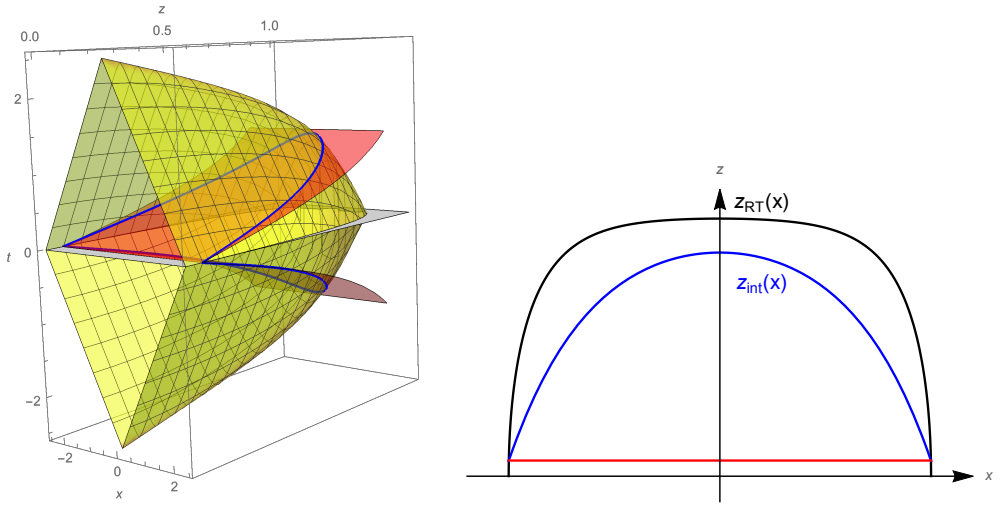

Figure 7.2: Region relevant to the action computation for a segment in the BTZ case, for $l = 5$. Left: Intersection of WDW patch with entanglement wedge in the (x,z,t) space. The boundary of the entanglement wedge is in yellow, while the boundary of the WDW patch is in red. Right: intersections in the (x,z) plane, with z_{RT} in black, z_{int} in blue and the cutoff $z = \varepsilon$ in red.

The RT surface is a spacelike geodesic which lies on a constant time slice $t = 0$ and which is anchored at the edges of the boundary subregion [178]:

$$x_\pm(z) = \frac{1}{4} z_h \left[\log\left(\frac{J+1}{J-1}\right)^2 + \log\left(\frac{z_h^2 - Jz^2 \pm \sqrt{z_h^4 - (1+J^2)z_h^2 z^2 + J^2 z^4}}{z_h^2 + Jz^2 \pm \sqrt{z_h^4 - (1+J^2)z_h^2 z^2 + J^2 z^4}}\right)^2\right], \tag{7.36}$$

where

$$J = \coth\left(\frac{l}{2z_h}\right). \tag{7.37}$$

The turning point of the geodesic is at $x_{\pm}(z_*) = 0$, where

$$z_* = z_h \tanh\left(\frac{l}{2z_h}\right). \tag{7.38}$$

Since $z_* < z_h$ for every value of the boundary subregion size l, the geodesic never penetrates inside the event horizon of the black hole[1]. It is convenient to invert eq. (7.36) for the following computations:

$$z_{RT} = z_h \sqrt{\frac{\cosh\left(\frac{l}{z_h}\right) - \cosh\left(\frac{2x}{z_h}\right)}{\cosh\left(\frac{l}{z_h}\right) + 1}}. \tag{7.39}$$

In our static case, the entanglement wedge coincides with the causal wedge [179–181], which can be constructed by sending null geodesics from the causal diamond on the boundary into the bulk. The explicit expressions of such geodesics are [180]

$$\begin{aligned} \tilde{x}_{\rm EW}(z,j) &= \frac{z_h}{2}\log\left(\frac{\sqrt{z_h^2 + j^2(z^2 - z_h^2)} + jz}{\sqrt{z_h^2 + j^2(z^2 - z_h^2)} - jz}\right), \\ \tilde{t}_{\rm EW}(z,j) &= \pm\left[\frac{l}{2} + \frac{z_h}{2}\log\left(\frac{\sqrt{z_h^2 + j^2(z^2 - z_h^2)} - z}{\sqrt{z_h^2 + j^2(z^2 - z_h^2)} + z}\right)\right]. \end{aligned} \tag{7.40}$$

We obtain an analytical expression for the boundary of the entanglement wedge in terms of a unique explicit relation between (t,z,x) by determining $j = j(z,x)$ from the first equation in (7.40) and then inserting it into the second equation of (7.40). The result can be written as

$$t_{\rm EW} = \pm\left[\frac{l}{2} - z_h\,\mathrm{arccoth}\left(\frac{\sqrt{2}z_h\cosh\left(\frac{x}{z_h}\right)}{\sqrt{2z^2 + z_h^2\cosh\left(\frac{2x}{z_h}\right) - z_h^2}}\right)\right]. \tag{7.41}$$

The WDW patch is delimited by the radial null geodesics

$$t_{\rm WDW} = \pm\frac{z_h}{4}\log\left(\frac{z_h + z}{z_h - z}\frac{z_h - \varepsilon}{z_h + \varepsilon}\right)^2. \tag{7.42}$$

[1] In a certain sense, this is opposite in spirit with respect to the motivations for introducing complexity: a quantity measuring the evolution of the Einstein-Rosen bridge connecting the interior of black holes, in a context where the WDW reaches the singularities. In time-dependent configurations, the RT can go deep inside the horizon, while in the static case we observe that it does not happen. Anyway, we will be able to find some important conclusions and a relation with the entanglement entropy.

We will need again the intersection between the boundaries of the WDW patch and of the entanglement wedge

$$t_{\rm int} = t_{\rm WDW}\,, \qquad z_{\rm int} = z_h \frac{\cosh\left[\frac{l}{2z_h} + \operatorname{arctanh}\left(\frac{\varepsilon}{z_h}\right)\right] - \cosh\left(\frac{x}{z_h}\right)}{\sinh\left[\frac{l}{2z_h} + \operatorname{arctanh}\left(\frac{\varepsilon}{z_h}\right)\right]}\,. \tag{7.43}$$

This curve is plotted in fig. 7.2. As in the AdS case, we denote by $x_{\rm max}$ the maximum value of the transverse coordinate, which is reached when we evaluate the RT surface at $z = \varepsilon$:

$$x_{\rm max} \equiv x_{\rm RT}(z=\varepsilon) = z_h \operatorname{arccosh}\left[\sqrt{1-\frac{\varepsilon^2}{z_h^2}}\cosh\left(\frac{l}{2z_h}\right)\right]. \tag{7.44}$$

7.2.1 Bulk contribution

We split the integration region as in the AdS case, see eqs. (7.12,7.13). The total bulk action is given by $I_{\mathscr{V}} = 4(I^1_{\mathscr{V}} + I^2_{\mathscr{V}})$, which combine into the expression

$$\begin{aligned} I_{\mathscr{V}} = \frac{L}{8\pi G z_h}\int_0^{x_{max}(\varepsilon)} dx \Bigg\{ & \frac{4\sinh\left[\frac{l}{2z_h} + \operatorname{arctanh}\left(\frac{\varepsilon}{z_h}\right)\right]}{\cosh\left(\frac{l}{2z_h} + \operatorname{arctanh}\left(\frac{\varepsilon}{z_h}\right)\right) - \cosh\left(\frac{x}{z_h}\right)} - \frac{4z_h}{\varepsilon} \\ & + 2\coth\left(\frac{x}{z_h}\right)\log\left|\frac{\sinh\left(\frac{l-2x}{2z_h}\right)\sinh^2\left[\frac{l+2x+2z_h\operatorname{arctanh}(\varepsilon/z_h)}{4z_h}\right]}{\sinh\left(\frac{l+2x}{2z_h}\right)\sinh^2\left[\frac{l-2x+2z_h\operatorname{arctanh}(\varepsilon/z_h)}{4z_h}\right]}\right|\Bigg\}\,. \end{aligned} \tag{7.45}$$

This integral can be computed analytically, giving

$$I_{\mathscr{V}} = -\frac{L}{4\pi G}\frac{l}{\varepsilon} - \frac{L}{2\pi G}\log\left(\frac{\varepsilon}{l}\right) + \frac{L}{2\pi G}\log\left[\frac{2z_h}{l}\sinh\left(\frac{l}{2z_h}\right)\right] + \frac{\pi L}{16G}\,. \tag{7.46}$$

7.2.2 Null normals

In order to compute the counterterms due to the null surfaces and the joint contributions, the null normals are needed. It is convenient to use an affine parameterization, which can be found using the following Lagrangian description of geodesics:

$$\mathscr{L} = \frac{L^2}{z^2}\left(-f(z)\,\dot{t}^2 + \frac{\dot{z}^2}{f(z)} + \dot{x}^2\right) \tag{7.47}$$

where the dot represents the derivative with respect to the affine parameter λ. Since the Lagrangian does not depend on t and x, we have two constants of motion

$$E = -\frac{1}{2}\frac{\partial\mathscr{L}}{\partial\dot{t}} = \frac{L^2}{z^2}f(z)\,\dot{t}\,, \qquad J = \frac{1}{2}\frac{\partial\mathscr{L}}{\partial\dot{x}} = \frac{L^2}{z^2}\dot{x}\,. \tag{7.48}$$

Imposing the null condition $\mathscr{L} = 0$ and making use of eq. (7.48) leads to

$$\dot{z} = \pm \frac{z^2}{L^2} \sqrt{E^2 - J^2 f(z)} \,. \tag{7.49}$$

Therefore, from eqs. (7.48) and (7.49), the tangent vector to the null geodesic is

$$V^\mu = (\dot{t}, \dot{z}, \dot{x}) = \left(\frac{z^2}{L^2 f(z)} E, \pm \frac{z^2}{L^2} \sqrt{E^2 - J^2 f(z)}, \frac{z^2}{L^2} J \right) . \tag{7.50}$$

Lowering the contravariant index with the metric tensor, we get the normal one-form to the null geodesic

$$\mathbf{V} = V_\mu dx^\mu = -E\, dt \pm \frac{\sqrt{E^2 - J^2 f(z)}}{f(z)} dz + J\, dx \,. \tag{7.51}$$

The null geodesics which bound the WDW patch are x-constant curves, and then they correspond to the choice $J = 0$. This gives the normals

$$\mathbf{k}^+ = k^+_\mu dx^\mu = \alpha \left(dt - \frac{dz}{f(z)} \right) , \qquad \mathbf{k}^- = k^-_\mu dx^\mu = \alpha \left(-dt - \frac{dz}{f(z)} \right) , \tag{7.52}$$

where α is an arbitrary constant.

The null geodesics that bound the entanglement wedge are normal to the RT surface, *i.e.*

$$V_\mu \frac{dX^\mu_{RT}(x)}{dx} = 0 \,, \qquad X^\mu_{\rm RT}(x) = (0, z_{RT}, x) \,, \tag{7.53}$$

where z_{RT} is given in eq. (7.39). With this condition and eqs. (7.51) and (7.53), we find a relation between the two constants of motion E and J which gives (for $t > 0$ and $t < 0$ respectively)

$$\mathbf{w}^\pm = w^\pm_\mu dx^\mu = \beta \left(\pm dt + a\, dz + b\, dx \right) , \tag{7.54}$$

where

$$a = \frac{e^{-\frac{x}{z_h}} \left(e^{\frac{2x}{z_h}} + 1 \right) z z_h^2}{\left(z_h^2 - z^2 \right) \sqrt{4z^2 + e^{-\frac{2x}{z_h}} \left(e^{\frac{2x}{z_h}} - 1 \right)^2 z_h^2}} , \qquad b = \frac{e^{-\frac{x}{z_h}} \left(e^{\frac{2x}{z_h}} - 1 \right) z_h}{\sqrt{4z^2 + e^{-\frac{2x}{z_h}} \left(e^{\frac{2x}{z_h}} - 1 \right)^2 z_h^2}} . \tag{7.55}$$

7.2.3 Null boundaries and counterterms

The term in eq. (7.16) vanishes because we used an affine parameterization. The counterterm in eq. (7.20) gives:

- For the null normals of the boundary of the entanglement wedge, this contribution vanishes because $\Theta = D_\mu (w^\pm)^\mu = 0$.

- For the null normals of the boundary of the WDW patch, a direct calculation gives $\Theta = \frac{\alpha z}{L^2}$ and:

$$
\begin{aligned}
I_{\text{ct}}^{\text{WDW}} &= -\frac{L}{2\pi G}\int_0^{x_{\max}} dx \int_{\varepsilon}^{z_{\text{int}}(x)} dz\, \frac{1}{z^2}\log\left|\frac{\tilde{L}}{L^2}\,\alpha z\right| = \\
&= \frac{L}{2\pi G}\int_0^{x_{\max}} dx \left\{ \frac{1+\log\left|\frac{\tilde{L}}{L^2}\,\alpha\varepsilon\right|}{\varepsilon} + \frac{\sinh\left(\frac{l}{2z_h}+\operatorname{arctanh}\left(\frac{\varepsilon}{z_h}\right)\right)}{z_h\left[\cosh\left(\frac{x}{z_h}\right)-\cosh\left(\frac{l}{2z_h}\right)+\operatorname{arctanh}\left(\frac{\varepsilon}{z_h}\right)\right]}\times \right. \\
&\left. \times\left(1+\log\left|\frac{\tilde{L}z_h\alpha}{L^2}\,\frac{\cosh\left(\frac{l}{2z_h}+\operatorname{arctanh}\left(\frac{\varepsilon}{z_h}\right)\right)-\cosh\left(\frac{x}{z_h}\right)}{\cosh\left(\frac{l}{2z_h}+\operatorname{arctanh}\left(\frac{\varepsilon}{z_h}\right)\right)}\right|\right)\right\}.
\end{aligned}
\tag{7.56}
$$

7.2.4 Joint contributions

We evaluate the joint terms in eq (7.23):

- The joint at the cutoff surface:

$$
I_{\mathscr{J}}^{\text{cutoff}} = -\frac{L}{4\pi G}\int_0^{x_{\max}}\frac{dx}{\varepsilon}\left|\frac{\alpha^2 z_h^2\varepsilon^2}{L^2(z_h^2-\varepsilon^2)}\right|. \tag{7.57}
$$

- The joint at the RT surface:

$$
I_{\mathscr{J}}^{\text{RT}} = -\frac{L}{4\pi G z_h}\int_0^{x_{\max}} dx\,\frac{\sinh\left(\frac{l}{z_h}\right)}{\cosh\left(\frac{l}{z_h}\right)-\cosh\left(\frac{2x}{z_h}\right)}\log\left|\frac{\beta^2 z_h^2}{2L^2}\,\frac{\cosh\left(\frac{l}{z_h}\right)-\cosh\left(\frac{2x}{z_h}\right)}{\cosh^2\left(\frac{x}{z_h}\right)}\right|. \tag{7.58}
$$

- The two joints coming from the intersection between the null boundaries of the WDW patch and the ones of the entanglement wedge:

$$
\begin{aligned}
I_{\mathscr{J}}^{\text{int}} = \frac{L}{2\pi G z_h}\int_0^{x_{\max}} dx\,&\frac{\sinh\left(\frac{l}{2z_h}+\operatorname{arctanh}\left(\frac{\varepsilon}{z_h}\right)\right)}{\cosh\left(\frac{l}{2z_h}+\operatorname{arctanh}\left(\frac{\varepsilon}{z_h}\right)\right)-\cosh\left(\frac{x}{z_h}\right)}\times \\
&\times\log\left|\frac{e^{x/z_h}\alpha\beta z_h^2}{L^2}\,\frac{\left[\cosh\left(\frac{l}{2z_h}+\operatorname{arctanh}\left(\frac{\varepsilon}{z_h}\right)\right)-\cosh\left(\frac{x}{z_h}\right)\right]^2}{1+e^{2x/z_h}\cosh\left(\frac{l}{2z_h}+\operatorname{arctanh}\left(\frac{\varepsilon}{z_h}\right)\right)-2e^{x/z_h}}\right|.
\end{aligned}
\tag{7.59}
$$

All the joints contributions and the counterterm are correctly regularized by the prescription induced from the UV cutoff at $z=\varepsilon$.

7.2.5 Complexity

We performed all the integrals analytically and we further simplified the result using various dilogarithm identities, including the relation

$$8\,\mathrm{Re}\left[\mathrm{Li}_2\left(\frac{1+ie^{\frac{y}{2}}}{1+e^{\frac{y}{2}}}\right)-\mathrm{Li}_2\left(\frac{1}{1+e^{\frac{y}{2}}}\right)-\mathrm{Li}_2\left(1+ie^{\frac{y}{2}}\right)-\mathrm{Li}_2\left(\frac{e^{\frac{y}{2}}-i}{1+e^{\frac{y}{2}}}\right)\right]=$$
$$=-\frac{7\pi^2}{6}+4\left(\log\left(1+e^{\frac{y}{2}}\right)\right)^2+\log 2\left[2y-4\log\left(\frac{e^y-1}{y}\right)+4\log\left(\frac{2}{y}\sinh\frac{y}{2}\right)\right], \tag{7.60}$$

which can be proved by taking a derivative of both side of the equation with respect to y. In this way the action subregion complexity is given by

$$\mathscr{C}_A^{\mathrm{BTZ}}=\frac{c}{3\pi^2}\left\{\frac{l}{2\varepsilon}\log\left(\frac{\tilde{L}}{L}\right)-\log\left(\frac{2\tilde{L}}{L}\right)\log\left(\frac{2z_h}{\varepsilon}\sinh\left(\frac{l}{2z_h}\right)\right)+\frac{\pi^2}{8}\right\}. \tag{7.61}$$

Introducing the entanglement entropy of an interval

$$S^{\mathrm{BTZ}}=\frac{c}{3}\log\left(\frac{2z_h}{\varepsilon}\sinh\left(\frac{l}{2z_h}\right)\right), \tag{7.62}$$

we can then write it in the form

$$\mathscr{C}_A^{\mathrm{BTZ}}=\frac{l}{\varepsilon}\frac{c}{6\pi^2}\log\left(\frac{\tilde{L}}{L}\right)-\log\left(\frac{2\tilde{L}}{L}\right)\frac{S^{\mathrm{BTZ}}}{\pi^2}+\frac{1}{24}c. \tag{7.63}$$

The divergencies of eqs. (7.63) are the same as in the AdS case eqs. (7.32), which is recovered for $z_h=0$.

A non-trivial cross-check can be done in the $l\gg z_h$ limit. Keeping just the terms linear in l in eq. (7.61), we find agreement with the subregion complexity $\mathscr{C}_A^{\mathrm{BTZ,R}}$ computed for one side of the Kruskal diagram, see [163, 164]:

$$\mathscr{C}_A^{\mathrm{BTZ,R}}=\frac{c}{6}\frac{l}{\pi^2}\left[\frac{1}{\varepsilon}\log\left(\frac{\tilde{L}}{L}\right)-\frac{1}{z_h}\log\left(\frac{2\tilde{L}}{L}\right)\right]. \tag{7.64}$$

Note that in this limit the $\log\varepsilon$ divergence disappears because it is suppressed by the segment length l.

For comparison, the volume complexity of an interval for the BTZ [140, 161] is:

$$\mathscr{C}_V^{\mathrm{BTZ}}=\frac{2c}{3}\left(\frac{l}{\varepsilon}-\pi\right), \tag{7.65}$$

and it is non-trivially independent on temperature. Subregion $\mathscr{C}_V$ at equilibrium is a topologically protected quantity: for multiple intervals, the authors of [161] found the following result using the the Gauss-Bonnet theorem

$$\mathscr{C}_V^{\mathrm{AdS}}=\mathscr{C}_V^{\mathrm{BTZ}}=\frac{2c}{3}\left(\frac{l_{tot}}{\varepsilon}+\kappa\right), \tag{7.66}$$

where l_{tot} is the total length of all the segments and κ is the finite part, that depends on topology

$$\kappa = -2\pi\chi + \frac{\pi}{2}m\,, \tag{7.67}$$

where χ is the Euler characteristic of the extremal surface (which is equal to 1 for a disk) and m is the number of ninety degrees junctions between RT surface and boundary segments. It would be interesting to see if a similar result could be established for the CA conjecture. This motivates us to study the two segment case in the next section.

7.3 Subregion complexity for two segments in AdS_3

In this section we evaluate the holographic subregion action complexity for a disjoint subregion on the boundary of AdS_3 spacetime. We consider two segments of size l with a separation equal to d, located on the constant time slice $t = 0$. For simplicity, we work with a symmetric configuration, in which the two boundary subregions are respectively given by $x \in [-l - d/2, -d/2]$ and $x \in [d/2, l + d/2]$. According to the values of the subregions size l and of the separation d, there are two possible extremal surfaces anchored at the boundary at the edges of the two subregions [182, 183]:

- The extremal surface (which in this number of dimension is a geodesic) is given by the union of the RT surfaces for the individual subregions. This is the minimal surface for $d > d_0$, where d_0 is a critical distance.

- The extremal surface connects the two subregions. This configuration is minimal for $d < d_0$.

The two cases are shown in Fig. 7.3. The geodesic with the minimal area provides the holographic entanglement entropy for the union of the disjoint subregions. The critical distance corresponds to the distance for which both the extremal surfaces have the same length, *i.e.*

$$d_0 = (\sqrt{2} - 1)l\,. \tag{7.68}$$

In the first configuration (see left in Fig. 7.3), we have two non-intersecting entanglement wedges and then

$$\mathscr{C}_A^1 = 2\,\mathscr{C}_A^{\text{AdS}}\,. \tag{7.69}$$

For the second configuration (right in Fig. 7.3), we must perform a new computation. The spacetime region of interest is symmetric both with respect to the $x = 0$ slice and to the $t = 0$ one. As a consequence, we can evaluate the action on the region with $t > 0$ and $x > 0$ and introduce opportune symmetry factors. A schematic representation is shown in fig. 7.4.

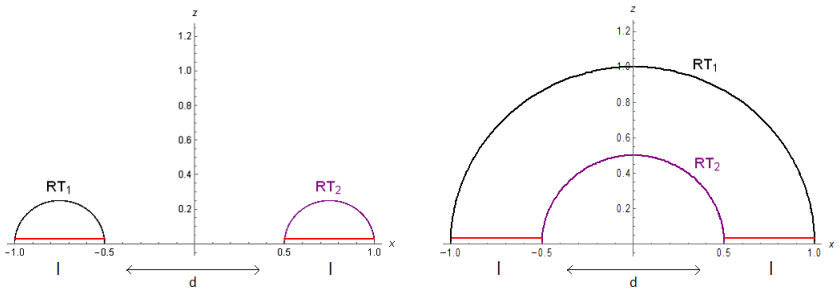

Figure 7.3: The possible RT surfaces for disjoint subregions of length $l = 0.5$ with a separation $d = 1$, on the slice $t = 0$.

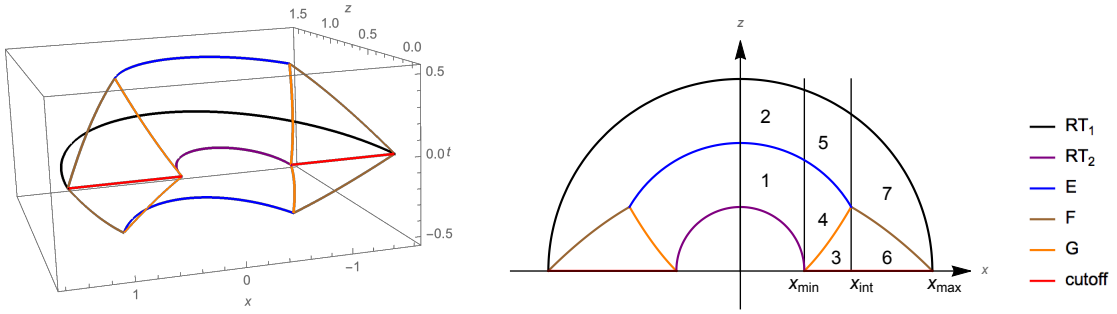

Figure 7.4: Left: Bulk region relevant to the action subregion calculation for two segments in AdS. Right: projection in the (x,z) plane. The regions in which the bulk integral is splitted are numbered.

The RT surface is the union of the spacelike geodesics anchored at the edges of the region $x \in [-l-d/2, l+d/2]$ and $x \in [-d/2, d/2]$. We will denote such geodesics as RT_1 and RT_2, respectively:

$$z_{RT_1}(x) = \sqrt{\left(\frac{2l+d}{2}\right)^2 - x^2}\,, \qquad z_{RT_2}(x) = \sqrt{\left(\frac{d}{2}\right)^2 - x^2}\,. \tag{7.70}$$

With the introduction of the cutoff surface at $z = \varepsilon$, RT_2 is truncated at $x = x_{min}$ and RT_1 at $x = x_{max}$, defined by

$$x_{min} \equiv x_{\mathrm{RT}_2}(z=\varepsilon) = \sqrt{\left(\frac{d}{2}\right)^2 - \varepsilon^2}\,, \qquad x_{max} \equiv x_{\mathrm{RT}_1}(z=\varepsilon) = \sqrt{\left(\frac{d+2l}{2}\right)^2 - \varepsilon^2}\,. \tag{7.71}$$

The null boundaries of the entanglement wedge can be built by sending null geodesics from RT_1 and RT_2:

$$t_{EW_1} = \frac{2l+d}{2} - \sqrt{z^2+x^2}\,, \qquad t_{EW_2} = -\frac{d}{2} + \sqrt{z^2+x^2}\,. \tag{7.72}$$

The WDW patch, anchored at the cutoff in the present regularization, is bounded by the null surface

$$t_{WDW} = z - \varepsilon\,. \tag{7.73}$$

The intersection curve E between the null boundaries of the entanglement wedge, (built from RT_1 and RT_2, see eq. (7.72)) is

$$t_E = \frac{l}{2}, \qquad z_E = \frac{1}{2}\sqrt{(d+l)^2 - 4x^2}. \tag{7.74}$$

The intersection F between the boundary of the WDW patch eq. (7.73) and the null surface anchored at RT_1 is:

$$t_F = \frac{1}{4}\left[d + 2(l-\varepsilon) - \frac{4x^2}{d+2(l+\varepsilon)}\right], \qquad z_F = t_F + \varepsilon. \tag{7.75}$$

The intersection G between the WDW patch eq. (7.73) and the null surface anchored at RT_2 gives

$$t_G = -\frac{d}{4} + \frac{x^2}{d-2\varepsilon} - \frac{\varepsilon}{2}, \qquad z_G = t_G + \varepsilon. \tag{7.76}$$

The intersection among the three curves described above (obtained solving the condition $z_E = z_F = z_G$) gives

$$x_{int}(\varepsilon) = \frac{\sqrt{(d-2\varepsilon)\,[d+2(l+\varepsilon)]}}{2}. \tag{7.77}$$

7.3.1 Bulk contribution

As shown in Fig. 7.4, the total bulk contribution can be divided into 7 parts for computational reasons:

$$I_{\mathscr{V}} = 4\sum_{i=1}^{7} I^i_{bulk}, \tag{7.78}$$

where

$$\begin{aligned}
I^1_{\mathscr{V}} &= -\frac{L}{4\pi G}\int_0^{x_{min}} dx \int_{z_{RT_2}}^{z_E} dz \int_0^{t_{EW_2}} \frac{dt}{z^3} \\
I^2_{\mathscr{V}} &= -\frac{L}{4\pi G}\int_0^{x_{min}} dx \int_{z_E}^{z_{RT_1}} dz \int_0^{t_{EW_1}} \frac{dt}{z^3} \\
I^3_{\mathscr{V}} &= -\frac{L}{4\pi G}\int_{x_{min}}^{x_{int}} dx \int_{\varepsilon}^{z_G} dz \int_0^{t_{WDW}} \frac{dt}{z^3} \\
I^4_{\mathscr{V}} &= -\frac{L}{4\pi G}\int_{x_{min}}^{x_{int}} dx \int_{z_G}^{z_E} dz \int_0^{t_{EW_2}} \frac{dt}{z^3} \\
I^5_{\mathscr{V}} &= -\frac{L}{4\pi G}\int_{x_{min}}^{x_{int}} dx \int_{z_E}^{z_{RT_1}} dz \int_0^{t_{EW_1}} \frac{dt}{z^3} \\
I^6_{\mathscr{V}} &= -\frac{L}{4\pi G}\int_{x_{int}}^{x_{max}} dx \int_{\varepsilon}^{z_F} dz \int_0^{t_{WDW}} \frac{dt}{z^3} \\
I^7_{\mathscr{V}} &= -\frac{L}{4\pi G}\int_{x_{int}}^{x_{max}} dx \int_{z_F}^{z_{RT_1}} dz \int_0^{t_{EW_1}} \frac{dt}{z^3}.
\end{aligned} \tag{7.79}$$

All the integrals can be evaluated analytically. Since the expressions are rather cumbersome, we only write just the total expression

$$\begin{aligned} I_{\mathscr{V}} &= -\frac{c}{6\pi}\left\{\frac{2l}{\varepsilon}-2\log\frac{d(d+2l)}{\varepsilon^2}+\frac{\pi^2}{2}+8\,\mathrm{arctanh}\sqrt{\frac{d}{d+2l}}\right. \\ &\left.-2\left[\mathrm{Li}_2\left(\frac{\sqrt{d(d+2l)}}{d+l}\right)-\mathrm{Li}_2\left(-\frac{\sqrt{d(d+2l)}}{d+l}\right)\right]\right\}. \end{aligned} \tag{7.80}$$

We already expressed the result in terms of the central charge for later convenience.

7.3.2 Counterterms

The counterterms for the null boundaries of the entanglement wedge vanish as usual. We can separate the counterterm for the null boundaries of the WDW patch in two contributions:

$$\begin{aligned} I_{ct,I} &= \frac{L}{2\pi G}\int_{x_{min}}^{x_{int}}dx\int_{\varepsilon}^{z_G}\frac{dz}{z^2}\log\left(\frac{\tilde{L}\,\alpha\, z}{L^2}\right), \\ I_{ct,II} &= \frac{L}{2\pi G}\int_{x_{int}}^{x_{max}}dx\int_{\varepsilon}^{z_F}\frac{dz}{z^2}\log\left(\frac{\tilde{L}\,\alpha\, z}{L^2}\right). \end{aligned} \tag{7.81}$$

7.3.3 Joint contributions

We have to include several joint contributions to the action:

- Joints on the cutoff at $z=\varepsilon$. The null normals are

$$\mathbf{k}^{\pm}=\alpha\,(\pm dt-dz)\,, \tag{7.82}$$

  and the contribution is:

$$I_{\varepsilon}=-\frac{L}{4\pi G}\int_{x_{min}}^{x_{max}}dx\,\frac{\log\left(\frac{\alpha^2\varepsilon^2}{L^2}\right)}{\varepsilon}=-\frac{L}{2\pi G}\frac{l\log\left(\frac{\alpha\varepsilon}{L}\right)}{\varepsilon}. \tag{7.83}$$

- Joint on RT_1. The null normals to such surfaces are

$$\mathbf{w}_{\mathbf{1}}^{\pm}=\beta\left(\pm dt+\frac{z}{\sqrt{z^2+x^2}}dz+\frac{x}{\sqrt{z^2+x^2}}dx\right), \tag{7.84}$$

  which gives

$$\begin{aligned} I_{RT_1} &= -\frac{L}{2\pi G}\int_0^{x_{max}}dx\,\frac{d+2l}{(d+2l)^2-4x^2}\log\frac{\beta^2\left[(d+2l)^2-4x^2\right]}{4L^2}= \\ &= \frac{L}{4\pi G}\log(\varepsilon)\log\left(\frac{\beta^2\varepsilon}{L^2}\right)-\frac{L}{4\pi G}\log(d+2l)\log\frac{(d+2l)\,\beta^2}{L^2}+\frac{L\pi}{48G}. \end{aligned} \tag{7.85}$$

- Joint on RT_2. The null normals to these surfaces are

$$\mathbf{w}_{\mathbf{2}}^{\pm} = \gamma\left(\pm dt - \frac{z}{\sqrt{z^2+x^2}}dz - \frac{x}{\sqrt{z^2+x^2}}dx\right), \tag{7.86}$$

and the action is:

$$\begin{aligned} I_{RT_2} &= -\frac{L}{2\pi G}\int_0^{x_{min}} dx\,\frac{d}{d^2-4x^2}\log\frac{\gamma^2\left(d^2-4x^2\right)}{4L^2} = \\ &= \frac{L}{4\pi G}\log(\varepsilon)\log\left(\frac{\gamma^2\,\varepsilon}{L^2}\right) - \frac{L}{4\pi G}\log(d)\log\frac{d\,\gamma^2}{L^2} + \frac{L\pi}{48G}. \end{aligned} \tag{7.87}$$

- Joints between the two null boundaries of the entanglement wedge, curve E. The normals are $\mathbf{w}_{\mathbf{1}}^{+}$ and $\mathbf{w}_{\mathbf{2}}^{+}$. The contribution gives

$$I_E = \frac{L}{\pi G}\int_0^{x_{int}} dx\,\frac{d+l}{(d+l)^2-4x^2}\log\left[\frac{\beta\,\gamma\left[(d+l)^2-4x^2\right]}{4L^2}\right]. \tag{7.88}$$

- Joint between the null boundary of the WDW patch and the null boundary of the entanglement wedge anchored at RT_1, curve F. The normals are $\mathbf{k}^{+}$ and $\mathbf{w}_{\mathbf{1}}^{+}$. The term gives

$$I_F = \frac{2L}{\pi G}\int_{x_{int}}^{x_{max}} dx\,\frac{d+2(l+\varepsilon)}{(d+2(l+\varepsilon))^2-4x^2}\log\left[\frac{\alpha\,\beta\left[(d+2(l+\varepsilon))^2-4x^2\right]^2}{16L^2\left[(d+2(l+\varepsilon))^2+4x^2\right]}\right]. \tag{7.89}$$

- Joint between the null boundary of the WDW patch and the null boundary of the entanglement wedge anchored at RT_2 (curve G) with normals $\mathbf{k}^{+}$ and $\mathbf{w}_{\mathbf{2}}^{+}$. The contribution gives

$$I_G = \frac{2L}{\pi G}\int_{x_{min}}^{x_{int}} dx\,\frac{d-2\varepsilon}{4x^2-(d-2\varepsilon)^2}\log\left[\frac{\alpha\,\gamma(d-2\varepsilon+2x)^2(d-2\varepsilon-2x)^2}{16L^2\left[4x^2+(d-2\varepsilon)^2\right]}\right]. \tag{7.90}$$

7.3.4 Complexity

Adding up all the contributions and using polylog identities, we find:

$$\begin{aligned} \mathscr{C}_A^2 = \frac{c}{3\pi^2}\Bigg\{ &\log\left(\frac{\tilde{L}}{L}\right)\frac{l}{\varepsilon} - \log\left(\frac{2\tilde{L}}{L}\right)\log\left(\frac{d(d+2l)}{\varepsilon^2}\right) - \frac{\pi^2}{4} \\ &+ \left[\log\left(\frac{\tilde{L}}{L}\right) + \log\left(\frac{2(d+l)}{\sqrt{d(d+2l)}}\right)\right]\log\left(\frac{(d+l+\sqrt{d(d+2l)})^2}{l^2}\right) \\ &+ \mathrm{Li}_2\left(\frac{\sqrt{d(d+2l)}}{d+l}\right) - \mathrm{Li}_2\left(-\frac{\sqrt{d(d+2l)}}{d+l}\right)\Bigg\}. \end{aligned} \tag{7.91}$$

The divergences of (7.91) are the same as in eq. (7.69); in particular, the subleading divergences are still poportional to the entanglement entropy

$$S = \frac{c}{3}\log\frac{d(d+2l)}{\varepsilon^2}\,. \tag{7.92}$$

The finite part is instead a more complicated function of d, l compared to the single interval case.

7.4 Mutual complexity

Consider a physical system which is splitted into two sets A, B. The mutual information is defined as

$$I(A|B) = S(A) + S(B) - S(A\cup B)\,. \tag{7.93}$$

Since the entanglement entropy is shown to exhibit a subadditivity behaviour, *i.e.* the entanglement entropy of the full system is less than the sum of the entropies related to the two subsystems, the mutual information is a positive quantity.

Another quantity which measures the correlations between two physical subsystems was defined in [164, 128] and called *mutual complexity*:

$$\Delta\mathscr{C} = \mathscr{C}(\hat{\rho}_A) + \mathscr{C}(\hat{\rho}_B) - \mathscr{C}(\hat{\rho}_{A\cup B})\,. \tag{7.94}$$

where $\hat{\rho}_A$, $\hat{\rho}_B$ are the reduced density matrices in the Hilbert spaces localised in A and B. If $\Delta\mathscr{C}$ is always positive, complexity is subadditive; if it is always negative, complexity is superadditive. By construction, in the CV conjecture complexity is always superadditive, i.e. $\Delta\mathscr{C} \leq 0$. Instead, in the *CA* conjecture, no general argument is known which fixes the sign of $\Delta\mathscr{C}$. $\Delta\mathscr{C}$ is a finite quantity in all the holographic conjectures. Moreover, $\Delta\mathscr{C} = 0$ for $d > d_0$ because in this case the RT surface is disconnected and then $\mathscr{C}(\hat{\rho}_A) + \mathscr{C}(\hat{\rho}_B) = \mathscr{C}(\hat{\rho}_{A\cup B})$. We will check that this quantity is generically discontinuous at $d = d_0$.

In the case of two disjoint intervals, from eq. (7.91) we find that the action mutual complexity is:

$$\begin{aligned}\Delta\mathscr{C}_A = \mathscr{C}_A^1 - \mathscr{C}_A^2 = \frac{c}{3\pi^2}\Bigg\{&\log\left(\frac{2\tilde{L}}{L}\right)\log\left(\frac{d(d+2l)}{l^2}\right) + \frac{\pi^2}{2}\\ &- \left[\log\left(\frac{\tilde{L}}{L}\right) + \log\left(\frac{2(d+l)}{\sqrt{d(d+2l)}}\right)\right]\log\left(\frac{(d+l+\sqrt{d(d+2l)})^2}{l^2}\right)\\ &-\mathrm{Li}_2\left(\frac{\sqrt{d(d+2l)}}{d+l}\right) + \mathrm{Li}_2\left(-\frac{\sqrt{d(d+2l)}}{d+l}\right)\Bigg\}\,.\end{aligned} \tag{7.95}$$

The function $\Delta\mathscr{C}_A$ is plotted in figure 7.5 for various $\eta = \tilde{L}/L$. From the figure, we see that this quantity can be either positive or negative. At small d, the behavior of $\Delta\mathscr{C}_A$ is:

$$\Delta\mathscr{C}_A \approx \frac{c}{3\pi^2}\log\left(\frac{2\tilde{L}}{L}\right)\log\left(\frac{2d}{l}\right). \tag{7.96}$$

For the value $\tilde{L}/L = 1/2$, the behaviour of $\Delta\mathscr{C}_A$ at $d \to 0$ switches from $-\infty$ to ∞.

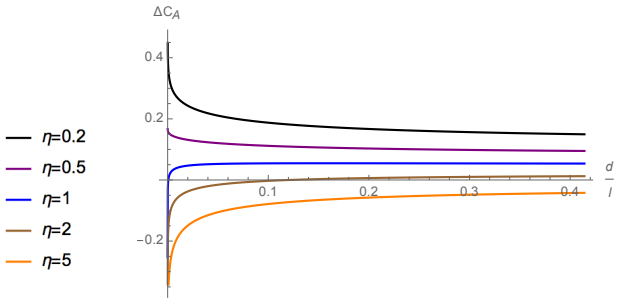

Figure 7.5: Mutual complexity $\Delta\mathscr{C}_A$ for several values of $\eta = \tilde{L}/L$ as a function of $\frac{d}{l} \in [0, \frac{d_0}{l} = \sqrt{2}-1]$.

If $\eta \leq 1/2$, CA is subadditive for all values of d/l. For $\eta > 1/2$, it is always possible to find small enough distances giving a superadditive behaviour. Moreover, there is a critical $\eta_0 \approx 2.465$ in such a way that complexity of two disjoint intervals is always superadditive if $\eta > \eta_0$. In order to have a positive definite subregion complexity, we should require $\eta > 1$. So it seems that it is not possible to achieve an universally subadditive complexity in a physically consistent setting.

A similar behaviour of subregion CA is found in the thermofield double state where the subsystems are taken as the two disconnected boundaries of spacetime. This case was investigated for asymptotically AdS black holes in D dimensions [163, 164], showing that the complexity=action is subadditive when $\eta < \hat{\eta}_D$ and superadditive for $\eta > \hat{\eta}_D$. The value of $\hat{\eta}_D$ is given by the zero of $g_D(\eta)$ [163]:

$$g_D(\eta) = \log((D-2)\eta) + \frac{1}{2}\left(\psi_0(1) - \psi_0\left(\frac{1}{D-1}\right)\right) + \frac{D-2}{D-1}\pi, \tag{7.97}$$

where $\psi_0(z) = \Gamma'(z)/\Gamma(z)$ is the digamma function. For $D = 3$, $\hat{\eta}_3 \approx 0.1$.

In the CV conjecture, we can use eqs. (7.66) and (7.67) from [161] to determine mutual complexity. Considering the case of a double segment, we find that for $d < d_0$ the mutual complexity is constant:

$$\Delta\mathscr{C}_V = -\frac{4c}{3}\pi. \tag{7.98}$$

7.4.1 Strong super/subaddivity for overlapping segments

Given two generically overlapping regions A and B, entanglement entropy satisfies the strong subadditivity property:

$$\tilde{\Delta}S = S(A) + S(B) - S(A \cup B) - S(A \cap B) \geq 0\,. \tag{7.99}$$

Inspired by this relation, we can define [128] by analogy a generalization of the mutual complexity as:

$$\tilde{\Delta}\mathscr{C}(A,B) = \mathscr{C}(\hat{\rho}_A) + \mathscr{C}(\hat{\rho}_B) - \mathscr{C}(\hat{\rho}_{A\cup B}) - \mathscr{C}(\hat{\rho}_{A\cap B})\,. \tag{7.100}$$

This definition generalizes eq. (7.94) to the case where $A \cap B \neq \emptyset$. We can investigate the sign of this quantity in the case of two overlapping segments.

Suppose that we consider the regions given by two intervals of lengths a, b which intersect in a segment of length c. The union of these intervals is a segment of total length $a + b - c$. From eq. (7.63) we find

$$\tilde{\Delta}\mathscr{C}_A^{\text{BTZ}} = -\log\left(\frac{2\tilde{L}}{L}\right)\tilde{\Delta}S^{\text{BTZ}}\,, \tag{7.101}$$

where $\tilde{\Delta}S^{\text{BTZ}}$ is the quantity defined in (7.99), computed for the two overlapping intervals in the BTZ background. Then $\mathscr{C}_A$ is strongly subadditive for $\tilde{L}/L < 1/2$ and strongly superadditive for $\tilde{L}/L > 1/2$.

7.5 Comments and discussion

We studied the CA subregion complexity conjecture in AdS_3 and in the BTZ background. The main results of this chapter are:

- In the case of one segment, we find that subregion complexity for AdS_3 and for the BTZ can be directly related to the entanglement entropy, see eqs. (7.1).
- In the case of a two segments subregion, complexity in AdS_3 is a more complicated function of the lengths and the relative separation of the segments, see eqs. (7.91). Subregion complexity carries a different amount of information compared to the entanglement entropy. In particular, for two disjoint segments the mutual complexity (defined in eq. (7.94)) is not proportional to mutual information.

We find that the sign of action mutual complexity $\Delta\mathscr{C}_A$ of a two disjoint segments subregion depends drastically on $\eta = \tilde{L}/L$ (see figure 7.5):

- For $\eta \geq \eta_0 \approx 2.465$, $\Delta\mathscr{C}_A$ is always negative, and so $\mathscr{C}_A$ is superadditive as $\mathscr{C}_V$ and $\mathscr{C}_{V2.0}$.
- For $\frac{1}{2} < \eta < \eta_0$, $\Delta\mathscr{C}_A$ is negative at small d and positive at large d. This region should be partially unphysical, because in order to obtain a positive-definite $\mathscr{C}_A$, we have to require $\tilde{L} > L$ and so $\eta > 1$.

- In the unphysical region $0 < \eta \leq 1/2$, action complexity is subadditive.

Chapter 8

Conclusions and outlook

In this thesis we studied various aspects of non-relativistic theories, both from the point of view of quantum field theory and of gravity computations in the context of general relativity. We briefly summarize the results and we give some hints for further directions to follow for future investigations.

Trace anomaly

The terms entering the trace anomaly for a $2+1$ dimensional Galilean-invariant field theory coupled to a Newton-Cartan background split into an infinite number of sectors which are invariant under Weyl transformations

$$\langle T^i_{\ i} - 2T^0_{\ 0} \rangle = \sum_{k=0}^{\infty} \mathscr{A}_k \,. \tag{8.1}$$

Each sector is distinguished only from the number of appearances[1] of the one-form n giving the local time direction in Newton-cartan geometry. In particular, there exists one sector which can be written as the dimensional reduction along a null direction of the $3+1$ dimensional relativistic trace anomaly

$$\mathscr{A}_0 = aE_4 - cW^2_{MNPQ} + \mathscr{A}_{\rm ct} \,, \tag{8.2}$$

while the next-to minimal subsector with one appearance of n has vanishing trace anomaly $\mathscr{A}_1 = 0$. The classification for the other sectors in not known, apart from the existence of an infinite tower of type B anomalies which can be built using the Weyl tensor.

Studying the trace anomaly in the specific cases of a free scalar and a free fermion minimally coupled to Newton-Cartan gravity, we found that the coefficients of the minimal sector $\mathscr{A}_0$ of the trace anomaly are the same of the $3+1$ dimensional relativistic case, apart from an overall normalization $1/m$ involving the mass of the non-relativistic particle. This result suggests the existence of an $a-$theorem for the coefficient of the Euler density as in the relativistic parent theory, whose physical interpretation could be the fact that bound states tend to be broken when adding energy to the system.

[1] In the previous formula, the index k indeed counts the number of appearances of n.

We also investigated what happens when a source for the particle number is turned on, finding a surprising violation of the invariance under gauge transformations and Milne boosts, the local version of Galilean boosts. On the other hand, we found that no gravitational anomaly arises, even when adding the particle number source.

There are several open questions to answer. We propose the following ones:

- The relation between the anomaly coefficients and the correlation functions of the energy-momentum tensor multiplet should be clarified [3, 11]. In the case of vacuum correlation function, these correlators have support just at coincident points. It would be interesting to check if the anomaly coefficients can be related to the form of the finite-density correlators evaluated at separated points.

- It would be interesting to attempt a perturbative proof using Osborn's local renormalization group approach; this was initiated in [18]. The main missing ingredient to the proof is to control the positivity of some anomaly coefficients whose relativistic analog turn out to be proportional to the Zamolodchikov metric. Local renormalization group for Lifshitz theories was studied in [184].

- The relation between the anomaly and the dilaton effective action should be investigated; in the relativistic case, this leads to a proof of the a-theorem [4]. The study of non-relativistic dilaton was initiated in [185].

- The anomaly coefficients for anyons coupled to Newton-Cartan backgrounds should be computed. This may be interesting for condensed matter applications, as the quantum Hall effect.

- An analysis of the Wess-Zumino consistency conditions for trace anomalies in presence of gauge and Milne boost violations would clarify the nature of the anomalies and their possible relevance for the properties of the Renormalization Group flow. Due to the large number of terms involved, this seems a rather challenging task.

Supersymmetry

We considered a $\mathcal{N} = 2$ Galilean-invariant Wess-Zumino model in $2+1$ dimensions obtained as the null reduction of the relativistic parent in one higher dimension. Using the null reduction technique, we build a non-relativistic formulation of the superspace and we obtain a supergraph formalism with D-algebra rules which is very similar to the relativistic one. As a result, the non-renormalization theorem can be easily imported and then we find that no quantum corrections arise in the superpotential.

Furthermore, the properties of the model to conserve the particle number and to have a retarded propagator, coming from the non-relativistic invariance, allow to produce a set of selection rules which greatly constrain the quantume corrections of the model. This not only allows to find more simplifications than in the relativistic case, but we also find that the self-energy is one-loop exact.

This study can be considered as the starting point for many other developments:

- The result we have found is reminiscent of relativistic gauge theories with extended supersymmetry, like for instance the relativistic $\mathcal{N} = 2$ SYM in 3+1 dimensions [186]. In that case extended supersymmetry constrains the corrections to the Kähler potential to be related to the F-terms, which are protected by the non-renormalization theorem. In the non-relativistic model discussed in this paper, instead the protection of the Kähler potential is related to the $U(1)$ charge conservation at each vertex, which in many diagrammatic contributions constrains arrows to form a closed loop, so leading to a vanishing integral. It would be interesting to investigate if a common hidden mechanism exists, which is responsible of the similar mild UV behavior of these two rather different classes of theories.

- As a continuation of the study of non-relativistic conformal anomalies in curved Newton-Cartan background [15–17, 187, 83, 184, 18], it would be interesting to study superconformal anomalies of a Galilean supersymmetric theory in the presence of a classical Newton-Cartan supergravity source.

- A non-relativistic theory of a chiral superfield coupled to a Chern-Simons gauge field, which is invariant under the conformal extension of the $\mathscr{S}_2\mathscr{G}$ algebra, was constructed in [42]. We expect that further examples of $\mathscr{S}_2\mathscr{G}$ theories may be constructed by coupling the F-term interacting theory discussed in this paper to a Chern-Simons gauge field. These examples should contain trilinear derivative couplings between scalars and fermions and then should be different from existing constructions of non-relativistic SUSY Chern Simons theory built from the $c \to \infty$ non relativistic limit (see e.g. [188–192]). In analogy to the non-SUSY example studied in [193], we expect that for special values of the F-term coupling g the resulting theory is conformal. We leave this as a topic for further work. These extensions may provide a useful theoretical SUSY setting for studying non-abelian anyons [192, 194] and non-relativistic particle-vortex dualities [195].

- The opposite ultra-relativistic limit $c \to 0$ gives the Carroll group and can be found from a particular choice of the parameters in the Bargmann algebra [196]. It would be interesting to build supersymmetric extensions of the Carroll group starting from the supersymmetric extensions of the Bargamann algebra.

Complexity

We studied the holographic Complexity=Volume and Complexity=Action conjectures for black holes in asymptotically warped AdS_3 spacetime. The volume rate is a monotonically increasing function of time which goes to a constant for late times, while the action rate is always positive, but reaches a maximum and then decreases to a constant for late times. In the action case, we also observe that when the black hole is non-rotating, there exists a critical time under which the complexity rate vanishes. In both cases, the value reached for $t \to \infty$ is proportional to the product TS of temperature and entropy,

and vanishes in the extremal case. All these properties are qualitatively the same as for the BTZ black hole.

We also investigated the complexity conjectures in the warped case when the state on the boundary is mixed, in particular when only one of the two boundaries is taken as a subregion. In this case, we found that there is a richer structure of divergences than in the BTZ case, containing both a linear and a logarithmic divergence in the UV cutoff. In the volume case the behaviour of subregion complexity is superadditive; in the action case, the leading linear divergence depends from a length scale $\tilde{L}$ appearing in a counterterm needed to have reparametrization invariance of the action. While this behaviour is the same of the AdS case, the presence of an additional logarithmic divergence is responsible for the fact that the action is also superadditive, contrarily to the BTZ black hole, where the property depends from the counterterm scale. Furthermore, the coefficient of the logarithmic divergence is temperature-dependent and the behaviour is different between the volume and the action: this allows to discern between the two conjectures.

Finally, we studied the subregion complexity=action in the BTZ background for a generic segment on the boundary. We learnt from the analytic computation that the result for a single interval is very elegant: the result is a sum of a divergent term in the UV cutoff which is linear in the length of the region on the boundary, a term proportional to the entaglement entropy of the configuration, and a constant contribution which seems to be a topological term. The analysis of the case with two disjoint intervals reveals that the result still holds for the divergent part of complexity, but we have an additional finite term given by a function of the distance between the two intervals and their length. This tells us that the mutual complexity carries different information with respect to the mutual information, which is the analog quantity computed with the entanglement entropy instead of complexity.

There are some possible future developments that we can be intersted to study:

- Warped black holes can be realized also as solutions of Topological Massive Gravity and New Massive Gravity. It would be interesting to study both Action and Volume in these examples, in order to get control on both the conjectures in the case of higher derivatives terms in the gravity action. The Action conjecture for higher derivatives gravity was already studied by several authors in in [141, 142, 123, 143], but always in the late-time limit. In particular, ref. [123] studied the late-time limit of Action conjecture for warped black holes in Topological Massive Gravity; the asymptotic growth of the action is not proportional to TS.

- It would be interesting to study complexity from the field theory side. A proper definition of complexity in quantum field theory has several subtleties, including the choice of the reference state and the allowed set of elementary quantum gates. Recently, concrete calculations have been performed in the case of free field theories and an approach based on tensor networks in connection with the Liouville action was proposed in [131].

- In the CV conjecture, subregion complexity for multiple intervals in the BTZ background is independent of temperature and can be computed using topology from the Gauss-Bonnet

theorem, see [161]. It would be interesting to investigate if a similar relation with topology holds also for CA. The complicated structure of the finite terms in eqs. (7.91) suggests that such relation, if exists, is more intricated than in CV.

- One of the obscure aspects of the CA conjecture is the physical meaning of the scale $\tilde{L}$ appearing in the action counterterm eq. (5.93) on the null boundaries. A deeper understanding of the role of this parameter is desirable. In particular, its relation with the field theory side of the correspondence remains completely unclear.

Appendix A

Conventions

In this Appendix we collect SUSY conventions in $3+1$ and $2+1$ dimensions. For conventions in four dimensions we primarily refer to [197].

Spinors

In $3+1$ dimensional Minkowski space-time we take the metric $\eta^{MN} = \text{diag}(-1,1,1,1)$ and denote left-handed Weyl spinors as ψ_α, while right-handed ones as $\bar{\chi}^{\dot{\alpha}}$.

Spinorial indices are raised and lowered as

$$\psi^\alpha = \varepsilon^{\alpha\beta}\psi_\beta\,, \qquad \bar{\chi}_{\dot{\alpha}} = \varepsilon_{\dot{\alpha}\dot{\beta}}\bar{\chi}^{\dot{\beta}} \tag{A.1}$$

where the Levi-Civita symbol is chosen to be

$$\varepsilon^{\alpha\beta} = \varepsilon^{\dot{\alpha}\dot{\beta}} = -\varepsilon_{\alpha\beta} = -\varepsilon_{\dot{\alpha}\dot{\beta}} = \begin{pmatrix} 0 & 1 \\ -1 & 0 \end{pmatrix} \tag{A.2}$$

Contractions of spinorial quantities are given by

$$\chi\cdot\psi = \chi^\alpha\psi_\alpha = \psi\cdot\chi\,, \qquad \bar{\chi}\cdot\bar{\psi} = \bar{\chi}_{\dot{\alpha}}\bar{\psi}^{\dot{\alpha}} = \bar{\psi}\cdot\bar{\chi} \tag{A.3}$$

Complex conjugation changes the chirality of spinors. The prescription for the signs is

$$(\psi^\alpha)^\dagger = \bar{\psi}^{\dot{\alpha}}\,, \qquad (\psi_\alpha)^\dagger = \bar{\psi}_{\dot{\alpha}}\,, \qquad (\bar{\chi}^{\dot{\alpha}})^\dagger = \chi^\alpha\,, \qquad (\bar{\chi}_{\dot{\alpha}})^\dagger = \chi_\alpha \tag{A.4}$$

We use sigma matrices

$$\sigma^M = (\mathbf{1},\sigma^i)\,, \qquad \bar{\sigma}^M = (\mathbf{1},-\sigma^i) \tag{A.5}$$

where we have defined $(\bar{\sigma}^M)^{\dot{\alpha}\alpha} = \varepsilon^{\dot{\alpha}\dot{\beta}}\varepsilon^{\alpha\beta}(\sigma^M)_{\beta\dot{\beta}}$. They satisfy the following set of useful identities

$$\begin{aligned} &(\sigma^M)_{\alpha\dot{\alpha}}(\bar{\sigma}_M)^{\dot{\beta}\beta} = -2\delta_\alpha^{\ \beta}\delta_{\dot{\alpha}}^{\ \dot{\beta}}\,, \quad (\sigma^M)_{\alpha\dot{\alpha}}(\sigma_M)_{\beta\dot{\beta}} = -2\varepsilon_{\alpha\beta}\varepsilon_{\dot{\alpha}\dot{\beta}}\,, \quad \text{Tr}(\sigma^M\bar{\sigma}^N) = -2\eta^{MN}\,, \\ &\left(\sigma^M\bar{\sigma}^N + \sigma^N\bar{\sigma}^M\right)_\alpha^{\ \beta} = -2\eta^{MN}\delta_\alpha^{\ \beta}\,, \qquad \left(\bar{\sigma}^M\sigma^N + \bar{\sigma}^N\sigma^M\right)_{\dot{\alpha}}^{\ \dot{\beta}} = -2\eta^{MN}\delta_{\dot{\alpha}}^{\ \dot{\beta}} \end{aligned} \tag{A.6}$$

Spinorial derivatives

In order to manipulate expressions with spinorial objects it is useful to adopt a notation where spinorial indices are manifest. For the case of vectors and in particular for partial derivatives this is achieved by

defining

$$\partial_{\alpha\dot{\alpha}} = (\sigma^M)_{\alpha\dot{\alpha}}\partial_M\,, \qquad \partial^{\alpha\dot{\alpha}} = \varepsilon^{\alpha\beta}\varepsilon^{\dot{\alpha}\dot{\beta}}\partial_{\beta\dot{\beta}} = (\bar{\sigma}^M)^{\dot{\alpha}\alpha}\partial_M\,, \qquad \partial_M = -\frac{1}{2}(\bar{\sigma}_M)^{\dot{\alpha}\alpha}\partial_{\alpha\dot{\alpha}} \tag{A.7}$$

which in particular imply

$$\Box \equiv \partial^M\partial_M = -\frac{1}{2}\partial^{\alpha\dot{\alpha}}\partial_{\alpha\dot{\alpha}}\,, \qquad \partial^{\alpha\dot{\gamma}}\partial_{\dot{\gamma}\beta} = -\delta^\alpha_\beta\Box \tag{A.8}$$

We assign rules for the coordinates consistently with the requirement $\partial_M x^M = \partial_{\alpha\dot{\alpha}}x^{\alpha\dot{\alpha}} = 4$, that is

$$x^{\alpha\dot{\alpha}} = -\frac{1}{2}(\bar{\sigma}_M)^{\dot{\alpha}\alpha}x^M\,, \qquad x^M = (\sigma^M)_{\alpha\dot{\alpha}}x^{\alpha\dot{\alpha}} \tag{A.9}$$

It follows that $x^2 \equiv x^M x_M = -2x^{\alpha\dot{\alpha}}x_{\alpha\dot{\alpha}}$.

Finally, we define partial spinorial derivatives acting on Grassmann variables as

$$\partial_\alpha\theta^\beta = \delta_\alpha^{\ \beta}\,, \qquad \partial^\beta\theta_\alpha = -\delta_\alpha^{\ \beta}\,, \qquad \bar{\partial}_{\dot{\alpha}}\bar{\theta}^{\dot{\beta}} = \delta_{\dot{\alpha}}^{\ \dot{\beta}}\,, \qquad \bar{\partial}^{\dot{\beta}}\bar{\theta}_{\dot{\alpha}} = -\delta^{\dot{\alpha}}_{\ \dot{\beta}} \tag{A.10}$$

Imposing the reality of $\delta_M^N = [\partial_M, x^N]$ and $\delta_\alpha^{\ \beta} = \{\partial_\alpha, \theta^\beta\}$ we find that spacetime derivatives are anti-hermitian, $(\partial_M)^\dagger = -\partial_M$, while the spinorial ones are hermitian, $(\partial_\alpha)^\dagger = \bar{\partial}_{\dot{\alpha}}$.

Superspace

The SUSY generators can be written as

$$P_{\alpha\dot{\alpha}} = -i\partial_{\alpha\dot{\alpha}}\,, \qquad \mathcal{Q}_\alpha = i\left(\partial_\alpha + \frac{i}{2}\bar{\theta}^{\dot{\alpha}}\partial_{\alpha\dot{\alpha}}\right), \qquad \bar{\mathcal{Q}}_{\dot{\alpha}} = -i\left(\bar{\partial}_{\dot{\alpha}} + \frac{i}{2}\theta^\alpha\partial_{\alpha\dot{\alpha}}\right) \tag{A.11}$$

such that the algebra is $\{\mathcal{Q}_\alpha, \bar{\mathcal{Q}}_{\dot{\alpha}}\} = i\partial_{\alpha\dot{\alpha}} = -P_{\alpha\dot{\alpha}}$. The covariant differential operators which anticommute with the supercharges are

$$\mathcal{D}_\alpha = \partial_\alpha - \frac{i}{2}\bar{\theta}^{\dot{\alpha}}\partial_{\alpha\dot{\alpha}} = -i\mathcal{Q}_\alpha - i\bar{\theta}^{\dot{\alpha}}\partial_{\alpha\dot{\alpha}}\,, \qquad \bar{\mathcal{D}}_{\dot{\alpha}} = \bar{\partial}_{\dot{\alpha}} - \frac{i}{2}\theta^\alpha\partial_{\alpha\dot{\alpha}} = i\bar{\mathcal{Q}}_{\dot{\alpha}} - i\theta^\alpha\partial_{\alpha\dot{\alpha}} \tag{A.12}$$

and they satisfy

$$\{\mathcal{D}_\alpha, \bar{\mathcal{D}}_{\dot{\alpha}}\} = -i\partial_{\alpha\dot{\alpha}} = P_{\alpha\dot{\alpha}} \tag{A.13}$$

With these conventions, we obtain

$$\bar{\mathcal{Q}}_{\dot{\alpha}} = (\mathcal{Q}_\alpha)^\dagger\,, \qquad \bar{\mathcal{D}}_{\dot{\alpha}} = (\mathcal{D}_\alpha)^\dagger \tag{A.14}$$

We define

$$\mathcal{Q}^2 \equiv \frac{1}{2}\mathcal{Q}^\alpha\mathcal{Q}_\alpha\,, \qquad \bar{\mathcal{Q}}^2 \equiv \frac{1}{2}\bar{\mathcal{Q}}_{\dot{\alpha}}\bar{\mathcal{Q}}^{\dot{\alpha}}\,, \qquad \mathcal{D}^2 \equiv \frac{1}{2}\mathcal{D}^\alpha\mathcal{D}_\alpha\,, \qquad \bar{\mathcal{D}}^2 \equiv \frac{1}{2}\bar{\mathcal{D}}_{\dot{\alpha}}\bar{\mathcal{D}}^{\dot{\alpha}} \tag{A.15}$$

Chiral superfields

Chiral superfields satisfy $\bar{\mathcal{D}}_{\dot{\alpha}}\Sigma(x^M, \theta^\alpha, \bar{\theta}^{\dot{\alpha}}) = 0$, and can be written as

$$\Sigma(x_L, \theta, \bar{\theta}) = \phi(x_L) + \theta^\alpha\psi_\alpha(x_L) - \theta^2F(x_L)\,, \qquad x_L^{\alpha\dot{\alpha}} \equiv x^{\alpha\dot{\alpha}} - i\theta^\alpha\bar{\theta}^{\dot{\alpha}} \tag{A.16}$$

Similarly, anti-chiral superfields satisfy $\mathscr{D}_\alpha \bar{\Sigma}(x^M, \theta^\alpha, \bar{\theta}^{\dot{\alpha}}) = 0$, whose solution is

$$\bar{\Sigma}(x_R, \theta, \bar{\theta}) = \bar{\phi}(x_R) + \bar{\theta}_{\dot{\alpha}} \bar{\psi}^{\dot{\alpha}}(x_R) - \bar{\theta}^2 \bar{F}(x_R), \qquad x_R^{\alpha\dot{\alpha}} \equiv x^{\alpha\dot{\alpha}} + i\theta^\alpha \bar{\theta}^{\dot{\alpha}} \tag{A.17}$$

Using definitions $\theta^2 \equiv \frac{1}{2}\theta^\alpha \theta_\alpha$, $\bar{\theta}^2 \equiv \frac{1}{2}\bar{\theta}_{\dot{\alpha}}\bar{\theta}^{\dot{\alpha}}$, we find the following compact expression for the components of a chiral superfield

$$\phi = \Sigma|, \qquad \psi_\alpha = \mathscr{D}_\alpha \Sigma|, \qquad F = \mathscr{D}^2 \Sigma| \tag{A.18}$$

where $|$ means that we evaluate the expression at $\theta = \bar{\theta} = 0$. The anti-chiral components are simply given by the complex conjugated of these expressions.

Pauli matrices in light-cone coordinates

Pauli matrices matrices in light-cone coordinates are

$$\begin{aligned} \sigma^\pm &= \frac{1}{\sqrt{2}}(\sigma^3 \pm \sigma^0), & \bar{\sigma}^\pm &= \frac{1}{\sqrt{2}}(\bar{\sigma}^3 \pm \bar{\sigma}^0) \\ \sigma^- &= -\bar{\sigma}^+ = \sqrt{2}\begin{pmatrix} 0 & 0 \\ 0 & -1 \end{pmatrix}, & \sigma^+ &= -\bar{\sigma}^- = \sqrt{2}\begin{pmatrix} 1 & 0 \\ 0 & 0 \end{pmatrix} \end{aligned} \tag{A.19}$$

Therefore, for instance we write (from (A.7))

$$\begin{aligned} \partial_{\alpha\dot{\alpha}} &= (\sigma^+)_{\alpha\dot{\alpha}}\,\partial_+ + (\sigma^-)_{\alpha\dot{\alpha}}\,\partial_- + (\sigma^1)_{\alpha\dot{\alpha}}\,\partial_1 + (\sigma^2)_{\alpha\dot{\alpha}}\,\partial_2 \\ \partial^{\alpha\dot{\alpha}} &= (\bar{\sigma}^+)^{\dot{\alpha}\alpha}\,\partial_+ + (\bar{\sigma}^-)^{\dot{\alpha}\alpha}\,\partial_- + (\bar{\sigma}^1)^{\dot{\alpha}\alpha}\,\partial_1 + (\bar{\sigma}^2)^{\dot{\alpha}\alpha}\,\partial_2 \end{aligned} \tag{A.20}$$

with $\partial_\pm = \frac{1}{\sqrt{2}}(\partial_3 \pm \partial_0)$.

Conventions in 2+1 dimensions

Non-relativistic quantities in 2+1 dimensions are obtained from the null reduction of 3+1 dimensional Minkowski spacetime. The prescription is to introduce light-cone coordinates $x^M = (x^-, x^+, x^1, x^2) = (x^-, x^\mu)$, compactify along a small circle in the x^- direction and perform the identifications

$$\partial_- \to im, \qquad \partial_+ \to \partial_t, \qquad \phi(x^M) = e^{imx^-}\varphi(x^\mu) \tag{A.21}$$

where m is the adimensional eigenvalue of the $U(1)$ mass operator and $\phi(x^M)$ is a local field.

Non-relativistic fermions in 2+1 dimensions are parametrized by two complex Grassmann scalars $\xi(x^\mu)$ and $\chi(x^\mu)$. Under null reduction the identification with the 3+1 dimensional left-handed Weyl spinor $\psi(x^M)$ works as follows

$$\psi_\alpha(x^M) = e^{imx^-}\tilde{\psi}_\alpha(x^\mu) = e^{imx^-}\begin{pmatrix} \xi(x^\mu) \\ \chi(x^\mu) \end{pmatrix} \tag{A.22}$$

Under complex conjugation we choose the prescription

$$\bar{\psi}_{\dot{\alpha}} = (\psi_\alpha)^\dagger = e^{-imx^-}(\tilde{\psi}_\alpha)^\dagger \equiv e^{-imx^-}\begin{pmatrix} \bar{\xi}(x^\mu) \\ \bar{\chi}(x^\mu) \end{pmatrix} \tag{A.23}$$

Using identities (A.1) it is easy to infer the identification with the components of ψ^α and $\bar{\psi}^{\dot{\alpha}}$.

Taking the mass as a dimensionless parameter enforces the energy dimensions of the non-relativistic fermion to be

$$[\xi] = E^2\,, \qquad [\chi] = E \tag{A.24}$$

These assignments immediately follow when performing the null reduction of the Weyl Lagrangian

$$\mathscr{L} = i\psi^\dagger \bar{\sigma}^M \partial_M \psi \to \sqrt{2} m \bar{\xi}\xi + \sqrt{2} i \bar{\chi}\partial_t \chi - i\bar{\xi}(\partial_1 - i\partial_2)\chi - i\bar{\chi}(\partial_1 + i\partial_2)\xi \tag{A.25}$$

We observe that the only dynamical component is χ, while ξ turns out to be an auxiliary field that can be integrated out from the action.

Since null reduction affects only space-time coordinates without modifying the spinorial ones, we obtain $\mathscr{N} = 2$ supersymmetry in three dimensions. According to the ordinary pattern for which the three dimensional $\mathscr{N} = 2$ superspace is "equal" to the four-dimensional $\mathscr{N} = 1$ superspace, all the properties related to manipulations of covariant derivatives and supercharges, *e.g.* the D-algebra procedure, are directly inherited from the (3+1) relativistic theory under a suitable re-interpretation of the spinorial objects.

In particular, the algebra of covariant derivatives reads

$$\{D_\alpha, \bar{D}_\beta\} = -i\partial_{\alpha\beta}\,, \qquad \{D^\alpha, \bar{D}^\beta\} = -i\partial^{\beta\alpha} \tag{A.26}$$

where, as follows from (A.20), the three-dimensional derivatives are given by

$$\partial_{\alpha\beta} = \begin{pmatrix} \sqrt{2}\partial_t & \partial_1 - i\partial_2 \\ \partial_1 + i\partial_2 & -i\sqrt{2}M \end{pmatrix} \qquad \partial^{\alpha\beta} = \begin{pmatrix} -i\sqrt{2}M & -(\partial_1 - i\partial_2) \\ -(\partial_1 + i\partial_2) & \sqrt{2}\partial_t \end{pmatrix} \tag{A.27}$$

They satisfy the following identities

$$\partial^{\alpha\beta} = \varepsilon^{\alpha\delta}\varepsilon^{\beta\gamma}\partial_{\gamma\delta} \qquad \partial_{\beta\alpha} = \varepsilon_{\alpha\gamma}\varepsilon_{\beta\delta}\,\partial^{\gamma\delta} \tag{A.28}$$

Therefore, we have for instance $\bar{\xi}_\alpha \partial^{\alpha\beta}\chi_\beta = \bar{\xi}^\alpha \partial_{\beta\alpha}\chi^\beta$. Identities which turn out to be useful for the reduction of the action to components are

$$\begin{aligned} &[D^\alpha, \bar{D}^2] = i\partial^{\beta\alpha}\bar{D}_\beta\,, \qquad [\bar{D}^\alpha, D^2] = -i\partial^{\alpha\beta}D_\beta \\ &D^2\bar{D}^2 + \bar{D}^2 D^2 = (2iM\partial_t + \partial_i^2) + D^\alpha \bar{D}^2 D_\alpha = (2iM\partial_t + \partial_i^2) + \bar{D}_\alpha D^2 \bar{D}^\alpha \end{aligned} \tag{A.29}$$

Spin connection

The explicit expression for the spin connection is:

$$\begin{aligned} \omega_{MAB} \;=\; & \frac{1}{2}\left[e^N_{\ A}\left(\partial_M e_{NB} - \partial_N e_{MB}\right) - e^N_{\ B}\left(\partial_M e_{NA} - \partial_N e_{MA}\right)\right. \\ & \left. - e^N_{\ A} e^P_{\ B}\left(\partial_N e_{PC} - \partial_P e_{NC}\right) e^C_{\ M}\right]\,. \end{aligned} \tag{A.30}$$

We thus obtain the components:

$$
\begin{aligned}
\underset{(M)}{\omega_{-AB}} &= -\frac{1}{2}e^{\mu}{}_{A}e^{\nu}{}_{B}\tilde{F}_{\mu\nu}\,, \quad \underset{(A)}{\omega_{\mu-A}} = -\frac{1}{2}e^{\nu}{}_{A}\tilde{F}_{\mu\nu}\,, \\
\underset{(A)}{\omega_{\mu+a}} &= \frac{1}{2}v^{\nu}\left(\partial_{\mu}e^{a}{}_{\nu}-\partial_{\nu}e^{a}{}_{\mu}\right)-\frac{1}{2}e^{\nu}{}_{a}F_{\mu\nu}-\frac{1}{2}v^{\nu}e^{\rho}{}_{a}\left[A_{\mu}\tilde{F}_{\nu\rho}+n_{\mu}F_{\nu\rho}+e^{b}{}_{\mu}\left(\partial_{\nu}e^{b}{}_{\rho}-\partial_{\rho}e^{b}{}_{\nu}\right)\right], \\
\omega_{\mu ab} &= \frac{1}{2}e^{\nu}{}_{a}\left(\partial_{\mu}e^{b}{}_{\nu}-\partial_{\nu}e^{b}{}_{\mu}\right)-\frac{1}{2}e^{\nu}{}_{b}\left(\partial_{\mu}e^{a}{}_{\nu}-\partial_{\nu}e^{a}{}_{\mu}\right)+ \\
&\quad -\frac{1}{2}e^{\nu}{}_{a}e^{\rho}{}_{b}\left[A_{\mu}\tilde{F}_{\nu\rho}+n_{\mu}F_{\nu\rho}+e^{c}{}_{\mu}\left(\partial_{\nu}e^{c}{}_{\rho}-\partial_{\rho}e^{c}{}_{\nu}\right)\right]. \qquad \text{(A.31)}
\end{aligned}
$$

Note that $\underset{(M)}{\omega_{--B}} = 0$.

Appendix B

Explicit calculation of the heat kernel perturbative expansion

In this Appendix we show the explicit calculation of the perturbative expansion of the heat kernel applied to a non-relativistic differential operator as in eq. (3.56). The terminology of the insertion terms refers to the decomposition in eq. (3.63), which induces the splitting at first and second order as in eqs. (3.65),(3.70). For simplicity, we will omit the subscript E referred to the Euclidean version of the Schrödinger operator.

We start with the case where the insertion operators are time-independent and then we switch to the time-dependent case.

B.1 First order expansion of the heat kernel operator

We start with the simplest case, when we consider the single insertion of a multiplicative function $P(x)$. By definition

$$K_{1P}(\tau) = \int_0^\tau d\tau' \, \langle x,t|e^{(\tau-\tau')\triangle} P(x) e^{\tau'\triangle}|x',t'\rangle \,. \tag{B.1}$$

We insert a completeness relation in order to use the expression of the flat space heat kernel operator inside the previous integral

$$\begin{aligned} K_{1P}(\tau) &= \int_0^\tau d\tau' \int d^d\tilde{x} \int d\tilde{t} \, \langle x,t|e^{(\tau-\tau')\triangle}|\tilde{x},\tilde{t}\rangle P(\tilde{x}) \langle \tilde{x},\tilde{t}|e^{\tau'\triangle}|x',t'\rangle = \\ &= \frac{1}{(2\pi)^2} \int_0^\tau d\tau' \, \frac{1}{(4\pi(\tau-\tau'))^{d/2}} \frac{1}{(4\pi\tau')^{d/2}} \int d\tilde{t} \, \frac{m(\tau-\tau')}{m^2(\tau-\tau')^2 + \frac{(t-\tilde{t})^2}{4}} \frac{m\tau'}{m^2\tau'^2 + \frac{(\tilde{t}-t')^2}{4}} \times \\ &\times \int d^d\tilde{x} P(\tilde{x}) \exp\left[-\frac{(x-\tilde{x})^2}{4(\tau-\tau')} - \frac{(\tilde{x}-x')^2}{4\tau'} \right] . \end{aligned} \tag{B.2}$$

We Fourier-transform the $P(\tilde{x})$ function

$$P(\tilde{x}) = \frac{1}{(2\pi)^{d/2}} \int d^d k \, e^{ik\tilde{x}} P(k) \tag{B.3}$$

and we perform explicitly the time integration to get

$$K_{1P}(\tau) = \frac{1}{(2\pi)^2}\int_0^\tau d\tau' \frac{1}{(4\pi(\tau-\tau'))^{d/2}}\frac{1}{(4\pi\tau')^{d/2}}\frac{8\pi m\tau}{4m^2\tau^2+(t-t')^2}\times \\ \times\int d^d\tilde{x}\int\frac{d^dk}{(2\pi)^{d/2}}P(k)\exp\left[-\frac{(x-\tilde{x})^2}{4(\tau-\tau')}-\frac{(\tilde{x}-x')^2}{4\tau'}+ik\tilde{x}\right]. \tag{B.4}$$

The Gaussian integral in the spatial coordinates can be performed exactly to find

$$K_{1P}(\tau) = \frac{1}{(2\pi)^2}\int_0^\tau d\tau' \frac{1}{(4\pi\tau)^{d/2}}\frac{8\pi m\tau}{4m^2\tau^2+(t-t')^2}\times \\ \times\int\frac{d^dk}{2\pi^{d/2}}\exp\left[-\frac{(x-x')^2}{4\tau}+ik\cdot\left(x\frac{\tau}{\tau'}+x'\frac{\tau-\tau'}{\tau}\right)-k^2\frac{\tau'}{\tau}(\tau-\tau')\right]P(k). \tag{B.5}$$

Setting $x=x', t=t'$ means that we compute the trace of this insertion

$$\mathrm{Tr}K_{1P}(\tau) = \frac{1}{2\pi}\int_0^\tau d\tau'\frac{1}{(4\pi\tau)^{d/2}}\frac{1}{m\tau}\int\frac{d^dk}{2\pi^{d/2}}\exp\left[ik\cdot x-k^2\frac{\tau'}{\tau}(\tau-\tau')\right]P(k) = \\ = \frac{1}{2\pi}\frac{1}{(4\pi\tau)^{d/2}}\frac{1}{m\tau}\int_0^\tau d\tau'\exp\left[\frac{\tau'}{\tau}(\tau-\tau')\partial_x^2\right]P(x), \tag{B.6}$$

and a Taylor expansion of the exponential around $\tau=0$ gives

$$\mathrm{Tr}K_{1P}(\tau) = \frac{2}{m(4\pi\tau)^{d/2+1}}\left(\tau P(x)+\frac{1}{6}\tau^2\partial_x^2P(x)+\mathscr{O}(\tau^3)\right). \tag{B.7}$$

The single insertion of the operators $S(x), Q_i(x)$ can be reduced to derivatives acting on the previous expression. In particular we find

$$K_{1S}(\tau) = \int_0^\tau d\tau'\int d^d\tilde{x}\int d\tilde{t}\,\langle x,t|e^{(\tau-\tau')\triangle}|\tilde{x},\tilde{t}\rangle S(\tilde{x})\sqrt{-\partial_{\tilde{t}}^2}\langle\tilde{x},\tilde{t}|e^{\tau'\triangle}|x',t'\rangle = \\ = \sqrt{-\partial_{t'}^2}\left(\int_0^\tau d\tau'\int d^d\tilde{x}\int d\tilde{t}\,\langle x,t|e^{(\tau-\tau')\triangle}|\tilde{x},\tilde{t}\rangle S(\tilde{x})\langle\tilde{x},\tilde{t}|e^{\tau'\triangle}|x',t'\rangle\right) = \\ = \sqrt{-\partial_{t'}^2}\,K_{1P}(\tau)|_{P(x)=S(x)}. \tag{B.8}$$

In the last step, we recognized the expression for the multiplicative insertion $P(x)$, when calling in a different way the function $S(x)$ in the integrand. In order to perform the differentiation, it is helpful to use the Fourier transform (t,ω are the conjugate variables)

$$\mathscr{F}\left(\frac{1}{1+\frac{t^2}{A^2}}\right) = \sqrt{\frac{\pi}{2}}A\,e^{-A|\omega|} \tag{B.9}$$

to obtain

$$\sqrt{-\partial_t^2}\left(\frac{1}{1+\frac{t^2}{A^2}}\right) = \frac{A(A^2-t^2)}{(A^2+t^2)^2}. \tag{B.10}$$

Using this method and computing the trace, we similarly obtain

$$\mathrm{Tr}K_{1S}(\tau) = \frac{2}{m(4\pi\tau)^{d/2+1}}\,\mathrm{tr}\left(\frac{S}{2m}+\frac{\tau}{12m}\partial_i^2S+\frac{\tau^2}{120m}\partial_i^4S+\mathscr{O}(\tau^3)\right), \tag{B.11}$$

where the tr on the r.h.s. refers to internal indices of the operators, while on the l.h.s Tr refers also to the sum over the spacetime coordinates.

A similar trick can be applied to the operator $Q_i(x)$ with the spatial derivative, by observing that

$$\begin{aligned} K_{1Q_i}(\tau) &= \int_0^\tau d\tau' \int d^d\tilde{x} \int d\tilde{t}\, \langle x,t|e^{(\tau-\tau')\triangle}|\tilde{x},\tilde{t}\rangle Q_i(\tilde{x}) \partial_{\tilde{x}_i} \langle \tilde{x},\tilde{t}|e^{\tau'\triangle}|x',t'\rangle = \\ &= -\partial_{x'_i}\left(\int_0^\tau d\tau' \int d^d\tilde{x} \int d\tilde{t}\, \langle x,t|e^{(\tau-\tau')\triangle}|\tilde{x},\tilde{t}\rangle Q_i(\tilde{x}) \langle \tilde{x},\tilde{t}|e^{\tau'\triangle}|x',t'\rangle \right) = \\ &= -\partial_{x'_i} K_{1P}(\tau)|_{P(x)=Q_i(x)} \,. \end{aligned} \tag{B.12}$$

Similar computations give (no sum on the index i)

$$\mathrm{Tr}\, K_{1Q_i}(\tau) = \frac{2}{m(4\pi\tau)^{d/2+1}} \,\mathrm{tr}\left(-\frac{\tau}{2}\partial_i Q_i - \frac{\tau^2}{12}\partial_i\partial_k^2 Q_i + \mathscr{O}(\tau^3) \right) . \tag{B.13}$$

B.2 Second order expansion of the heat kernel operator

In this section we consider double insertions of the operators appearing in the heat kernel expansion in the terms $K_{2X_1X_2}(\tau)$, where

$$X_1 = \{P(x_1), S(x_1), Q_i(x_1)\} \,, \qquad X_2 = \left\{P(x_2), S(x_2), Q_j(x_2)\right\} \,, \tag{B.14}$$

whose explicit expression is

$$K_{2X_1X_2}(\tau) = \int_0^\tau d\tau_2 \int_0^{\tau_2} d\tau_1 \langle x',t'|e^{-(\tau-\tau_2)\triangle}|x_2,t_2\rangle \hat{X}_2 \langle x_2,t_2|e^{-(\tau_2-\tau_1)\triangle}|x_1,t_1\rangle \hat{X}_1 \langle x_1,t_1|e^{-\tau_1\triangle}|x,t\rangle \,, \tag{B.15}$$

where

$$\hat{X}_1 = \left\{ P(x_1), S(x_1)\sqrt{-\partial_{t_1}^2}, Q_i(x_1)\partial_{i,x_1} \right\} , \qquad \hat{X}_2 = \left\{ P(x_2), S(x_2)\sqrt{-\partial_{t_2}^2}, Q_j(x_2)\partial_{j,x_2} \right\} . \tag{B.16}$$

Notice that the order in which the operators appear as subscripts is opposite to the order in which they enter the integral expression.

The strategy to follow is technically more difficult, but theoretically analog to the first order case:

- We insert some completeness identities in order to make the coordinate-basis representation of the flat heat kernel appearing explicitly
- We Fourier-transform the inserted operators
- We perform the integration along the inserted spacetime coordinates
- We finally take the trace and we Taylor-expand the result in τ

Following this method, we can always put the insertions in the form

$$K_{2X_1X_2}(\tau) = \int_0^\tau d\tau_2 \int_0^{\tau_2} d\tau_1 \frac{1}{(4\pi(\tau-\tau_2))^{d/2}} \frac{1}{(4\pi(\tau_2-\tau_1))^{d/2}} \frac{1}{(4\pi\tau_1)^{d/2}} \Xi^{X_1X_2} \Psi^{X_1X_2} \,, \tag{B.17}$$

where $\Xi^{X_1X_2}$ and $\Psi^{X_1X_2}$ correspond to the space and time part of the integrals, respectively. Following the previous prescription, it is useful to Fourier-transform

$$\Xi^{X_1X_2} = \int \frac{d^dk_1}{(2\pi)^{d/2}} \frac{d^dk_2}{(2\pi)^{d/2}} \tilde{\Xi}^{X_1X_2} \,, \tag{B.18}$$

and to introduce the quantity

$$\Upsilon = \exp\left(ik_1x_1 + ik_2x_2 - \frac{(x'-x_2)^2}{4(\tau-\tau_2)} - \frac{(x_2-x_1)^2}{4(\tau_2-\tau_1)} - \frac{(x_1-x)^2}{4\tau_1} \right). \tag{B.19}$$

Since the spatial and temporal integrals factorize, we can treat them separately. In particular we obtain the following Fourier transforms of the spatial part

$$\begin{aligned}
\tilde{\Xi}^{PP} &= \int dx_1 \int dx_2 \Upsilon P(k_1)P(k_2)\,, \\
\tilde{\Xi}^{Q_iP} &= -\partial_{x,i}\left[\int dx_1 \int dx_2 \Upsilon Q_i(k_1)P(k_2) \right], \\
\tilde{\Xi}^{Pa_j} &= \int dx_1 \int dx_2 \left[-\frac{(x_2-x_1)_j}{2(\tau_2-\tau_1)} \right] \Upsilon P(k_1)Q_j(k_2)\,, \\
\tilde{\Xi}^{Q_iQ_j} &= -\partial_{x,i}\left[\int dx_1 \int dx_2 \left[-\frac{(x_2-x_1)_j}{2(\tau_2-\tau_1)} \right] \Upsilon Q_i(k_1)Q_j(k_2) \right],
\end{aligned} \tag{B.20}$$

where $P(k)$ and $Q_i(k)$ are the Fourier transform of $P(x)$ and $Q_i(x)$. The temporal part, on the other hand, is given by

$$\begin{aligned}
\Psi^{PP} &= \frac{1}{(2\pi)^3} \int dt_1 \int dt_2 \frac{m(\tau-\tau_2)}{m^2(\tau-\tau_2)^2 + \frac{(t_2-t')^2}{4}} \frac{m(\tau_2-\tau_1)}{m^2(\tau_2-\tau_1)^2 + \frac{(t_2-t_1)^2}{4}} \frac{m\tau_1}{m^2\tau_1^2 + \frac{(t_1-t)^2}{4}}\,, \\
\Psi^{SP} &= \frac{1}{4\pi^3} \int dt_1 \int dt_2 \frac{m(\tau-\tau_2)}{m^2(\tau-\tau_2)^2 + \frac{(t_2-t')^2}{4}} \frac{m(\tau_2-\tau_1)}{m^2(\tau_2-\tau_1)^2 + \frac{(t_2-t_1)^2}{4}} \frac{4m^2\tau_1^2 - (t_1-t)^2}{(4m^2\tau_1^2 + (t_1-t)^2)^2}\,, \\
\Psi^{PS} &= \frac{1}{4\pi^3} \int dt_1 \int dt_2 \frac{m(\tau-\tau_2)}{m^2(\tau-\tau_2)^2 + \frac{(t_2-t')^2}{4}} \frac{4m^2(\tau_2-\tau_1)^2 - (t_2-t_1)^2}{(4m^2(\tau_2-\tau_1)^2 + (t_2-t_1)^2)^2} \frac{ms_1}{m^2\tau_1^2 + \frac{(t_1-t)^2}{4}}\,, \\
\Psi^{SS} &= \frac{1}{2\pi^3} \int dt_1 \int dt_2 \frac{m(\tau-\tau_2)}{m^2(\tau-\tau_2)^2 + \frac{(t_2-t')^2}{4}} \frac{4m^2(\tau_2-\tau_1)^2 - (t_2-t_1)^2}{(4m^2(\tau_2-\tau_1)^2 + (t_2-t_1)^2)^2} \frac{4m^2\tau_1^2 - (t_1-t)^2}{(4m^2\tau_1^2 + (t_1-t)^2)^2}\,.
\end{aligned} \tag{B.21}$$

While it seems that this list is not exaustive, one should observe that the insertion of the operator $S(x)$ must be considered at the same level of a $P(x)$ insertion when considering the spatial integration, while the insertion of $Q_i(x)$ must be treated as a $P(x)$ insertion for the time part. These rules follow from the fact that $S(x)$ operators carry time derivatives which do not affect the spatial part, while $Q_i(x)$ carry spatial derivatives which do not influence the time part.

The basic building blocks for the previous computations are found to give

$$\begin{aligned}
\tilde{\Xi}^{PP} &= (4\pi)^d \left(\frac{\tau_1(\tau-\tau_2)(\tau_2-\tau_1)}{s} \right)^{d/2} \\
&\quad \exp\left(\frac{ik_1\tau_1x'}{\tau} + \frac{ik_2\tau_2x'}{\tau} - \frac{ik_1\tau_1x}{\tau} - \frac{ik_2\tau_2x}{\tau} + \frac{k_1^2\tau_1^2}{\tau} + \frac{k_2^2\tau_2^2}{\tau} - k_1^2\tau_1 - 2k_1k_2\tau_1 - k_2^2\tau_2 \right. \\
&\quad \left. + \frac{2k_1k_2\tau_1\tau_2}{\tau} + ik_1x + ik_2x - \frac{x^2}{4\tau} + \frac{xx'}{2\tau} - \frac{(x')^2}{4\tau} \right) P(k_1)P(k_2)\,,
\end{aligned} \tag{B.22}$$

$$\begin{aligned}\tilde{\Xi}^{PQ_j} &= \exp\left(\frac{ik_1\tau_1x'}{\tau}+\frac{ik_2\tau_2x'}{\tau}-\frac{ik_1\tau_1x}{\tau}-\frac{ik_2\tau_2x}{\tau}+\frac{k_1^2\tau_1^2}{\tau}+\frac{k_2^2\tau_2^2}{\tau}-k_1^2\tau_1-2k_1k_2\tau_1-k_2^2\tau_2\right.\\ &\left.+\frac{2k_1k_2\tau_1\tau_2}{\tau}+ik_1x+ik_2x+\frac{xx'}{2\tau}-\frac{(x')^2}{4\tau}-\frac{x^2}{4\tau}\right)(4\pi)^d\left(\frac{\tau_1(\tau_1-\tau_2)(\tau_2-\tau)}{\tau}\right)^{d/2}\\ &\frac{\left(ik_1\tau_1+ik_2\tau_2-ik_2\tau+\frac{x-x'}{2}\right)_i}{\tau}P(k_1)Q_j(k_2)\,,\end{aligned} \tag{B.23}$$

while the expressions for $\tilde{\Xi}^{Q_iP}$ and $\tilde{\Xi}^{Q_iQ_j}$ can be obtained differentiating $\tilde{\Xi}^{PP}$ and $\tilde{\Xi}^{PQ_j}$ with respect to x_i.

On the other hand, we obtain for the time integration

$$\begin{aligned}\Psi^{PP} &= \frac{1}{\pi}\frac{2m\tau}{4m^2\tau^2+(t-t')^2}\,, \qquad \Psi^{SS}=\frac{1}{\pi}\frac{4m\tau\left(4m^2\tau^2-3(t-t')^2\right)}{\left(4m^2\tau^2+(t-t')^2\right)^3}\,,\\ \Psi^{PS} &= \Psi^{SP}=\frac{1}{\pi}\frac{\left(4m^2\tau^2-(t-t')^2\right)}{\left(4m^2\tau^2+(t-t')^2\right)^2}\,.\end{aligned} \tag{B.24}$$

Combining all the expressions, putting $x=x',t=t'$ and Taylor-expanding around $\tau=0$ we obtain (tr is the trace over the internal indices, there is no sum over the index i of the operator Q_i)

$$\mathrm{Tr}\,K_{2PP}=\frac{2}{m(4\pi\tau)^{d/2+1}}\mathrm{tr}\left(\frac{\tau^2}{2}P(x)^2+\mathscr{O}(\tau^3)\right)\,, \tag{B.25}$$

$$\begin{aligned}\mathrm{Tr}\,K_{2SS}=&\frac{2}{m(4\pi\tau)^{d/2+1}}\mathrm{tr}\left(\frac{S^2}{4m^2}+\frac{\tau}{12m^2}S\partial^2S+\frac{\tau}{24m^2}\partial_kS\partial_kS+\frac{\tau^2}{120m^2}S\partial^4S+\right.\\ &\left.+\frac{\tau^2}{144m^2}\partial^2S\partial^2S+\frac{\tau^2}{60m^2}\partial_i\partial^2S\partial_iS+\frac{\tau^2}{180m^2}\partial_{ij}S\partial_{ij}S+\mathscr{O}(\tau^3)\right)\,,\end{aligned} \tag{B.26}$$

$$\mathrm{Tr}\,K_{2PS}=\tilde{K}_{2SP}=\frac{1}{m(4\pi\tau)^{d/2+1}}\mathrm{tr}\left(\frac{\tau}{2m}SP+\frac{\tau^2}{12m}S\partial^2P+\frac{\tau^2}{12m}\partial^2SP+\frac{\tau^2}{12m}\partial_iS\partial_iP+\mathscr{O}(\tau^3)\right)\,, \tag{B.27}$$

$$\begin{aligned}\mathrm{Tr}\,K_{2Q_jQ_i}=&\frac{2}{m(4\pi\tau)^{d/2+1}}\mathrm{tr}\left[-\frac{\tau}{4}Q_iQ_i-\frac{\tau^2}{24}(\partial_jQ_i)(\partial_ia_j)\right.\\ &\left.+\frac{\tau^2}{8}(\partial_iQ_i)(\partial_ja_j)-\frac{\tau^2}{12}Q_i(\partial^2Q_i)-\frac{\tau^2}{24}(\partial_ia_j)^2+\mathscr{O}(\tau^3)\right]\,,\end{aligned} \tag{B.28}$$

$$\mathrm{Tr}\,K_{2Q_iP}=\frac{2}{m(4\pi\tau)^{d/2+1}}\mathrm{tr}\left(-\frac{\tau^2}{3}P(\partial_iQ_i)-\frac{\tau^2}{6}(\partial_iP)Q_i+\mathscr{O}(\tau^3)\right)\,, \tag{B.29}$$

$$\mathrm{Tr}\,K_{2PQ_i}=\frac{2}{m(4\pi\tau)^{d/2+1}}\mathrm{tr}\left(\frac{\tau^2}{6}Q_i(\partial_iP)-\frac{\tau^2}{6}(\partial_iQ_i)P+\mathscr{O}(\tau^3)\right)\,, \tag{B.30}$$

$$\begin{aligned}\mathrm{Tr}\,K_{2Q_iS}=&\frac{2}{m(4\pi\tau)^{d/2+1}}\mathrm{tr}\left[-\frac{\tau}{24m^2}\left(S\partial_k^2S+\frac{1}{2}(\partial_kS)^2\right)+\right.\\ &\left.-\frac{\tau^2}{80m^2}\left(\frac{1}{2}S\partial_k^2\partial_j^2S+\frac{7}{12}(\partial_k^2S)^2+\frac{13}{12}\partial_kS(\partial_k\partial_j^2S)+\frac{1}{3}(\partial_k\partial_jS)^2\right)+\mathscr{O}(\tau^3)\right]\,,\end{aligned} \tag{B.31}$$

$$\begin{aligned}\mathrm{Tr}\,K_{2SQ_i} = &\frac{2}{m(4\pi\tau)^{d/2+1}}\mathrm{tr}\left[\frac{\tau}{48m^2}\left((\partial_k S)^2 - S\partial_k^2 S\right) + \right.\\ &\left. + \frac{\tau^2}{80m^2}\left(-\frac{1}{3}S\partial_k^2\partial_j^2 S - \frac{1}{4}(\partial_k^2 S)^2 + \frac{1}{4}\partial_k S(\partial_k\partial_j^2 S) + \frac{1}{3}(\partial_k\partial_j S)^2\right) + \mathscr{O}(\tau^3)\right].\end{aligned} \tag{B.32}$$

B.3 Time-dependent insertion contributions to the heat kernel (first order)

We generalize to the time-dependent case the insertion operators appearing in the heat kernel expansion needed to compute the trace anomaly for the NC background (3.106).

We start with the single insertion of a multiplicative operator $P(x,t)$. Since we have an additional time dependence, the Fourier transform is

$$P(x,t) = \int \frac{d^d k}{(2\pi)^{d/2}} \int \frac{d\omega}{\sqrt{2\pi}} P(k,\omega) e^{i(kx-\omega t)} \tag{B.33}$$

and it is required to compute

$$\begin{aligned}K_{1P}(\tau) = &\int_0^\tau d\tau' \int d^d\tilde{x} \int d\tilde{t}\, \langle xt|e^{(\tau-\tau')\triangle}|\tilde{x}\tilde{t}\rangle P(\tilde{x},\tilde{t}) \langle \tilde{x}\tilde{t}|e^{\tau'\triangle}|x't'\rangle = \\ = &\int_0^\tau d\tau' \frac{1}{(2\pi)^2} \frac{1}{(4\pi(\tau-\tau'))^{d/2}} \frac{1}{(4\pi\tau')^{d/2}} \int \frac{d\omega}{\sqrt{2\pi}} \int d\tilde{t} e^{-i\omega\tilde{t}} \frac{m(\tau-\tau')}{m^2(\tau-\tau')^2 + \frac{(t-\tilde{t})^2}{4}} \\ &\frac{m\tau'}{m^2\tau'^2 + \frac{(\tilde{t}-t')^2}{4}} \int \frac{d^d k}{(2\pi)^{d/2}} e^{ik\tilde{x}} \exp\left(-\frac{(x-\tilde{x})^2}{4(\tau-\tau')} - \frac{(\tilde{x}-x')^2}{4\tau'}\right) P(k,\omega)\,.\end{aligned} \tag{B.34}$$

We observe that, despite the additional time dependence, the time and spatial parts of the integral still decouple and factorize. We can then use the same intermediate step in eq. (B.5)

$$\begin{aligned}&\int d^d\tilde{x} \int \frac{d^d k}{(2\pi)^{d/2}} e^{ik\tilde{x}} \exp\left(-\frac{(x-\tilde{x})^2}{4(\tau-\tau')} - \frac{(\tilde{x}-x')^2}{4s'}\right) = \\ &= \int \frac{d^d k}{2\pi^{d/2}} \exp\left(-\frac{(x-x')^2}{4\tau} + ik\cdot\left(x\frac{\tau'}{\tau} + x'\frac{\tau-\tau'}{\tau}\right) - k^2\frac{\tau'}{\tau}(\tau-\tau')\right),\end{aligned} \tag{B.35}$$

which in the case $x = x'$ gives

$$\int \frac{d^d k}{2\pi^{d/2}} \exp\left(ik\cdot x - k^2\frac{\tau'}{\tau}(\tau-\tau')\right). \tag{B.36}$$

The time integral $I(\omega)$ is better evauated after studying the analytic structure in the complex plane of the integrand

$$\begin{aligned}I(\omega) = &\int d\tilde{t} e^{-i\omega\tilde{t}} \frac{m(\tau-\tau')}{m^2(\tau-\tau')^2 + \frac{(t-\tilde{t})^2}{4}} \frac{m\tau'}{m^2\tau'^2 + \frac{(\tilde{t}-t')^2}{4}} = \\ = &4\alpha\beta e^{-i\omega t'} \int d\tilde{t} \frac{e^{-i\omega\tilde{t}}}{(\tilde{t}+i\beta)(\tilde{t}-i\beta)(\tilde{t}-\Delta t+i\alpha)(\tilde{t}-\Delta t-i\alpha)},\end{aligned} \tag{B.37}$$

where we sent $\tilde{t} \to \tilde{t} + t'$ and we defined

$$\alpha = 2m(\tau - \tau'), \qquad \beta = 2m\tau', \qquad \Delta t = t - t'. \tag{B.38}$$

The quantities α, β are positive by construction. We use the residue theorem to find

$$\begin{aligned} I(\omega) = {} & 4\alpha\beta e^{-i\omega t'}\theta(\omega)\left[\frac{\pi e^{-\beta\omega}}{\beta((\Delta t + i\beta)^2 + \alpha^2)} + \frac{\pi e^{-\alpha\omega - i\Delta t\omega}}{\alpha((\Delta t - i\alpha)^2 + \beta^2)}\right] + \\ & + 4\alpha\beta e^{-i\omega t'}\theta(-\omega)\left[\frac{\pi e^{\beta\omega}}{\beta((\Delta t - i\beta)^2 + \alpha^2)} + \frac{\pi e^{\alpha\omega - i\Delta t\omega}}{\alpha((\Delta t + i\alpha)^2 + \beta^2)}\right]. \end{aligned} \tag{B.39}$$

It can be found that the expression for $\omega = 0$ gives the time-independent results found in Appendix B.1 when using the prescription $\theta(0) = 1/2$ for the Heaviside distribution:

$$I(0) = \frac{8\pi ms}{4m^2\tau^2 + (t - t')^2} = \int d\tilde{t} \frac{m(\tau - \tau')}{m^2(\tau - \tau')^2 + \frac{(t-\tilde{t})^2}{4}} \frac{m\tau'}{m^2\tau'^2 + \frac{(\tilde{t}-t')^2}{4}}. \tag{B.40}$$

The trace of the insertion is found putting $t = t'$ to obtain

$$I(\omega, t = t') = \frac{2\pi}{m\tau}\frac{1}{\tau - 2\tau'}\left[e^{-2m\tau'|\omega|}(\tau - \tau') - \tau' e^{-2m(\tau - \tau')|\omega|}\right] = \frac{2\pi}{m\tau} + \mathscr{O}(\tau). \tag{B.41}$$

Using eqs. (B.36) and (B.41) inside eq. (B.34) and expanding in the auxiliary time τ we finally obtain the result

$$\mathrm{Tr}\, K_{1P}(\tau) = \frac{2}{m(4\pi\tau)^{d/2+1}}\mathrm{tr}\left(\tau P(x,t) + \frac{1}{6}\tau^2\partial_i^2 P(x,t) + \mathscr{O}(\tau^3)\right). \tag{B.42}$$

This is the same result of the case without time-dependence because the first order of the expansion of exponential terms vanishes.

Next we consider the single insertion of an operator with a spatial derivative acting on the fields. It turns out that the same trick of the time-independent case works, *i.e.*

$$K_{1Q_i}(s) = -\frac{\partial}{\partial x_i'}\left[\int_0^{s'} ds' \int d^d\tilde{x} \int d\tilde{t}\, \langle xt|e^{(s-s')\triangle}|\tilde{x}\tilde{t}\rangle Q_i(\tilde{x},\tilde{t})\langle\tilde{x}\tilde{t}|e^{s'\triangle}|x't'\rangle\right]. \tag{B.43}$$

Since the expression in parenthesis does not change if we add a time dependence to the operators of the heat kernel expansion, and since spatial and temporal parts of the integral factorize, we obtain an equivalent formula also for

$$\mathrm{Tr}\, K_{1Q_i}(\tau) = \frac{2}{m(4\pi\tau)^{d/2+1}}\mathrm{tr}\left(-\frac{\tau}{2}\partial_i Q_i(x,t) - \frac{\tau^2}{12}\partial_i\partial^2 Q_i(x,t) + \mathscr{O}(\tau^3)\right). \tag{B.44}$$

Single insertions of operators with a time derivative applied to the dynamical fields $S(x,t)$ can be modified by time dependence, but since they vanish on the background (3.106) we will not consider them.

B.4 Time-dependent insertion contributions to the heat kernel (second order)

We start with the double insertion of multiplicative operators of kind $P(x,t)$

$$\begin{aligned} K_{2P}(\tau) = &\int_0^\tau d\tau_2 \int_0^{\tau_2} d\tau_1 \int d^d x_1 \int d^d x_2 \int dt_1 \int dt_2 \, \langle xt|e^{(\tau-\tau_2)\triangle}|x_2 t_2\rangle \\ &P(x_2,t_2)\langle x_2 t_2|e^{(\tau_2-\tau_1)\triangle}|x_1 t_1\rangle P(x_1,t_1)\langle x_1 t_1|e^{\tau_1\triangle}|x' t'\rangle = \\ = &\int_0^\tau d\tau_2 \int_0^{\tau_2} d\tau_1 \frac{1}{(2\pi)^3} \frac{1}{(4\pi(\tau-\tau_2))^{d/2}} \frac{1}{(4\pi(\tau_2-\tau_1))^{d/2}} \frac{1}{(4\pi\tau_1)^{d/2}} \int d^d x_1 \int d^d x_2 \\ &\int \frac{d^d k_1}{(2\pi)^{d/2}} \int \frac{d^d k_2}{(2\pi)^{d/2}} \int \frac{d\omega_1}{\sqrt{2\pi}} \int \frac{d\omega_2}{\sqrt{2\pi}} \Upsilon \Psi^{PP} e^{-i\omega_1 t_1 - i\omega_2 t_2} P(k_2,\omega_2) P(k_1,\omega_1)\,, \end{aligned} \tag{B.45}$$

where Υ was given in eq. (B.19), while the Ψ^{PP} term in eq. (B.21). The time and spatial parts factorize again; the latter was evaluated in eq. (B.22) and at coincident points it is given by

$$\begin{aligned} &\int d^d x_1 \int d^d x_2 \, \Upsilon = (4\pi)^d \left(\frac{\tau_1(\tau-\tau_2)(\tau_2-\tau_1)}{\tau}\right)^{d/2} \times \\ &\times \exp\left(ik_1 x_1 + ik_2 x_2 + k_1^2\left(\frac{\tau_1^2}{\tau} - \tau_1\right) + k_2^2\left(\frac{\tau_2^2}{\tau} - \tau_2\right) + 2k_1 k_2\left(\frac{\tau_1\tau_2}{\tau} - \tau_1\right)\right) \quad . \end{aligned} \tag{B.46}$$

The temporal part Ψ^{PP} can be integrated along the t_1 coordinate using the same technique of the single insertion case. Using the definitions

$$\alpha = 2m(\tau_2-\tau_1)\,, \qquad \beta = 2m\tau_1\,, \qquad \Delta t = t_2 - t'\,, \tag{B.47}$$

we obtain

$$\begin{aligned} I(\omega_1) = &\int dt_1 e^{-i\omega_1 t_1} \frac{m(\tau_2-\tau_1)}{m^2(\tau_2-\tau_1)^2 + \frac{(t-\tilde{t})^2}{4}} \frac{m\tau_1}{m^2\tau_1^2 + \frac{(t-\tilde{t})^2}{4}} = \\ &= 4\alpha\beta e^{-i\omega t'}\theta(\omega_1)\left[\frac{\pi e^{-\beta\omega_1}}{\beta((\Delta t+i\beta)^2+\alpha^2)} + \frac{\pi e^{-\alpha\omega - i\Delta t\omega}}{\alpha((\Delta t - i\alpha)^2+\beta^2)}\right] + \\ &+ 4\alpha\beta e^{-i\omega t'}\theta(-\omega_1)\left[\frac{\pi e^{\beta\omega}}{\beta((\Delta t-i\beta)^2+\alpha^2)} + \frac{\pi e^{\alpha\omega - i\Delta t\omega}}{\alpha((\Delta t+i\alpha)^2+\beta^2)}\right]. \end{aligned} \tag{B.48}$$

The last step in the time integration consists in evaluating

$$\Psi(t,t',\omega_1,\omega_2) = \int dt_2 e^{-i\omega_2 t_2} \frac{m(\tau-\tau_2)}{m^2(\tau-\tau_2)^2 + \frac{(t-t_2)^2}{4}} I(\omega_1)\,. \tag{B.49}$$

The formal result is very cumbersome, but it can be checked that, using the prescription $\theta(0) = 1/2$, it gives exactly the time-independent result in the limit of vanishing frequencies:

$$\Psi(t=t',\omega_1=\omega_2=0) = \frac{16\pi^2\theta^2(0)}{ms} = \frac{4\pi^2}{ms}\,. \tag{B.50}$$

Moreover, in order to compute the insertions of time-dependent operators we only need the lowest orders of the expansion around $\tau = 0$ of the solution at coincident points, which is

$$\Psi(t = t', \omega_1, \omega_2) = \frac{4\pi^2}{ms} e^{-i(\omega_1+\omega_2)t} + \mathscr{O}(s) . \tag{B.51}$$

The zeroth order in the variable τ vanishes.

Combining eqs. (B.46) and (B.51) into (B.45) we find the same result of the time-independent case

$$\mathrm{Tr}\, K_{2PP} = \frac{2}{m(4\pi\tau)^{d/2+1}} \mathrm{tr} \left(\frac{\tau^2}{2} P(x,t)^2 + \mathscr{O}(\tau^3) \right) . \tag{B.52}$$

Additional new terms can contribute only to higher orders in τ, but they do not modify the a_4 coefficient.

Since time and space integrals factorize and there are no contributions to lower-order terms in the heat kernel expansion, we can similarly find that $\mathrm{Tr}\, K_{2X}$ have the same expressions of the time-independent case, if we choose among the set

$$X = \{P(x,t), Q_i(x,t)\} . \tag{B.53}$$

Additional terms could appear in insertions concerning the operator $S(x,t)$. They will not be considered here because $S(x,t)$ vanishes in the background (3.106).

Appendix C

Non-relativistic Wess-Zumino model in components

In this Appendix we show an alternative way to study quantum corrections to the Galilean Wess-Zumino model using component field formalism, which is more used in the literature concerning non-relativistic physics.

In Section 4.3 we applied null reduction to derive the action in terms of superfields, and after decomposing them into the components of the supermultiplet, we found the action in terms of fundamental fields. The same expression can be found with a slightly different procedure:

- Take the relativistic WZ model (4.19) in superfield formalism
- Express the action in terms of the relativistic component fields
- Perform the null reduction on the component fields.

The fact that this procedure gives the same result of Section 4.3 confirms that the prescription we gave to apply null reduction at the level of superfields works well. Moreover, it is possible to apply the DLCQ prescription after integrating out the auxiliary fields appearing after the reduction of the WZ action in components, and we find again the same result.

We start the analysis of quantum corrections considering the action in components (4.46). Scalars and fermions share the same kinetic operator and then the tree-level propagators are

$$\begin{aligned}\langle\varphi_1(\omega,\vec{p})\bar{\varphi}_1(-\omega,-\vec{p})\rangle &= \langle\chi_1(\omega,\vec{p})\bar{\chi}_1(-\omega,-\vec{p})\rangle = \frac{i}{2m\omega-\vec{p}^2+i\varepsilon}\\ \langle\varphi_2(\omega,\vec{p})\bar{\varphi}_2(-\omega,-\vec{p})\rangle &= \langle\chi_2(\omega,\vec{p})\bar{\chi}_2(-\omega,-\vec{p})\rangle = \frac{i}{4m\omega-\vec{p}^2+i\varepsilon}\end{aligned} \tag{C.1}$$

Figure C.1: Propagators for the dynamical non-relativistic fields. The bosons are denoted by dashed lines, while the fermions with continuous lines. The number of arrows denote the particle number.

Interaction vertices can be read directly from the lagrangian and are shown in fig. C.2 and C.3, where we use dashed and continous lines to denote scalars and fermions, respectively. The cubic vertices contain derivative interactions and then depend explicitly from the spatial momentum along the lines, while quartic vertices do not depend from the momentum.

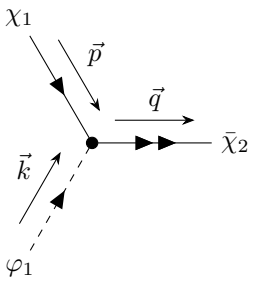

(a) $-\sqrt{2}ig\,[(q_1 - iq_2) - 2(p_1 - ip_2)]$

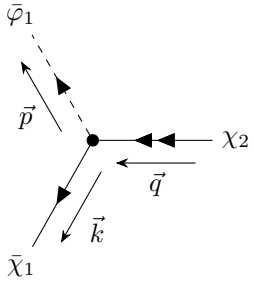

(b) $\sqrt{2}ig^*\,[(q_1 + iq_2) - 2(k_1 + ik_2)]$

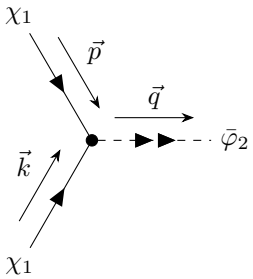

(c) $-2ig\,[(k_1 - ik_2) - (p_1 - ip_2)]$

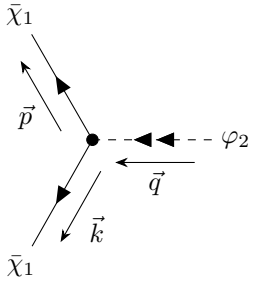

(d) $2ig^*\,[(k_1 + ik_2) - (p_1 + ip_2)]$

Figure C.2: Feynman rules for three-point vertices. Scalars are denoted by dashed lines, while fermions by continuous lines.

In order to classify the admitted diagrams, we can take into account that the reduction in components does not affect the propagators as functions of ω and $\vec{p}$. Therefore, the arguments that led to formulate the fundamental selection rule 4.4.1 are still true. Moreover, the conservation of particle number at each vertex still provides the driving rule to select the admissible topologies and arrows configurations.

In order to properly define physical quantities and Green functions, we introduce renormalized fields and couplings defined as

$$\begin{cases} \varphi_a = Z_a^{-1/2}\,\varphi_a^{(B)} = \left(1 - \frac{1}{2}\delta_{\varphi_a}\right)\varphi_a^{(B)} & a = 1,2 \\ \chi_a = Z_a^{-1/2}\,\chi_a^{(B)} = \left(1 - \frac{1}{2}\delta_{\chi_a}\right)\chi_a^{(B)} & \\ m = Z_m^{-1} m^{(B)} = (1 - \delta_m) m^{(B)} & \\ g = \mu^{-\varepsilon} Z_g^{-1} g^{(B)} = \mu^{-\varepsilon}(1 - \delta_g) g^{(B)} & \end{cases} \tag{C.2}$$

Spatial integrals are computed in dimension $d = 2 - \varepsilon$ and we have introduced the mass scale μ to keep the coupling constant dimensionless.

One-loop corrections to the self-energies

By applying selection rule 4.4.1 and particle number conservation we find that there are no admissible one-loop self-energy diagrams for particles in sector 1, while there is a non-vanishing contribution both for the scalar and the fermion in sector 2 corresponding to the diagrams in fig. C.4. Direct inspection leads to the integral

$$i\mathscr{M}_{\mathrm{b}}^{(2)} = i\mathscr{M}_{\mathrm{f}}^{(2)} = \frac{2|g|^2}{(2\pi)^3} \int d\omega\, d^2k\, \frac{(\vec{p} - 2\vec{k})^2}{\left[2m\omega - \vec{k}^2 + i\varepsilon\right]\left[2m(\Omega - \omega) - (\vec{p} - \vec{k})^2 + i\varepsilon\right]} \tag{C.3}$$

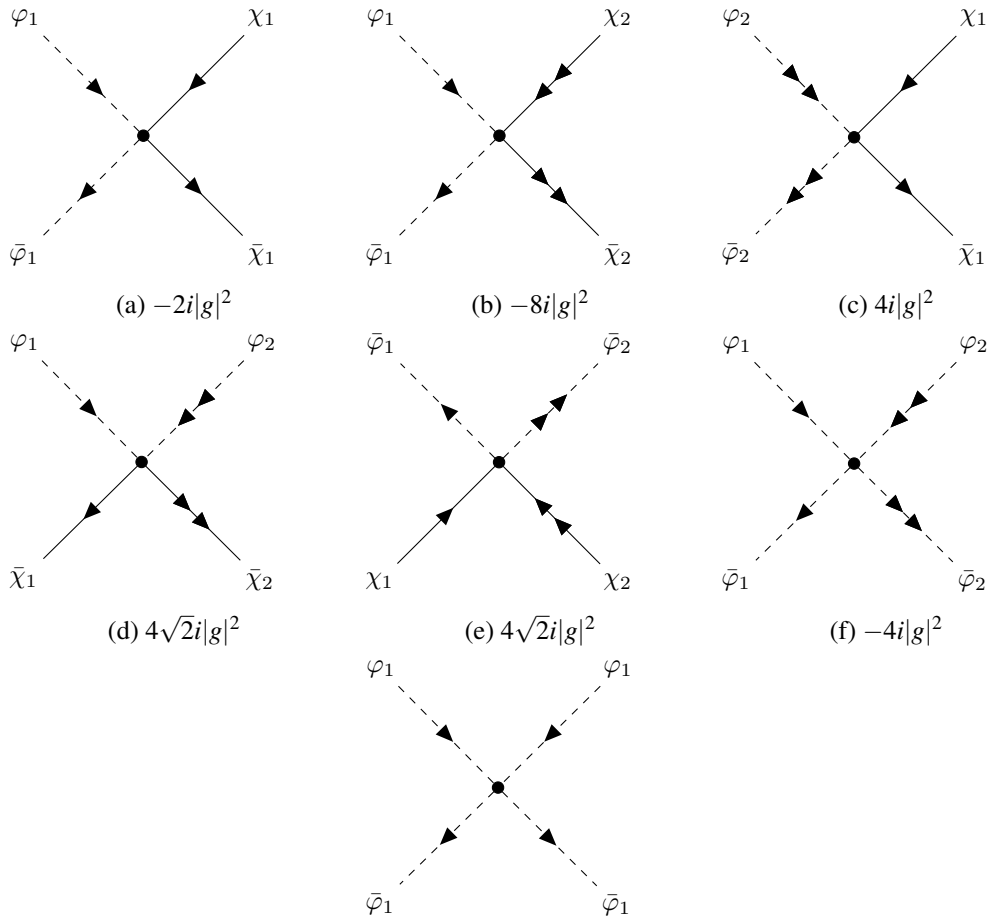

(a) $-2i|g|^2$ (b) $-8i|g|^2$ (c) $4i|g|^2$

(d) $4\sqrt{2}i|g|^2$ (e) $4\sqrt{2}i|g|^2$ (f) $-4i|g|^2$

(g) $-4i|g|^2$

Figure C.3: Feynman rules for four-point vertices. Scalars are denoted by dashed lines, while fermions by continuous lines.

Even if SUSY is not manifest in the component field formalism, we see that it shows via the equality of the quantum corrections of the fermionic and bosonic fields.

We solve the integration along the energy using the residue theorem

$$\mathscr{M}^{(2)} = -\frac{|g|^2}{m}\int \frac{d^2k}{(2\pi)^2}\,\frac{(\vec{p}-2\vec{k})^2}{2m\Omega-\vec{k}^2-(\vec{p}-\vec{k})^2+i\varepsilon}\,. \tag{C.4}$$

The remaining integral is UV divergent and can be computed with standard techniques of dimensional regularization. In generic dimensions d there exists a region in complex plane where the integral is convergent and we can translate the integration variable as

$$\vec{l}=\vec{k}-\frac{\vec{p}}{2}\,, \qquad d\vec{l}=d\vec{k}\,, \tag{C.5}$$

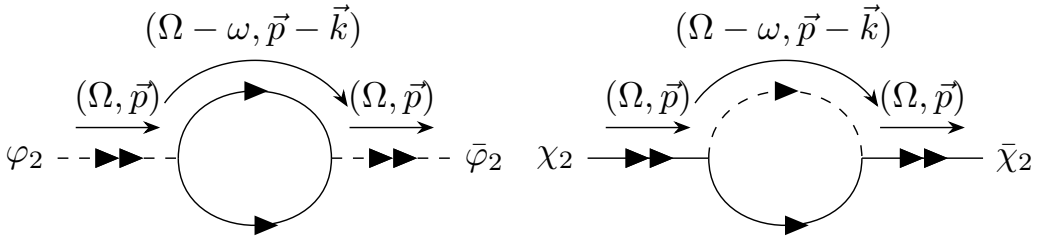

(a) $i\mathscr{M}_{\rm b}^{(2)}(\varphi_2,\bar{\varphi}_2)$ (b) $i\mathscr{M}_{\rm f}^{(2)}(\chi_2,\bar{\chi}_2)$

Figure C.4: 1-loop correction to the scalar (a) and fermionic (b) self-energies in sector 2.

giving

$$\mathscr{M}^{(2)}=\frac{2|g|^2\mu^{2(2-d)}}{(2\pi)^d}\int d^dl\,\frac{4l^2}{2m\Omega-2l^2-\frac{\vec{p}^2}{2}}=-\frac{4|g|^2\mu^{2(2-d)}}{(2\pi)^d}\frac{2\pi^{d/2}}{\Gamma(d/2)}\int_0^\infty dl\,\frac{l^{d+1}}{l^2-m\Omega+\frac{\vec{p}^2}{4}}\,. \tag{C.6}$$

After evaluating the remaining integral along the radial direction we find

$$\mathscr{M}^{(2)}=\frac{|g|^2}{m}\,d\,\frac{\mu^{2(2-d)}}{(4\pi)^{d/2}}\,\Gamma\left(-\frac{d}{2}\right)\left(\frac{\vec{p}^2}{4}-m\Omega\right)^{\frac{d}{2}}=\frac{|g|^2}{2\pi m}\left(2m\Omega-\frac{\vec{p}^2}{2}\right)\frac{1}{\varepsilon}+\text{finite} \tag{C.7}$$

In the minimal subtraction scheme the $1/\varepsilon$ pole is cancelled by setting in (C.2)

$$\delta_{\varphi_2}^{(1\text{loop})}=\delta_{\chi_2}^{(1\text{loop})}=-\frac{|g|^2}{4\pi m}\frac{1}{\varepsilon}\,,\qquad \delta_m^{(1\text{loop})}=0 \tag{C.8}$$

whereas $\delta_{\varphi_1}^{(1\text{loop})}=\delta_{\chi_1}^{(1\text{loop})}=0$. This result is consistent with the one-loop renormalization (4.72) that we have found in superspace.

One-loop corrections to three-point vertices

The action in components contains two kinds of three-point vertices (plus their complex conjugates). The vertex $\mathbf{V}_3(\chi_1,\chi_1,\bar{\varphi}_2)$ and its complex conjugate are not corrected at one loop because we cannot build any diagram consistent with particle number conservation. It then follows immediately that

$$\left(\delta_g+\delta_{\chi_1}+\frac{1}{2}\delta_{\varphi_2}^*\right)\Big|_{(1\text{loop})}=0 \tag{C.9}$$

Combining this relation with eq. (C.8), we find

$$\delta_g^{(1\text{loop})}=\frac{|g|^2}{8\pi m}\frac{1}{\varepsilon} \tag{C.10}$$

On the other hand, the vertex $\mathbf{V}_3(\varphi_1,\chi_1,\bar{\chi}_2)$ has in principle a one-loop contribution shown in fig. C.5.

After the integration by residues of the ω variable, this diagram gives

$$\mathscr{M}^{(3)}(\varphi_1,\chi_1,\bar{\chi}_2)=-\frac{|g|^2}{m}\frac{\sqrt{2}g}{(2\pi)^2}\int d^2l\,\frac{(p_1+k_1)-i(p_2+k_2)-2(l_1-il_2)}{2m(\omega_p+\omega_k)-\vec{l}^2-(\vec{p}+\vec{k}-\vec{l})^2+i\varepsilon} \tag{C.11}$$

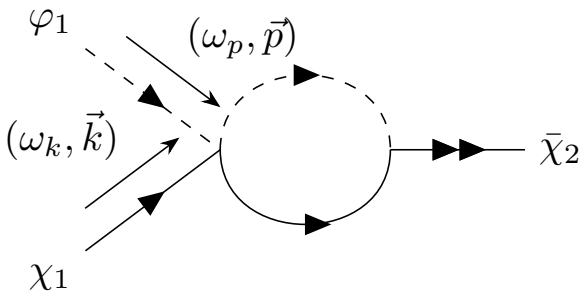

Figure C.5: 1-loop correction to the 3-point vertex.

We perform dimensional regularization along the spatial directions. Since the integrand contains in the numerator an expression which explicitly depends from the spatial momenta $\vec{l} = (l_1, l_2)$, we should give a prescription to define in a covariant way the numerator. For example we can assume that it comes from the contraction $\vec{v} \cdot \vec{l}$ and that the first vector in d dimensions is $\vec{v} = (1, -i)$, andis promoted in d dimensions to a vector whose only the first two entries are non-vanishing. In this way we obtain

$$\mathscr{M}^{(3)}(\varphi_1, \chi_1, \bar{\chi}_2) = -\frac{|g|^2}{m} \frac{\sqrt{2} g \mu^{3(2-d)}}{(2\pi)^d} \int d^d l \, \frac{\vec{v} \cdot (\vec{p} + \vec{k} - 2\vec{l})}{2m(\omega_p + \omega_k) - \vec{l}^2 - (\vec{p} + \vec{k} - \vec{l})^2 + i\varepsilon} \tag{C.12}$$

With the change of variables $\vec{q} = \vec{l} - \frac{\vec{p}+\vec{k}}{2}$ we find

$$\mathscr{M}^{(3)}(\varphi_1, \chi_1, \bar{\chi}_2) = -\frac{|g|^2}{m} \frac{\sqrt{2} g \mu^{3(2-d)}}{(2\pi)^d} \int d^d q \, \frac{\vec{v} \cdot \vec{q}}{q^2 - m(\omega_p + \omega_k) + \frac{(\vec{p}+\vec{k})^2}{4} + i\varepsilon} \tag{C.13}$$

This integral vanishes because the range is even and the integrand is odd. This implies that the following relation holds:

$$\left(\delta_g + \frac{1}{2}\delta_{\varphi_1} + \frac{1}{2}\delta_{\chi_1} + \frac{1}{2}\delta_{\chi_2} \right) \Big|_{(1\text{loop})} = 0 \tag{C.14}$$

This condition is automatically satisfied by results in eqs. (C.8) and (C.10).

We note that the one-loop result $\delta_g = -\frac{1}{2}\delta_{\chi_2}$ is the component version of the superspace non-renormalization theorem. As for the self-energy, we find that quantum corrections do not break SUSY.

One-loop corrections to four-point vertices

In principle, the one-loop evaluation of self-energies and three-point vertices allows to solve for all the unknowns in lagrangian (4.46). Moreover, we have verified that the corrections are all consistent between themselves and with the superspace results. However, we will provide further evidence of SUSY invariance at the level of component field formulation by considering the 1PI diagrams giving quantum corrections to the four-point vertices. This will also show how the non-renormalization theorem works at the level of fundamental fields.

Compared to the previous cases, we have far more possibilities to build four-point diagrams with the vertices at our disposal (see figs. C.2, C.3). All the topologies of diagrams consistent with particle number conservation at each vertex are reported in fig. C.6.

For example, we consider the first of such diagrams, *i.e.* the one-loop correction to the vertex $\mathbf{V}_4(\varphi_1, \varphi_1, \bar{\varphi}_1, \bar{\varphi}_1)$. This is the only graph among the many containing as external lines only fields from sector 1. We report the precise assignments of momenta and energy in fig. C.7.

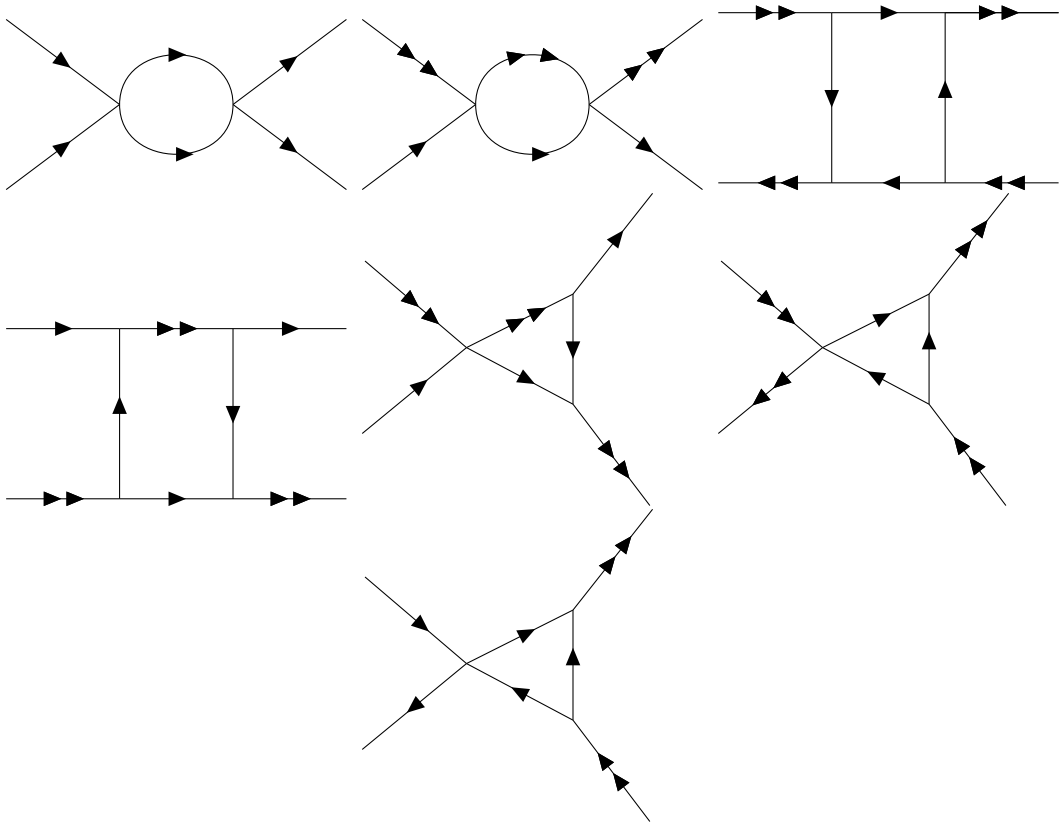

Figure C.6: Possible topologies of one-loop corrections to four-point vertices for the dynamical fields. In the picture we do not distinguish between bosonic and fermionic lines.

The t and u-channel diagrams vanish because we have circulating arrows in the internal loop. After integration in ω with the residue theorem, the integral corresponding to the s-channel diagram is

$$\mathscr{M}^{(4)}(\varphi_1,\varphi_1,\bar{\varphi}_1,\bar{\varphi}_1) = -\frac{4|g|^4}{m}\int \frac{d^2l}{(2\pi)^2}\,\frac{1}{2m(\omega_p+\omega_k)-\vec{l}^2-(\vec{p}+\vec{k}-\vec{l})^2+i\varepsilon} \tag{C.15}$$

Performing the change of variables $\vec{q} = \vec{l} - \frac{\vec{p}+\vec{k}}{2}$, in dimensional regularization we can write

$$\mathscr{M}^{(4)}(\varphi_1,\varphi_1,\bar{\varphi}_1,\bar{\varphi}_1) = \frac{4|g|^4}{m}\frac{\mu^{4(2-d)}}{(4\pi)^{d/2}}\frac{1}{\Gamma(d/2)}\int_0^\infty dq\,\frac{q^{d-1}}{q^2-m(\omega_p+\omega_k)+\frac{(\vec{p}+\vec{k})^2}{4}+i\varepsilon} \tag{C.16}$$

After performing the last integration and expanding in $\varepsilon = 2-d$ we obtain

$$\mathscr{M}^{(4)}(\varphi_1,\varphi_1,\bar{\varphi}_1,\bar{\varphi}_1) = \frac{|g|^4}{\pi m}\frac{1}{\varepsilon} + \text{finite} \tag{C.17}$$

The renormalization condition in minimal subtraction scheme requires

$$\mathscr{M}^{(4)}(\varphi_1,\varphi_1,\bar{\varphi}_1\bar{\varphi}_1) - 4|g|^2(2\delta_g + 2\delta_{\varphi_1}) = 0\,, \tag{C.18}$$

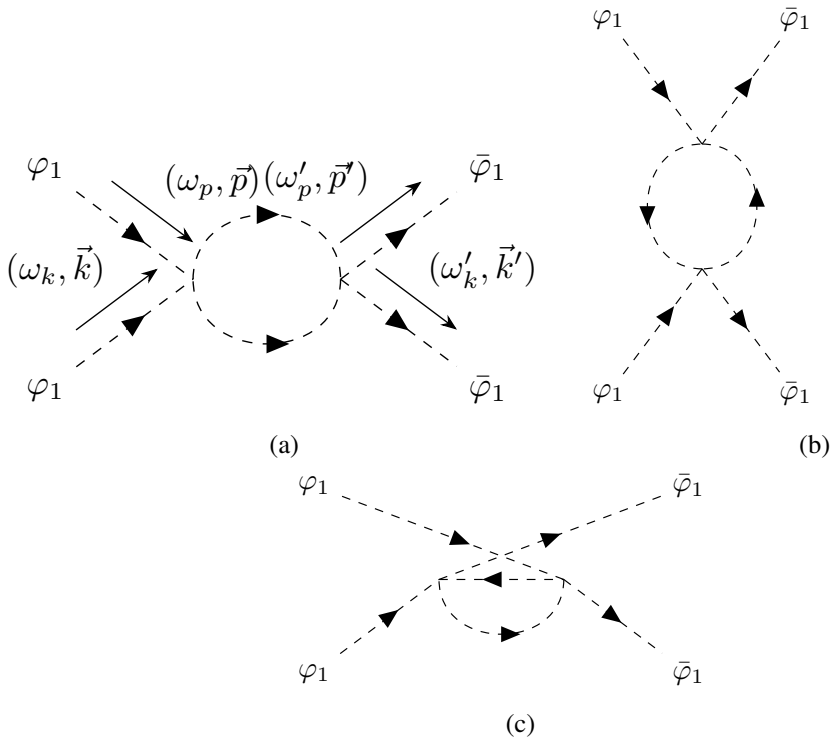

Figure C.7: 1-loop 1PI corrections to the 4-point vertex with external scalars from sector 1, coming from channels s, t and u respectively.

which means

$$\delta_g^{(1\text{loop})} = \frac{|g|^2}{8\pi m}\frac{1}{\varepsilon}. \tag{C.19}$$

This is consistent with (C.10) and confirms that SUSY is preserved by quantum corrections. Since the quantum corrections of the coupling constant g are completely determined by the wave-function renormalization, this is also a manifest way to see that the non-renormalization theorem works.

Two-loop corrections to the self-energy

We observe that in component field formalism the number of Feynman diagrams to study at every loop order is much greater than using the superfield approach. This makes the check of SUSY invariance and the study of quantum corrections more involved when the number of loops increase. However, the selection rules 4.4.1 and 4.4.2 help in decreasing the number of diagrams to consider in the non-relativistic case. In particular the 2-loop order for the self-energy is easily treatable and then we will consider it as an example of higher loop corrections in component field formalism.

It is in fact possible to find only one *a priori* non-vanishing diagram modifying the self-energy of the fermions in sector 2. This is depicted in Fig. C.8 and by consistency we expect to find that this contribution vanishes, because we do not find a diagram contributing to the bosonic superpartner. We now prove that this is indeed the case.

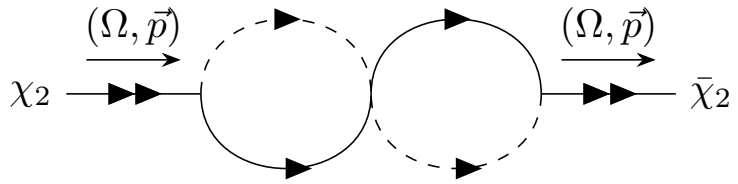

Figure C.8: Two-loop correction to the self-energy for the dynamical fermion in sector 2.

Writing down the corresponding integral and first performing the ω_k, ω_l integrations by using the residue technique we find

$$\mathscr{M}_{\mathrm{f}}^{(4)}(\chi_2,\bar{\chi}_2) = -\frac{|g|^4}{m^2}\int \frac{d^2k\,d^2l}{(2\pi)^4}\,\frac{\vec{p}^{\,2}+4\vec{l}\cdot\vec{k}+2(\vec{l}+\vec{k})\cdot\vec{p}}{\left[2m\Omega-\vec{k}^2-(\vec{p}-\vec{k})^2+i\varepsilon\right]\left[2m\Omega-\vec{l}^2-(\vec{p}-\vec{l})^2+i\varepsilon\right]} \tag{C.20}$$

Performing the change of variables

$$\vec{k} = \vec{K}+\frac{\vec{p}}{2}, \qquad \vec{l} = \vec{L}+\frac{\vec{p}}{2} \tag{C.21}$$

and continuing the integral to $d = 2-\varepsilon$ dimensions we find

$$\mathscr{M}_{\mathrm{f}}^{(4)}(\chi_2,\bar{\chi}_2) = -\frac{|g|^4}{m^2}\frac{\mu^{4(2-d)}}{(2\pi)^{2d}}\int d^dK\,d^dL\,\frac{4\vec{K}\cdot\vec{L}}{\left[2m\Omega-2K^2-\frac{\vec{p}^2}{4}+i\varepsilon\right]\left[2m\Omega-2L^2-\frac{\vec{p}^2}{2}+i\varepsilon\right]} \tag{C.22}$$

The two integrals vanish for symmetry reasons.

Appendix D

Additional details on the complexity computations

In this appendix we collect various additional technical details useful to the computations of the complexity conjectures.

D.1 An explicit model for WAdS black holes

We start with the explicit model whose entropy satisfies the area law and admitting the metric eq. (5.17) as a solution [145], which we introduced in Section 5.1.3. We will give a compendium of the dictionary required to match the notation used in the main text with the conventions of [145], and in this way we will find an alternative procedure to determine the conserved charges of the black hole.

In fact, in ref. [145] the conserved charges associated to the asymptotic isometries of the black hole have been computed starting from the following form of the metric in the coordinates $(\tilde{t},\tilde{r},\tilde{\theta})$:

$$ds^2 = p d\tilde{t}^2 + \frac{d\tilde{r}^2}{h^2 - pq} + 2h d\tilde{t} d\tilde{\theta} + q d\tilde{\theta}^2 , \tag{D.1}$$

with functions given by

$$p(\tilde{r}) = 8G\mu , \qquad q(\tilde{r}) = -\frac{4G\mathscr{J}}{\alpha} + 2\tilde{r} - 2\frac{\gamma^2}{L^2}\tilde{r}^2 , \qquad h(\tilde{r}) = -2\alpha\tilde{r} , \tag{D.2}$$

and $U(1)$ gauge field

$$A = A_{\tilde{t}} d\tilde{t} + A_{\tilde{\theta}} d\tilde{\theta} , \qquad A_{\tilde{t}}(\tilde{r}) = \frac{\alpha^2 L^2 - 1}{\gamma\alpha L} + \zeta , \qquad A_{\tilde{\theta}}(\tilde{r}) = -\frac{4G}{\alpha}Q + \frac{2\gamma}{L}\tilde{r} , \tag{D.3}$$

where

$$\gamma = \sqrt{\frac{1-\alpha^2 L^2}{8G\mu}} , \tag{D.4}$$

and ζ is a gauge constant.

We can put the metric (5.17) in the form (D.1) by means of the coordinate change

$$\tilde{t} = \sqrt{\frac{l^3}{\omega}} t , \qquad \tilde{r} = r - \frac{\sqrt{r_+ r_- (\nu^2+3)}}{2\nu} , \qquad \tilde{\theta} = \frac{\sqrt{\omega l^3}}{2}\theta , \tag{D.5}$$

where

$$\omega = \frac{\nu^2+3}{2\nu l}\left(\nu(r_+ + r_-) - \sqrt{r_+ r_-(\nu^2+3)}\right). \tag{D.6}$$

The previous set of transformations is such that the gauge field in the coordinates (t,r,θ) can be written as $A = adt + (b+cr)d\theta$, motivating the ansatz (5.40).

The quantities $\mu, \mathscr{J}, Q$ appearing in the previous solution are respectively identified with the mass, angular momentum and charge of the black hole. The equations of motion and the change of coordinates do not uniquely fix the charge Q, while we identify

$$\mu = \frac{\nu^2+3}{16Gl^2}\left(r_+ + r_- - \frac{\sqrt{r_+ r_-(\nu^2+3)}}{\nu}\right), \tag{D.7}$$

$$\mathscr{J} = \frac{2\nu(r_+ + r_-)\sqrt{r_+ r_-(\nu^2+3)} - (5\nu^2+3)r_+ r_-}{8Gl\left(\nu(r_+ + r_-) - \sqrt{r_+ r_-(\nu^2+3)}\right)}. \tag{D.8}$$

As it is pointed out in [145], the set $\{\mu, \mathscr{J}, Q\}$ satisfies the first law of thermodynamics in the form

$$d\mu = TdS + \Omega d\mathscr{J} + \Phi_{\text{tot}} dQ, \tag{D.9}$$

where the total electric potential is shown to be $\Phi_{\text{tot}} = 0$, thus eliminating the contribution from the charge of the black hole.

This special form of the first law of thermodynamics is a consequence of the choice of the Killing vectors associated to mass and angular momentum in [145], since all the contributions coming from the charge are eliminated.

A direct match with the mass M and angular momentum J coming from the thermodynamic analysis in (t,r,θ) coordinates gives:

$$\mu = \frac{M}{l^2}, \qquad \mathscr{J} = -\frac{4J}{\omega l^2}. \tag{D.10}$$

In order to get the conserved charges associated to isometries in (t,r,θ) coordinates, we need to adjust the normalization conditions:

- The angular range $0 \le \theta \le 2\pi$ corresponds to $0 \le \tilde{\theta} \le 2\pi\frac{\sqrt{\omega l^3}}{2}$, so extensive quantities, such as mass, entropy and angular momentum in (t,r,θ) coordinates get an extra $\frac{\sqrt{\omega l^3}}{2}$ factor if we want to preserve the length of the integration along $[0,2\pi]$.

- Killing vectors are transformed as:

$$\frac{\partial}{\partial t} = \sqrt{\frac{l^3}{\omega}}\frac{\partial}{\partial \tilde{t}}, \qquad \frac{\partial}{\partial \theta} = \frac{\sqrt{\omega l^3}}{2}\frac{\partial}{\partial \tilde{\theta}}. \tag{D.11}$$

- In [145] it is defined $\Omega = -h(r_+)/q(r_+)$, while in eq. (5.26),(5.27) we followed the conventions of [100], where an additional factor of l is put in the denominator both for the angular velocity and the Hawking temperature. Choosing the last normalization amounts to modify $\mu \to \mu/l$, with the other conserved charges of the black hole unchanged.

Taking into account all these corrections, we get that the mass in (t,r,θ) coordinates with the Killing $\frac{\partial}{\partial t}$ is $M/2$ and the angular momentum associated to the Killing $-\frac{\partial}{\partial \theta}$ is J. The $1/2$ factor in the normalization of the mass is reminiscent of Komar's anomalous factor and it is also pointed out for similar computations in [134].

D.2 Another way to compute the asymptotic growth of action for WAdS black holes

The asymptotic growth of the action of the WDW patch computed in section 5.3 can be derived in a different way following the procedure introduced in [57]. This is also a cross-check of our calculation.

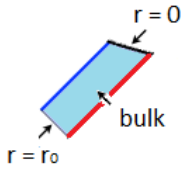

Figure D.1: Asymptotic contributions for the non-rotating case. In this picture we called the horizon radius r_0.

Non-rotating case: Following the argument in [57], the only relevant region of the WDW patch at late times is included between the horizon and the future singularity, as shown in fig. D.1. The time derivative of the gravitational action evaluated in this region contains three contributions:

- The time derivative of the bulk contribution is given by eq. (5.111).
- The time derivative of the GHY term nearby the singularity is given by eq. (5.113).
- The contribution from the joint at $r = r_m$ is replaced by the GHY term nearby the horizon:

$$\Delta I^{r_h}_{\text{GHY}} = \frac{(v^2+3)l}{16G}\Delta t_b \left[2r - r_h\right]_{r=r_h}, \tag{D.12}$$

  which in the asymptotic limit gives the same contribution as the null joint.

In this way, summing these terms, we find the same result of eq. (5.121).

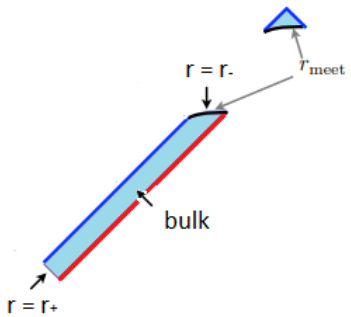

Figure D.2: Asymptotic contributions for the rotating case.

Rotating case: The region is depicted in figure D.2: in this case we need only the part of the WDW patch included between the inner and outer horizons. We consider the various contributions comparing with the computation in section 5.3:

- The bulk contribution is still given by eq. (5.127).
- The two null joints contributions are replaced by the GHY term evaluated on two constant-r surfaces, one at $r \approx r_-$ and one at $r \approx r_+$. The induced metric on these constant-r surfaces is:

$$h_{ij} = l^2 \begin{pmatrix} 1 & \nu r - \frac{1}{2}\sqrt{(3+\nu^2) r_+ r_-} \\ \nu r - \frac{1}{2}\sqrt{(3+\nu^2) r_+ r_-} & \frac{r}{4}\Psi(r) \end{pmatrix}, \tag{D.13}$$

$$\sqrt{h} = \frac{l^2}{2}\sqrt{(\nu^2+3)(r_+ - r)(r - r_-)}\,. \tag{D.14}$$

The normal vector to these slices is

$$n^\mu = \left(0, -\frac{1}{l}\sqrt{(\nu^2+3)(r_+ - r)(r-r_-)}, 0\right), \qquad n^\alpha n_\alpha = -1\,, \tag{D.15}$$

and the extrinsic curvature is

$$K = \frac{\sqrt{\nu^2+3}}{2l}\frac{2r - r_+ - r_-}{\sqrt{(r_+ - r)(r-r_-)}}\,. \tag{D.16}$$

The GHY term nearby the inner horizon gives:

$$\frac{dI^{r_-}_{\text{GHY}}}{dt_b} = -\frac{l}{4}\sqrt{\nu^2+3}\,[2r - r_+ - r_-]_{r=r_-}\,, \tag{D.17}$$

while the term from the outer horizon

$$\frac{dI^{r_+}_{\text{GHY}}}{dt_b} = \frac{l}{4}\sqrt{\nu^2+3}\,[2r - r_+ - r_-]_{r=r_+}\,. \tag{D.18}$$

These two contributions give the same result as the asymptotic contributions from the joints.

In this way, we find again a match with the late time result of eq. (5.133).

D.3 Divergence structure of the subregion complexity for WAdS black holes (non-rotating case)

In this appendix we consider in detail the non-rotating case for the subregion complexity of asymptotically WAdS_3 black holes considered in section 6.2 with $r_+ = r_h$ and $r_- = 0$, and we check that the divergences of complexity reproduce the appropriate limit from the rotating case.

D.3.1 Total action

We recover the expression of the bulk action from eq. (5.98):

$$I^{\text{tot}}_{\mathscr{V}} = \frac{\mathscr{I}}{2G}\int_0^\Lambda dr\,(r^*_\Lambda - r^*(r)) = -\frac{l}{4G}(\nu^2+3)\Lambda r^*_\Lambda + \frac{l}{4G}(\nu^2+3)\int_0^\Lambda dr\, r^*(r)\,. \tag{D.19}$$

The GHY term can be recovered from eq. (5.88)

$$I_{\mathscr{B}} = -\frac{(\nu^2+3)l}{4G}(2\varepsilon_0 - r_h)(r^*_\Lambda - r^*(\varepsilon_0)) = \frac{(\nu^2+3)l}{4G} r_h\,(r^*_\Lambda - r^*(0))\,, \tag{D.20}$$

where in the last step we performed the limit $\varepsilon_0 \to 0$ involving the IR cutoff. The expression is divergent after sending $\Lambda \to \infty$ due to the behaviour at infinity of the tortoise coordinate.

At $t_b = 0$, the joints of the WDW patch are located at both the IR and UV cutoffs. The former vanish as already observed, while the latter give a non-vanishing expression. If we conventionally decide to take the flow of time in the bulk as increasing when going upwards, these joints take a negative sign $\eta = -1$ in eq. (5.91) and we obtain

$$I_{\mathscr{J}} = 2 \times \frac{l}{4G} \sqrt{\frac{\Lambda}{4}\Psi(\Lambda)} \log \left| \frac{l^2}{A^2} \frac{f(\Lambda)}{2R(\Lambda)} \right| = \frac{l}{4G} \sqrt{\Lambda \Psi(\Lambda)} \log \left| \frac{l^2}{A^2} \frac{(\nu^2+3)(\Lambda - r_h)}{\Psi(\Lambda)} \right| . \tag{D.21}$$

Finally, we have to add the counterterm which renders the action diffeomorphism-invariant:

$$I_{\rm ct} = 4 \times \frac{l}{4G} \int_{\varepsilon_0}^{\Lambda} dr \, \frac{6(\nu^2-1)r + (\nu^2+3)r_h}{4\sqrt{r\Psi(r)}} \log \left| \frac{A\tilde{L}}{2l^2} \frac{6(\nu^2-1)r + (\nu^2+3)r_h}{\sqrt{r\Psi(r)}} \right| . \tag{D.22}$$

The integration can be done analytically and we can also perform the usual limit $\varepsilon_0 \to 0$ (where it was not evaluated yet), finding

$$\begin{aligned} I_{\rm ct} = \frac{l}{4G} \Bigg[& \frac{2(\nu^2+3)r_h}{\sqrt{3(\nu^2-1)}} \arctan \left(\frac{\sqrt{3(\nu^2-1)\Lambda}}{\sqrt{(\nu^2+3)r_h + 3(\nu^2-1)\Lambda}} \right) \\ & - \sqrt{\Lambda\Psi(\Lambda)} \log \left| \frac{4l^4}{A^2\tilde{L}^2} \frac{\Lambda\Psi(\Lambda)}{((\nu^2+3)r_h + 6(\nu^2-1)\Lambda)^2} \right| \Bigg] . \end{aligned} \tag{D.23}$$

Putting all these results together we obtain the expression for the total action in the WDW patch

$$\begin{aligned} I^{\rm tot} = & \frac{l}{4G}(\nu^2+3) \int_0^{\Lambda} dr\, r^*(r) - \frac{l}{4G}(\nu^2+3)\Lambda r_\Lambda^* + \frac{(\nu^2+3)l}{4G} r_h \left(r_\Lambda^* - r^*(0)\right) \\ & + \frac{l}{2G} \frac{(\nu^2+3)r_h}{\sqrt{3(\nu^2-1)}} \arctan \left(\frac{\sqrt{3(\nu^2-1)\Lambda}}{\sqrt{(\nu^2+3)r_h + 3(\nu^2-1)\Lambda}} \right) \\ & + \frac{l}{4G} \sqrt{\Lambda\Psi(\Lambda)} \log \left| \frac{\tilde{L}^2}{4l^2} \frac{(\nu^2+3)(\Lambda - r_h)\left[(\nu^2+3)r_h + 6(\nu^2-1)\Lambda\right]^2}{\Lambda\Psi^2(\Lambda)} \right| . \end{aligned} \tag{D.24}$$

The divergent parts of the total complexity are:

$$I^{\rm tot} = \frac{l}{4G} \sqrt{3(\nu^2-1)\Lambda} \left(\log \left| \frac{\tilde{L}^2}{l^2}(\nu^2+3) \right| - 1 \right) - \frac{l}{8G} \frac{\nu^2+3}{\sqrt{3(\nu^2-1)}} r_h \log\Lambda + \mathscr{O}(\Lambda^0) . \tag{D.25}$$

This reproduces eq. (6.28) in the $r_- \to 0$ limit.

D.3.2 External action

The bulk and the counterterm action can be obtained in the same way as in the previous section D.3.1:

$$I_{\mathscr{V}}^{\rm out} = -\frac{l}{4G} \sqrt{3(\nu^2-1)\Lambda} - \frac{l}{8G} \frac{7\nu^2-3}{\sqrt{3(\nu^2-1)}} r_h \log\Lambda + \frac{l}{4G}(\nu^2+3) r_h r_\Lambda^* + \mathscr{O}(\Lambda^0) , \tag{D.26}$$

$$I_{\rm ct}^{\rm out} = -\frac{l}{4G} \sqrt{\Lambda\psi(\Lambda)} \log \left| \frac{4l^4}{A^2\tilde{L}^2} \frac{\Lambda\Psi(\Lambda)}{\left[6(\nu^2-1)\Lambda + (\nu^2+3)r_h\right]^2} \right| + \mathscr{O}(\Lambda^0) . \tag{D.27}$$

There is no spacelike or timelike boundary, then there is no contribution from the GHY term.

As in the rotating case, we need to be careful with the regularization of the joints at the horizon; we use again the same method as in [163]. From (5.90) in this situation, we find

$$I^{\text{out}}_{\mathscr{J}} = -\frac{l}{4G}\sqrt{r_h\Psi(r_h)}\left[-\log\left|\frac{l^2}{A^2}\frac{f(r_{\varepsilon_U,\varepsilon_V})}{2R(r_h)}\right| + \log\left|\frac{l^2}{A^2}\frac{f(r_{U_0,\varepsilon_V})}{2R(r_h)}\right| + \log\left|\frac{l^2}{A^2}\frac{f(r_{\varepsilon_U,V_0})}{2R(r_h)}\right|\right] + \frac{l}{4G}\sqrt{\Lambda\Psi(\Lambda)}\log\left|\frac{l^2}{A^2}\frac{f(\Lambda))}{2R(\Lambda)}\right| . \tag{D.28}$$

In this case it is convenient to add and subtract the joint term $\frac{l}{2G}\nu r_h \log\left|\frac{l^2}{A^2}\frac{f(r_{\varepsilon_U,\varepsilon_V})}{2\nu r_h}\right|$ and to use the relation (6.32) to get

$$I^{\text{out}}_{\mathscr{J}} = -\frac{l}{2G}\nu r_h\left[\log(U_0V_0) + \log\left|\frac{l^2}{A^2}\frac{f(r_{\varepsilon_U,\varepsilon_V})}{2\nu r_h}\right| - \log(\varepsilon_U\varepsilon_V)\right] + \frac{l}{4G}\sqrt{\Lambda\Psi(\Lambda)}\log\left|\frac{l^2}{A^2}\frac{(\nu^2+3)(\Lambda-r_h)}{\Psi(\Lambda)}\right| . \tag{D.29}$$

Finally, the expression simplifies by means of eqs. (6.31) and (6.33):

$$I^{\text{out}}_{\mathscr{J}} = -\frac{l}{2G}\left[\nu r_h\left(\frac{\nu^2+3}{2\nu}r^*_\Lambda + F(r_h)\right) - \frac{1}{2}\sqrt{\Lambda\Psi(\Lambda)}\log\left|\frac{l^2}{A^2}\frac{(\nu^2+3)(\Lambda-r_h)}{\Psi(\Lambda)}\right|\right] . \tag{D.30}$$

The function $F(r)$, which can be obtained from eq. (6.34), is finite and it is not needed to find the divergence structure. Adding all the terms outside the horizon, we finally obtain

$$I^{\text{out}} = \frac{l}{4G}\sqrt{3(\nu^2-1)}\Lambda\left(\log\left|\frac{\tilde{L}^2}{l^2}(\nu^2+3)\right| - 1\right) - \frac{l}{8G}\frac{7\nu^2-3}{\sqrt{3(\nu^2-1)}}r_h\log\Lambda + \mathscr{O}(\Lambda^0) . \tag{D.31}$$

This results reproduces eq. (6.38) in the $r_- \to 0$ limit.

D.3.3 Volume

The non-rotating case of the subregion volume computation has to match with the limit $r_- \to 0$ of the computation in section 6.1. The volume of the extremal slice anchored at the boundary and bounded by the RT surface is given by the induced metric computed from the non-rotating metric

$$V(L) = \int_0^{2\pi} d\theta \int_{r_h}^{\Lambda} dr\sqrt{h} = 2\pi l^2\int_{r_h}^{\Lambda} dr\sqrt{\frac{3(\nu^2-1)r + (\nu^2+3)r_h}{4(\nu^2+3)(r-r_h)}} . \tag{D.32}$$

We introduce the convenient coordinate parametrization $R = r/r_h$ and we obtain

$$V(L) = 2\pi l^2 r_h\int_1^{\Lambda/r_h} dR\sqrt{\frac{3(\nu^2-1)R + (\nu^2+3)}{4(\nu^2+3)(R-1)}} . \tag{D.33}$$

This expression can be analytically solved, giving a primitive function

$$V(L) = 2\pi l^2 r_h \left[\sqrt{\frac{(\nu^2+3)+3R(\nu^2-1)}{\nu^2+3}} \frac{\sqrt{R-1}}{2} + \right. \\ \left. + \frac{2\nu^2 \log\left(\frac{\sqrt{3(\nu^2-1)(R-1)}+\sqrt{3+\nu^2+3R(\nu^2-1)}}{2\nu} \right)}{\sqrt{3(\nu^2-1)(\nu^2+3)}} \right]_{R=1}^{R=\Lambda/r_h} , \tag{D.34}$$

and consequently the result

$$V(L) = \pi l^2 \sqrt{\frac{3(\nu^2-1)}{\nu^2+3}} \Lambda + \frac{2\pi l^2 \nu^2 r_h}{\sqrt{3(\nu^2-1)(\nu^2+3)}} \log\left(\frac{\Lambda}{r_h}\right) + \\ + \pi l^2 r_h \frac{(3-\nu^2)+2\nu^2 \log\left[\frac{3(\nu^2-1)}{\nu^2}\right]}{2\sqrt{3(\nu^2-1)(\nu^2+3)}} + \mathscr{O}(\Lambda^{-1}) . \tag{D.35}$$

The divergent parts of this expression reproduce eq. (6.9) in the $r_- \to 0$ limit, as expected.

D.4 Subsystem complexity and temperature

In this Appendix we give the details for the computation of the temperature dependence of subregion complexity for the WAdS black holes as given in section 6.3.5. Let us compute the temperature dependence of M at constant J, which is the specific heat at constant J:

$$C_J = \frac{\partial M}{\partial T}\Big|_J = \frac{\partial M}{\partial r_+}\frac{\partial r_+}{\partial T} + \frac{\partial M}{\partial r_-}\frac{\partial r_-}{\partial T} . \tag{D.36}$$

The quantities $\frac{\partial r_+}{\partial T}$ and $\frac{\partial r_-}{\partial T}$ can be computed from the inverse of the matrix

$$\begin{pmatrix} \frac{\partial T}{\partial r_+} & \frac{\partial T}{\partial r_-} \\ \frac{\partial J}{\partial r_+} & \frac{\partial J}{\partial r_-} \end{pmatrix} , \tag{D.37}$$

which can be directly calculated from eqs. (5.24) and (5.27). This gives (here we define $\varepsilon = r_-/r_+$):

$$C_J = \frac{\pi l r_+}{4G} \frac{\nu(\varepsilon-1)\left(\varepsilon\left(-3\nu^2+2\nu\sqrt{(\nu^2+3)\varepsilon}+3\right)-2\nu\sqrt{(\nu^2+3)\varepsilon}\right)}{\varepsilon\left(\nu^2(4\varepsilon-1)-3\right)} . \tag{D.38}$$

The quantity C_J is negative for $0 < \varepsilon < \frac{\nu^2+3}{4\nu^2}$ and positive for $\frac{\nu^2+3}{4\nu^2} < \varepsilon < 1$. For $\varepsilon = 0$ and $\varepsilon = \frac{\nu^2+3}{4\nu^2}$, C_J is diverging and there is a second order phase transition, similar to the one which occurs for Kerr and Reissner-Nordström black holes in flat spacetime [198].

With a similar method, one can compute the temperature dependence of K_+ and K_-. The result is:

$$\frac{\partial K_+}{\partial T}\Big|_J = \frac{\hat{a}}{\hat{b}} , \qquad \frac{\partial K_-}{\partial T}\Big|_J = \frac{\hat{c}}{\hat{b}} , \tag{D.39}$$

where

$$\hat{a} = 2\pi l r_+ \left(\sqrt{(v^2+3)r_+^2\varepsilon} - 2vr_+\right)^2 \left(v\left(v^2((\varepsilon-18)\varepsilon-7)+3\varepsilon(\varepsilon+6)+3\right)\right.$$
$$\left.\sqrt{(v^2+3)r_+^2\varepsilon} - r_+\varepsilon\left(-31v^4+6v^2+\left(v^2+3\right)^2\varepsilon+9\right)\right), \tag{D.40}$$

$$\hat{b} = 3\left(v^2-1\right)\sqrt{(v^2+3)r_+^2\varepsilon}\left(4v\sqrt{(v^2+3)r_+^2\varepsilon}+\left(v^2+3\right)r_+(-\varepsilon-1)\right)$$
$$\left(2v(\varepsilon+1)\sqrt{(v^2+3)r_+^2\varepsilon}-\left(5v^2+3\right)r_+\varepsilon\right), \tag{D.41}$$

$$\hat{c} = 2\pi l r_+ \left(\sqrt{(v^2+3)r_+^2\varepsilon} - 2vr_+\right)^2 \left(v\left(v^2(\varepsilon(7\varepsilon+18)-1)-3(\varepsilon(\varepsilon+6)+1)\right)\right.$$
$$\left.\sqrt{(v^2+3)r_+^2\varepsilon} + r_+\varepsilon\left(\left(v^2+3\right)^2+\left(-31v^4+6v^2+9\right)\varepsilon\right)\right). \tag{D.42}$$

D.5 Another regularization for the subregion action of one segment in the BTZ background

In this Appendix we follow the prescription A introduced in section 7.1 to regularize the action, where the null boundaries of the WDW patch are sent from the true boundary $z = 0$ and we add a timelike cutoff surface at $z = \varepsilon$ cutting the bulk structure we integrate over. The geometry of the region is shown in figure D.3.

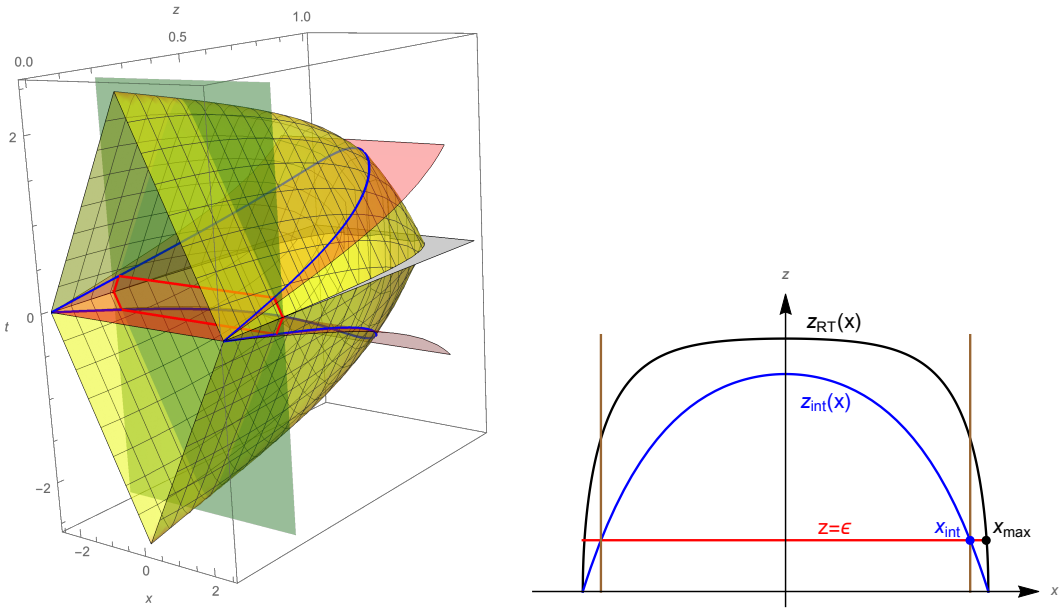

Figure D.3: Another regularization for the BTZ case.

The geometric data are slightly different than the ones introduced in Section 7.2. The RT surface and the corresponding entanglement wedge are the same, see eqs. (7.36) and (7.41), but the WDW patch starts from the true boundary $z=0$ and then the null lines which delimit it are parametrized by

$$t_{\rm WDW} = \pm\frac{z_h}{4}\log\left(\frac{z_h+z}{z_h-z}\right)^2 , \tag{D.43}$$

where $\pm$ refers to positive and negative times, respectively. The intersection curve between the WDW patch and the entanglement wedge is given in this case by

$$z_{\rm int} = \coth\left(\frac{l}{2z_h}\right) - \cosh\left(\frac{x}{z_h}\right)\operatorname{csch}\left(\frac{l}{2z_h}\right) . \tag{D.44}$$

The null normals to the boundaries of the WDW patch and the entanglement wedge are unchanged.

Unlike the case of the other regularization, the intersection curve and the RT surface do not meet at $z=\varepsilon$, but at the true boundary $z=0$. For this region, there are no codimension-three joints. The intersection curve between the boundaries of the WDW patch and the entanglement wedge meets the cutoff surface at:

$$x_{\rm int} = \operatorname{arccosh}\left[\cosh\left(\frac{l}{2z_h}\right) - \frac{\varepsilon}{z_h}\sinh\left(\frac{l}{2z_h}\right)\right] . \tag{D.45}$$

This expression is found by inverting eq. (D.44) and imposing $z=\varepsilon$. In the following sections we compute all the terms entering the gravitational action.

D.5.1 Bulk contribution

We split the contributions as follows

$$I_{\mathscr{V}} = 4\left(I^1_{\mathscr{V}} + I^2_{\mathscr{V}} + I^3_{\mathscr{V}}\right) , \tag{D.46}$$

where

$$\begin{aligned}
I^1_{\mathscr{V}} &= -\frac{L}{4\pi G}\int_0^{x_{\rm int}} dx \int_\varepsilon^{z_{\rm int}} dz \int_0^{t_{\rm WDW}} dt\, \frac{1}{z^3} , \\
I^2_{\mathscr{V}} &= -\frac{L}{4\pi G}\int_0^{x_{\rm int}} dx \int_{z_{\rm int}}^{z_{\rm RT}} dz \int_0^{t_{\rm EW}} dt\, \frac{1}{z^3} , \\
I^3_{\mathscr{V}} &= -\frac{L}{4\pi G}\int_{x_{\rm int}}^{x_{\rm max}} dx \int_\varepsilon^{z_{\rm RT}} dz \int_0^{t_{\rm EW}} dt\, \frac{1}{z^3} .
\end{aligned} \tag{D.47}$$

In this case the sum of bulk terms obtained by splitting the spacetime region with the intersection between the boundaries of the WDW patch and the entanglement wedge does not give the entire bulk action. We need to add $I^3_{\mathscr{V}}$ which accounts for the region between the values $x_{\rm int}$ and $x_{\rm max}$ of the transverse coordinate.

A direct evaluation gives

$$\begin{aligned}
I^1_{\mathscr{V}} + I^2_{\mathscr{V}} = \frac{L}{16\pi G z_h}\int_0^{x_{\rm int}(\varepsilon)} dx \Bigg\{ &\coth\left(\frac{x}{z_h}\right)\log\left|\frac{\sinh\left(\frac{l-2x}{2z_h}\right)\sinh^2\left[\frac{l+2x}{4z_h}\right]}{\sinh\left(\frac{l+2x}{2z_h}\right)\sinh^2\left[\frac{l-2x}{4z_h}\right]}\right| \\
&+ \frac{2\sinh\left(\frac{l}{2z_h}\right)}{\cosh\left(\frac{l}{2z_h}-\cosh\left(\frac{x}{z_h}\right)\right)} - \frac{2z_h}{\varepsilon} + \left(\frac{z_h^2}{\varepsilon^2}-1\right)\log\left|\frac{z_h-\varepsilon}{z_h+\varepsilon}\right| \Bigg\} .
\end{aligned} \tag{D.48}$$

$$I_{\mathscr{V}}^{3} = -\frac{L}{16\pi G}\,. \tag{D.49}$$

D.5.2 Gibbons-Hawking-York contribution

The Gibbons-Hawking-York (GHY) surface term in the action for timelike and spacelike boundaries is

$$I_{GHY} = \frac{1}{8\pi G}\int_{\partial\mathscr{B}} d^2x\sqrt{-\det h_{\mu\nu}}\,K \tag{D.50}$$

with $h_{\mu\nu}$ the induced metric on the boundary and K the trace of the extrinsic curvature. The only contribution of this kind comes from the timelike regularizing surface at $z=\varepsilon$.

The GHY contribution is conveniently splitted into by two parts: the first one involves the WDW patch, while the second one involves the entanglement wedge

$$I^{1}_{\text{GHY}} = \left[\frac{L}{8\pi G}\int_0^{x_{\text{int}}} dx\int_0^{t_{\text{WDW}}} dt\left(\frac{2}{z^2}-\frac{1}{z_h^2}\right)\right]_{z=\varepsilon} = \frac{L}{8\pi G}\frac{l}{\varepsilon}-\frac{L}{4\pi G}\,, \tag{D.51}$$

$$I^{2}_{\text{GHY}} = \left[\frac{L}{8\pi G}\int_{x_{\text{int}}}^{x_{max}} dx\int_0^{t_{\text{EW}}} dt\left(\frac{2}{z^2}-\frac{1}{z_h^2}\right)\right]_{z=\varepsilon} = \frac{L}{8\pi G}\,. \tag{D.52}$$

The total GHY contribution is

$$I_{\text{GHY}} = 4\left(I^{1}_{\text{GHY}}+I^{2}_{\text{GHY}}\right) = \frac{L}{2\pi G}\left(\frac{l}{\varepsilon}-1\right)\,. \tag{D.53}$$

D.5.3 Null boundaries counterterms

The details of calculation are very similar to the ones in section 7.2.3. The contribution in eq. (7.16) and the counterterm on the boundary of entanglement wedge again vanish. The counterterm on the boundary of the WDW patch gives:

$$\begin{aligned} I^{\text{WDW}}_{\text{ct}} &= -\frac{L}{2\pi G}\int_0^{x_{\text{int}}} dx\int_\varepsilon^{z_{\text{int}}} dz\,\frac{1}{z^2}\log\left|\frac{\tilde{L}}{L^2}\,\alpha z\right| = \\ &= \frac{L}{2\pi G}\int_0^{x_{\text{max}}} dx\left\{\frac{1+\log\left|\frac{\tilde{L}}{L^2}\,\alpha\varepsilon\right|}{\varepsilon}+\frac{\sinh\left(\frac{l}{2z_h}\right)}{z_h\left[\cosh\left(\frac{x}{z_h}\right)-\cosh\left(\frac{l}{2z_h}\right)\right]}\times\right. \\ &\left.\times\left(1+\log\left|\frac{\tilde{L}z_h\alpha}{L^2}\,\frac{\cosh\left(\frac{l}{2z_h}\right)-\cosh\left(\frac{x}{z_h}\right)}{\cosh\left(\frac{l}{2z_h}\right)}\right|\right)\right\}\,. \end{aligned} \tag{D.54}$$

D.5.4 Joint terms

The joint contribution to the gravitational action coming from a codimension-two surface given by the intersection of a codimension-one null surface and a codimension-one timelike (or spacelike) surface is

$$I_{\mathscr{J}} = \frac{\eta}{8\pi G}\int_{\mathscr{J}} dx\sqrt{\sigma}\log|\mathbf{k}\cdot\mathbf{n}|\,, \tag{D.55}$$

where σ is the induced metric determinant on the codimension-two surface and $\mathbf{n}$ and $\mathbf{k}$ are the outward-directed normals to the timelike (or spacelike) surface and the null one respectively. Moreover, the

sign in front of the expression can be determined with the rule

$$\eta = -\operatorname{sign}(\mathbf{k}\cdot\mathbf{n})\,\operatorname{sign}(\mathbf{k}\cdot\hat{t}) \tag{D.56}$$

in which $\hat{t}$ is the auxiliary unit vector in the tangent space of the boundary region, orthogonal to the joint and outward-directed from the region of interest [65].

The unit normal vector n^μ to the $z=\varepsilon$ surface is

$$n^\mu = \left(0, -\frac{z}{L}\sqrt{f(z)}, 0\right) \tag{D.57}$$

where the sign must be chosen so that the vector is outward-directed from the region of interest.

The joints give the following contributions:

- The joint involving the WDW patch boundary and the cutoff surface:

$$I_{\mathscr{J}}^{\text{cutoff1}} = -\frac{L}{2\pi G}\int_0^{x_{\text{int}}}\frac{dx}{\varepsilon}\log\left(\frac{\alpha\,\varepsilon}{L\sqrt{f(\varepsilon)}}\right) = -\frac{L}{4\pi G}\frac{l}{\varepsilon}\log\left(\frac{L}{\alpha\varepsilon}\right) - \frac{L}{2\pi G}\log\left(\frac{L}{\alpha\varepsilon}\right). \tag{D.58}$$

- The joint involving the cutoff surface and the entanglement wedge boundary:

$$I_{\mathscr{J}}^{\text{cutoff2}} = \mathscr{O}(\varepsilon\log\varepsilon)\,. \tag{D.59}$$

- The null-null joint contribution coming from the RT surface is the same as in the previous regularization, see eq. (7.58).

- The joints coming from the intersection between the null boundaries of the WDW patch and the ones of the entanglement wedge give a similar contribution as in eq. (7.59), The main difference is that the integral is in the range $[0, x_{\text{int}}(\varepsilon)]$ and the intersection is slightly different, because the WDW patch starts from $z=0$ in the present regularization:

$$I_{\mathscr{J}}^{\text{int}} = \frac{L}{2\pi G z_h}\int_0^{x_{\text{int}}} dx\,\frac{\sinh\left(\frac{l}{2z_h}\right)}{\cosh\left(\frac{l}{2z_h}\right)-\cosh\left(\frac{x}{z_h}\right)}\log\left|\frac{\alpha\beta z_h^2}{2L^2}\frac{\left(\cosh\left(\frac{l}{2z_h}\right)-\cosh\left(\frac{x}{z_h}\right)\right)^2}{\cosh\left(\frac{x}{z_h}\right)\cosh\left(\frac{l}{2z_h}\right)-1}\right|. \tag{D.60}$$

D.5.5 Complexity

Adding all the contributions and performing the integrals we finally get

$$\mathscr{C}_A^{\text{BTZ}} = \frac{l}{\varepsilon}\frac{c}{6\pi^2}\left(1+\log\left(\frac{\tilde{L}}{L}\right)\right) - \log\left(\frac{2\tilde{L}}{L}\right)\frac{S^{\text{BTZ}}}{\pi^2} - \frac{c}{3\pi^2}\left(\frac{1}{2}+\log\left(\frac{\tilde{L}}{L}\right)\right) + \frac{1}{24}c\,. \tag{D.61}$$

The difference with expression (7.63) consists only in the coefficient of the divergence $1/\varepsilon$ and in a finite piece proportional to the counterterm scale $\tilde{L}$ via a logarithm.

Recently other counterterms were proposed to give a universal behaviour of all the divergences of the action [174]. In particular, with this regularization we need to insert a codimension-one boundary term at the cutoff surface:

$$I_{\text{ct}}^{\text{cutoff}} = -\frac{1}{16\pi G}\int d^{d-1}x\,dt\,\sqrt{-h}\left(\frac{2(d-1)}{L}+\frac{L}{d-2}\tilde{R}\right), \tag{D.62}$$

being $\tilde{R}$ the Ricci scalar on the codimension-one surface. Adding the extra counterterm in eq. (D.62), we find

$$\mathscr{C}_A^{\mathrm{BTZ}} = \frac{l}{\varepsilon}\frac{c}{6\pi^2}\log\left(\frac{\tilde{L}}{L}\right) - \log\left(\frac{2\tilde{L}}{L}\right)\frac{S^{\mathrm{BTZ}}}{\pi^2} - \frac{c}{3\pi^2}\log\left(\frac{\tilde{L}}{L}\right) + \frac{1}{24}c\,. \tag{D.63}$$

The numerical coefficient of all the divergences is the same as in eq. (7.63). The two regularizations differ only by a finite piece dependent from the counterterm length scale $\tilde{L}$.

Bibliography

[1] A. B. Zamolodchikov, "Irreversibility of the Flux of the Renormalization Group in a 2D Field Theory," *JETP Lett.* **43** (1986) 730–732. [Pisma Zh. Eksp. Teor. Fiz.43,565(1986)].

[2] J. L. Cardy, "Is There a c Theorem in Four-Dimensions?," *Phys. Lett.* **B215** (1988) 749–752.

[3] H. Osborn, "Derivation of a Four-dimensional c Theorem," *Phys. Lett.* **B222** (1989) 97–102.

[4] Z. Komargodski and A. Schwimmer, "On Renormalization Group Flows in Four Dimensions," *JHEP* **12** (2011) 099, 1107.3987.

[5] S. Deser and A. Schwimmer, "Geometric classification of conformal anomalies in arbitrary dimensions," *Phys. Lett.* **B309** (1993) 279–284, hep-th/9302047.

[6] I. Adam, I. V. Melnikov, and S. Theisen, "A Non-Relativistic Weyl Anomaly," *JHEP* **09** (2009) 130, 0907.2156.

[7] M. Baggio, J. de Boer, and K. Holsheimer, "Anomalous Breaking of Anisotropic Scaling Symmetry in the Quantum Lifshitz Model," *JHEP* **07** (2012) 099, 1112.6416.

[8] T. Griffin, P. Horava, and C. M. Melby-Thompson, "Conformal Lifshitz Gravity from Holography," *JHEP* **05** (2012) 010, 1112.5660.

[9] I. Arav, S. Chapman, and Y. Oz, "Lifshitz Scale Anomalies," *JHEP* **02** (2015) 078, 1410.5831.

[10] I. Jack and H. Osborn, "Analogs for the c Theorem for Four-dimensional Renormalizable Field Theories," *Nucl. Phys.* **B343** (1990) 647–688.

[11] H. Osborn, "Weyl consistency conditions and a local renormalization group equation for general renormalizable field theories," *Nucl. Phys.* **B363** (1991) 486–526.

[12] K. Jensen and A. Karch, "Revisiting non-relativistic limits," *JHEP* **04** (2015) 155, 1412.2738.

[13] C. Duval, G. Burdet, H. P. Kunzle, and M. Perrin, "Bargmann Structures and Newton-cartan Theory," *Phys. Rev.* **D31** (1985) 1841–1853.

[14] D. T. Son, "Toward an AdS/cold atoms correspondence: A Geometric realization of the Schrodinger symmetry," *Phys. Rev.* **D78** (2008) 046003, 0804.3972.

[15] K. Jensen, "Anomalies for Galilean fields," *SciPost Phys.* **5** (2018), no. 1, 005, 1412.7750.

[16] I. Arav, S. Chapman, and Y. Oz, "Non-Relativistic Scale Anomalies," *JHEP* **06** (2016) 158, 1601.06795.

[17] R. Auzzi, S. Baiguera, and G. Nardelli, "On Newton-Cartan trace anomalies," *JHEP* **02** (2016) 003, 1511.08150. [Erratum: JHEP02,177(2016)].

[18] R. Auzzi, S. Baiguera, F. Filippini, and G. Nardelli, "On Newton-Cartan local renormalization group and anomalies," *JHEP* **11** (2016) 163, 1610.00123.

[19] C. R. Hagen, "Scale and conformal transformations in galilean-covariant field theory," *Phys. Rev.* **D5** (1972) 377–388.

[20] R. Jackiw and S.-Y. Pi, "Classical and quantal nonrelativistic Chern-Simons theory," *Phys. Rev.* **D42** (1990) 3500. [Erratum: Phys. Rev.D48,3929(1993)].

[21] T. Mehen, I. W. Stewart, and M. B. Wise, "Conformal invariance for nonrelativistic field theory," *Phys. Lett.* **B474** (2000) 145–152, hep-th/9910025.

[22] D. T. Son and M. Wingate, "General coordinate invariance and conformal invariance in nonrelativistic physics: Unitary Fermi gas," *Annals Phys.* **321** (2006) 197–224, cond-mat/0509786.

[23] Y. Nishida and D. T. Son, "Nonrelativistic conformal field theories," *Phys. Rev.* **D76** (2007) 086004, 0706.3746.

[24] D. T. Son, "Newton-Cartan Geometry and the Quantum Hall Effect," 1306.0638.

[25] M. Geracie, D. T. Son, C. Wu, and S.-F. Wu, "Spacetime Symmetries of the Quantum Hall Effect," *Phys. Rev.* **D91** (2015) 045030, 1407.1252.

[26] D. B. Kaplan, M. J. Savage, and M. B. Wise, "A New expansion for nucleon-nucleon interactions," *Phys. Lett.* **B424** (1998) 390–396, nucl-th/9801034.

[27] Y. Nishida and D. T. Son, "Unitary Fermi gas, epsilon expansion, and nonrelativistic conformal field theories," *Lect. Notes Phys.* **836** (2012) 233–275, 1004.3597.

[28] P. F. Bedaque, H. W. Hammer, and U. van Kolck, "Renormalization of the three-body system with short range interactions," *Phys. Rev. Lett.* **82** (1999) 463–467, nucl-th/9809025.

[29] P. F. Bedaque, H. W. Hammer, and U. van Kolck, "The Three boson system with short range interactions," *Nucl. Phys.* **A646** (1999) 444–466, nucl-th/9811046.

[30] E. Braaten and H. W. Hammer, "Universality in few-body systems with large scattering length," *Phys. Rept.* **428** (2006) 259–390, cond-mat/0410417.

[31] M. T. Grisaru, W. Siegel, and M. Rocek, "Improved Methods for Supergraphs," *Nucl. Phys.* **B159** (1979) 429.

[32] N. Seiberg, "Naturalness versus supersymmetric nonrenormalization theorems," *Phys. Lett.* **B318** (1993) 469–475, hep-ph/9309335.

[33] D. Friedan, Z.-a. Qiu, and S. H. Shenker, "Superconformal Invariance in Two-Dimensions and the Tricritical Ising Model," *Phys. Lett.* **151B** (1985) 37–43.

[34] T. Grover, D. N. Sheng, and A. Vishwanath, "Emergent Space-Time Supersymmetry at the Boundary of a Topological Phase," *Science* **344** (2014), no. 6181, 280–283, 1301.7449.

[35] Y. Yu and K. Yang, "Simulating Wess-Zumino Supersymmetry Model in Optical Lattices," *Phys. Rev. Lett.* **105** (2010) 150605, 1005.1399.

[36] L. Huijse, B. Bauer, and E. Berg, "Emergent Supersymmetry at the Ising–Berezinskii-Kosterlitz-Thouless Multicritical Point," *Phys. Rev. Lett.* **114** (2015), no. 9, 090404, 1403.5565.

[37] S.-K. Jian, Y.-F. Jiang, and H. Yao, "Emergent Spacetime Supersymmetry in 3D Weyl Semimetals and 2D Dirac Semimetals," *Phys. Rev. Lett.* **114** (2015), no. 23, 237001, 1407.4497.

[38] A. Rahmani, X. Zhu, M. Franz, and I. Affleck, "Emergent Supersymmetry from Strongly Interacting Majorana Zero Modes," *Phys. Rev. Lett.* **115** (2015), no. 16, 166401, 1504.05192. [Erratum: Phys. Rev. Lett.116,no.10,109901(2016)].

[39] J. Yu, R. Roiban, S.-K. Jian, and C.-X. Liu, "Finite-Scale Emergence of 2+1D Supersymmetry at First-Order Quantum Phase Transition," *Phys. Rev.* **B100** (2019), no. 7, 075153, 1902.07407.

[40] S.-S. Lee, "Emergence of supersymmetry at a critical point of a lattice model," *Phys. Rev.* **B76** (2007) 075103, cond-mat/0611658.

[41] R. Puzalowski, "GALILEAN SUPERSYMMETRY," *Acta Phys. Austriaca* **50** (1978) 45.

[42] M. Leblanc, G. Lozano, and H. Min, "Extended superconformal Galilean symmetry in Chern-Simons matter systems," *Annals Phys.* **219** (1992) 328–348, hep-th/9206039.

[43] T. E. Clark and S. T. Love, "NONRELATIVISTIC SUPERSYMMETRY," *Nucl. Phys.* **B231** (1984) 91–108.

[44] J. A. de Azcarraga and D. Ginestar, "Nonrelativistic limit of supersymmetric theories," *J. Math. Phys.* **32** (1991) 3500–3508.

[45] A. Meyer, Y. Oz, and A. Raviv-Moshe, "On Non-Relativistic Supersymmetry and its Spontaneous Breaking," *JHEP* **06** (2017) 128, 1703.04740.

[46] O. Bergman and C. B. Thorn, "SuperGalilei invariant field theories in (2+1)-dimensions," *Phys. Rev.* **D52** (1995) 5997–6007, hep-th/9507007.

[47] J. Beckers and V. Hussin, "Dynamical Supersymmetries of the Harmonic Oscillator," *Phys. Lett.* **A118** (1986) 319–321.

[48] J. P. Gauntlett, J. Gomis, and P. K. Townsend, "Particle Actions as Wess-Zumino Terms for Space-time (Super)symmetry Groups," *Phys. Lett.* **B249** (1990) 255–260.

[49] C. Duval and P. A. Horvathy, "On Schrodinger superalgebras," *J. Math. Phys.* **35** (1994) 2516–2538, hep-th/0508079.

[50] S. Chapman, Y. Oz, and A. Raviv-Moshe, "On Supersymmetric Lifshitz Field Theories," *JHEP* **10** (2015) 162, 1508.03338.

[51] I. Arav, Y. Oz, and A. Raviv-Moshe, "Holomorphic Structure and Quantum Critical Points in Supersymmetric Lifshitz Field Theories," 1908.03220.

[52] S. Ryu and T. Takayanagi, "Holographic derivation of entanglement entropy from AdS/CFT," *Phys. Rev. Lett.* **96** (2006) 181602, hep-th/0603001.

[53] A. Strominger and C. Vafa, "Microscopic origin of the Bekenstein-Hawking entropy," *Phys. Lett.* **B379** (1996) 99–104, hep-th/9601029.

[54] L. Susskind, "Entanglement is not enough," *Fortsch. Phys.* **64** (2016) 49–71, 1411.0690.

[55] J. M. Maldacena, "Eternal black holes in anti-de Sitter," *JHEP* **04** (2003) 021, hep-th/0106112.

[56] D. Stanford and L. Susskind, "Complexity and Shock Wave Geometries," *Phys. Rev.* **D90** (2014), no. 12, 126007, 1406.2678.

[57] A. R. Brown, D. A. Roberts, L. Susskind, B. Swingle, and Y. Zhao, "Complexity, action, and black holes," *Phys. Rev.* **D93** (2016), no. 8, 086006, 1512.04993.

[58] L. Lehner, R. C. Myers, E. Poisson, and R. D. Sorkin, "Gravitational action with null boundaries," *Phys. Rev.* **D94** (2016), no. 8, 084046, 1609.00207.

[59] J. Maldacena and L. Susskind, "Cool horizons for entangled black holes," *Fortsch. Phys.* **61** (2013) 781–811, 1306.0533.

[60] K. Papadodimas and S. Raju, "An Infalling Observer in AdS/CFT," *JHEP* **10** (2013) 212, 1211.6767.

[61] K. Papadodimas and S. Raju, "State-Dependent Bulk-Boundary Maps and Black Hole Complementarity," *Phys. Rev.* **D89** (2014), no. 8, 086010, 1310.6335.

[62] K. Papadodimas and S. Raju, "Remarks on the necessity and implications of state-dependence in the black hole interior," *Phys. Rev.* **D93** (2016), no. 8, 084049, 1503.08825.

[63] S. Detournay, T. Hartman, and D. M. Hofman, "Warped Conformal Field Theory," *Phys. Rev.* **D86** (2012) 124018, 1210.0539.

[64] K. Jensen, "Locality and anomalies in warped conformal field theory," *JHEP* **12** (2017) 111, 1710.11626.

[65] D. Carmi, R. C. Myers, and P. Rath, "Comments on Holographic Complexity," *JHEP* **03** (2017) 118, 1612.00433.

[66] C. W. Misner, K. S. Thorne, and J. A. Wheeler, *Gravitation*. W. H. Freeman, San Francisco, 1973.

[67] C. Hoyos and D. T. Son, "Hall Viscosity and Electromagnetic Response," *Phys. Rev. Lett.* **108** (2012) 066805, 1109.2651.

[68] K. Balasubramanian and J. McGreevy, "Gravity duals for non-relativistic CFTs," *Phys. Rev. Lett.* **101** (2008) 061601, 0804.4053.

[69] M. H. Christensen, J. Hartong, N. A. Obers, and B. Rollier, "Torsional Newton-Cartan Geometry and Lifshitz Holography," *Phys. Rev.* **D89** (2014) 061901, 1311.4794.

[70] J. Hartong, E. Kiritsis, and N. A. Obers, "Lifshitz space–times for Schrödinger holography," *Phys. Lett.* **B746** (2015) 318–324, 1409.1519.

[71] J. Hartong, E. Kiritsis, and N. A. Obers, "Schrödinger Invariance from Lifshitz Isometries in Holography and Field Theory," *Phys. Rev.* **D92** (2015) 066003, 1409.1522.

[72] J.-M. Levy-Leblond, "Nonrelativistic particles and wave equations," *Commun. Math. Phys.* **6** (1967) 286–311.

[73] J. F. Fuini, A. Karch, and C. F. Uhlemann, "Spinor fields in general Newton-Cartan backgrounds," *Phys. Rev.* **D92** (2015), no. 12, 125036, 1510.03852.

[74] C. Duval, P. A. Horvathy, and L. Palla, "Spinors in nonrelativistic Chern-Simons electrodynamics," *Annals Phys.* **249** (1996) 265–297, hep-th/9510114.

[75] K. Jensen, "On the coupling of Galilean-invariant field theories to curved spacetime," *SciPost Phys.* **5** (2018), no. 1, 011, 1408.6855.

[76] L. Bonora, P. Cotta-Ramusino, and C. Reina, "Conformal Anomaly and Cohomology," *Phys. Lett.* **126B** (1983) 305–308.

[77] R. Auzzi, S. Baiguera, and G. Nardelli, "Trace anomaly for non-relativistic fermions," *JHEP* **08** (2017) 042, 1705.02229.

[78] R. Auzzi, S. Baiguera, and G. Nardelli, "Nonrelativistic trace and diffeomorphism anomalies in particle number background," *Phys. Rev.* **D97** (2018), no. 8, 085010, 1711.00910.

[79] D. V. Vassilevich, "Heat kernel expansion: User's manual," *Phys. Rept.* **388** (2003) 279–360, hep-th/0306138.

[80] V. Mukhanov and S. Winitzki, *Introduction to quantum effects in gravity*. Cambridge University Press, 2007.

[81] S. N. Solodukhin, "Entanglement Entropy in Non-Relativistic Field Theories," *JHEP* **04** (2010) 101, 0909.0277.

[82] K. Fernandes and A. Mitra, "Gravitational anomalies on the Newton-Cartan background," *Phys. Rev.* **D96** (2017), no. 8, 085003, 1703.09162.

[83] S. Pal and B. Grinstein, "Heat kernel and Weyl anomaly of Schrödinger invariant theory," *Phys. Rev.* **D96** (2017), no. 12, 125001, 1703.02987.

[84] S. M. Christensen and M. J. Duff, "New Gravitational Index Theorems and Supertheorems," *Nucl. Phys.* **B154** (1979) 301–342.

[85] D. Z. Freedman and A. Van Proeyen, *Supergravity*. Cambridge Univ. Press, Cambridge, UK, 2012.

[86] R. Auzzi, S. Baiguera, G. Nardelli, and S. Penati, "Renormalization properties of a Galilean Wess-Zumino model," *JHEP* **06** (2019) 048, 1904.08404.

[87] E. Bergshoeff, J. Rosseel, and T. Zojer, "Newton–Cartan (super)gravity as a non-relativistic limit," *Class. Quant. Grav.* **32** (2015), no. 20, 205003, 1505.02095.

[88] O. Aharony, A. Hanany, K. A. Intriligator, N. Seiberg, and M. J. Strassler, "Aspects of N=2 supersymmetric gauge theories in three-dimensions," *Nucl. Phys.* **B499** (1997) 67–99, hep-th/9703110.

[89] Y. Nakayama, "Superfield Formulation for Non-Relativistic Chern-Simons-Matter Theory," *Lett. Math. Phys.* **89** (2009) 67–83, 0902.2267.

[90] J. Wess and B. Zumino, "Supergauge Transformations in Four-Dimensions," *Nucl. Phys.* **B70** (1974) 39–50. [,24(1974)].

[91] S. J. Gates, M. T. Grisaru, M. Rocek, and W. Siegel, "Superspace Or One Thousand and One Lessons in Supersymmetry," *Front. Phys.* **58** (1983) 1–548, hep-th/0108200.

[92] S. Weinberg, *The quantum theory of fields. Vol. 3: Supersymmetry*. Cambridge University Press, 2013.

[93] S. Y. Yong and D. T. Son, "Effective field theory for one-dimensional nonrelativistic particles with contact interaction," *Phys. Rev.* **A97** (2018), no. 4, 043630, 1711.10517.

[94] L. F. Abbott and M. T. Grisaru, "The Three Loop Beta Function for the Wess-Zumino Model," *Nucl. Phys.* **B169** (1980) 415–429.

[95] A. Sen and M. K. Sundaresan, "The Four Loop Beta Function for the Wess-Zumino Model," *Phys. Lett.* **101B** (1981) 61–63.

[96] O. Bergman, "Nonrelativistic field theoretic scale anomaly," *Phys. Rev.* **D46** (1992) 5474–5478.

[97] R. Auzzi, S. Baiguera, and G. Nardelli, "Volume and complexity for warped AdS black holes," *JHEP* **06** (2018) 063, 1804.07521.

[98] R. Auzzi, S. Baiguera, M. Grassi, G. Nardelli, and N. Zenoni, "Complexity and action for warped AdS black holes," *JHEP* **09** (2018) 013, 1806.06216.

[99] D. M. Hofman and A. Strominger, "Chiral Scale and Conformal Invariance in 2D Quantum Field Theory," *Phys. Rev. Lett.* **107** (2011) 161601, 1107.2917.

[100] D. Anninos, W. Li, M. Padi, W. Song, and A. Strominger, "Warped AdS(3) Black Holes," *JHEP* **03** (2009) 130, 0807.3040.

[101] D. Anninos, "Hopfing and Puffing Warped Anti-de Sitter Space," *JHEP* **09** (2009) 075, 0809.2433.

[102] D. M. Hofman and B. Rollier, "Warped Conformal Field Theory as Lower Spin Gravity," *Nucl. Phys.* **B897** (2015) 1–38, 1411.0672.

[103] D. Anninos, J. Samani, and E. Shaghoulian, "Warped Entanglement Entropy," *JHEP* **02** (2014) 118, 1309.2579.

[104] A. Castro, D. M. Hofman, and N. Iqbal, "Entanglement Entropy in Warped Conformal Field Theories," *JHEP* **02** (2016) 033, 1511.00707.

[105] T. Azeyanagi, S. Detournay, and M. Riegler, "Warped Black Holes in Lower-Spin Gravity," *Phys. Rev.* **D99** (2019), no. 2, 026013, 1801.07263.

[106] W. Song, Q. Wen, and J. Xu, "Generalized Gravitational Entropy for Warped Anti–de Sitter Space," *Phys. Rev. Lett.* **117** (2016), no. 1, 011602, 1601.02634.

[107] W. Song, Q. Wen, and J. Xu, "Modifications to Holographic Entanglement Entropy in Warped CFT," *JHEP* **02** (2017) 067, 1610.00727.

[108] J. L. Cardy, "Critical exponents of the chiral Potts model from conformal field theory," *Nucl. Phys.* **B389** (1993) 577–586, hep-th/9210002.

[109] P. Kraus and E. Perlmutter, "Partition functions of higher spin black holes and their CFT duals," *JHEP* **11** (2011) 061, 1108.2567.

[110] M. R. Gaberdiel, T. Hartman, and K. Jin, "Higher Spin Black Holes from CFT," *JHEP* **04** (2012) 103, 1203.0015.

[111] R.-G. Cai, S.-M. Ruan, S.-J. Wang, R.-Q. Yang, and R.-H. Peng, "Action growth for AdS black holes," *JHEP* **09** (2016) 161, 1606.08307.

[112] S. Chapman, H. Marrochio, and R. C. Myers, "Complexity of Formation in Holography," *JHEP* **01** (2017) 062, 1610.08063.

[113] D. Carmi, S. Chapman, H. Marrochio, R. C. Myers, and S. Sugishita, "On the Time Dependence of Holographic Complexity," *JHEP* **11** (2017) 188, 1709.10184.

[114] S. Chapman, D. Ge, and G. Policastro, "Holographic Complexity for Defects Distinguishes Action from Volume," *JHEP* **05** (2019) 049, 1811.12549.

[115] M. Moosa, "Evolution of Complexity Following a Global Quench," *JHEP* **03** (2018) 031, 1711.02668.

[116] M. Moosa, "Divergences in the rate of complexification," *Phys. Rev.* **D97** (2018), no. 10, 106016, 1712.07137.

[117] S. Chapman, H. Marrochio, and R. C. Myers, "Holographic complexity in Vaidya spacetimes. Part I," *JHEP* **06** (2018) 046, 1804.07410.

[118] S. Chapman, H. Marrochio, and R. C. Myers, "Holographic complexity in Vaidya spacetimes. Part II," *JHEP* **06** (2018) 114, 1805.07262.

[119] J. L. F. Barbon and E. Rabinovici, "Holographic complexity and spacetime singularities," *JHEP* **01** (2016) 084, 1509.09291.

[120] S. Bolognesi, E. Rabinovici, and S. R. Roy, "On Some Universal Features of the Holographic Quantum Complexity of Bulk Singularities," *JHEP* **06** (2018) 016, 1802.02045.

[121] M. Flory and N. Miekley, "Complexity change under conformal transformations in AdS_3/CFT_2," *JHEP* **05** (2019) 003, 1806.08376.

[122] M. Flory, "WdW-patches in AdS_3 and complexity change under conformal transformations II," *JHEP* **05** (2019) 086, 1902.06499.

[123] M. Ghodrati, "Complexity growth in massive gravity theories, the effects of chirality, and more," *Phys. Rev.* **D96** (2017), no. 10, 106020, 1708.07981.

[124] H. Dimov, R. C. Rashkov, and T. Vetsov, "Thermodynamic information geometry and complexity growth of a warped AdS black hole and the warped AdS_3/CFT_2 correspondence," *Phys. Rev.* **D99** (2019), no. 12, 126007, 1902.02433.

[125] R. Jefferson and R. C. Myers, "Circuit complexity in quantum field theory," *JHEP* **10** (2017) 107, 1707.08570.

[126] L. Hackl and R. C. Myers, "Circuit complexity for free fermions," *JHEP* **07** (2018) 139, 1803.10638.

[127] S. Chapman, J. Eisert, L. Hackl, M. P. Heller, R. Jefferson, H. Marrochio, and R. C. Myers, "Complexity and entanglement for thermofield double states," *SciPost Phys.* **6** (2019), no. 3, 034, 1810.05151.

[128] E. Caceres, S. Chapman, J. D. Couch, J. P. Hernandez, R. C. Myers, and S.-M. Ruan, "Complexity of Mixed States in QFT and Holography," 1909.10557.

[129] S. Chapman, M. P. Heller, H. Marrochio, and F. Pastawski, "Toward a Definition of Complexity for Quantum Field Theory States," *Phys. Rev. Lett.* **120** (2018), no. 12, 121602, 1707.08582.

[130] P. Caputa, N. Kundu, M. Miyaji, T. Takayanagi, and K. Watanabe, "Anti-de Sitter Space from Optimization of Path Integrals in Conformal Field Theories," *Phys. Rev. Lett.* **119** (2017), no. 7, 071602, 1703.00456.

[131] P. Caputa, N. Kundu, M. Miyaji, T. Takayanagi, and K. Watanabe, "Liouville Action as Path-Integral Complexity: From Continuous Tensor Networks to AdS/CFT," *JHEP* **11** (2017) 097, 1706.07056.

[132] A. Bhattacharyya, P. Caputa, S. R. Das, N. Kundu, M. Miyaji, and T. Takayanagi, "Path-Integral Complexity for Perturbed CFTs," *JHEP* **07** (2018) 086, 1804.01999.

[133] K. A. Moussa, G. Clement, and C. Leygnac, "The Black holes of topologically massive gravity," *Class. Quant. Grav.* **20** (2003) L277–L283, gr-qc/0303042.

[134] A. Bouchareb and G. Clement, "Black hole mass and angular momentum in topologically massive gravity," *Class. Quant. Grav.* **24** (2007) 5581–5594, 0706.0263.

[135] M. Banados, C. Teitelboim, and J. Zanelli, "The Black hole in three-dimensional space-time," *Phys. Rev. Lett.* **69** (1992) 1849–1851, hep-th/9204099.

[136] M. Banados, M. Henneaux, C. Teitelboim, and J. Zanelli, "Geometry of the (2+1) black hole," *Phys. Rev.* **D48** (1993) 1506–1525, gr-qc/9302012. [Erratum: Phys. Rev.D88,069902(2013)].

[137] G. Clement, "Warped AdS(3) black holes in new massive gravity," *Class. Quant. Grav.* **26** (2009) 105015, 0902.4634.

[138] E. Tonni, "Warped black holes in 3D general massive gravity," *JHEP* **08** (2010) 070, 1006.3489.

[139] R. M. Wald, "Black hole entropy is the Noether charge," *Phys. Rev.* **D48** (1993), no. 8, R3427–R3431, gr-qc/9307038.

[140] M. Alishahiha, "Holographic Complexity," *Phys. Rev.* **D92** (2015), no. 12, 126009, 1509.06614.

[141] M. Alishahiha, A. Faraji Astaneh, A. Naseh, and M. H. Vahidinia, "On complexity for F(R) and critical gravity," *JHEP* **05** (2017) 009, 1702.06796.

[142] W.-D. Guo, S.-W. Wei, Y.-Y. Li, and Y.-X. Liu, "Complexity growth rates for AdS black holes in massive gravity and $f(R)$ gravity," *Eur. Phys. J.* **C77** (2017), no. 12, 904, 1703.10468.

[143] M. M. Qaemmaqami, "Complexity growth in minimal massive 3D gravity," *Phys. Rev.* **D97** (2018), no. 2, 026006, 1709.05894.

[144] M. Gürses, "Perfect Fluid Sources in 2+1 Dimensions," *Class. Quant. Grav.* **11** (1994), no. 10, 2585.

[145] M. Banados, G. Barnich, G. Compere, and A. Gomberoff, "Three dimensional origin of Godel spacetimes and black holes," *Phys. Rev.* **D73** (2006) 044006, hep-th/0512105.

[146] G. Barnich and G. Compere, "Conserved charges and thermodynamics of the spinning Godel black hole," *Phys. Rev. Lett.* **95** (2005) 031302, hep-th/0501102.

[147] G. Compere, S. Detournay, and M. Romo, "Supersymmetric Godel and warped black holes in string theory," *Phys. Rev.* **D78** (2008) 104030, 0808.1912.

[148] S. Detournay and M. Guica, "Stringy Schrödinger truncations," *JHEP* **08** (2013) 121, 1212.6792.

[149] P. Karndumri and E. O. Colgáin, "3D Supergravity from wrapped D3-branes," *JHEP* **10** (2013) 094, 1307.2086.

[150] A. Castro and M. J. Rodriguez, "Universal properties and the first law of black hole inner mechanics," *Phys. Rev.* **D86** (2012) 024008, 1204.1284.

[151] G. Giribet and M. Tsoukalas, "Warped-AdS3 black holes with scalar halo," *Phys. Rev.* **D92** (2015), no. 6, 064027, 1506.05336.

[152] F. Jugeau, G. Moutsopoulos, and P. Ritter, "From accelerating and Poincare coordinates to black holes in spacelike warped AdS_3, and back," *Class. Quant. Grav.* **28** (2011) 035001, 1007.1961.

[153] T. Hartman and J. Maldacena, "Time Evolution of Entanglement Entropy from Black Hole Interiors," *JHEP* **05** (2013) 014, 1303.1080.

[154] Y. Neiman, "On-shell actions with lightlike boundary data," 1212.2922.

[155] K. Parattu, S. Chakraborty, B. R. Majhi, and T. Padmanabhan, "A Boundary Term for the Gravitational Action with Null Boundaries," *Gen. Rel. Grav.* **48** (2016), no. 7, 94, 1501.01053.

[156] G. Hayward, "Gravitational action for space-times with nonsmooth boundaries," *Phys. Rev.* **D47** (1993) 3275–3280.

[157] S. Lloyd, "An ultimate physical limit to computation," *Nature* **406** (2000) 1047–1054.

[158] R. Auzzi, S. Baiguera, A. Mitra, G. Nardelli, and N. Zenoni, "Subsystem complexity in warped AdS," *JHEP* **09** (2019) 114, 1906.09345.

[159] M. Headrick, V. E. Hubeny, A. Lawrence, and M. Rangamani, "Causality & holographic entanglement entropy," *JHEP* **12** (2014) 162, 1408.6300.

[160] O. Ben-Ami and D. Carmi, "On Volumes of Subregions in Holography and Complexity," *JHEP* **11** (2016) 129, 1609.02514.

[161] R. Abt, J. Erdmenger, H. Hinrichsen, C. M. Melby-Thompson, R. Meyer, C. Northe, and I. A. Reyes, "Topological Complexity in AdS_3/CFT_2," *Fortsch. Phys.* **66** (2018), no. 6, 1800034, 1710.01327.

[162] R. Abt, J. Erdmenger, M. Gerbershagen, C. M. Melby-Thompson, and C. Northe, "Holographic Subregion Complexity from Kinematic Space," *JHEP* **01** (2019) 012, 1805.10298.

[163] C. A. Agón, M. Headrick, and B. Swingle, "Subsystem Complexity and Holography," *JHEP* **02** (2019) 145, 1804.01561.

[164] M. Alishahiha, K. Babaei Velni, and M. R. Mohammadi Mozaffar, "Black hole subregion action and complexity," *Phys. Rev.* **D99** (2019), no. 12, 126016, 1809.06031.

[165] E. Cáceres, J. Couch, S. Eccles, and W. Fischler, "Holographic Purification Complexity," *Phys. Rev.* **D99** (2019), no. 8, 086016, 1811.10650.

[166] P. Roy and T. Sarkar, "Note on subregion holographic complexity," *Phys. Rev.* **D96** (2017), no. 2, 026022, 1701.05489.

[167] P. Roy and T. Sarkar, "Subregion holographic complexity and renormalization group flows," *Phys. Rev.* **D97** (2018), no. 8, 086018, 1708.05313.

[168] E. Bakhshaei, A. Mollabashi, and A. Shirzad, "Holographic Subregion Complexity for Singular Surfaces," *Eur. Phys. J.* **C77** (2017), no. 10, 665, 1703.03469.

[169] A. Bhattacharya, K. T. Grosvenor, and S. Roy, "Entanglement Entropy and Subregion Complexity in Thermal Perturbations around Pure-AdS," 1905.02220.

[170] B. Chen, W.-M. Li, R.-Q. Yang, C.-Y. Zhang, and S.-J. Zhang, "Holographic subregion complexity under a thermal quench," *JHEP* **07** (2018) 034, 1803.06680.

[171] R. Auzzi, G. Nardelli, F. I. Schaposnik Massolo, G. Tallarita, and N. Zenoni, "On volume subregion complexity in Vaidya spacetime," 1908.10832.

[172] M. Ghodrati, X.-M. Kuang, B. Wang, C.-Y. Zhang, and Y.-T. Zhou, "The connection between holographic entanglement and complexity of purification," *JHEP* **09** (2019) 009, 1902.02475.

[173] R.-Q. Yang, C. Niu, and K.-Y. Kim, "Surface Counterterms and Regularized Holographic Complexity," *JHEP* **09** (2017) 042, 1701.03706.

[174] A. Akhavan and F. Omidi, "On the Role of Counterterms in Holographic Complexity," 1906.09561.

[175] R. Auzzi, S. Baiguera, A. Legramandi, G. Nardelli, P. Roy, and N. Zenoni, "On subregion action complexity in AdS_3 and in the BTZ black hole," 1910.00526.

[176] A. R. Brown, D. A. Roberts, L. Susskind, B. Swingle, and Y. Zhao, "Holographic Complexity Equals Bulk Action?," *Phys. Rev. Lett.* **116** (2016), no. 19, 191301, 1509.07876.

[177] E. Poisson, *A Relativist's Toolkit: The Mathematics of Black-Hole Mechanics*. Cambridge University Press, 2009.

[178] V. Balasubramanian, A. Bernamonti, J. de Boer, N. Copland, B. Craps, E. Keski-Vakkuri, B. Muller, A. Schafer, M. Shigemori, and W. Staessens, "Holographic Thermalization," *Phys. Rev.* **D84** (2011) 026010, 1103.2683.

[179] B. Czech, J. L. Karczmarek, F. Nogueira, and M. Van Raamsdonk, "The Gravity Dual of a Density Matrix," *Class. Quant. Grav.* **29** (2012) 155009, 1204.1330.

[180] V. E. Hubeny and M. Rangamani, "Causal Holographic Information," *JHEP* **06** (2012) 114, 1204.1698.

[181] A. C. Wall, "Maximin Surfaces, and the Strong Subadditivity of the Covariant Holographic Entanglement Entropy," *Class. Quant. Grav.* **31** (2014), no. 22, 225007, 1211.3494.

[182] M. Rangamani and T. Takayanagi, "Holographic Entanglement Entropy," *Lect. Notes Phys.* **931** (2017) pp.1–246, 1609.01287.

[183] M. Headrick, "Lectures on entanglement entropy in field theory and holography," 1907.08126.

[184] S. Pal and B. Grinstein, "Weyl Consistency Conditions in Non-Relativistic Quantum Field Theory," *JHEP* **12** (2016) 012, 1605.02748.

[185] I. Arav, I. Hason, and Y. Oz, "Spontaneous Breaking of Non-Relativistic Scale Symmetry," *JHEP* **10** (2017) 063, 1702.00690.

[186] A. Bilal, "Introduction to supersymmetry," hep-th/0101055.

[187] R. Auzzi and G. Nardelli, "Heat kernel for Newton-Cartan trace anomalies," *JHEP* **07** (2016) 047, 1605.08684.

[188] Y. Nakayama, S. Ryu, M. Sakaguchi, and K. Yoshida, "A Family of super Schrodinger invariant Chern-Simons matter systems," *JHEP* **01** (2009) 006, 0811.2461.

[189] Y. Nakayama, M. Sakaguchi, and K. Yoshida, "Interacting SUSY-singlet matter in non-relativistic Chern-Simons theory," *J. Phys.* **A42** (2009) 195402, 0812.1564.

[190] K.-M. Lee, S. Lee, and S. Lee, "Nonrelativistic Superconformal M2-Brane Theory," *JHEP* **09** (2009) 030, 0902.3857.

[191] C. Lopez-Arcos, J. Murugan, and H. Nastase, "Nonrelativistic limit of the abelianized ABJM model and the ADS/CMT correspondence," *JHEP* **05** (2016) 165, 1510.01662.

[192] N. Doroud, D. Tong, and C. Turner, "On Superconformal Anyons," *JHEP* **01** (2016) 138, 1511.01491.

[193] O. Bergman and G. Lozano, "Aharonov-Bohm scattering, contact interactions and scale invariance," *Annals Phys.* **229** (1994) 416–427, hep-th/9302116.

[194] N. Doroud, D. Tong, and C. Turner, "The Conformal Spectrum of Non-Abelian Anyons," *SciPost Phys.* **4** (2018), no. 4, 022, 1611.05848.

[195] C. Turner, "Bosonization in Non-Relativistic CFTs," 1712.07662.

[196] P. M. Zhang, M. Cariglia, M. Elbistan, and P. A. Horvathy, "Scaling and conformal symmetries for plane gravitational waves," 1905.08661.

[197] S. P. Martin, "A Supersymmetry primer," hep-ph/9709356. [Adv. Ser. Direct. High Energy Phys.18,1(1998)].

[198] P. C. W. Davies, "Thermodynamics of Black Holes," *Proc. Roy. Soc. Lond.* **A353** (1977) 499–521.